May 2021

NEW MEXICO OZONE ATTAINMENT INITIATIVE PHOTOCHEMICAL MODELING STUDY – DRAFT FINAL AIR QUALITY TECHNICAL SUPPORT DOCUMENT

RAMBOLL

WESTAR
Western States Air Resources Council

NEW MEXICO OZONE ATTAINMENT INITIATIVE PHOTOCHEMICAL MODELING STUDY – DRAFT FINAL AIR QUALITY TECHNICAL SUPPORT DOCUMENT

Project name	**New Mexico Ozone Attainment Initiative Photochemical Modeling Study**
Project no.	**1690017454**
Recipient	**New Mexico Environmental Division**
Document type	**Draft Final Technical Report**
Version	**V8.0**
Date	**May 2021**
Prepared by	**Ralph Morris, Marco Rodriguez, Tejas Shah, Jeremiah Johnson, Jung Chien, Pradeepa Vennam and Fiona Jiang, Ramboll US Consulting, Inc.** **Tom Moore and Mary Uhl, Western States Air Resources Council**

Ramboll
7250 Redwood Blvd.
Suite 105
Novato, CA 94945

T +1 415 899 0700
www.ramboll.com

CONTENTS

TABLE OF TABLES

TABLE OF FIGURES

ACRONYMS AND ABBREVIATIONS

3SAQS	Three-State Air Quality Study
AIRS	Aerometric Information Retrieval System
AMET	Atmospheric Model Evaluation Tool
APCA	Anthropogenic Precursor Culpability Assessment
AQ	Air Quality
AQS	Air Quality System
AQTSD	Air Quality Technical Support Document
BC	Boundary Condition
BLM	Bureau of Land Management
CAMx	Comprehensive Air-quality Model with extensions
CARB	California Air Resources Board
CASTNet	Clean Air Status and Trends Network
CB6r2	Carbon Bond mechanism version 6, revision 2
CMAQ	Community Multiscale Air Quality modeling system
CONUS	Continental United States
CPC	Center for Prediction of Climate
CSAPR	Cross State Air Pollution Rule
CSN	Chemical Speciation Network
DV	Ozone Design Value
DVC	Current Year Ozone Design Value
DVF	Future Year Ozone Design Value
EC	Elemental Carbon Fine Particulate Matter
ECMWF	European Center for Medium Range Weather Forecasting
EGU	Electrical Generating Units
EIS	Environmental Impact Statement
EPA	Environmental Protection Agency
ERA5	ECMWF global hourly meteorological forecasts at 30-km
ERG	Eastern Research Group
FB	Fractional Bias
FE	Fractional Error
FRM	Federal Reference Method
GCM	Global Chemistry Model
GEOS-Chem	Goddard Earth Observing System (GEOS) global chemistry model
GIRAS	Geographic Information Retrieval and Analysis System
IMPROVE	Interagency Monitoring of PROtected Visual Environments
IWDW	Intermountain West Data Warehouse
LCC	Lambert Conformal Conic projection
LSM	Land Surface Model
MADIS	Meteorological Assimilation Data Ingest System
MATS	Modeled Attainment Test Software
MCIP	Meteorology-Chemistry Interface Processor
MEGAN	Model of Emissions of Gases and Aerosols in Nature
MNGE	Mean Normalized Gross Error
MNB	Mean Normalized Bias
MNE	Mean Normalized Error
MOVES	Motor Vehicle Emissions Simulator
MOZART	Model for OZone And Related chemical Tracers

MPE	Model Performance Evaluation
MSKF	Multi-Scale Kain-Fritsch Cumulus Parameterization
NAAQS	National Ambient Air Quality Standard
NAM	North American Mesoscale Forecast System
NCAR	National Center for Atmospheric Research
NCEP	National Center for Environmental Prediction
NCDC	National Climatic Data Center
NEI	National Emissions Inventory
NEPA	National Environmental Policy Act
NH_4	Ammonium Fine Particulate Matter
NMB	Normalized Mean Bias
NME	Normalized Mean Error
NMED	New Mexico Environmental Department
NO_2	Nitrogen Dioxide
NO_3	Nitrate Fine Particulate Matter
NOAA	National Oceanic and Atmospheric Administration
OA	Organic Aerosol Fine Particulate Matter
OAI	Ozone Attainment Initiative
OC	Organic Carbon Fine Particulate Matter
OSAT	Ozone Source Apportionment Technology
O&G	Oil and Gas
PAVE	Package for Analysis and Visualization
PBL	Planetary Boundary Layer
PGM	Photochemical Grid Model
PM	Particulate Matter
PPB	Parts Per Billion
PPM	Parts Per Million
PPM	Piecewise Parabolic Method
QA	Quality Assurance
QC	Quality Control
RMP	Resource Management Plan
RRF	Relative Response Factor
SCC	Source Classification Code
SIP	State Implementation Plan
SMAT	Software for Modeled Attainment Test
SMOKE	Sparse Matrix Kernel Emissions modeling system
SNMOS	Southern New Mexico Ozone Study
SOA	Secondary Organic Aerosol
SO_2	Sulfur Dioxide
SO_4	Sulfate Fine Particulate Matter
TCEQ	Texas Commission on Environmental Quality
UNC-IE	University of North Carolina Institute for the Environment
USFS	United States Forest Service
VERDI	Visualization Environment for Rich Data Interpretation
VMT	Vehicle Miles Traveled
WBD	Wind Blown Dust model
WAQS	Western Air Quality Study
WESTAR	Western States Air Resources Council
WestJumpAQMS	West-Wide Jump-Start Air Quality Modeling Study

WESTUS	Western United States
WRAP	Western Regional Air Partnership
WGA	Western Governors' Association
WRF	Weather Research Forecast model

1. INTRODUCTION

This is a draft final Air Quality Technical Support Document (AQTSD) for the New Mexico (NM) Ozone Attainment Initiative (OAI) Photochemical Modeling Study ("NM OAI Study"). The NM OAI Study has developed a 2014 base year photochemical grid model (PGM) modeling platform and conducted 2028 future year modeling for a Base Case and an Oil and Gas (O&G) Control Strategy scenario that implemented proposed controls on 2028 New Mexico O&G sources. The New Mexico Environmental Department (NMED) has contracted with a team consisting of Western States Air Resources Council (WESTAR) and Ramboll US Corporation (Ramboll) to conduct the NM OAI Study.

The NM OAI Study leverages the 2014 PGM modeling platform developed by the Western Regional Air Partnership (WRAP) in the Western Air Quality Study (WAQS) and enhances it by adding a 4-km grid resolution modeling domain covering New Mexico and adjacent regions. The NM OAI Study AQTSD documents the 2014 base case, 2028 future year base case and 2028 NM O&G control strategy modeling and includes a summary of the development of the 2014 PGM modeling platform with more details found on the NM OAI Study Website[1] and reports:

- New Mexico Ozone Attainment Initiative Photochemical Modeling Study – Draft Modeling Protocol (Ramboll and WESTAR, 2020a).[2]
- New Mexico Ozone Attainment Initiative Photochemical Modeling Study – Draft Work Plan (Ramboll and WESTAR, 2020b).[3]
- New Mexico Ozone Attainment Initiative Photochemical Modeling Study – 2014 Modeling Platform Development and Model Evaluation (Ramboll and WESTAR2020c).[4]
- New Mexico Ozone Attainment Initiative Photochemical Modeling Study – Revised 2014v2 Base Case and Model Performance Evaluation (Ramboll and WESTAR, 2021).[5]

Although the WESTAR/Ramboll team conducted the 2014 base year and 2028 base and O&G Control Strategy future year modeling, the implementation of the proposed NMED O&G ozone precursor control strategy in the 2028 O&G emissions was conducted by Eastern Research Group (ERG) under separate contract with NMED so is not documented in this report.

1.1 NM OAI Photochemical Modeling Study Genesis

The NMED Air Quality Bureau has authority over air quality management activities throughout the state of New Mexico, with the exception Bernalillo County and Tribal Lands. The City of Albuquerque/Air Quality Division has authority in Bernalillo County and, except for where Tribal Implementation Plans have been approved, EPA oversees air quality issues in Tribal Lands. The New Mexico Air Quality Control Act (NMAQCA) requires the NMED to develop a plan to address elevated ozone levels when air quality

[1] https://www.wrapair2.org/NMOAI.aspx
[2] https://www.wrapair2.org/pdf/NM_OAI_Modeling_Protocol_v5.pdf.
[3] https://www.wrapair2.org/pdf/NM_OAI_Work_Plan_v2.pdf
[4] https://www.wrapair2.org/pdf/NM_OAI_2014_BaseCase_MPE_v3.pdf
[5] https://www.wrapair2.org/NMOAI.aspx

is within 95% of the ozone NAAQS (74-3-5.3, NMSA 1978[6]). The ozone NAAQS was revised in 2015 with a threshold of 0.070 ppm (70 ppb) with the relevant metric being the ozone Design Value (DV) that is expressed as the three-year average of the fourth highest Maximum Daily Average 8-hour (MDA8) ozone concentrations. Table 1-1 lists the observed ozone DVs at New Mexico monitoring sites from 2010 to 2019. The DVs are color-coded when they exceed the 75 ppb 2008 ozone NAAQS (red), 70 ppb 2015 ozone NAAQS (yellow) and within 95% of the 70 ppb ozone NAAQS (green, i.e., ≥ 67 ppb). In more recent years, the ozone DVs have exceeded the 70 ppb 2015 ozone NAAQS at several sites in southern New Mexico (e.g., in Doña Ana and Eddy Counties). In particular, the 2017-2019 ozone DVs are particularly high and even exceeded the 75 ppb 2008 ozone NAAQS at three sites in southern New Mexico (colored red in Table 1-1).

[6] https://law.justia.com/codes/new-mexico/2017/chapter-74/article-2/section-74-2-5.3/

Table 1-1. Ozone design values (ppm) at sites in New Mexico from 2010 to 2019. Red above the 75 ppb 2008 NAAQS, yellow above 2015 70 ppb NAAQS and green within 95% of the 2015 NAAQS.

AQS Site ID	Local Site Name	County Name	2008-2010	2009-2011	2010-2012	2011-2013	2012-2014	2013-2015	2014-2016	2015-2017	2016-2018	2017-2019
350010023	Del Norte HS	Bernalillo	0.064	0.066	0.068	0.070	0.068	0.066	0.065	0.067	0.070	0.070
350010024	SE Heights	Bernalillo	0.066	0.068	0.070	0.070	0.068					
350010027	Westside	Bernalillo	0.067	0.068	0.071	0.071						
350010029	South Valley	Bernalillo	0.066	0.067	0.069	0.070	0.067	0.066	0.065	0.065	0.066	0.067
350010032	Westside	Bernalillo			0.070	0.070	0.067					
350011012	Foothills	Bernalillo	0.068	0.070	0.074	0.072	0.067	0.064	0.064	0.067	0.069	0.071
350011013	North Valley	Bernalillo	0.067	0.068	0.069	0.069						
350130008	La Union	Doña Ana	0.064	0.062	0.065	0.067	0.067	0.066	0.066	0.068	0.068	0.070
350130017	Sunland Park	Doña Ana	0.064	0.065	0.068	0.067	0.067					
350130020	Chaparral	Doña Ana	0.066	0.067	0.067	0.069	0.068	0.067	0.066	0.068	0.071	0.073
350130021	Desert View	Doña Ana	0.070	0.069	0.072	0.072	0.072	0.072	0.072	0.072	0.074	0.077
350130022	Santa Teresa	Doña Ana	0.067	0.066	0.070	0.075	0.074	0.072	0.068	0.072	0.074	0.076
350130023	Solano	Doña Ana	0.063	0.063	0.065	0.065	0.065	0.065	0.065	0.066	0.067	0.070
350151005	Carlsbad City	Eddy	0.067	0.068	0.071	0.071	0.071	0.069	0.067	0.068	0.074	0.079
350153001	Carlsbad Caverns	Eddy									0.071	
350171003	Chino Copper	Grant	0.063	0.065	0.067	0.063	0.062					
350250008	Hobbs Jefferson	Lea	0.059	0.061	0.061	0.066	0.065	0.067	0.066	0.067	0.070	0.071
350290003	Deming Airport	Luna	0.057	0.058	0.064	0.067	0.066					
350390026	Coyote Ranger District	Rio Arriba							0.064	0.065	0.067	0.067
350431001	Bernalillo	Sandoval	0.060	0.061	0.061	0.063	0.063	0.065	0.064	0.065	0.068	0.068
350439004	Pueblo of Jemez	Sandoval		0.062								
350450009	Bloomfield	San Juan	0.060	0.061	0.067	0.068	0.067	0.064	0.062	0.064	0.069	0.068
350450018	Navajo Lake	San Juan			0.071	0.071	0.068	0.067	0.066	0.068	0.070	0.069
350451005	Substation	San Juan	0.063	0.063	0.067	0.068	0.066	0.063	0.062	0.064	0.069	0.069
350490021	Santa Fe Airport	Santa Fe	0.063	0.062	0.065	0.066	0.066	0.064	0.063	0.063	0.066	0.066
350610008	Los Lunas	Valencia			0.067	0.070	0.069	0.066	0.064	0.065	0.067	0.068

To address the high observed ozone concentrations in New Mexico, the NMED has embarked on an Ozone Attainment Initiative (OAI[7]) to protect the ozone attainment status of the state and ensure health and welfare of the residents of the state for future generations. The OAI was initiated in Spring 2018. As part of the OAI, NMED released a Request for Proposal (RFP#20 667 4040 0001) for the NM OAI Study and the NM OAI Study PGM modeling was awarded to a contracting team of WESTAR and Ramboll.

[7] https://www.env.nm.gov/air-quality/o3-initiative/

1.2 Overview of NM OAI Study Modeling Approach

The procedures used for the NM OAI Study photochemical modeling were described in a detailed Modeling Protocol dated May 19, 2020 (Ramboll and WESTAR, 2020a). A description of the tasks and schedule for completing the NM OAI Study is contained in a Work Plan (Ramboll and WESTAR, 2020b) with presentations, results and reports posted to the NM OAI Study webpage[8] as they are produced. One objective of the study was to evaluate a proposed regulation to control ozone precursor emissions from oil and gas (O&G) development sources in New Mexico. The original future year emissions scenario in the NM OAI Study was 2023, when the proposed O&G rule would not be fully implemented. Thus, the future year to be modeled was changed to 2028 in a December 2020 Contract Amendment from NMED to the WESTAR/Ramboll team.

The NM OAI Study is conducting PGM modeling by enhancing the WRAP-WAQS 2014v2 36/12-km PGM modeling platform[9] with the addition of a new 4-km grid resolution domain covering New Mexico and surrounding areas, especially the O&G production regions in the Permian and San Juan Basins. The NM OAI Study PGM modeling is performing 2014 base year modeling and model performance evaluation. 2028 future year modeling was also conducted. The NM OAI Study PGM modeling is being conducted in accordance with EPA's guidance for ozone State Implementation Plan (SIP) ozone attainment demonstration modeling (EPA, 2018).

1.2.1 WRAP-WAQS 2014 PGM Platform Development

The WRAP-WAQS developed an annual 2014 PGM modeling platform to address air quality issues in the western states. An initial WRAP-WAQS 2014v1 PGM modeling platform was developed in 2019 for the CAMx and CMAQ PGMs that is documented in a webpage[10] on the Intermountain West Data Warehouse (IWDW). Additional diagnostic sensitivity tests were conducted to address several model performance issues culminating in the WRAP-WAQS 2014v2 36/12-km CAMx modeling database that was used as the starting point for the NM OAI Study CAMx summer of 2014 36/12/4-km modeling database. The development of the WRAP-WAQS 2014v2 PGM database and model performance evaluation is available in a webpage[11] on the IWDW.

The WRAP-WAQS 2014v2 CAMx platform used a 36/12-km grid resolution domain structure with meteorological inputs based on the WAQS 2014 36/12-km WRF meteorological model simulation (Bowden, Talgo and Adelman, 2016[12]). The 2014 emissions were based on the 2014 National Emissions Inventory (2014NEI[13]) with updates from western states[14]. Boundary Condition (BC) inputs were based on a WRAP 2014 GEOS-Chem model simulation.

Because the NM OAI Study requires a 4-km modeling domain for New Mexico, new summer of 2014 36/12/4-km WRF meteorological modeling was conducted, as

[8] https://www.wrapair2.org/NMOAI.aspx
[9] http://views.cira.colostate.edu/wiki#WAQS-2014-Modeling-Platform
[10] http://views.cira.colostate.edu/iwdw/docs/waqs_2014v1_shakeout_study.aspx
[11] https://views.cira.colostate.edu/iwdw/docs/WRAP_WAQS_2014v2_MPE.aspx
[12] http://views.cira.colostate.edu/wiki/Attachments/Modeling/WAQS_2014_WRF_MPE_January2016.pdf
[13] https://www.epa.gov/air-emissions-inventories/2014-national-emissions-inventory-nei-data
[14] https://www.wrapair2.org/pdf/WRAP%20Regional%20Haze%20SIP%20Emissions%20Inventory%20Review%20Documentation_for_Docket%20Feb2019.pdf

described in Chapter 2, that was used to develop 36/12/4-km meteorological inputs for CAMx. The NM OAI Study defined their 36/12-km domains to match WRAP-WAQS 2014v2 36/12-km domains so the WRAP-WAQS 2014v2 36/12-km emission and some other inputs (e.g., BCs) can be used directly in the NM OAI Study PGM modeling. Figure 1-1 shows the 36/12/4-km modeling domains used for the NM OAI Study PGM modeling with the 4-km grid resolution New Mexico domain shown in Figure 1-2.

1.2.2 Episode Selection

The May-August 2014 modeling period was selected as it has a high quality emissions inventory with western state updates and has a PGM platform already developed from the WRAP-WAQS regional haze modeling that can be leveraged for the NM OAI Study. Details on the episode selection are contained in Chapter 3 of the NM OAI Study Modeling Protocol (Ramboll and WESTAR, 2020a).

1.2.3 Model Selection

Details on the rationale for model selection are provided in Chapter 2 of the NM OAI Study Modeling Protocol (Ramboll and WESTAR, 2020a). The Weather Research Forecast (WRF) prognostic meteorological model was selected. Emissions modeling was conducted using the Sparse Matric Operator Kernel Emissions (SMOKE) model for most source categories. The Model of Emissions of Gases and Aerosols from Nature (MEGAN v3.1) was used initially for biogenic emissions in the 4-km domain for the original CAMx 2014 Base Case, but was ultimately replaced by biogenic emission based on the BEIS v3.7 model in the final CAMx 2014v2 base case. There are special processors for fires, windblown dust (WBD), lightning NO_x (LNO_x) and oceanic sea salt (NaCl) and Dimethyl Sulfide (DMS) emissions that were used. The 2014 version of the Motor Vehicle Emissions Simulator (MOVES2014b) on-road mobile source emissions model was used with SMOKE-MOVES and WRF meteorological data to generate on-road mobile source emissions for the 4-km New Mexico modeling domain.

The Comprehensive Air-quality Model with extensions (CAMx) photochemical grid model (PGM) was used because it supports two-way grid nesting, was used in the WRAP-WAQS regional haze modeling, contains a well-vetted ozone source apportionment tool and has a rich and successful history of successful application to the region.

1.2.4 Domain Selection

The NM OAI Study modeling is using the same 36-km 36US and 12-km 12WUS2 domains as used in the WRAP-WAQS 2014 modeling platform. A new 4-km New Mexico domain was added to the 36/12-km domain structure. Figure 1-1 displays the 36/12/4-km domain structure with Figure 1-1 showing the 4-km New Mexico domain. New WRF 2014 36/12/4-km meteorological modeling was conducted to generate finer scale 4-km meteorological conditions for the New Mexico domain and consistent meteorology among the 36/12/4-km domains. The domains use a Lambert Conformal Conic (LCC) projection using the parameters given in Table 1-2 with the definitions of the extent of the 36/12/4-km domains given in Table 1-3. CAMx was run using the 36/12/4-km domain structure shown in Figure 1-1 using two-way interactive grid nesting.

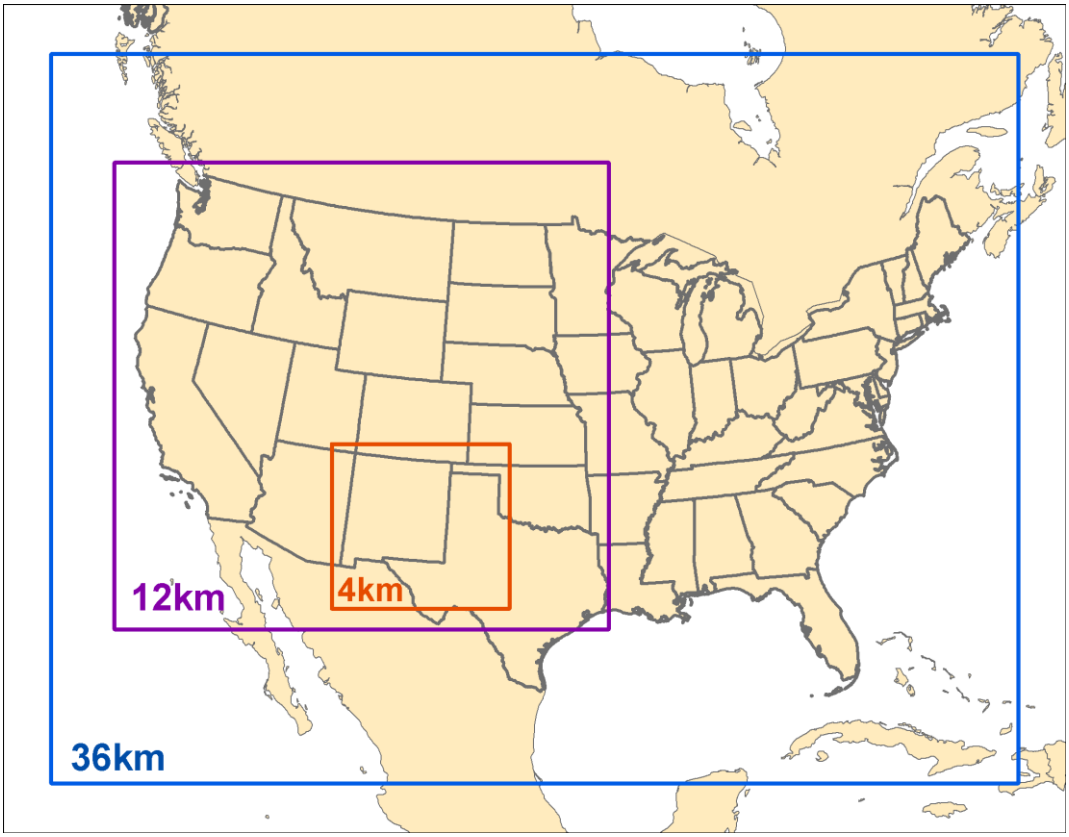

Figure 1-1. NM OAI Study 2014 36/12/4-km PGM and emissions modeling domains.

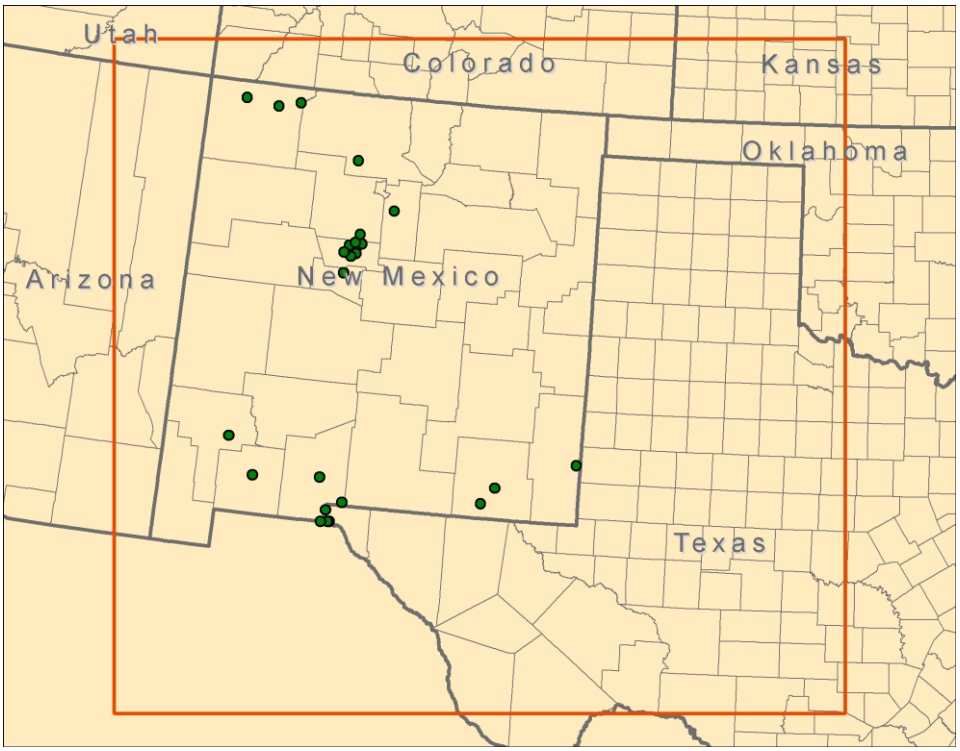

Figure 1-2. 4-km New Mexico modeling domain for PGM and emissions modeling, with locations of New Mexico ozone monitors that were operating during some portion of 2014.

Table 1-2. Lambert Conformal Conic (LCC) projection parameters for the NM OAI Study 36/12/4 modeling domains.

Parameter	Value
Projection	Lambert-Conformal
1st True Latitude	33 degrees N
2nd True Latitude	45 degrees N
Central Longitude	-97 degrees W
Central Latitude	40 degrees N

Table 1-3. Grid definitions for CAMx NM OAI Study 2014 36/12/4-km modeling domains.

Grid	Origin (SW) (km)	Extent (NE) (km)	NX	NY
36-km	(-2736, -2088)	(2592, 1944)	148	112
12-km*	(-2388, -1236)	(336, 1344)	227	215
4-km*	(-1192, -1120)	(-212, -212)	245	227

*Definition includes outer row/column of buffer cells required by CAMx for nested domains

1.2.5 Base and Future Year Emissions Data

The 2014 base year emissions data were based on the WRAP-WAQS 2014v2 emissions that were in turn based on the 2014NEIv2 with updates from western states. New emissions were generated for natural emission sources (e.g., biogenic and LNO_x). 2028 emissions were based on the WRAP 2028 On-the-Books (2028OTBa2) emissions scenario with updated 2028 O&G emissions for New Mexico and using actual 2014 fires instead of Representative Baseline fires as used in the WRAP 2028OTBa2 scenario. The development of the 2014 and 2028 emission scenarios are discussed in Chapter 4.

1.2.6 Initial and Boundary Conditions Development

The first two-weeks of May were run on the 36/12/4-km domains to spin-up the model before the first high ozone day in New Mexico (68 ppb on May 17). This washed out the influence of the initial concentrations (IC) before elevated ozone concentrations occur in New Mexico.

Boundary conditions (BC) for the outer 36-km 36US domain were based on a 2014 simulation of the GEOS-Chem global chemistry model conducted by WRAP processed by the GC2CAMx converter. The result is day-specific diurnally varying BCs for the lateral boundaries around the 36-km 36US modeling domain. The top BC was based on a zero-gradient assumption where concentrations above the top of the model (above 50 mb, or ~19-km above sea level) are assumed to be the same as in the top vertical layer of CAMx.

Due to uncertainties in projecting future year international emissions, the CAMx BCs based on the 2014 GEOS-Chem global model simulation were held constant for the 2028 modeling. This is likely a conservative estimate of 2028 BCs.

Chapter 3 provides a summary of the development of the 2014 CAMx BC inputs with more details in Ramboll and WESTAR (2020c) and on the WRAP-WAQS 2014v2 modeling website.

1.2.7 Diagnostic Sensitivity Analyses

The NM OAI Study conducted four diagnostic sensitivity tests for the CAMx 2014 36/12/4-km base case that compared the CAMx ozone performance for four alternative meteorological inputs. The NM OAI Study conducted two WRF 2014 36/12/4-km WRF simulations that used different analysis fields as input. The two 2014 36/12/4-km WRF outputs were processed with WRFCAMx using two different options for vertical turbulent exchange (i.e., vertical mixing) coefficients (Kv). This resulted in four different CAMx meteorological inputs that were evaluated using CAMx diagnostic sensitivity tests that are summarized in Chapter 5 with details provided in Ramboll and WESTAR (2020c).

1.2.8 Model Performance Evaluation

The NM OAI Study CAMx 2014 36/12/4-km base case simulation Model Performance Evaluation (MPE) followed EPA's MPE recommendations in their ozone modeling guidance (EPA, 2018) and other sources (e.g., Simon, Baker and Phillips, 2012; Emery et al., 2016). The CAMx 2014 36/12/4-km base case simulation MPE focused on ozone model performance within the 4-km New Mexico domain, and especially within New Mexico. Two CAMx 2014 base case simulations were performed and subjected to an MPE. An original CAMx 2014 base case simulation used CAMx v7.0 and biogenic

emissions in the 4-km NM domain based on the MEGAN v3.1 model whose evaluation is documented in NM OAI Study 2014 platform development and 2014 base case modeling report (Ramboll and WESTAR, 2020c). A revised 2014v2 base case was conducted using CAMx v7.1 and biogenic emissions based on the BEIS v3.7, whose results are documented in an Addendum to the 2014 base case modeling report (Ramboll and WESTAR, 2021).

1.2.9 2028 Future Year Base and Control Strategy Modeling

2028 future year ozone modeling was conducted using the WRAP 2028OTBa2 emissions scenario with updated 2028 O&G emissions in New Mexico and using 2014 actual fires instead of the Representative Baseline fires used in the 2028OTBa2 scenario. These fire inventories were prepared for the WRAP Fire and Smoke Work Group and are documented in a report (Air Sciences, 2020) and presentation.[15] A CAMx 2028 future year 36/12/4-km base case simulation was conducted using CAMx v7.1 and used to project 2028 future year ozone design values (DVs). The procedures to calculate projected ozone DVs followed EPA's latest guidance (EPA, 2018). These procedures use the modeling results in a relative fashion to scale the current year observed 2012-2016 8-hour ozone design values (i.e., $DVC_{2012\text{-}2016}$) to project 2028 future year ozone Design Values (DVFs). The scaling factors are called Relative Response Factors (RRFs) and are the ratio of the future-year to current-year modeling results for the 10 highest base year modeled MDA8 ozone days near the monitoring site. EPA has developed the Speciated Modeled Attainment Test (SMAT[16]) tool that includes the recommended procedures in the latest EPA guidance for projecting ozone DVFs.

The NM OAI Study also conducted future year modeling for a 2028 O&G Control Strategy that implemented controls on ozone precursors from O&G sources within the San Juan and Permian Basins. The WESTAR/Ramboll team provided the 2028 NM O&G emissions to ERG who, under separate contract to NMED, implemented the proposed NM O&G ozone precursor control strategy in the 2028 NM O&G emissions and provided them to WESTAR/Ramboll for ozone modeling. This report does not document the implementation of the NM O&G ozone precursor control strategy as that was not performed by WESTAR/Ramboll.

1.2.10 Future Year Source Apportionment Modeling

The NM OAI Study also is conducting future year ozone source apportionment modeling for the 2028 O&G Control Strategy scenario using the CAMx ozone source apportionment tool. The CAMx 2028 Source Sector APCA ozone source apportionment modeling examined the ozone contributions of several major anthropogenic emission source sectors in New Mexico and other states as well as contributions of International anthropogenic emissions on ozone concentrations in New Mexico and is discussed in Chapter 9. CAMx 2028 VOC/NO_x Sensitivity OSAT ozone source apportionment modeling was also conducted to examine the level of VOC sensitive versus NO_x sensitive ozone formation in New Mexico and is discussed in Chapter 10.

[15] https://www.wrapair2.org/pdf/FireEIandFutureScenariosResults_to_regional_planners_20200520.pptx
[16] https://www.epa.gov/scram/photochemical-modeling-tools

2. 2014 WRF METEOROLOGICAL MODELING

The NM OAI Study conducted WRF meteorological modeling for the summer of 2014 to generate CAMx meteorological inputs for the 36/12/4-km horizontal domain structure shown in Figure 1-1.

2.1 WRF Meteorological Model

The Weather Research and Forecasting (WRF) Model is a mesoscale numerical weather prediction system designed to serve both operational forecasting and atmospheric research needs (Skamarock, 2004; 2006; Skamarock et al., 2005; 2008; 2019). The Advanced Research WRF (ARW) version of WRF was used in the NM OAI Study.

This chapter summarizes the application and evaluation of the WRF meteorological model to generate 2014 36/12/4-km meteorological inputs for CAMx photochemical grid modeling with more details provided in Chapter 2 of Ramboll and WESTAR (2020c).

2.2 WRF Horizontal Modeling Domain

The WRF 2014 36/12/4-km modeling domains were defined slightly larger than the PGM 36/12/4-km domains (Figure 1-1) so that any modeling artifacts that occur near the WRF boundaries as the boundary conditions (BCs) come into dynamic balance with the WRF numerical algorithms are not present in the PGM meteorological inputs.

2.3 WRF Model Configuration

WRF version 4.2 was used for this modeling analysis. The NM OAI Study 36/12-km WRF/PGM grid configuration (e.g., horizontal domains and vertical layer structure) was designed to be identical to the WRAP-WAQS 2014 WRF/PGM grid configuration in order to facilitate the use of data between the two studies. A 4-km domain was added covering New Mexico and adjacent regions.

The WAQS 2011/2014 WRF modeling used 36 vertical levels (35 vertical layers) from the surface to a 50 mb (hPa) height (approximately 19-km above sea level). The EPA 2014, 2015 and 2016 WRF modeling also used 35 vertical layers up to a 50 mb height.

Table 2-1 displays the 36-vertical layer structure used in the WRAP-WAQS 2011/2014 WRF modeling that was also adopted for the NM OAI Study WRF 2014 36/12/4-km modeling.

Table 2-1. WRF 36 level vertical layer structure for the NM OAI study. This is the same WRF layer structure as used in WAQS 2011/2014/2016 and EPA 2016 WRF modeling.

WRF Layer	Sigma	Pressure (mb)	Height (m)	Thickness (m)
36	0.0000	50.00	19260	2055
35	0.0270	75.65	17205	1850
34	0.0600	107.00	15355	1725
33	0.1000	145.00	13630	1701
32	0.1500	192.50	11930	1389
31	0.2000	240.00	10541	1181
30	0.2500	287.50	9360	1032
29	0.3000	335.00	8328	920
28	0.3500	382.50	7408	832
27	0.4000	430.00	6576	760
26	0.4500	477.50	5816	701
25	0.5000	525.00	5115	652
24	0.5500	572.50	4463	609
23	0.6000	620.00	3854	461
22	0.6400	658.00	3393	440
21	0.6800	696.00	2954	421
20	0.7200	734.00	2533	403
19	0.7600	772.00	2130	388
18	0.8000	810.00	1742	373
17	0.8400	848.00	1369	271
16	0.8700	876.50	1098	177
15	0.8900	895.50	921	174
14	0.9100	914.50	747	171
13	0.9300	933.50	577	84
12	0.9400	943.00	492	84
11	0.9500	952.50	409	83
10	0.9600	962.00	326	82
9	0.9700	971.50	243	82
8	0.9800	981.00	162	41
7	0.9850	985.75	121	24
6	0.9880	988.60	97	24
5	0.9910	991.45	72	16
4	0.9930	993.35	56	16
3	0.9950	995.25	40	16
2	0.9970	997.15	24	12
1	0.9985	998.58	12	12
0	1.0000	1000.00	0	

2.3.1 Vertical Coordinate

Since its inception, WRF has used the eta (sometimes called sigma or "terrain-following") vertical coordinate system. One weakness of the eta coordinate is that variations in terrain (especially steep topography) can increase numerical errors in the model. To reduce these errors, Park et al., (2018) developed a hybrid sigma–pressure coordinate that is now included as the default vertical coordinate system for the WRF model (Skamarock et al., 2019).

For the NM OAI Study 2014 36/12/4-km WRF modeling, we used the new hybrid vertical coordinate system and a new version of the WRFCAMx processor that has been updated to use WRF's hybrid vertical coordinate. The hybrid vertical coordinate system and use of 4-km New Mexico domain are the two biggest differences between the NM OAI Study and WRAP-WAQS 2014 WRF modeling. The WRAP-WAQS 2014 WRF/CAMx modeling did not use the hybrid vertical coordinate system in WRF because at the time it was not supported in the WRFCAMx processor.

2.3.2 Topographic Inputs

Topographic information for WRF was based on a combination of the standard WRF terrain databases and high-resolution terrain. The 36-km 36US domain used the 10-minute global data, the 12-km 12WUS2 domain used the 2-minute data, and the 4-km New Mexico domain used the 30 second data.

2.3.3 Vegetation Type and Land Use Inputs

Vegetation type and land use information used the United States Geological Survey (USGS) land use databases from the most recently released WRF databases provided with the WRF distribution. Standard WRF surface characteristics corresponding to each land use category was employed.

2.3.4 Atmospheric Data Inputs

WRF relies on other model or re-analysis output meteorological fields to provide initial and boundary conditions (IC/BC) and fields for the four-dimensional data assimilation (FDDA). FDDA refers to the nudging of the WRF meteorological fields to observed analysis fields so that the WRF meteorological fields better represent what was observed and prevent the model from drifting away from the observed meteorology. The NM OAI Study conducted two WRF simulations that used two different analysis fields that were evaluated for their performance against meteorological variables as well as their effect on CAMx ozone model performance. Both the 12-km resolution North American Model (NAM) and the ~30-km resolution European Center for Medium-Range Weather Forecasting (ECMWF) Re-Analysis (ERA5[17]) dataset analysis fields were used for IC/BC and FDDA in the two WRF 2014 36/12/4-km sensitivity simulations.

Analysis nudging (i.e., FDDA) was used for winds, temperature, and humidity on the 36-km and 12-km domains. Both surface and aloft nudging was used but nudging for temperature and mixing ratio was not performed within the boundary layer. Observation nudging was not used, even on the 4-km domain.

[17] https://www.ecmwf.int/en/forecasts/datasets/archive-datasets/reanalysis-datasets/era5

The effects of the two 2014 WRF simulations on CAMx ozone performance was evaluated in diagnostic sensitivity simulations and the best performing configuration selected as the final CAMx meteorological inputs, as described in Chapter 5.

2.3.5 New Lightning Data Assimilation

More recently, the assimilation of lightning data in WRF simulations has shown to improve the locations and amounts of convective precipitation. The use of lighting detection networks, such as the National Lightning Detection Network (NLDN), have been used in WRF simulations and used to force deep convection (thunderstorms) when lightning is observed and only allow shallow convection when lightning is not present. The use of the new lightning assimilation approach has been demonstrated to improve both WRF convective precipitation as well as PGM concentration and deposition performance (Heath et al., 2016). The new lightning data assimilation algorithms was not used in the NM OAI Study 2014 WRF modeling for the following reasons: (1) it would have to be tested and evaluated and there is insufficient time in the schedule to conduct such diagnostic testing; (2) the NLDN data used to date with the WRF lightning assimilation is a commercial product that is expensive and not within the budget; (3) the implementation of the lightning detection data assimilation in WRF has a flaw that it doesn't distinguish between no lightning detects and missing data and suppresses convection in areas with missing data (e.g., over the Gulf of Mexico); and (4) most importantly, the lightning detection data assimilation algorithm has not been implemented in the latest versions of WRF so its use would limit the use of other model new options, such as the hybrid vertical coordinate system.

2.3.6 PBL and LSM Physics Options

As used in the WRAP-WAQS 2014 WRF modeling, the YSU Planetary Boundary Layer (PBL) and Noah Land Surface Model (LSM) physics options were used in the NM OAI Study 2014 36/12/4-km WRF modeling. Previous WRF sensitivity modeling for the intermountain west region found the YSU/Noah PBL/LSM schemes produces the most realistic meteorological fields. Note that EPA's 2014/2015/2016 WRF modeling uses the ACM2 PBL and Pleim-Xiu (PX) LSM schemes (EPA, 2019).

2.3.7 Remaining WRF Physics Options

Table 2-2 lists the remaining WRF physics options for the NM OAI Study 2014 36/12/4-km WRF application. These are standard WRF physics options and consistent with the WRF options used in the WRAP-WAQS 2014 and EPA 2014/2015/2016 WRF modeling. Our comparison of 2014 WRAP-WAQS and 2014 EPA WRF modeling for summertime precipitation performance in New Mexico found that the WRAP-WAQS WRF meteorological model performance was better than EPA WRF for most variables. Therefore, we used the same microphysics and cumulus schemes for the NM OAI Study as used in 2014 WRAP-WAQS (Thompson and Multi-Scale Kain-Fritsch, respectively) and most of the same other physics options (see Table 2-2).

Table 2-2. NM OAI Study 2014 WRF model configuration and comparison with the WRF configuration used in the WRAP-WAQS 2014 and EPA 2014/2015/2016 WRF modeling.

WRF Option	NM OAI Study	2014 WRAP-WAQS	2014 EPA
Horizontal Domains	36/12/4-km	36/12/4-km	12-km
Vertical Coordinate	Hybrid Sigma	Sigma	Sigma
Microphysics	Thompson	Thompson	Morrison 2
LW Radiation	RRTMG	RRTMG	RRTMG
SW Radiation	RRTMG	RRTMG	RRTMG
Sfc Layer Physics	MM5 similarity	MM5 similarity	MM5 similarity
LSM	Noah	Noah	Pleim-Xiu
PBL scheme	Yonsei University (YSU)	YSU	ACM2
Cumulus	36/12/4-km Multi-scale Kain Fritsch	36/12-km Multi-scale_Kain Fritsch; 4-km None	Kain-Fritsch
BC, IC Analysis Nudging Source	36/12-km NAM & ERA5	36/12-km NAM	12-km NAM
Analysis Nudging Grids	36/12-km	36/12-km	12-km
Obs Nudging	None	4-km	None
Sea Sfc Temp	FNMOC	FNMOC	FNMOC

2.3.8 Application Methodology

The WRF model was executed in 5.5-day blocks initialized at 12Z every five days. Model results were output every 60 minutes, split at twelve (12) hour intervals. Twelve (12) hours of spin-up is included in each 5-day block before the data is used in the subsequent evaluation and PGM meteorological inputs.

2.4 WRF Model Evaluation

Quantitative and qualitative evaluations of the NM OAI Study 2014 WRF 36/12/4-km simulation meteorological performance was conducted for both the WRF/NAM and WRF/ERA5 applications. The quantitative evaluations compare integrated surface hourly meteorological observations with WRF predictions matched by time and location and included the calculation of model performance statistical metrics that were compared against performance benchmarks. The qualitative evaluations compared time series plots of modeled wind speed and wind direction to the observations at specific sites. The qualitative evaluation also compared spatial plots of WRF precipitation estimates against spatial maps of precipitation analysis fields based on observations

2.4.1 Quantitative Evaluation Using METSTAT

METSTAT was used to evaluate the WRF/NAM and WRF/ERA model performance against observed surface meteorological observations of wind speed and direction, temperature and mixing ratio (humidity). Figure 2-1 displays the WRF/NAM and WRF/ERA5 wind speed soccer plot that compares monthly measures of wind speed bias and error across surface monitoring sites in New Mexico with the simple and complex performance benchmarks. The monthly wind speed performance of the two WRF simulations are remarkably similar with both having near zero bias that achieves the simple benchmark (≤±0.5 m/s). The error (RMSE) for the two WRF simulations falls between the simple

and complex benchmarks (i.e., between 2.0 and 2.5 m/s) for all four months (May through August).

The monthly wind direction bias and error statistics for the two WRF simulations are also nearly identical with bias values of ~5 degrees that achieves the ≤±5 degree simple benchmark and error statistics that falls between the 30 degree simple and 50 degree complex benchmarks (Figure 2-2).

There are differences in the two WRF simulations temperature performance and more differences in the monthly values than seen for winds (Figure 2-3). The WRF/ERA5 simulations has a near zero temperature bias in May and June with the bias and error achieving the simple benchmark for both months. The WRF/NAM has a warm bias for May and June that straddle the simple benchmark upper bound (+0.5 K). The two WRF simulations have similar July and August performance that have a warm bias of ~1.0 K that fails to achieve the simple benchmark. For both WRF simulations, the temperature bias is right at, but mostly within, the 2.0 K simple benchmark.

The WRF/ERA5 clearly has better surface humidity performance than WRF/NAM (Figure 2-4). For July and August, the WRF/NAM has a wet bias in July and August of ~1.5 g/kg so fails to achieve the simple (≤±0.8 g/kg) and complex (≤±1.0 g/kg) bias benchmarks. The WRF/ERA5 also has a wet bias for July and August that is not as large as WRF/NAM as it is right at the simple benchmark (~ 1.0 g/kg) but achieving the complex benchmark. The WRF/ERA5 also has better humidity error performance in July and August, although both simulations achieve the error performance benchmarks.

The two WRF simulations have better humidity performance in May and June that achieves the simple benchmark, albeit with a moist bias. May is the best performing month with nearly identical humidity model performance with a bias of ~0.6 g/kg and error of ~0.9 g/kg. In June, the WRF/ERA5 humidity performance is slightly better than WRF/NAM.

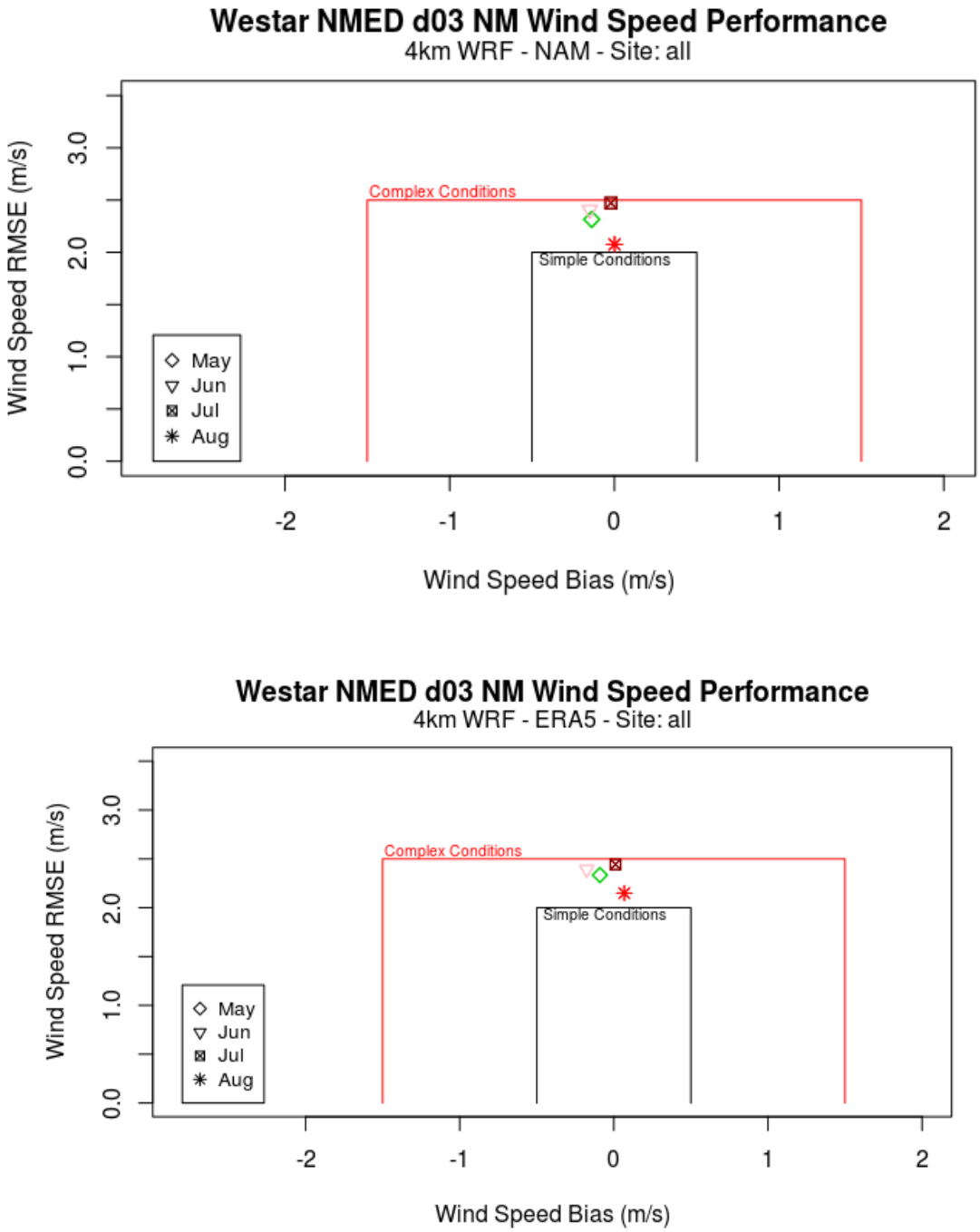

Figure 2-1. Soccer plot comparing WRF/NAM (top) and WRF/ERA5 (bottom) surface wind speed (m/s) model performance against the Simple and Complex Benchmarks for monthly RMSE (y-axis) and Mean Bias (x-axis).

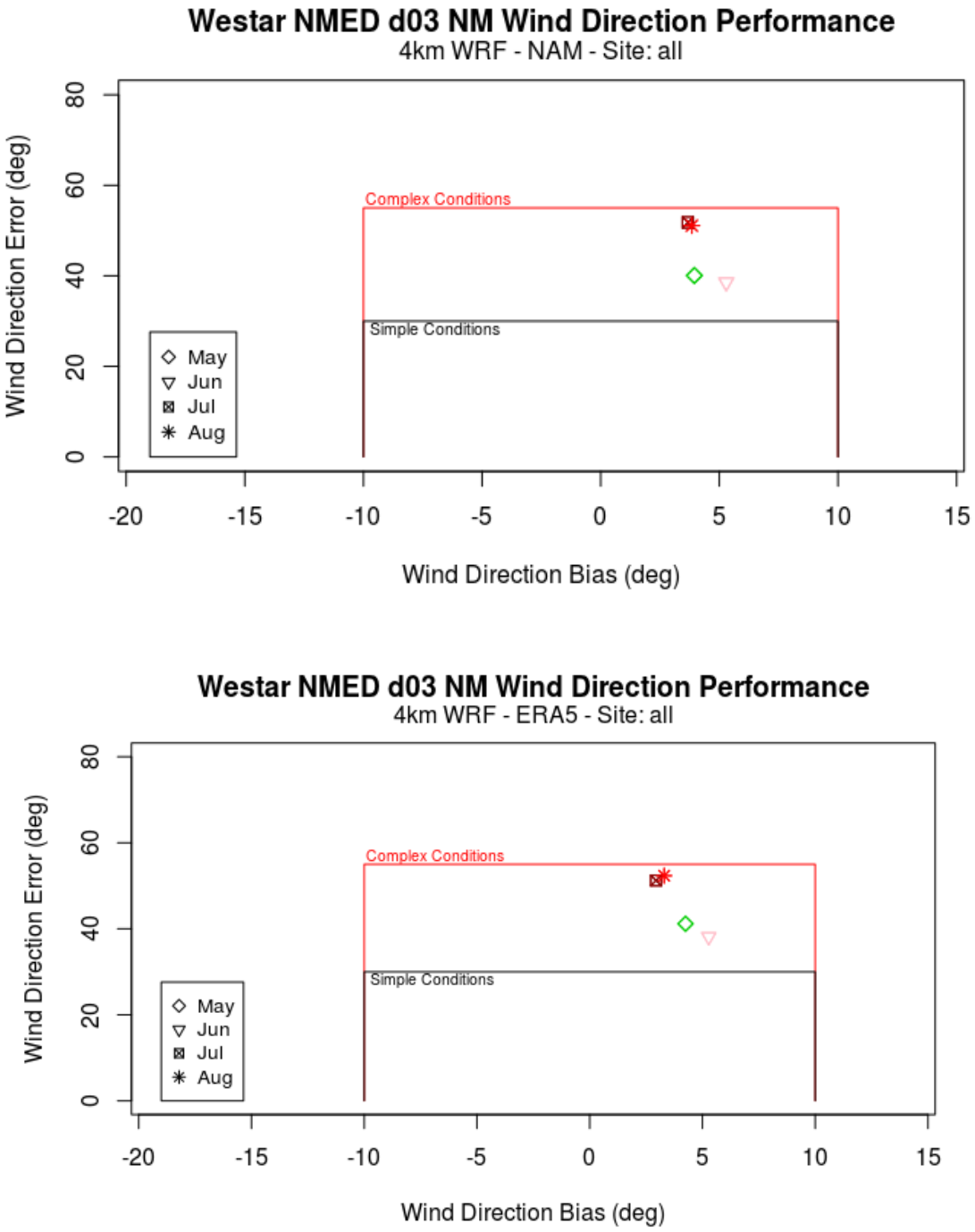

Figure 2-2. Soccer plot comparing WRF/NAM (top) and WRF/ERA5 (bottom) surface wind direction (degrees) model performance against the Simple and Complex Benchmarks for monthly RMSE (y-axis) and Mean Bias (x-axis).

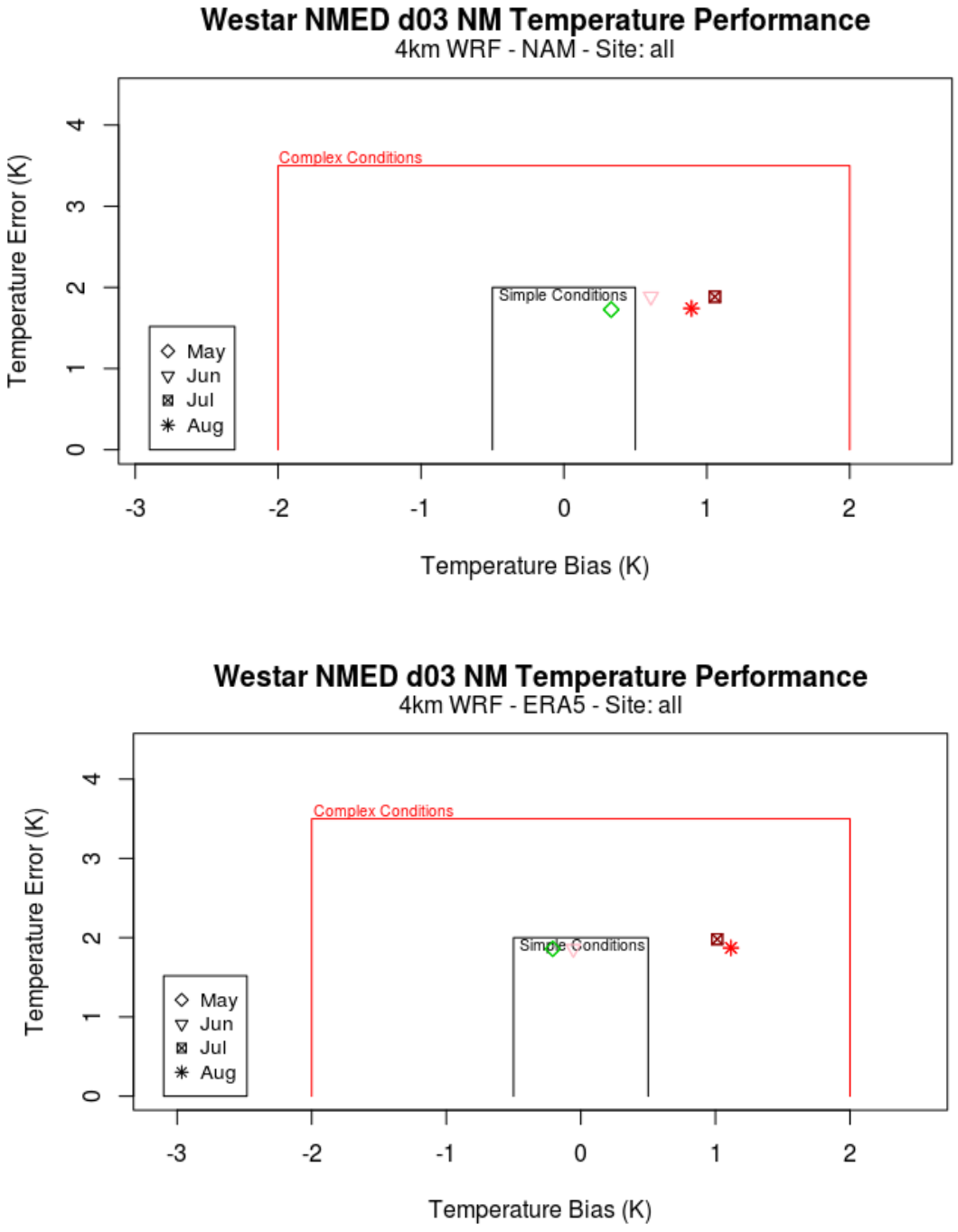

Figure 2-3. Soccer plot comparing WRF/NAM (top) and WRF/ERA5 (bottom) surface temperature (K) model performance against the Simple and Complex Benchmarks for monthly RMSE (y-axis) and Mean Bias (x-axis).

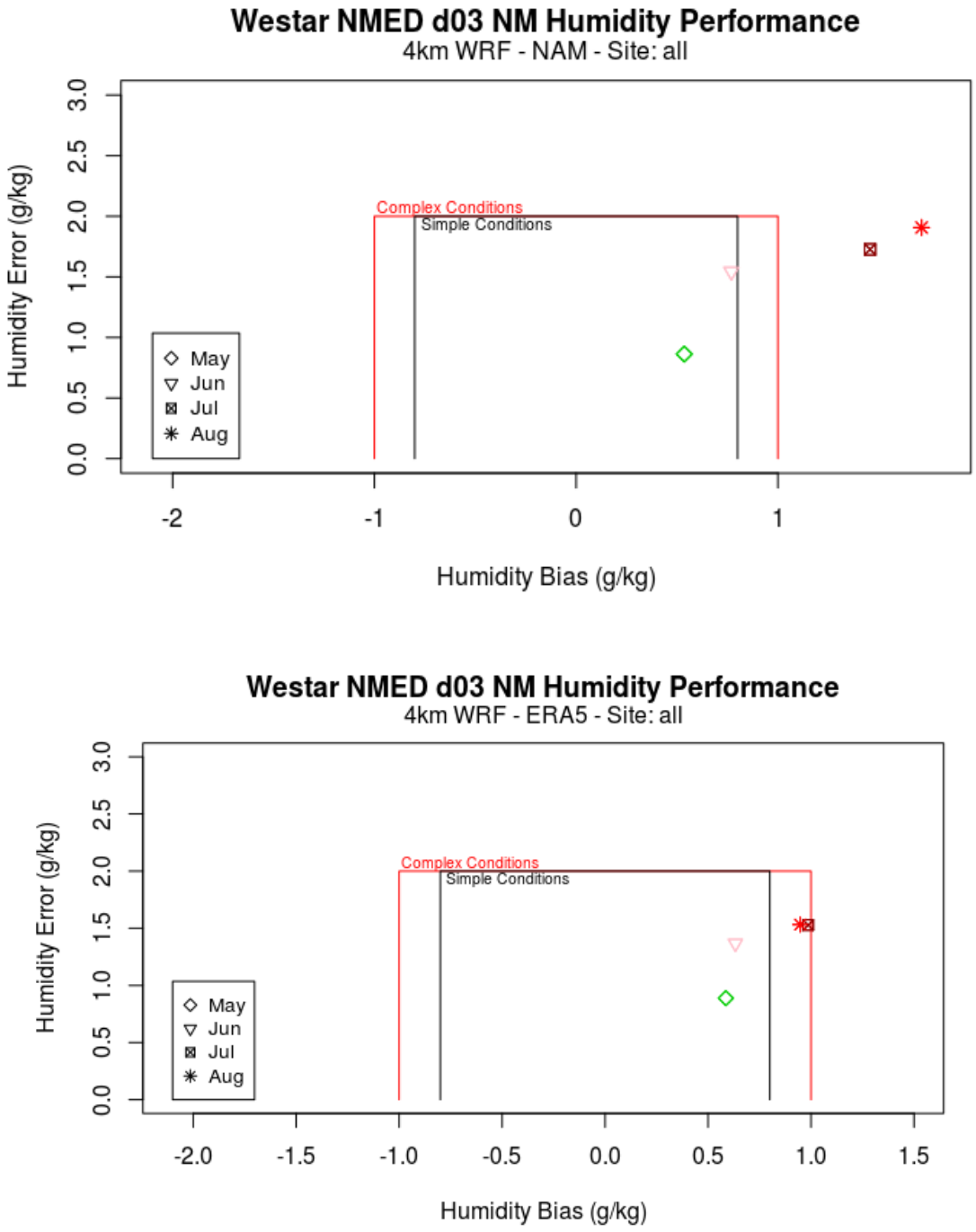

Figure 2-4. Soccer plot comparing WRF/NAM (top) and WRF/ERA5 (bottom) surface humidity (g/kg) model performance against the Simple and Complex Benchmarks for monthly RMSE (y-axis) and Mean Bias (x-axis).

2.4.2 Qualitative Evaluations for Precipitation Using PRISM Data

Oregon State University (OSU) publishes precipitation analysis fields based on observations that can be used to qualitatively evaluate the WRF precipitation fields. The Parameter-elevation Relationships on Independent Slopes Model (PRISM[18]) is used to generate the precipitation analysis fields (Daly et al., 2008). The PRISM interpolation method of observed precipitation reflects, as closely as possible, the current state of knowledge of spatial climate patterns in the United States. PRISM calculates a climate – elevation regression for each digital elevation model (DEM) grid cell, and stations entering the regression are assigned weights based primarily on the physiographic similarity of the station to the grid cell.

Figures 2-5 and 2-6 compares the PRISM monthly total precipitation across the 4-km New Mexico domain with the WRF/NAM and WRF/ERA5 model estimates for, respectively, July and August. Results for other months can be found in Ramboll and WESTAR (2020c). WRF/NAM overestimates the July monthly precipitation over northeast New Mexico, with WRF/ERA5 having an overestimation bias in most northerly Texas. But both WRF simulations have a dry bias for monthly precipitation over the remainder of New Mexico.

WRF/ERA5 does a better job at reproducing the locations and magnitudes of the August monthly PRISM precipitation than WRF/NAM (Figure 2-6). WRF/NAM overstates the August precipitation in central-south New Mexico.

[18] http://prism.oregonstate.edu/

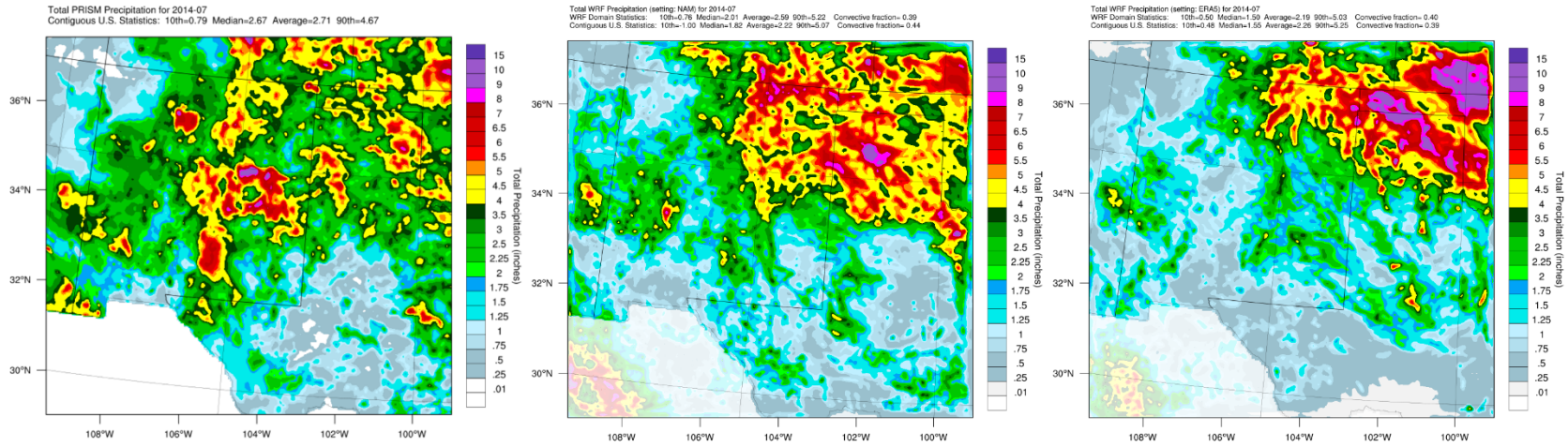

Figure 2-5. July monthly precipitation amounts from PRISM based on observations (left) and predicted by WRF/NAM (middle) and WRF/ERA5 (right).

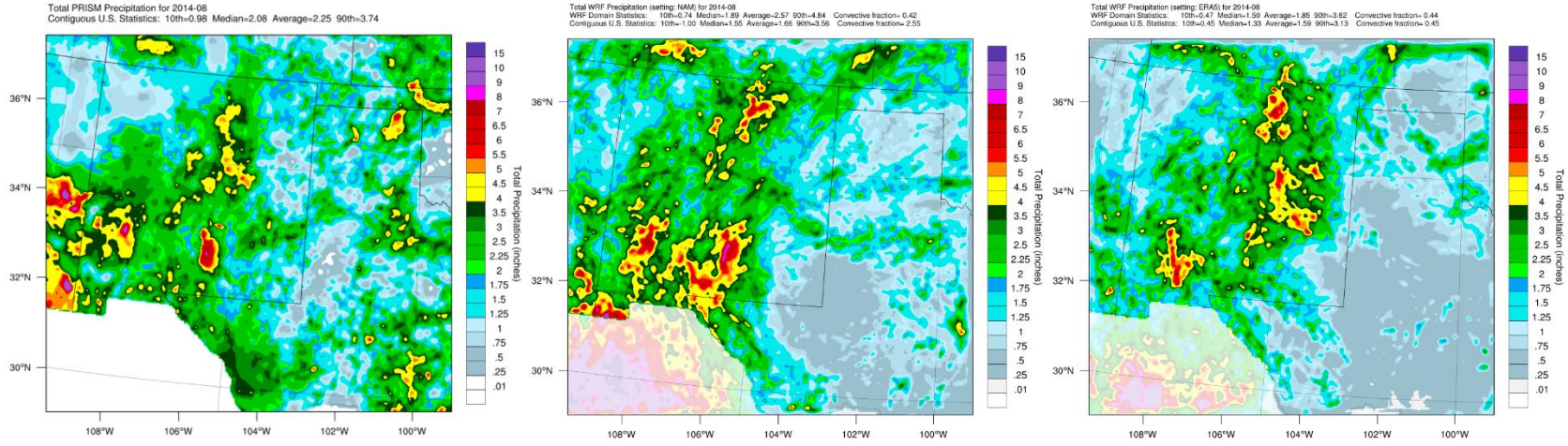

Figure 2-6. August monthly precipitation amounts from PRISM based on observations (left) and predicted by WRF/NAM (middle) and WRF/ERA5 (right).

2.4.3 Conclusions of 2014 WRF Model Performance

The model performance of the WRF/NAM and WRF/ERA5 simulations are reasonable and very similar for most meteorological variables (e.g., winds and temperature). This is in contrast to the WRAP-WAQS and EPA WRF 2014 simulations that had very different performance characteristics over New Mexico.[19] The biggest difference in the performance of the two WRF simulations was for humidity and precipitation. The WRF/NAM simulation had a moist bias for June-August that is likely partly associated with overactive convective precipitation that was greater in WRF/NAM than WRF/ERA5. It is unclear whether the WRF/NAM overstated precipitation is due to overactive convective events when they occur, or having events occur when they are not observed.

From the meteorological model performance evaluation, it is not possible to determine which set of WRF meteorological inputs will produce better ozone model performance when used as meteorological inputs for CAMx. There are variations in spatial and temporal model performance that are difficult to estimate what effects they will have on ozone concentrations. Furthermore, there may be meteorological inputs (e.g., level of mixing) that are more important for ozone modeling than the parameters we have observed data to evaluate the meteorological model for (i.e., winds, temperature, humidity and precipitation). Although it appears that WRF/NAM overstates the monthly precipitation if that does not occur on high ozone days it may not matter to the ozone model performance.

CAMx was run for a portion of the summer of 2014 episode with meteorological inputs based on both the WRF/NAM and WRF/ERA5 simulations and the ozone estimates compared to determine which meteorological inputs performed best so were selected for use in the final CAMX 2014 36/12/4-km base case simulation. The meteorological diagnostic sensitivity tests using the CAMx photochemical model are described in Chapter 5.

[19] https://www.wrapair2.org/pdf/NM_OAI_Study_Webinar1_2020-05-28.pdf

3. BOUNDARY CONDITION INPUTS

The Boundary Conditions (BCs) for the CAMx most outer 36-km 36US modeling domain lateral boundaries were based on output from a 2014 simulation of the GEOS-Chem global chemistry conducted by WRAP for their 2014v2 modeling platform.

3.1 WRAP 2014 GEOS-Chem Modeling

The WRAP-WAQS 2014v1 36/12-km CAMx and CMAQ base case simulations used BCs based on EPA's 2014 GEOS-Chem simulation that was used in EPA's 2014 modeling platform used in the 2014 National Air Toxics Assessment (NATA[20]). The CAMx and CMAQ 2014v1 base case simulation and sensitivity modeling found that the BCs based on EPA's 2014 GEOS-Chem caused year-long ozone overestimation bias throughout the western U.S.[21] Thus, WRAP conducted their own 2014 GEOS-Chem simulation using a newer version of the model and with updated emissions that resulted in much better CAMx ozone model performance without the systematic ozone over-prediction bias.[22] Table 3-1 presents the WRAP 2014 GEOS-Chem model configuration.

Table 3-1. 2014 GEOS-Chem simulation model configuration used by WRAP whose output is used to define the 2014 day-specific diurnally varying BC inputs for the NM OAI Study photochemical modeling.

Science Options	WRAP 2014 GEOS-Chem Base Case
Version	Version 12.2.0 (release date: 2019-02-19)
Vertical Grid Mesh	72 Layers
Chemistry mechanism	GEOS-Chem standard chemistry with complex SOA option[23].
Horizontal Grids	2x2.5 degree (Nx, Ny = 144, 91)
Initial Conditions	6-month spin-up; starting from provided initial conditions for standard chemistry
Meteorology	2014 GEOS-FP meteorology
Photolysis mechanism	Default (FAST-J)
Advection Scheme	Default (TPCORE)
Cloud convection scheme	On / Relaxed Arakawa-Schubert
Planetary Boundary Layer mixing	On / non-local scheme implemented by Lin and McElroy
Dry deposition scheme	Default (Wesely)
Chemistry Solver	Default (FLEXCHEM)
Parallelization	Open Multi-Processing (OMP)

[20] https://www.epa.gov/national-air-toxics-assessment
[21] http://views.cira.colostate.edu/iwdw/docs/waqs_2014v1_shakeout_study.aspx
[22] https://www.wrapair2.org/pdf/WRAP_Shake-Out_Phase-III_Update_RTOWG_2019-09-10v3a.pptx
[23] We recommend turning off semivolatile primary organic aerosol (POA) chemistry and isoprene SOA reactions via the volatility-based scheme (VBS) [Pye et al., 2010] to avoid risk of double-counting in the complex SOA chemistry scheme. For more information, see http://maraisresearchgroup.co.uk/Publications/GC-v11-02-SOA-options.pdf

3.2 2014 GEOS-Chem Model Evaluation

The results of the WRAP 2014 GEOS-Chem simulation and CAMx sensitivity modeling using the new BCs can be found on the WAQS-WRAP2014v2 model evaluation webpage[24]. Relevant for the NM OAI Study is the fact that this updated 2014 GEOS-Chem BCs do lead to better CAMx model performance for ozone concentrations and corrects a persistent year-long ozone overestimation bias that occurred using the previous 2014 GEOS-Chem simulation conducted by EPA and used in the EPA 2014 modeling platform. The NM OAI Study evaluated the use of the WRAP 2014 GEOS-Chem BCs for CAMx modeling at several sites in New Mexico and found good ozone performance that achieved ozone model performance goals.[25] Thus, the WAQS-WRAP 2014v2 BC inputs based on the WRAP 2014 GEOS-Chem simulation were used "as is" for the NM OAI Study.

[24] http://views.cira.colostate.edu/iwdw/docs/WRAP_WAQS_2014v2_MPE.aspx
[25] https://www.wrapair2.org/pdf/NM_OAI_Study_Webinar1_2020-05-28.pdf

4. 2014 AND 2028 EMISSION INPUTS

4.1 Summary of Emissions Used in 2014 and 2028 Modeling

The emissions inventories for the CAMx 2014 36/2/4-km base case modeling were based on the WRAP-WAQS 2014v2 emissions inventory. Within the 36-km 36US North American and 12-km 12WUS2 western U.S. domains, the WRAP-WAQS CAMx 2014v2 base case emission inputs were used without any changes.

For the 4-km New Mexico domain, the WRAP-WAQS 2014v2 emissions have been reviewed and updated as needed by the NMED. For on-road mobile sources, the 4-km domain emissions were based on MOVES2014 model, 2014 activity data and day-specific hourly gridded 2014 WRF 4-km meteorology run through SMOKE-MOVES.

For the NM OAI Study future year 2028 Base Case and 2028 New Mexico O&G Control Strategy, the emissions were based on the WRAP 2028OTBa2 emissions inventory with updated New Mexico O&G emissions and use of 2014 actual fires instead of the Representative Baseline fires. The 2028OTBa2 CAMx-ready emission inputs for the 36/12-km domains were used "as is", substituting the 2014v2 actual 20014 fires for the Representative Baseline fires. For the 4-km NM domain, the 2028OTBa2 emissions were processed using SMOKE, with the new 2028 New Mexico (NM) oil and gas (O&G) emissions substituted for the NM O&G emissions used in the 2028OTBa2 emissions scenario.

The NM OAI Study 2028 O&G Control Strategy scenario used the exact same emissions as the NM OAI Study 2028 Base Case, only the controlled 2028 O&G emissions were used in New Mexico. The 2028 NM O&G Control Strategy oil and gas emissions were provided by ERG under separate contract to NMED.

4.2 Development of CAMx 2014 Base Case Emission Inputs

The CAMx 2014 base case emission inputs for the 36/12-km domains were based on the WRAP 2014v2 CAMx model-ready emission inputs and were used "as is." For the 4-km NM domain, the New Mexico emissions from the 2014v2 database were reviewed and updated by the NMED. The 2014v2 emissions for New Mexico and portions of surrounding states within the 4-km New Mexico domain were then processed by the Sparse Matrix Operator Kernel Emissions (SMOKE) modeling system (UNC, 2015). SMOKE version 4.7 was used, which was released in October 2019.[26]

4.2.1 Day-Specific On-Road Mobile Source Emissions

The 2014 on-road mobile source emission inputs for the 4-km New Mexico domain were generated using the SMOKE-MOVES emissions model. SMOKE-MOVES used a 2014 mobile source emission factor (EF) lookup table generated by the Motor Vehicle Emission Simulator (MOVES2014[27]) model (EPA, 2014a,b,c). The SMOKE-MOVES default county-level 2014 vehicle activity data for New Mexico was reviewed by NMED and updated as needed. SMOKE-MOVES uses the 2014 MOVES EF lookup table, hourly gridded 4-km meteorological data from the 2014 WRF simulation conducted in this study (see Chapter 2) and 2014 county-level activity data (e.g., vehicle miles travelled

[26] https://www.cmascenter.org/smoke/
[27] https://www.epa.gov/moves/moves-onroad-technical-reports#moves2014

[VMT], speed, etc.) to generate 2014 day-specific hourly gridded on-road mobile source emission inputs for CAMx and the 4-km New Mexico domain.

4.2.2 Point Source Emissions

2014 point source emissions were based on the WRAP-WAQS 2014v2 emissions inventory. The 2014v2 New Mexico point source emissions were reviewed and updated by NMED. Point sources were processed in two streams: (1) major point sources with Continuous Emissions Monitoring (CEM) devices, which are primarily fossil-fueled Electrical Generating Units (EGU) with capacity of 25 MW or greater; and (2) point sources without CEMs. For point sources with CEM data, day-specific hourly NO_X and SO_2 emissions were used for the 2014 base case emissions scenario. The VOC, CO, and PM emissions for point sources with CEM data were based on the annual emissions data in the 2014v2 inventory temporally allocated to each hour of the year using the CEM hourly heat input.

4.2.3 Area and Non-Road Source Emissions

The 2014 area and non-road sources were spatially allocated to the 4-km New Mexico grid using an appropriate surrogate distribution (e.g., population for home heating, etc.). The area sources were temporally allocated by month and by hour of day using the SMOKE source-specific temporal allocation factors, while chemical speciation used the SMOKE source-specific CB6r4 speciation allocation profiles.

4.2.4 Episodic Biogenic Emissions

Two different CAMx 2014 base case simulations were conducted using two different biogenic emission inputs within the 4-km NM domain. The first CAMx 2014 base case 4-km domain biogenic emissions were generated using Version 3.1 of the MEGAN biogenic emissions model. MEGAN v3.1 is a new version of MEGAN and comes with a Leaf Area Index (LAI) database that defines the vegetative biomass and type that when combined with temperature and light dependent emission factors produces biogenic VOC emissions using the day-specific hourly gridded WRF meteorology. However, the new LAI data in MEGAN v3.1 were missing for urban areas producing "holes" in the biogenic VOC emission inputs. Thus, revised CAMx 2014v2 base case 4-km NM biogenic emission inputs used the BEIS v3.7 biogenic emissions model. BEIS3.7 is the most recent version of BEIS released by EPA in October 2020. BEIS3.7 uses updated biomass and emissions factors, and the Biogenic Emissions Landcover Database version 5 (BELD5). Table 4-1 compares the biogenic NO_x and VOC emissions by month (in tons/month) for the 4-km NM domain and the two biogenic models. The BEIS NO_x emissions are substantially lower than MEGAN, and VOC emissions are mostly lower except early summer month showing slightly higher emissions with BEIS. Figure 4-1 displays the spatial distributions of emissions in the 4-km NM domain expressed as episode average tons per day. The BEIS NO_x and VOC emissions are mostly lower than MEGAN throughout the domain. The missing biogenic VOC emissions in urban areas (e.g., El Paso/Juarez) using MEGAN v3.1 is also evident in the spatial maps.

Table 4-1. 2014 biogenic emissions (tons/month) in the 4-km NM domain estimated by MEGAN3.1 and BEIS3.7.

Tons/month		MEGAN	BEIS	% Diff (BEIS-MEGAN)
NO_x	May	35,050	10,602	-69.8%
	Jun	42,445	13,134	-69.1%
	Jul	51,639	12,838	-75.1%
	Aug	41,002	11,923	-70.9%
VOC	May	128,323	159,809	24.5%
	Jun	267,055	256,379	-4.0%
	Jul	317,697	251,562	-20.8%
	Aug	354,570	216,032	-39.1%

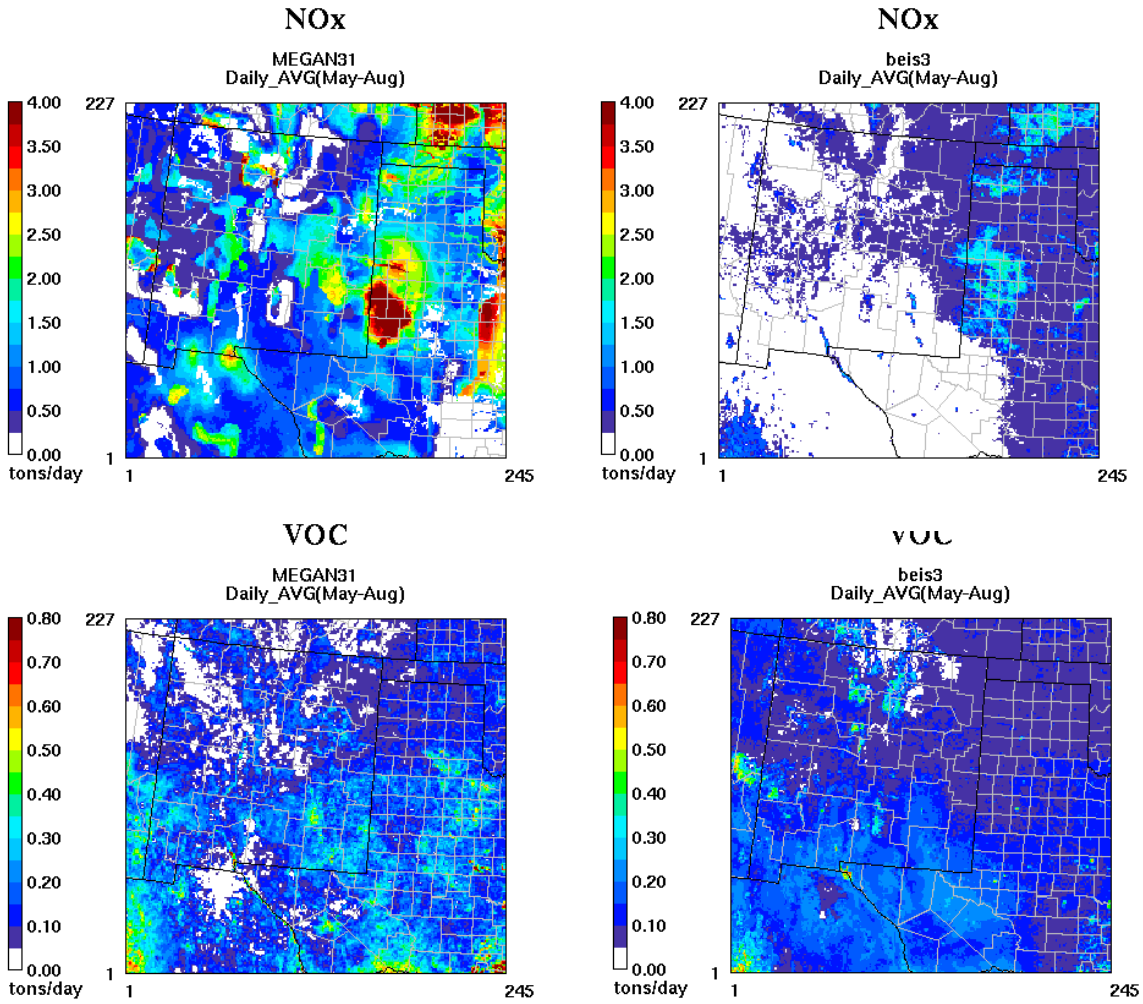

Figure 4-1. Spatial distribution of NO_x (top panel) and VOC (bottom panel) biogenic emissions (episode average tons per day) in the 4-km NM domain estimated by MEGAN3.1 (left) and BEIS3.7 (right).

4.2.5 Wildfires, Prescribed Burns, Agricultural Burns

2014 emissions from open-land burning including wildfires, wildland prescribed burns and agricultural burning were based on the WRAP-WAQS 2014v2 emissions inventory. The WRAP Fire and Smoke Work Group (FSWG[28]) processed the 2014NEIv2 Bluesky/SMARTFIRE fire emissions for the U.S. and classified them as either wildfires (WF), wildland prescribed burns (Rx) or agricultural burning (Ag) and made other updates for the 2014v2 inventory. The 2014NEIv2 fire emissions for Mexico and Canada were used without any changes. Table 4-2 displays NO_x and VOC emissions by month and fire type within the 4-km NM domain. Figure 4-2 displays spatial maps of NO_x emissions from 2014 summer fires for the 4-km NM domain. Emissions are expressed as episode average tons per day per grid cell. We see some hotspots on the wildfires plot in New Mexico and Arizona near the western boundary of the 4-km domain.

[28] https://www.wrapair2.org/FSWG.aspx

Table 4-2. 2014 fire emissions summary (tons/month) by fire type for the 4-km NM domain

Tons/month	Pollutant	Ag fires	Prescribed fires	Wildfires	Mexico fires
NO_x	May	36	90	597	49
	Jun	11	81	1,056	32
	Jul	18	13	332	8
	Aug	18	69	39	2
VOC	May	60	617	6,663	92
	Jun	18	736	17,641	187
	Jul	29	82	4,985	40
	Aug	28	1,376	371	13

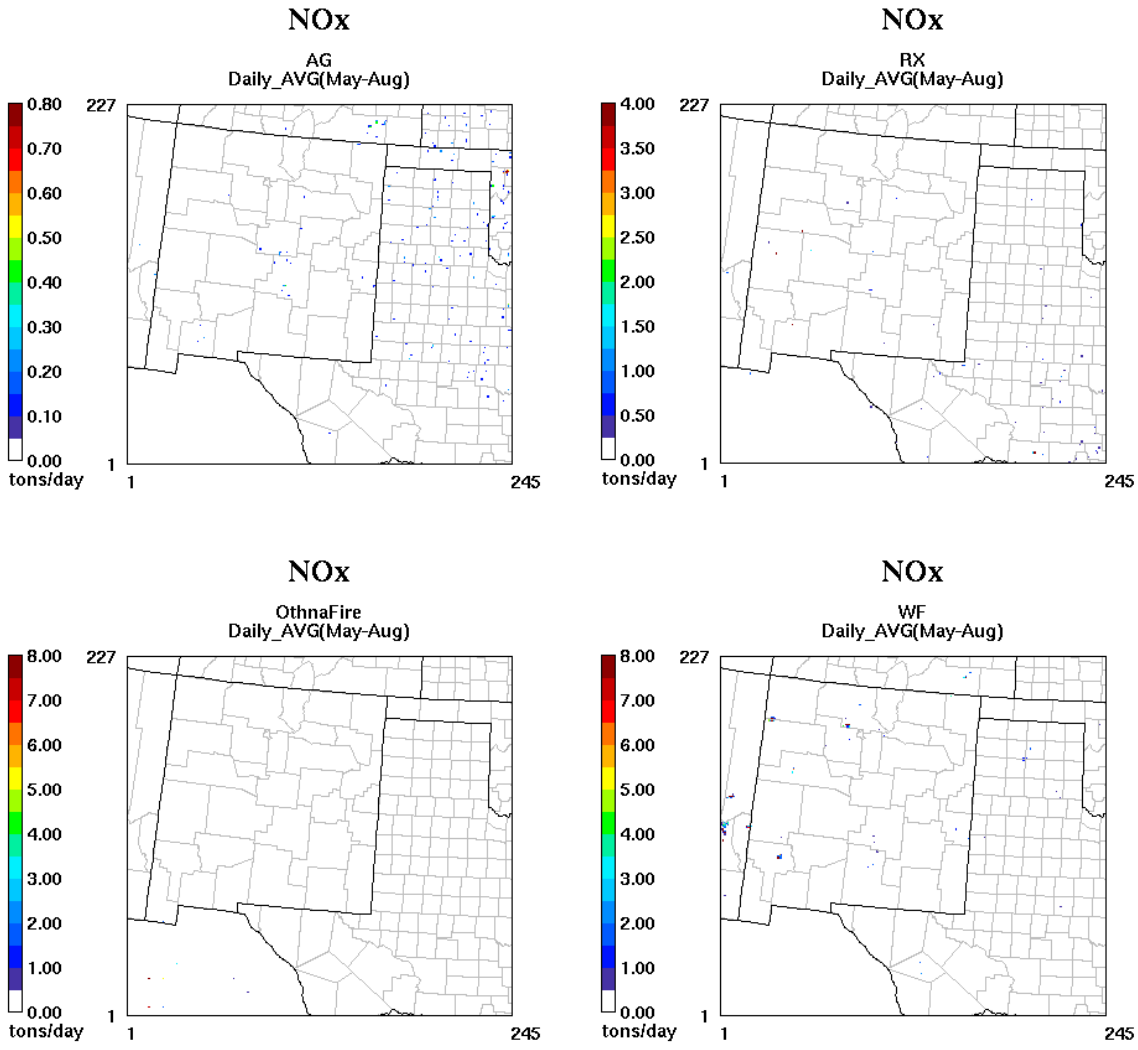

Figure 4-2. Spatial distribution of agricultural fires, prescribed fires, wildfires and Mexico fires (clockwise starting from top left) NO_x emissions (episode avg tons per day) for New Mexico 4-km domain.

4.2.6 Other Natural Emissions

Lightning NO_x (LNO_X), and windblown dust (WBD) emissions were generated for the 4-km domain using special CAMx processors and WRF 2014 meteorological data. Oceanic emissions such as sea salt spray aerosol (SSA) and dimethyl sulphide (DMS) were not generated for the 4-km New Mexico domain since this domain does not include any ocean within it. However, the LNO_X, WBD and oceanic emissions for the 36-km and 12km were based on the WRAP-WAQS 2014v2 emissions and were included in the modeling.

4.2.7 2014 Emission Results

Table 4-3 summarizes the 2014 criteria air pollutant emissions in episode average short tons per day by source category for the 4-km New Mexico domain. These data represent the model-ready emissions input to the CAMx air quality model for the 2014

base case. Mostly, emissions are summarized from the SMOKE reports generated by the SMKMRG program. There are a couple of exceptions to this general approach, fugitive dust and EGU sources. The fugitive dust emissions were adjusted after SMOKE processing to account for fugitive dust correction factors that are derived from the Biogenic Emission Landuse Database version 4 (BELD4). The correction factors are necessary to account for dust removal due to local vegetation scavenging so are not transported downwind. Model-ready emissions for EGU and Mexico point sources were obtained from WRAP/WAQS 2014 platform so were summarized for the 4-km domain outside of SMOKE.

Table 4-3. 2014 base case anthropogenic emissions summary (episode average short tons per day) by source category for the 4-km New Mexico domain.

Country/ Category	Source Category	CO	NH_3	NO_x	$PM_{2.5}$	PM_{10}	SO_2	VOC
US Anthro	Area fugitive dust	0.0	0.0	0.0	253.3	1,788.2	0.0	0.0
	Agricultural ammonia sources	0.0	764.7	0.0	0.0	0.0	0.0	43.4
	Non-point Oil and Gas for 7 WRAP States (CO, MT, NM, ND, SD, UT, WY)	237.7	0.0	157.8	4.4	4.4	11.3	567.3
	Remaining Non-point Oil and Gas	286.8	0.0	311.7	6.9	6.9	30.0	1,642.5
	Residential Wood Combustion	7.0	0.1	0.1	0.5	0.5	0.0	1.2
	Other nonpoint sources	141.3	1.5	28.5	9.3	13.4	4.5	213.2
	On-road mobile	1,476.2	6.0	444.5	13.2	20.1	1.7	150.6
	Locomotive	22.9	0.1	122.7	2.9	3.1	0.1	6.2
	Non-road mobile	570.3	0.2	133.4	9.0	9.4	0.3	73.2
	EGU point sources	89.2	3.4	210.6	12.9	17.8	160.0	5.0
	Point Oil and Gas for 7 WRAP States (CO, MT, NM, ND, SD, UT, WY)	89.9	0.0	114.7	1.4	1.4	23.8	56.1
	Remaining Point Oil and Gas	113.8	0.1	205.2	3.2	3.3	27.1	48.4
	Non-EGU point sources	74.4	4.9	47.5	11.4	32.5	49.3	24.4
Mexico Anthro	Mexico area	19.9	33.2	42.2	5.8	15.7	1.7	103.3
	Mexico on-road mobile	356.3	0.6	98.4	1.5	2.6	1.4	34.4
	Mexico point sources	28.4	0.7	20.2	4.8	5.7	16.4	8.3

Figure 4-3 presents pie charts showing VOCs and NO_x emissions from anthropogenic sources by source category for New Mexico and portion of surrounding states within the 4-km domain. Point and non-point oil and gas sectors account for majority of NO_x emissions followed by on-road mobile and EGU sources. In New Mexico, oil and gas sources are the largest anthropogenic VOC emitters and accounts for nearly 80% of 4-km domain VOC emissions.

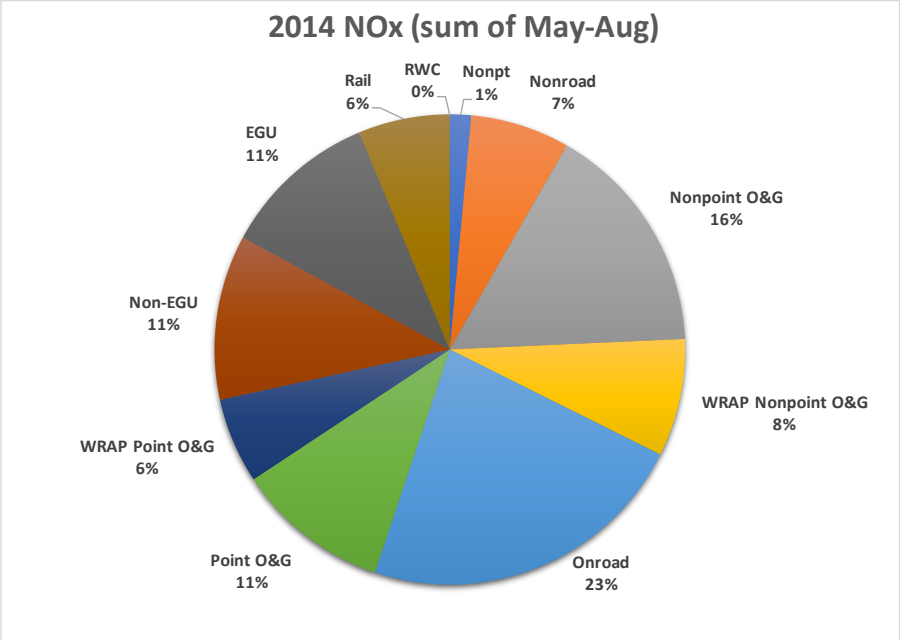

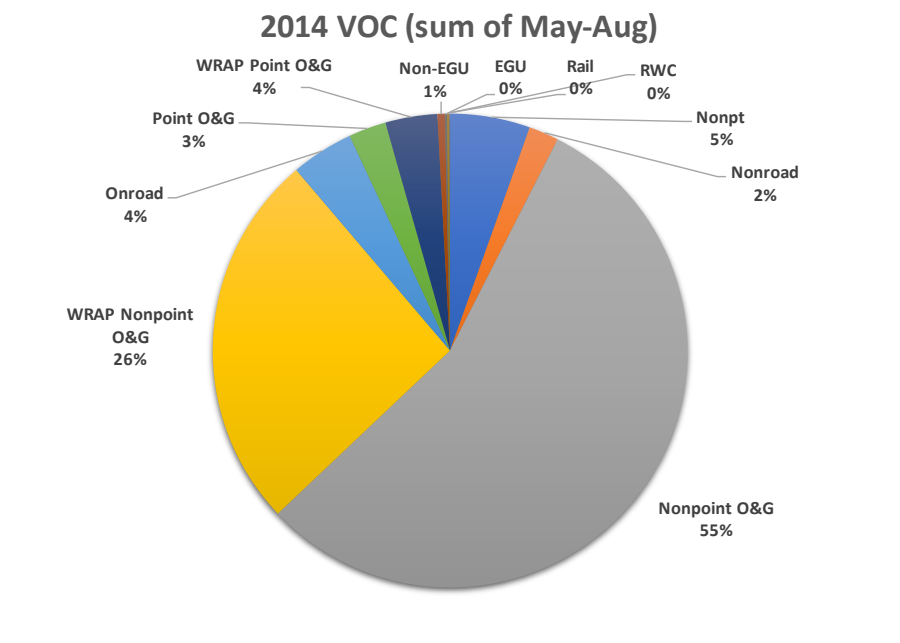

Figure 4-3. New Mexico 2014 base case anthropogenic NO_x and VOC emissions by source category.

Figure 4-4 displays spatial maps of NO_x and VOC anthropogenic emissions from the oil and gas sector across the 4-km New Mexico domain. Top panel shows emission maps for non-point O&G sources while bottom panel shows point O&G sources. The San Juan and Permian basins are clearly visible on the emissions map and confirm correct spatial allocation of oil and gas emissions. Figure 4-5 shows emission maps for on-road mobile (top panel), rail (middle panel) and non-point sources including non-road equipment (bottom panel).

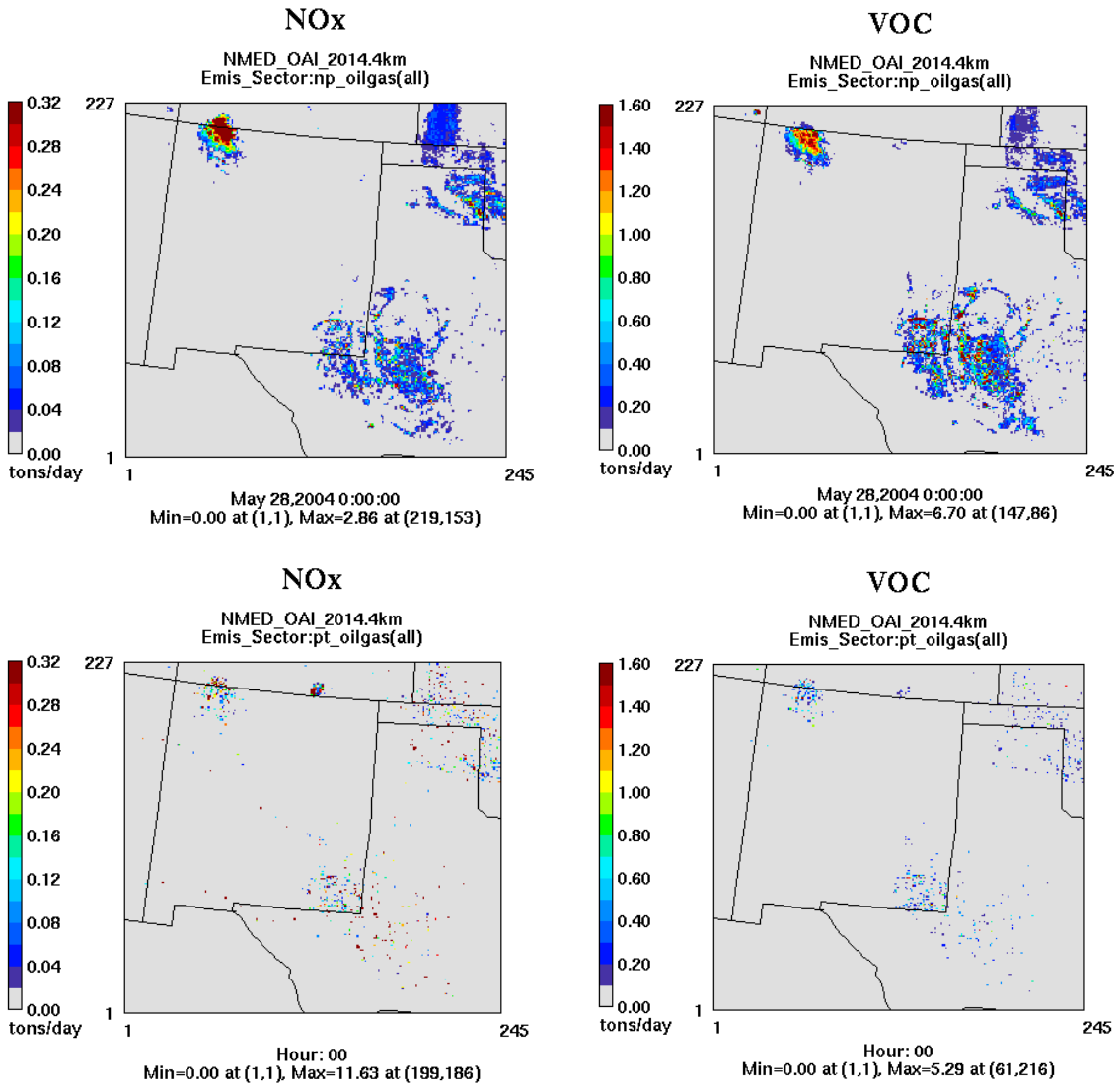

Figure 4-4. Spatial distribution of the non-point (top) and point (bottom) source oil and gas NO_x (left) and VOC (right) emissions (episode avg tons per day) for New Mexico 4-km domain.

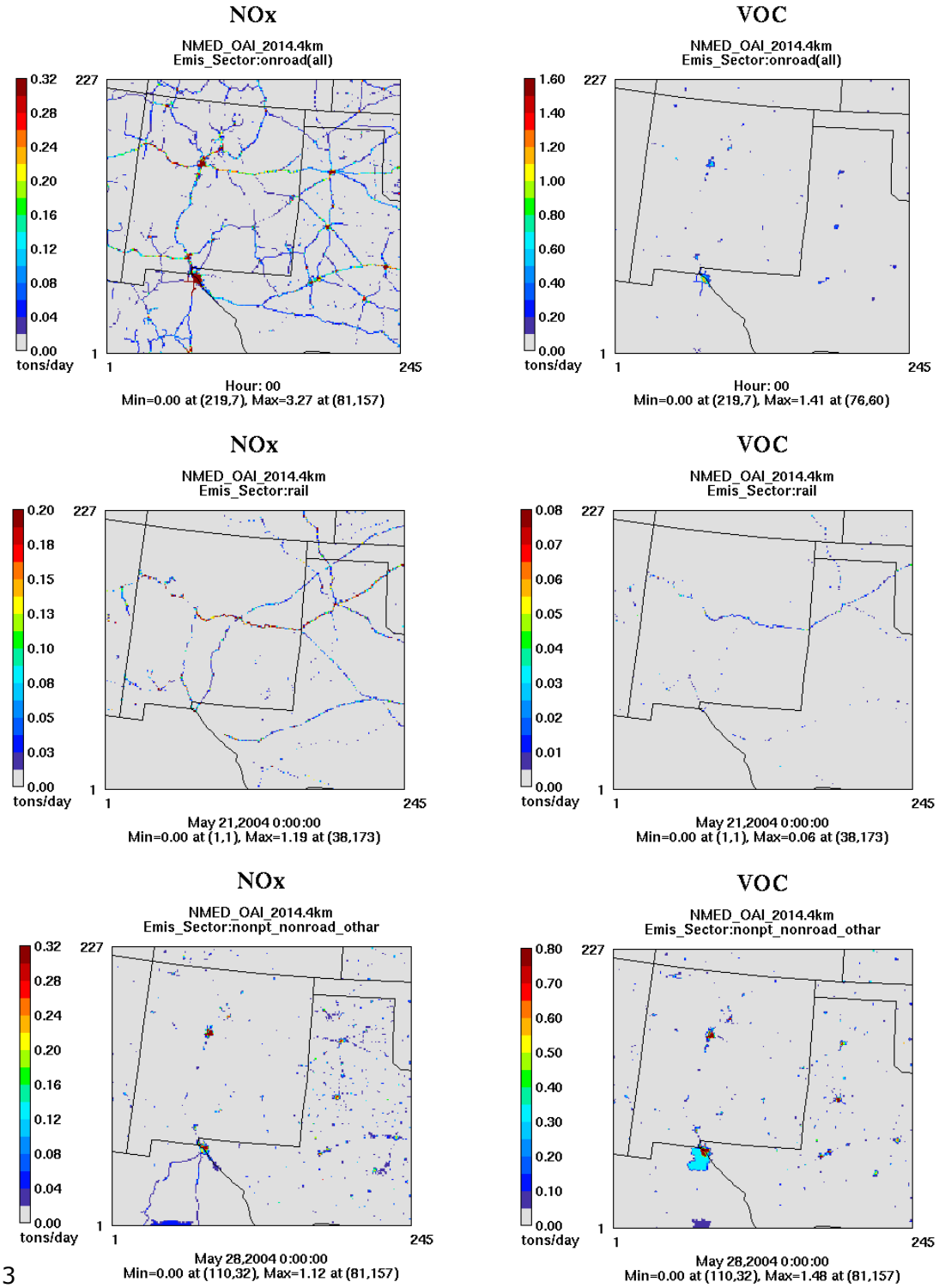

3

Figure 4-5. Spatial distribution of on-road (top), rail (middle) and non-point/non-road equipment (bottom) NO_x (left) and VOC (right) emissions (episode avg tons per day) for New Mexico 4-km domain.

4.3 Development of CAMx 2028 Emission Scenarios

The NM OAI Study 2028 base case and 2028 O&G Control Strategy emissions were based on the WRAP 2028OTBa2 emissions inventory with updates to NM O&G emissions and using 2014 actual fires. Details on the 2028OTBa2 emission assumptions are contained in the WRAP Representative Baseline (RepBase2) and 2028 On-the-Books (2028OTBa2) CAMx Simulation Run Specification Sheet.[29] The original WRAP 2028OTBa emissions scenario used EPA's 2028 emission projections from their 2016v1 modeling platform[30] for several source sectors (e.g., non-EGU Point Sources). However, some of EPA's 2028 emission projections were inconsistent with the WRAP 2014v2 emission updates for the western states and there were double counted sources in EPA's 2016v1 platform 2028 emission projections. Thus, WRAP elected to use more source sector emissions from the EPA 2016v1 and WRAP 2014v2 emissions inventories that were vetted by many states resulting in the following source sectors used in the 2028OTBa2 emissions inventory with deviations from the WRAP 2028OTBa2 from the NM OAI Study 2028 base case discussed below (see details in Run Specification Sheet cited in footnote):

- The California Air Resources Board provided 2028 emissions for California and all source sectors.
- 2028 emissions for Electrical Generating Units (EGU) for fossil-fueled EGUs in WRAP states were reviewed in detail by the individual states starting from the results of the WRAP EGU Analysis Project.[31] 2028 emissions for Non-fossil-fueled EGU in the WRAP region and all EGUs outside of the WRAP region were based on EPA's 2016v1 modeling platform 2028 projections.
- 2028 O&G emissions for New Mexico were based on new estimates developed in the NM OAI Study as described later in this chapter. 2028 O&G emissions for other non-New Mexico WRAP region O&G basins are based on the WRAP projections out to 2023 (Ramboll, 2020a). The EPA 2016v1 platform 2016 O&G emissions were used for non-WRAP states. The 2028OTBa2 O&G emissions were reviewed in detail by WRAP region states to eliminate duplications and update sources as needed.
- Non-EGU Point Source emissions for the WRAP states were reviewed in detail by the individual states starting from the WRAP 2014v2 emissions, while the EPA 2016v1 platform emissions for 2016 were used for non-WRAP states.
- The SMOKE-MOVES model with 2014 meteorology, 2028 vehicle activity and 2028 MOVES2014 Emissions Factor Look-Up tables were used to generate 2028 on-road mobile source emissions by either WRAP[32] for the 12-km domain or the NM OAI Study for the 4-km domain.
- 2028 Non-road emissions were based on 2028 estimates by WRAP in the Mobile Source Emissions Inventory Projection Project for the WRAP region and EPA's 2028 estimates for the non-WRAP states.

[29] https://views.cira.colostate.edu/docs/iwdw/platformdocs/WRAP_2014/EmissionsSpecifications_WRAP_RepBase2_and_2028OTBa2_RegionalHazeModelingScenarios_Sept30_2020.pdf

[30] https://www.epa.gov/air-emissions-modeling/2016v1-platform

[31] https://www.wrapair2.org/EGU.aspx

[32] WRAP Mobile Source Emissions Inventory Projections Project

- WRAP region 2014v2 and EPA 2016v1 emissions were used for the Non-Point source sector in the 2028OTBa2 emissions scenario.
- The NM OAI Study 2028 fires were based on the WRAP region 2014v2 actual fire estimates.
- Natural emissions (biogenic, lighting NO_x, windblown dust and oceanic) were the same as used in the WRAP 2014v2, RepBase2 and 2028OTBa2 emission scenarios

4.3.1 2028 Base Case New Mexico Oil and Gas Emissions

A circa 2028 forecast oil and gas (O&G) emission inventory was developed for New Mexico for use in the NM OAI Study 2028 Base Case emission scenario. The basis of the forecast O&G emission inventory is circa 2028 O&G activity estimates provided by BLM[33] and emissions and emission per unit of O&G activity from the future year WRAP Oil and Gas Working Group (OGWG) emission inventory (Ramboll, 2020a). The WRAP OGWG developed 2023 future year O&G emissions for 7 of the WRAP states.

The 2028 New Mexico O&G emission inventory includes wellsite, gathering, and processing subsectors, which are items 1, 5, and 6 in Figure 4-6. Item 1 are On-Shore Petroleum and Natural Gas Production is referred to as "wellsite" sources; emissions from wellsite sources are classified as nonpoint sources. Item 2 are Gathering and Boosting sources. Item 6 consists of Gas Processing Plants are collectively referred to as "midstream" sources; emissions from midstream sources are classified as point sources. The classification of well-site emissions as nonpoint and midstream emissions as point sources is consistent with other O&G emission inventory classifications used in prior studies, such as the BLM Colorado Air Resource Management Modeling Study (CARMMS)[34].

[33] Email communication from BLM Staff (Forrest Cook) to Ramboll (John Grant). September 15, 2020.
[34] https://www.blm.gov/programs/natural-resources/soil-air-water/air/colorado

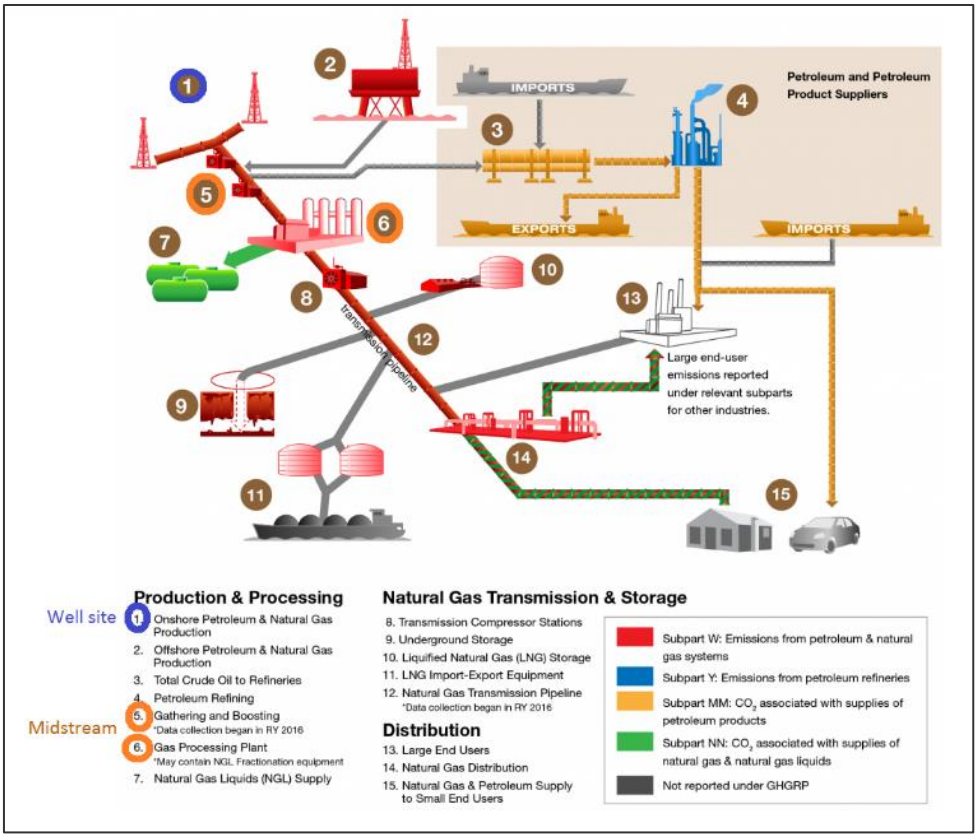

Figure 4-6. Example Petroleum and Natural Gas Industry schematic[35].

The BLM O&G forecast factors were used to project New Mexico O&G emissions to 2028. Table 4-4 compares the New Mexico O&G VOC and NO_x activity for the WRAP 2014 and 2023 scenarios with the NM OAI Study 2028 base case activity based on BLM forecasts. With the exception of spud count, the 2028 NM O&G activity is greater than 2014.

A comparison of the WRAP OGWG 2014 and 2023 New Mexico O&G emissions with the 2028 values from the NM OAI Study are given in Table 4-5. Across New Mexico, 2028 O&G NO_x and VOC emissions are, respectively, 29% and 15% higher than in 2014. In the Permian Basin, New Mexico 2028 O&G NO_x emissions are 64% higher than 2014, with VOC emissions 19% higher. The 2028 and 2014 New Mexico O&G emissions in the San Juan Basin are more comparable, with 2028 NO_x and VOC emissions, respectively, 1% and 10% higher than 2014.

[35] Source: https://www.epa.gov/ghgreporting/ghgrp-and-oil-and-gas-industry, accessed in April 2020.

Table 4-4. Comparison of WRAP OGWG 2014 and 2023 New Mexico O&G emissions used in the 2014v2 and 2028OTBa2 scenarios with the NM OAI study 2028 base case New Mexico O&G emissions based on BLM forecast.

Activity Metric	WRAP OGWG		BLM Forecast
	2014	2023	Circa- 2028
Permian Basin (NM)			
Oil Production (million bbl)	119	276	166
Gas Production (BCF)	508	1,190	790
Well Count	28,615	27,335	40,478
Spud Count	1,178	651	794
San Juan Basin (NM)			
Oil Production (million bbl)	6	7	7
Gas Production (BCF)	713	440	1,138
Well Count	21,687	19,604	23,073
Spud Count	146	64	94
Las Vegas-Raton Basin (NM)			
Oil Production (million bbl)	0	0	0
Gas Production (BCF)	24	24	20
Well Count	835	835	835
Spud Count	0	0	0
Sierra Grande Uplift (NM)			
Oil Production (million bbl)	0	0	0
Gas Production (BCF)	0.02	0.02	0.27
Well Count	1	1	8
Spud Count	34	34	0.4

Table 4-5. Comparison of WRAP OGWG 2014 and 2023 NO_x and VOC New Mexico O&G emissions with the NM OAI Study 2028 base case.

Pollutant	WRAP OGWG		NMED OAI EI
	2014	2023	2028
New Mexico State Total			
NOx	81,188	93,719	104,955
VOC	185,269	226,032	213,073
Permian , NM			
NOx	35,251	52,074	57,922
VOC	97,977	149,609	116,896
San Juan , NM			
NOx	44,730	39,789	45,200
VOC	86,567	75,670	95,500
Estancia Basin , NM			
NOx	113	645	645
VOC	5	26	26
Orogrande Basin , NM			
NOx	541	548	548
VOC	28	30	29
Raton , NM			
NOx	8	8	6
VOC	646	646	600
Pedregosa Basin , NM			
NOx	262	373	373
VOC	6	9	9
Basin-And-Range Province , NM			
NOx	261	261	261
VOC	10	11	11
Sierra Grande Uplift , NM			
NOx	23	23	0
VOC	31	31	2

4.4 Summary of 2014 and 2028 Base Case Emissions

Tables 4-6 through 4-8 summarizes the total emissions in New Mexico for the 2014 and 2028 base case emission scenarios and their differences. Graphical comparisons of the changes in NO_x and VOC emissions between 2014 and 2028 base cases are shown in, respectively, Figures 4-7 and 4-8. And the distribution of NO_x and VOC emissions across source sectors are shown in Figures 4-9 and 4-10, respectively. Total NO_x emissions in New Mexico are estimated to be reduced by -28% between 2014 and 2028 with the largest reductions coming from on-road mobile (-72%), EGU point (-69%) and non-road mobile (-51%) source sectors (Table 4-6 and Figure 4-7). These NO_x emission reductions were offset somewhat by increases in O&G point (+40%) and non-point (+36%) source sectors. Although there are large reductions in on-road (-61%) and non-road (-49%) mobile source VOC emissions between 2014 and 2028 base cases, the total reduction in New Mexico VOC emissions between 2014 and 2028 is only -6% because non-point O&G dominates (~75%; Figure 4-10) anthropogenic VOC emissions in New Mexico and they are only reduced by -5%.

Table 4-6. Summary of total emissions (tons/year) in New Mexico for the 2014 base case emissions scenario.

Category	CO	NH_3	NO_X	$PM_{2.5}$	PMC	SO_2	VOC
Fugitive Dust	0	0	0	31,152	188,801	0	0
Agricultural	0	28,774	0	0	0	0	2,825
Non-Point	23,039	262	5,934	1,561	794	937	28,621
Non-Road	77,821	13	7,334	548	40	18	9,397
O&G Non-Point	76,949	0	45,476	1,362	0	4,129	321,608
On-Road	246,144	939	75,861	2,194	1,042	252	26,275
O&G Point	23,458	0	31,125	436	0	8,623	40,744
EGU Point	11,309	422	43,071	1,507	650	11,911	429
Non-EGU Point	5,479	54	3,829	592	1,577	308	2,043
Rail	3,527	11	20,114	490	52	12	1,033
RWC	1,375	10	23	93	0	4	214
Total	469,102	30,485	232,766	39,935	192,956	26,194	433,188

Table 4-7. Summary of total emissions (tons/year) in New Mexico for the 2028 base case emissions scenario.

Category	CO	NH_3	NO_X	$PM_{2.5}$	PMC	SO_2	VOC
Fugitive Dust	0	0	0	31,152	188,801	0	0
Agricultural	0	28,774	0	0	0	0	2,825
Non-Point	23,039	262	5,934	1,561	794	937	28,621
Non-Road	69,460	15	3,618	244	24	11	4,767
O&G Non-Point	106,267	0	61,987	1,989	0	21,789	304,635
On-Road	111,251	821	21,610	688	1,178	143	10,311
O&G Point	37,205	0	43,480	706	55	11,912	53,212
EGU Point	7,173	301	13,389	1,292	755	3,385	256
Non-EGU Point	5,479	54	4,126	592	1,577	639	2,043
Rail	3,845	12	14,493	300	11	14	603
RWC	1,375	10	23	93	0	4	214
Total	365,093	30,248	168,661	38,617	193,195	38,834	407,488

Table 4-8. Percent differences in total New Mexico emissions between the 2014 and 2028 emission scenarios.

Category	CO	NH_3	NO_X	$PM_{2.5}$	PMC	SO_2	VOC
Fugitive Dust				0%	0%		
Agricultural		0%					0%
Non-Point	0%	0%	0%	0%	0%	0%	0%
Non-Road	-11%	17%	-51%	-56%	-41%	-37%	-49%
O&G Non-Point	38%		36%	46%	-98%	428%	-5%
On-Road	-55%	-13%	-72%	-69%	13%	-43%	-61%
O&G Point	59%		40%	62%		38%	31%
EGU Point	-37%	-29%	-69%	-14%	16%	-72%	-40%
Non-EGU Point	0%	0%	8%	0%	0%	107%	0%
Rail	9%	9%	-28%	-39%	-78%	9%	-42%
RWC	0%	0%	0%	0%	0%	0%	0%
Total	-22%	-1%	-28%	-3%	0%	48%	-6%

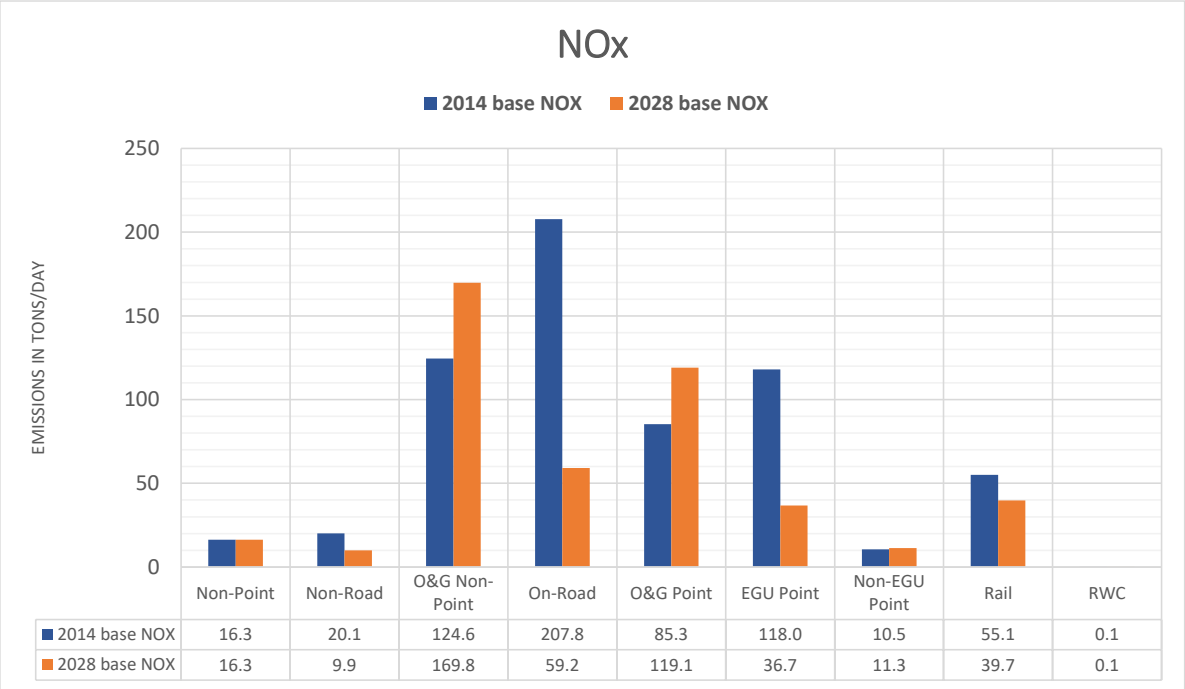

Figure 4-7. Comparison of 2014 and 2028 New Mexico NO_X emissions by source sector.

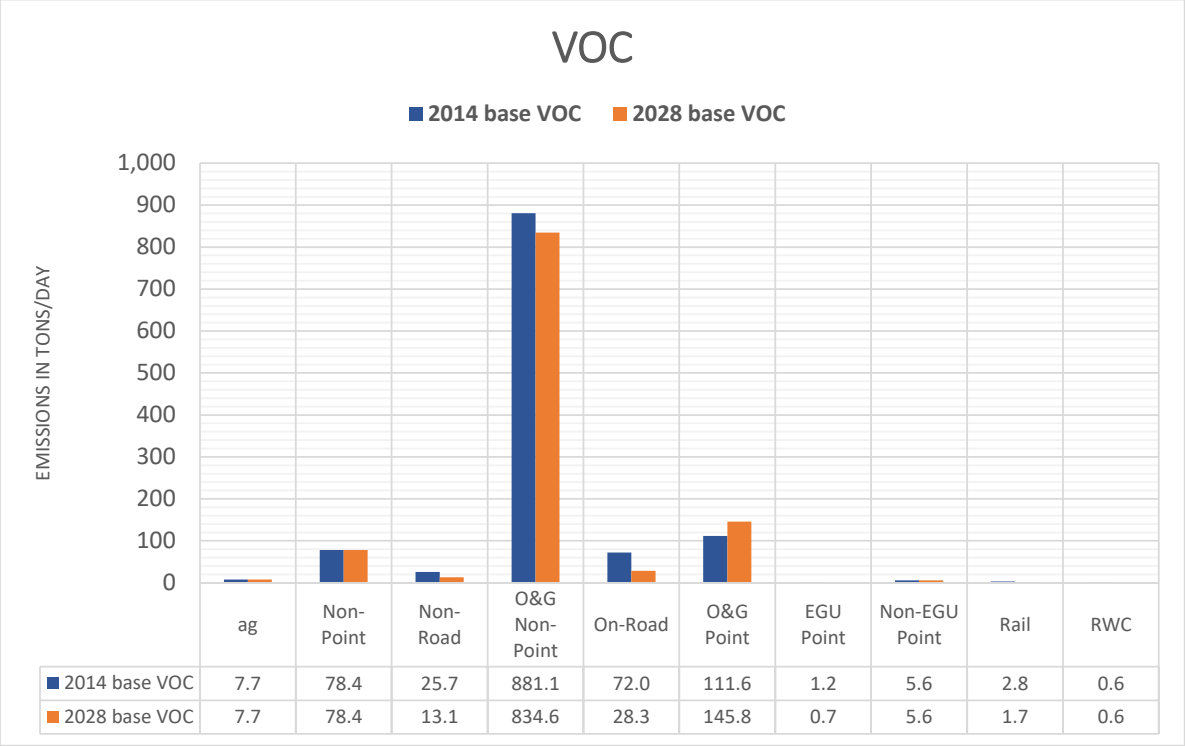

Figure 4-8. Comparison of 2014 and 2028 New Mexico NO_X emissions by source sector.

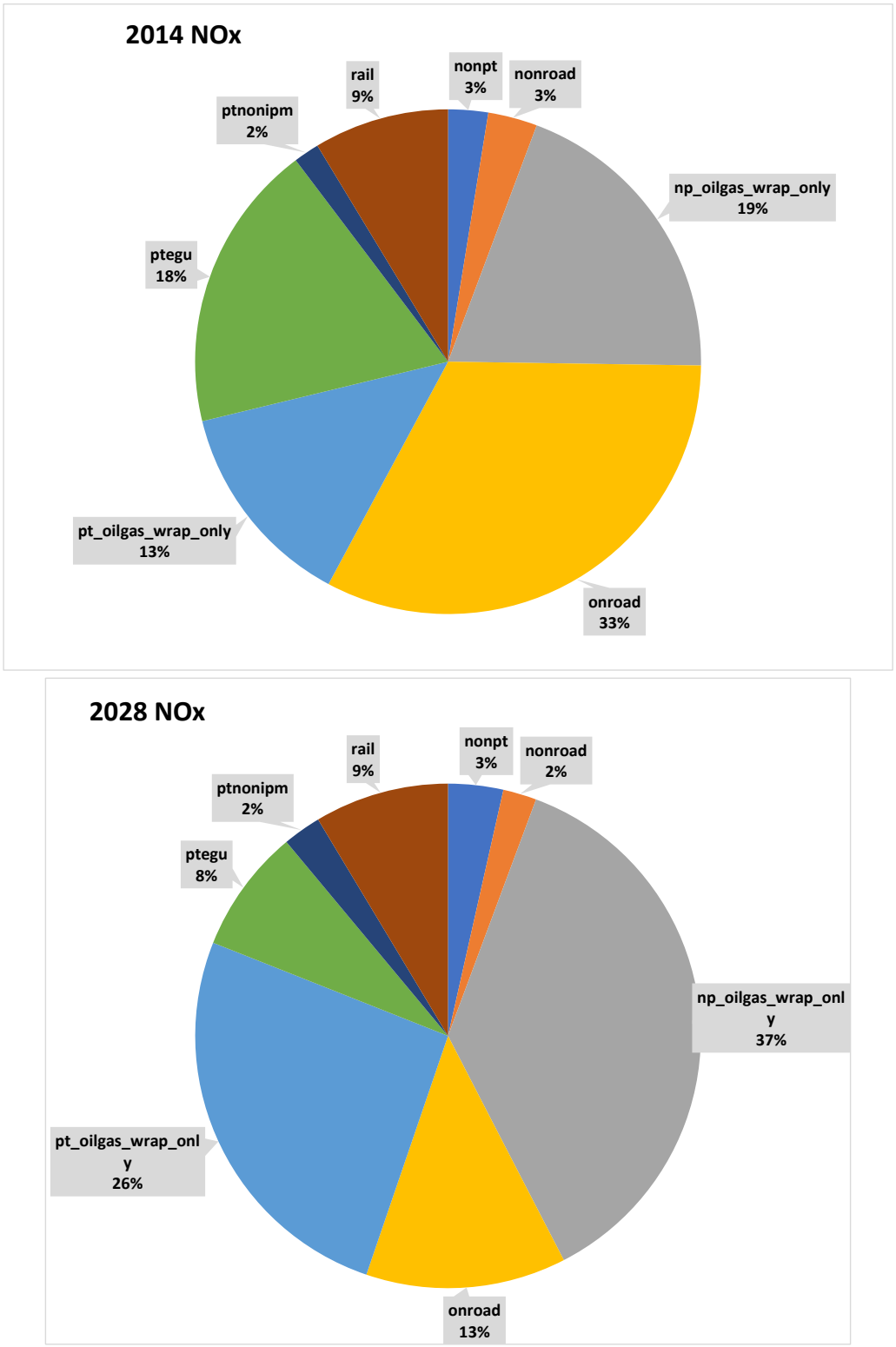

Figure 4-9. Distribution of New Mexico NO_x emissions across source sectors for the 2014 (top) and 2028 (bottom) base cases.

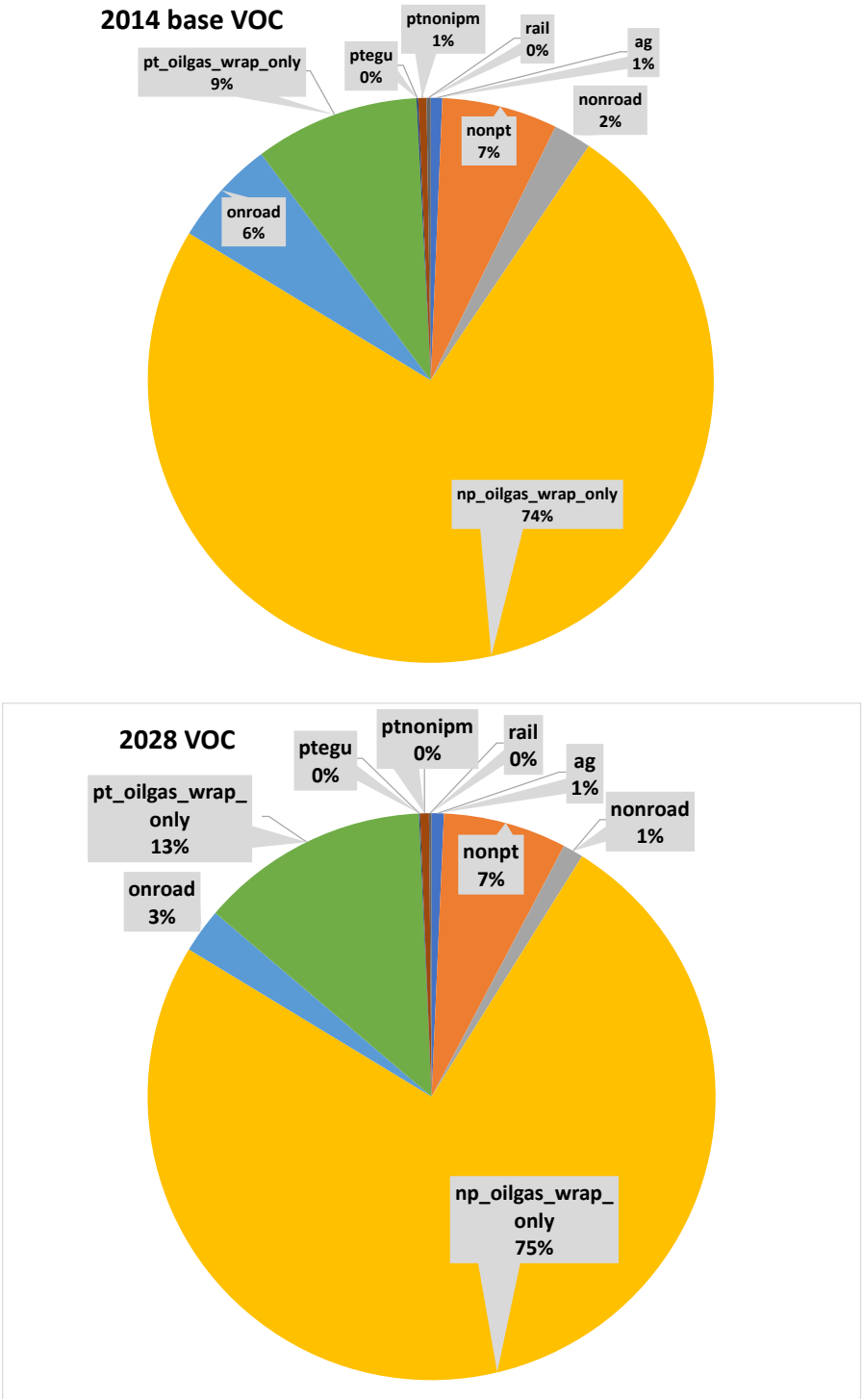

Figure 4-10. Distribution of New Mexico VOC emissions across source sectors for the 2014 (top) and 2028 (bottom) base cases.

4.5 2028 New Mexico Oil and Gas Control Strategy

The WESTAR/Ramboll Team provided the New Mexico 2028 O&G base case emissions to the NMED. The Eastern Research Group (ERG) under separate contract with NMED implemented the emission controls in the 2028 NM O&G emissions based on their interpretation of the proposed New Mexico "Ozone Precursor Rule for Oil and Natural Gas Sector."[36] The 2028 O&G Control Strategy reduced O&G emissions in 7 counties in New Mexico.

The 2028 NM O&G controlled emissions were processed by SMOKE and substituted for the 2028 NM O&G Base Case emissions to create the 2028 O&G Control Strategy emissions scenario. The only difference between the NM OAI Study 2028 Base Case and 2028 O&G Control Strategy were the controls on O&G emissions in New Mexico as implemented by ERG.

Table 4-9 displays the New Mexico state-wide O&G emissions for the 2028 Base Case and 2028 O&G Control Strategy. State-wide O&G NO_x emissions are reduced approximately -45% with similar reductions from both the Point and Non-Point source sectors. State-wide O&G VOC emission reductions are reduced approximately -50% with more reductions coming from the Non-Point (-53%) than Point (-35%) source sectors.

Table 4-9. New Mexico NO_x and VOC O&G emissions (tons per year) for the 2028 Base Case and 2028 NM O&G control strategy.

Source Sector	NO_x Emissions (TPY)			VOC Emissions (TPY)		
	Base	Control	Diff	Base	Control	Diff
Non-Point	61,245	33,144	-46%	181,252	85,564	-53%
Point	41,066	22,872	-44%	30,340	19,608	-35%
Total	102,311	56,016	-45%	211,592	105,172	-50%

Figures 4-11 and 4-12 display the changes in, respectively, NO_x and VOC emissions in the Permian and San Juan Basins between the 2028 base and 2028 control cases. In the Permian Basin, O&G NO_x emissions are estimated to be reduced by approximately 21,000 TPY (64%). In the San Juan Basin, O&G NO_x emissions are estimated to be reduced by approximately 25,000 TPY (44%). 2028 VOC O&G emissions in the Permian and San Juan Basins are estimated to be reduced by approximately 53,000 TPY each (-46% and -55% reduction, respectively).

Figure 4-13 shows the spatial distribution of the differences Non-Point and Point O&G NO_x and VOC emissions between the 2028 Base Case and 2028 O&G Control Strategy scenario. The O&G emission reductions are restricted to the New Mexico portions of the San Juan and Permian Basins.

[36] https://www.env.nm.gov/new-mexico-methane-strategy/wp-content/uploads/sites/15/2020/07/Draft-Ozone-Precursor-Rule-for-Oil-and-Natural-Gas-Sector-Version-Date-7.20.20.pdf

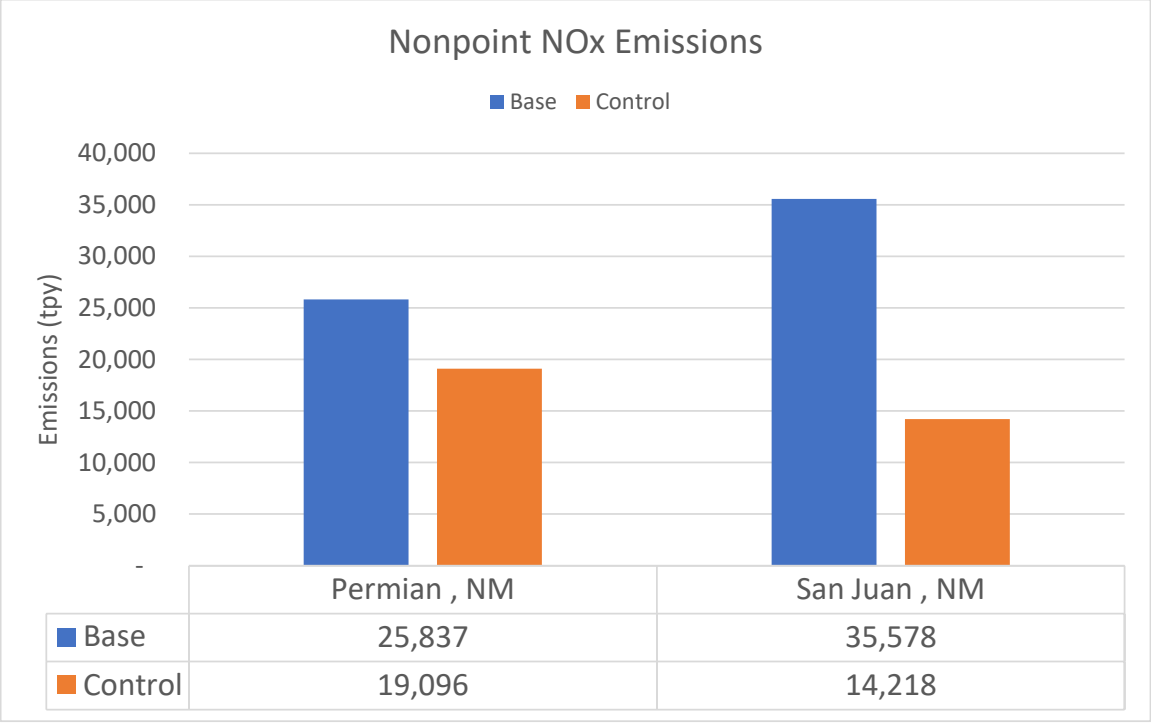

	Permian , NM	San Juan , NM
Base	25,837	35,578
Control	19,096	14,218

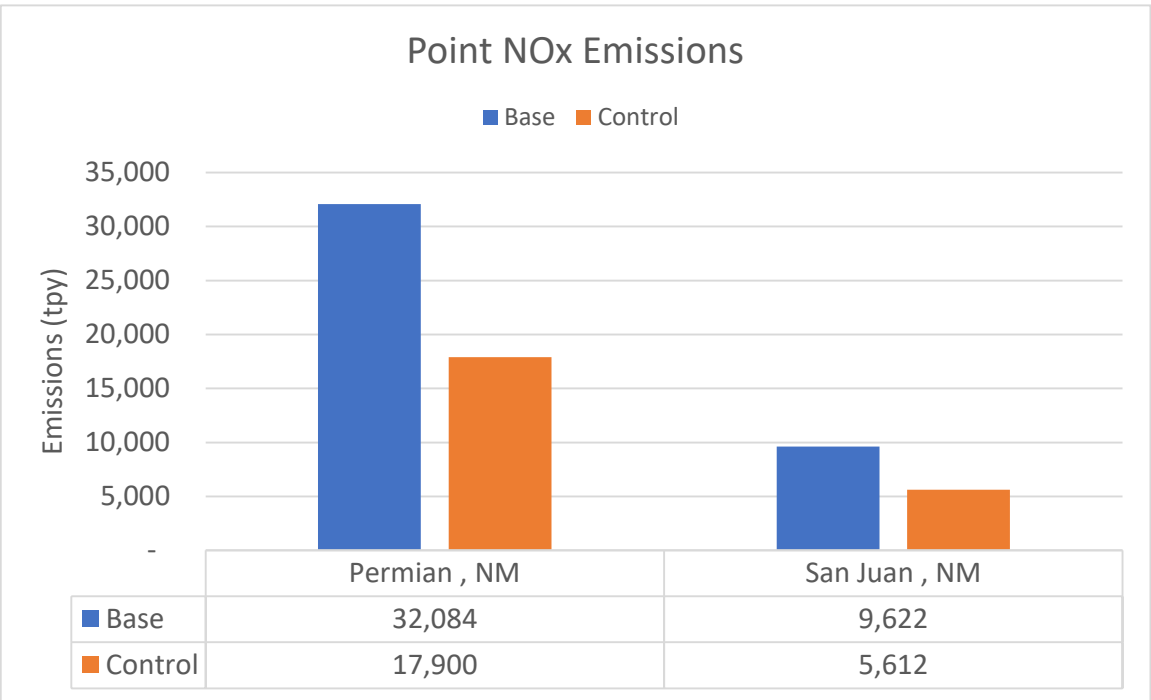

	Permian , NM	San Juan , NM
Base	32,084	9,622
Control	17,900	5,612

Figure 4-11. Comparison of 2028 Base Case and 2028 NM O&G control strategy NO_x emissions for the Non-Point (top) and Point (bottom) source sectors and the Permian (left) and San Juan (right) basins.

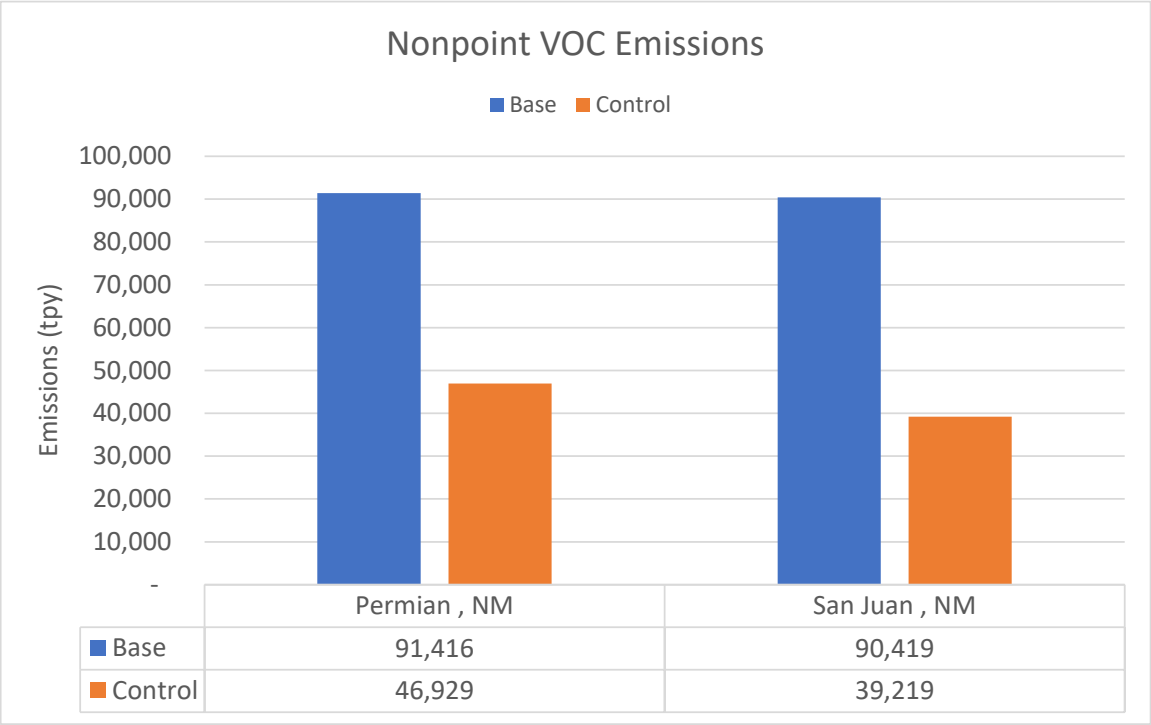

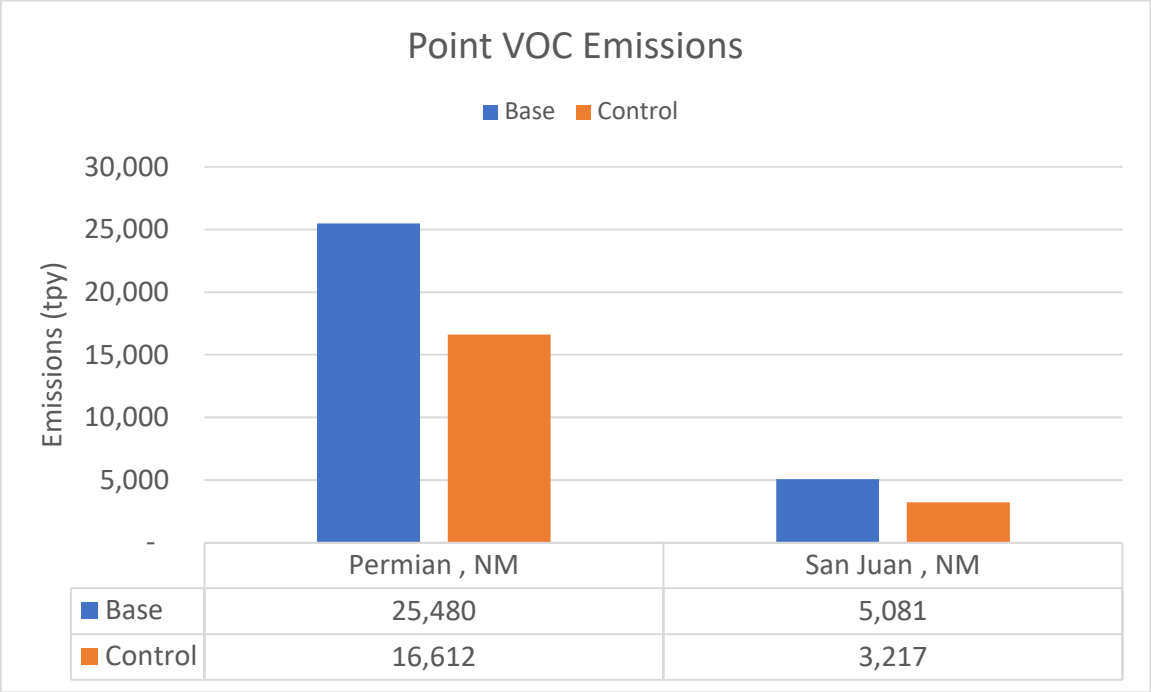

Figure 4-12. Comparison of 2028 Base Case and 2028 NM O&G control strategy VOC emissions for the Non-Point (top) and Point (bottom) source sectors and the Permian (left) and San Juan (right) basins.

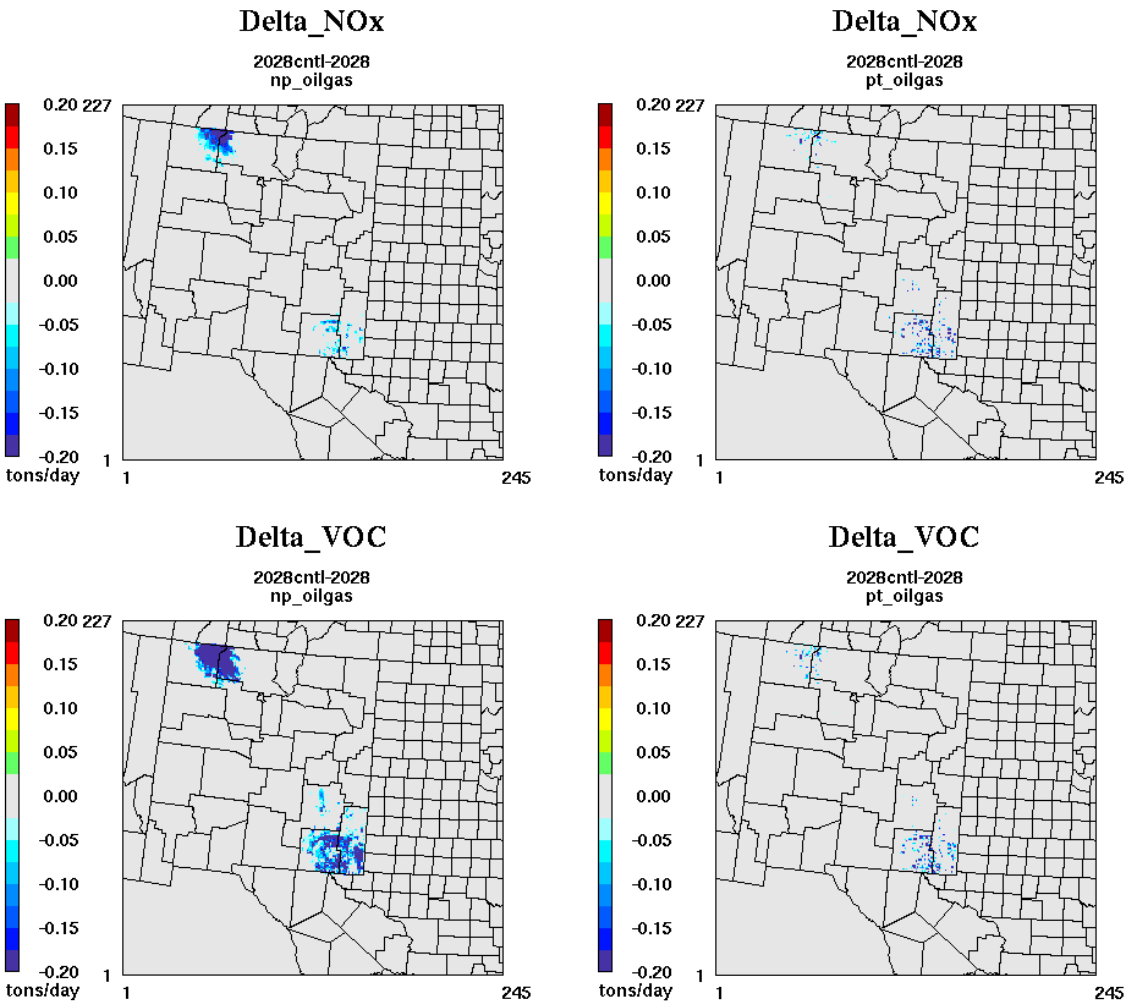

Figure 4-13. Differences in 2028 O&G Control Strategy and 2028 Base Case oil and gas NO_x (top) and VOC (bottom) emissions for the Non-Point (left) and Point (right) source sectors.

5. DIAGNOSTIC SENSITIVITY TESTS

Several CAMx diagnostic sensitivity tests were conducted to evaluate the effects that alternative meteorological inputs have on ozone concentrations.

5.1 WRFCAMx Processing of 2014 WRF Output

The WRFCAMx processor maps WRF meteorological fields to the format required by CAMx. It also calculates turbulent vertical exchange coefficients that define the rate and depth of vertical mixing in CAMx. Several options are available in WRFCAMx to derive vertical turbulent exchange coefficient (also known as Kv or vertical diffusivity) fields from WRF output. The Kv fields are diagnosed from wind, temperature, and Planetary Boundary Layer (PBL) parameters in WRFCAMx. For this application, the WRFCAMx processing was performed to generate two sets of Kv profiles using two different Kv options in WRFCAMx, the CMAQ-like and YSU Kv profile options.

The CAMx Kv_patch pre-processor program was used to set the minimum Kv value to 0.1 to 1.0 m^2/s in the lowest 100 m of the atmosphere depending on the amount urban land use category in a grid cell. This is done to account for the urban heat island effect that enhances vertical mixing through-out the day and night.

WRF was run with 36 vertical levels (35 vertical layers) as shown in Table 2-1. For the NM OAI Study, a layer collapsing strategy was employed that reduced the 35 WRF vertical layers to 25 layers in CAMx, which reduces the CAMx run time by about a third. Table 5-1 displays the WRF to CAMx layer collapsing strategy. This is the same layer collapsing study employed by WRAP-WAQS 2014 modeling platform.

5.2 CAMx Meteorological Diagnostic Sensitivity Tests

Four separate CAMx 2014 36/12/4-km diagnostic sensitivity tests were conducted for the first portion of the summer 2014 modeling episode that spanned May 15 to June 4, 2014. The purpose of the four meteorological inputs CAMx sensitivity tests was to identify the optimal meteorological inputs for the final CAMx 2014 base case simulation. The four sets of CAMx simulations were based on the WRF/NAM and WRF/ERA5 2014 36/12/4-km simulations described in Chapter 2 processed by WRFCAMx to generate two sets of vertical mixing coefficient (Kv) as described above:

1. WRF/NAM with CMAQ Kv
2. WRF/NAM with YSU Kv
3. WRF/ERA5 with CMAQ Kv
4. WRF/ERA5 with YSU Kv

Table 5-1. WRF to CAMx vertical layer collapsing strategy used in the NM OAI Study.

CAMx Layers	WRF Layers	WRF hybrid eta	WRF Pressure (mb)	Height (m)
	0	1.0000	1000.0	0
	1	0.9985	998.6	12
1	2	0.9970	997.2	24
	3	0.9950	995.3	40
2	4	0.9930	993.4	56
	5	0.9910	991.5	72
3	6	0.9880	988.6	97
	7	0.9850	985.8	121
4	8	0.9800	981.0	162
5	9	0.9700	971.5	243
6	10	0.9600	962.0	326
7	11	0.9500	952.5	409
	12	0.9400	943.0	492
8	13	0.9300	933.5	577
9	14	0.9100	914.5	747
10	15	0.8900	895.5	921
11	16	0.8700	876.5	1098
12	17	0.8400	848.0	1369
13	18	0.8000	810.0	1742
14	19	0.7600	772.0	2130
15	20	0.7200	734.0	2533
16	21	0.6800	696.0	2954
17	22	0.6400	658.0	3393
18	23	0.6000	620.0	3854
19	24	0.5500	572.5	4463
	25	0.5000	525.0	5115
20	26	0.4500	477.5	5816
	27	0.4000	430.0	6576
21	28	0.3500	382.5	7408
	29	0.3000	335.0	8328
22	30	0.2500	287.5	9360
	31	0.2000	240.0	10541
23	32	0.1500	192.5	11930
	33	0.1000	145.0	13630
24	34	0.0600	107.0	15355
	35	0.0270	75.7	17205
25	36	0.0000	50.0	19260

Figures 5-1 and 5-2 summarize the CAMx MDA8 ozone normalized mean bias (NMB) and error (NME) statistical performance metrics for each site in New Mexico and the four WRF meteorological inputs sensitivity tests. The statistics presented in these figures were calculated using a 60 ppb cutoff value relative to observed MDA8 ozone concentrations to understand the performance of each sensitivity test when ozone concentrations are most relevant to the NAAQS. Figure 5-1 shows that the NMB is generally within ±10% (colored grey) at almost all sites (note that the NMB performance goal is within ±5% and performance criteria is within ±15%). All of the sensitivity simulations have an under-prediction bias for observed ozone greater than 60 ppb at sites in the southern portion of the domain such that for one or two sites have a bias even lower than -10% (i.e., colored bright green). The WRF/NAM with CMAQ Kv sensitivity test has slightly better performance than the others with less underestimation bias (e.g., all sites but one are within ±10% compared to two sites for the other tests). Figure 5-2 shows that the NME is also generally within the performance goal (less than 15%) in all cases, with the southern portions of NM showing the largest errors but still within the performance criteria (less than 25%). The figure shows that CAMx using the WRF/NAM inputs tends to have slightly lower error and better ozone performance than when the WRF/ERA5 meteorological inputs are used.

Figure 5-3 presents soccer plots of bias and error for observed ozone above 60 ppb and all four CAMx sensitivity tests. This figure plots site-specific bias versus error with performance lines in the shape of a soccer goal, when the site-specific bias and error symbol falls within the soccer goal area (i.e., the red box) it is easy to see when the ozone performance goals are achieved. The figure shows that all sites have NMB and NME that fall within the performance criteria for bias (≤±15%) and error (≤25%), with most sites having an underestimation bias of the high (> 60 ppb) observed ozone concentrations. The CAMx simulations with the WRF/NAM meteorological inputs has slightly better performance than when the WRF/ERA5 inputs are used as more sites fall within the performance goal area. Comparison between the NAM cases indicate that the CAMx sensitivity test with CMAQ Kv has slightly smaller errors relative to the test with YSU Kv.

NAM CMAQ

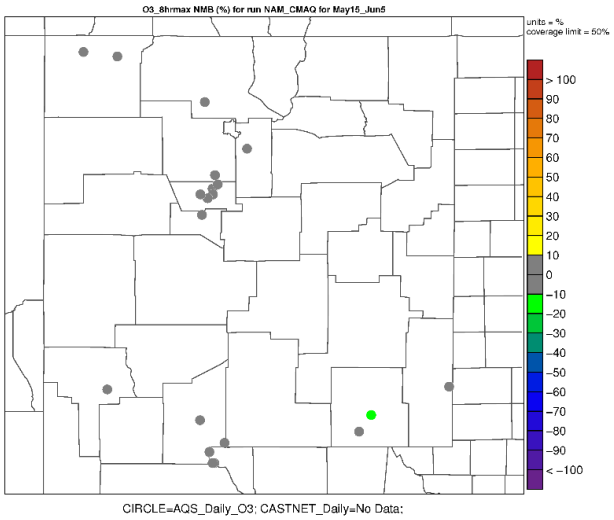

ERA5 CMAQ

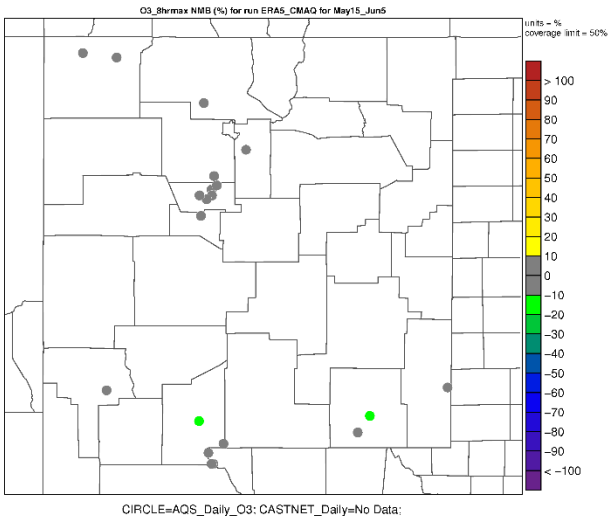

NAM YSU

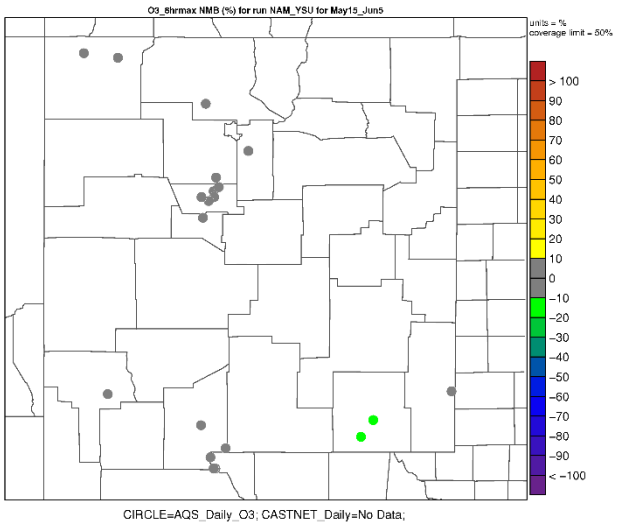

ERA5 YSU

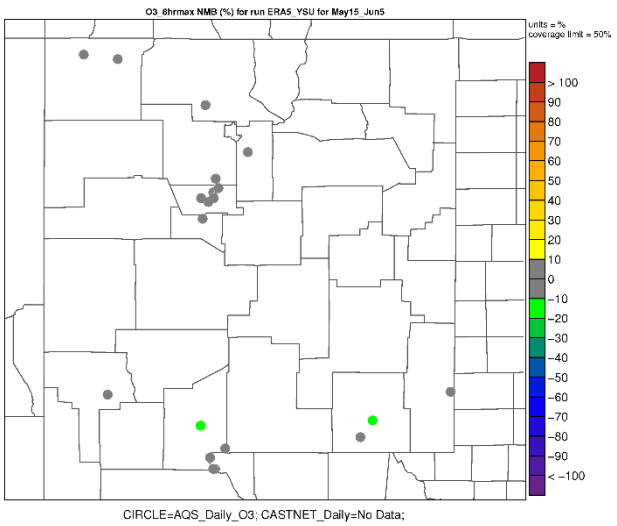

Figure 5-1. Comparison of sensitivity tests NMB with 60 ppb cutoff spatial plots over NM.

NAM CMAQ

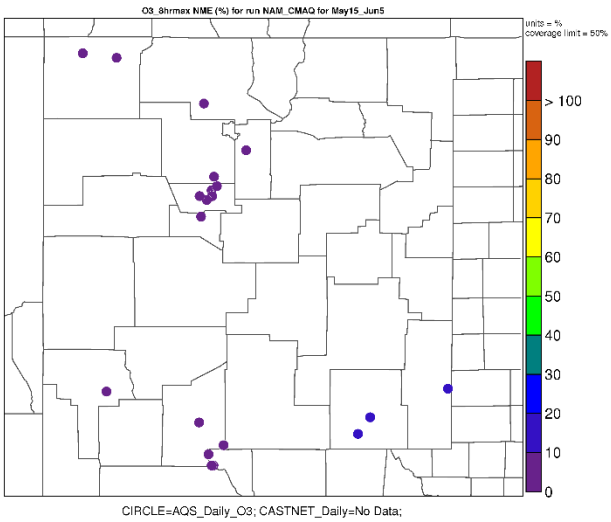

ERA5 CMAQ

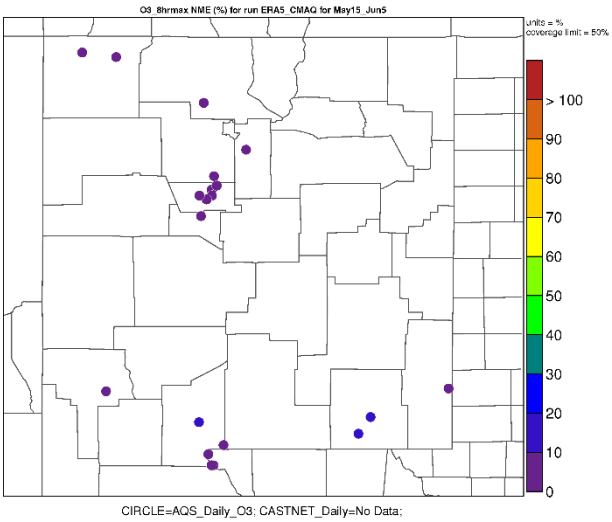

NAM YSU

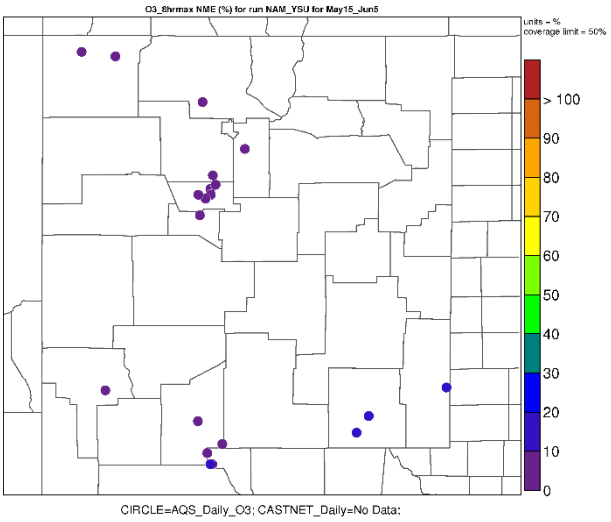

ERA5 YSU

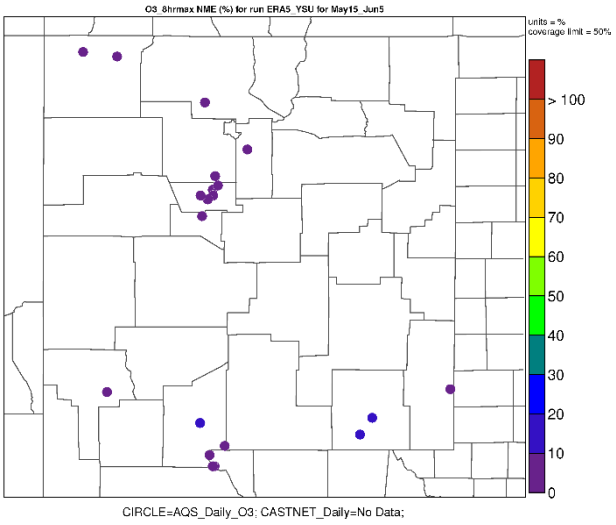

Figure 5-2. Comparison of sensitivity tests NME with 60 ppb cutoff spatial plots over NM.

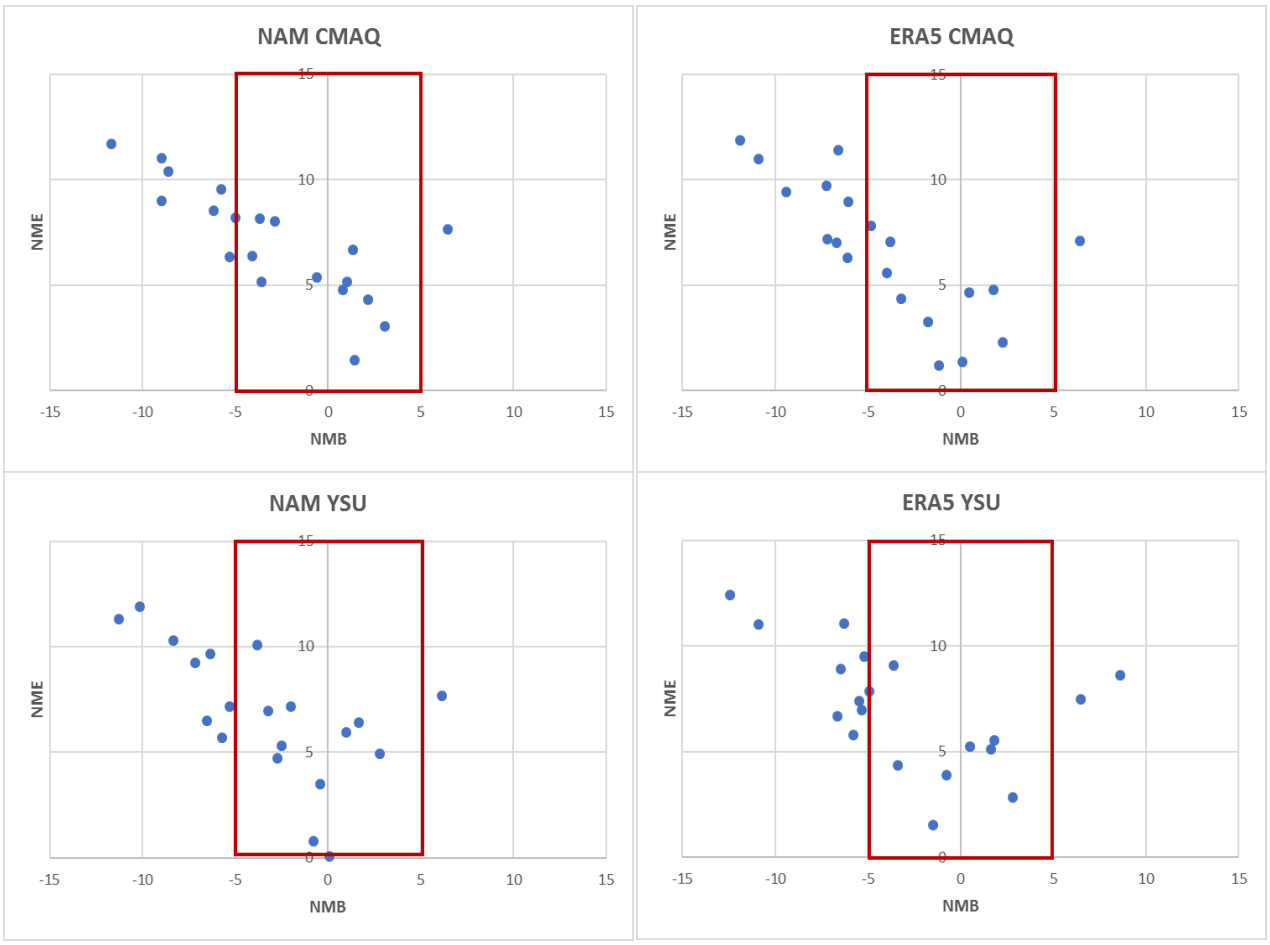

Figure 5-3. Comparison of sensitivity tests soccer plots with 60 ppb cutoff. Red rectangle indicates the performance goal soccer area.

Figures 5-4 to 5-7 present time series of predicted and observed MDA8 ozone concentrations for selected sites in Doña Ana, Eddy and Sandoval counties. At the Solano Road site in Doña Ana County the time series shows that the observed peak ozone concentration on May 29 is matched very well by the CAMx WRF/NAM sensitivity tests, while the CAMx WRF/ERA5 sensitivity test under-predicts by approximately 10 ppb (Figure 5-4). At the Desert View site, which is also in Doña Ana County, all four CAMx sensitivity tests underestimate the high observed ozone on May 28-29, but the CAMx WRF/NAM tests perform slightly better than the CAMx WRF/ERA5 test (Figure 5-5). At the Carlsbad site in Eddy County all test cases under-predict the high ozone concentration from May 27 to May 31 (Figure 5-6). For the site in Sandoval county (Figure 5-7) all four CAMx sensitivity tests track the daily variations of the observed MDA8 ozone including getting the timing and values of the observed ozone peak on May29, but the CAMx WRF/NAM with CMAQ Kv test exhibits the lowest biases.

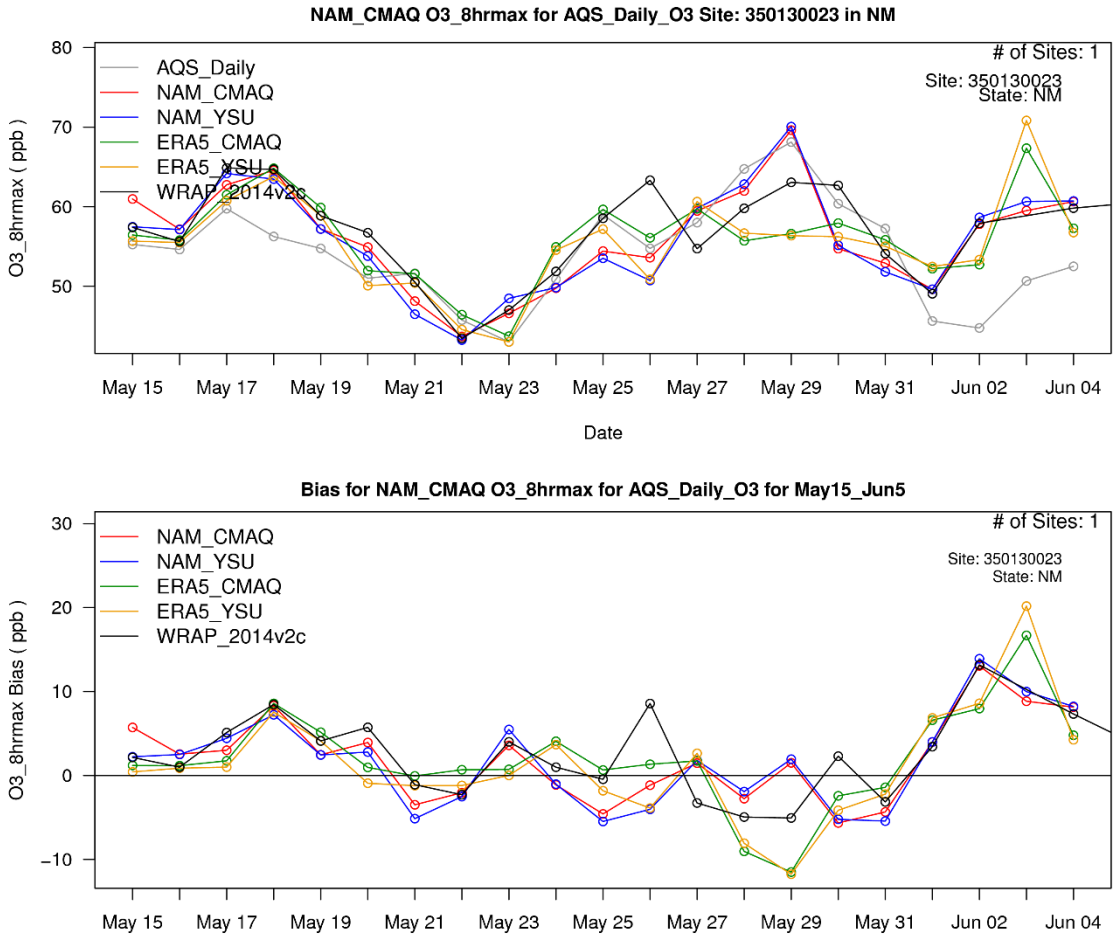

Figure 5-4. Timeseries comparison of sensitivity tests with observations (top) and bias (bottom) at Solano Road site in Doña Ana County

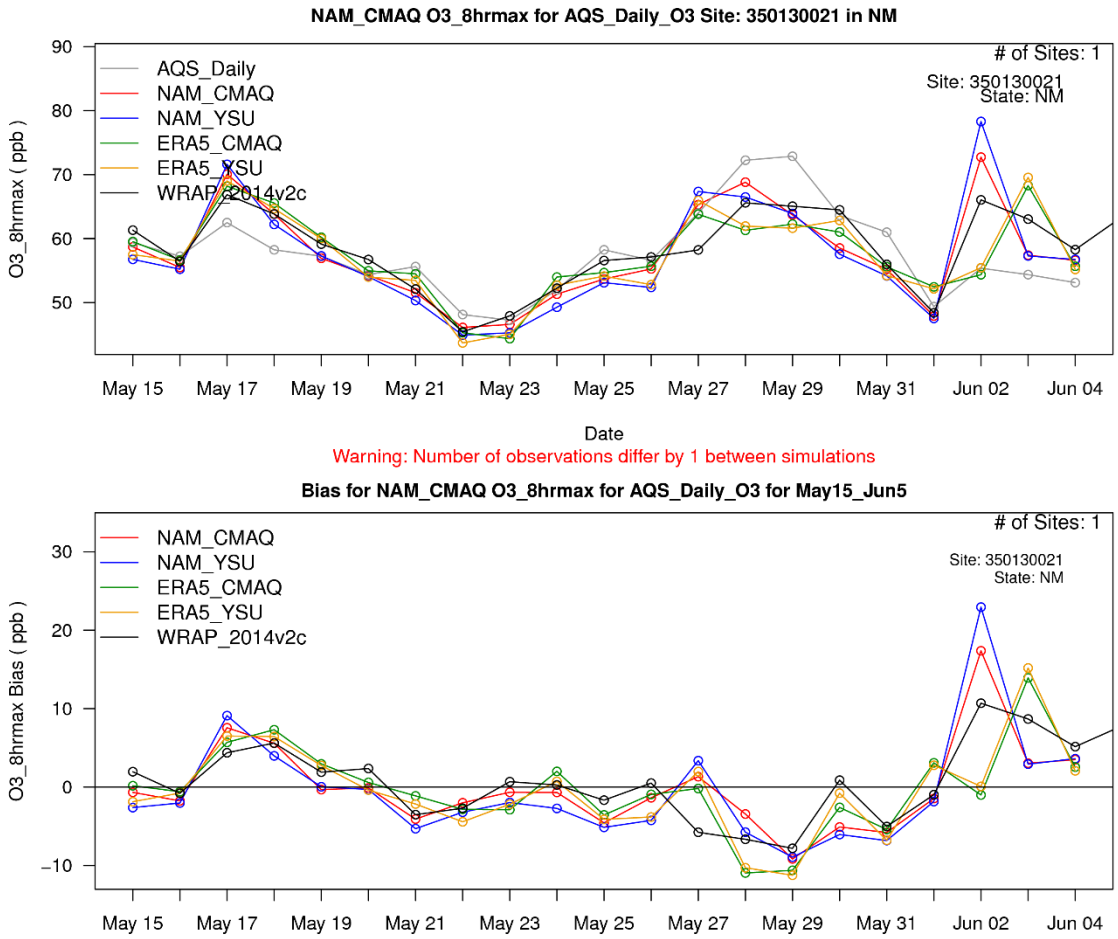

Figure 5-5. Timeseries comparison of sensitivity tests with observations (top) and bias (bottom) at Desert View site in Doña Ana County

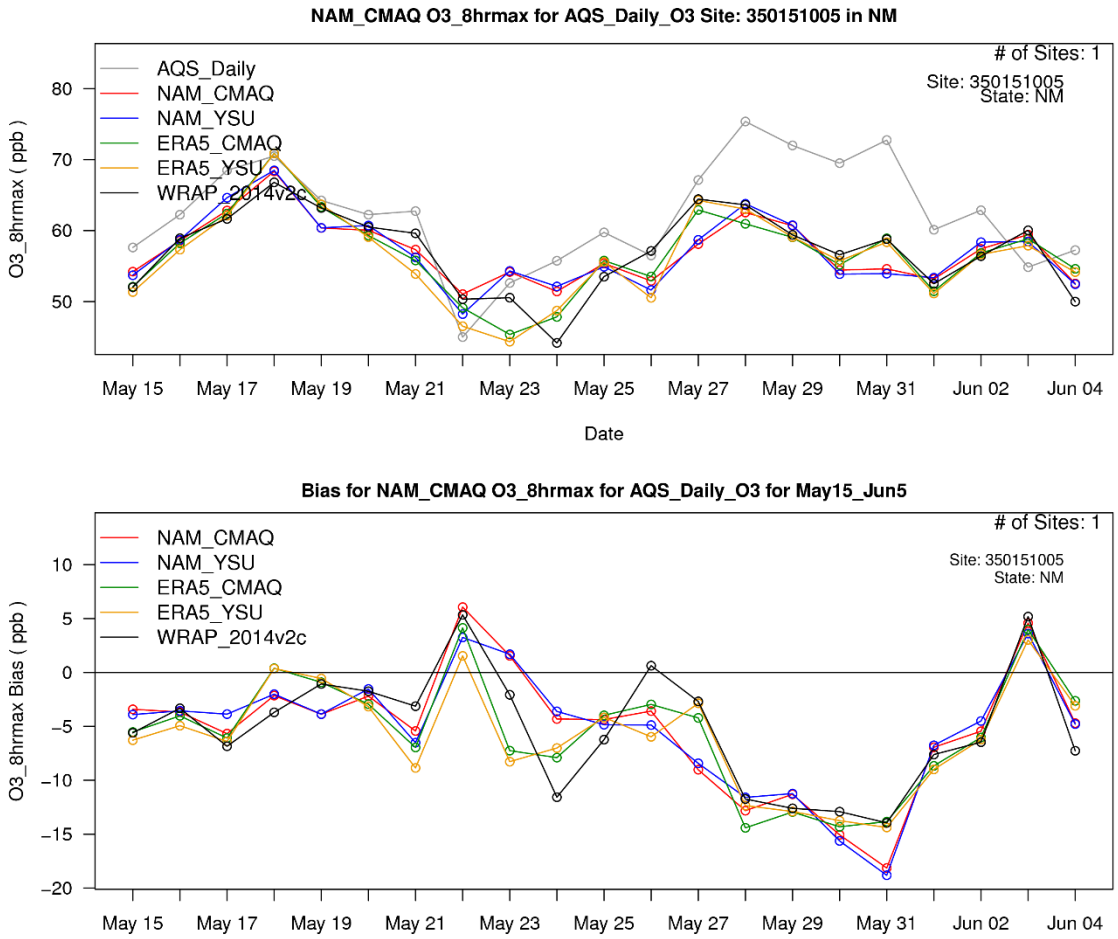

Figure 5-6. Timeseries comparison of sensitivity tests with observations (top) and bias (bottom) at Carlsbad site in Eddy County

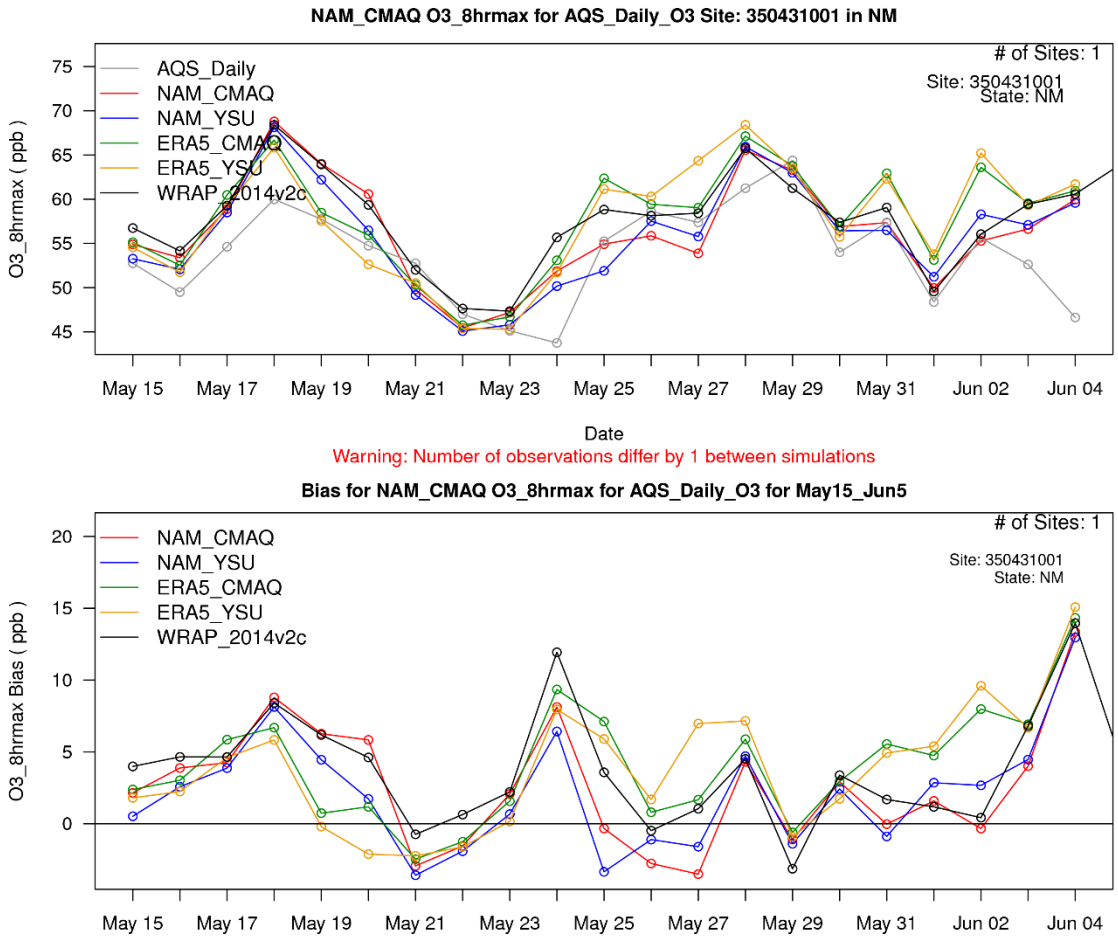

Figure 5-7. Timeseries comparison of sensitivity tests with observations (top) and bias (bottom) at Albuquerque site in Sandoval County

5.3 Summary of CAMx Diagnostic Sensitivity Tests

All four of the CAMx meteorological sensitivity cases have biases and errors well within the performance criteria and in most cases even within the more stringent performance goals. For the modeled episode, the differences in performance among all the cases considered are relatively minor. On some sites and days, CAMx using the WRF/NAM meteorology tends to capture peak ozone concentrations better than when the WRF/ERA5 meteorology is used. Based on the results presented here, the final CAMx 2014 base case model configuration used the WRF/NAM with CMAQ Kv treatment meteorological inputs.

6. 2014 BASE CASE MODELING AND MODEL PERFORMANCE EVALUATION

The NM OAI Study conducted two CAMx 2014 36/12/4-km base case simulations. The original 2014 base case simulation used CAMx v7.0 and biogenic emissions in the 4-km based on the MEGAN v3.1 model and is documented in Ramboll and WESTAR (2020c). There were errors in the CAMx v7.0 source apportionment algorithms that did not significantly affect the CAMx v7.0 2014 base case ozone estimates but would affect planned future year ozone source apportionment modeling. So, a second CAMx 2014v2 base case simulation was performed using CAMx v7.1 that had corrections to the ozone source apportionment algorithms. The revised CAMx v7.1 2014v2 base case simulation also updated the biogenic emissions in the 4-km domain using the BEIS v3.7 biogenic emissions model. The MEGAN v3.1 biogenic model used in the first CAMx v7.0 2014 base case was missing leaf area index (LAI) data for urban areas so produced zero biogenic VOC emissions for the urban land use type. The development of New Mexico-specific urban LAI inputs was beyond the resource and time constraints of the study, so BEIS biogenic emissions were used for the revised 2014v2 CAMX base case simulation. Details on the CAMx 2014v2 final base case simulation and model performance are provided in Ramboll and WESTAR (2021) with a summary provided below.

6.1 Final CAMx 2014v2 Base Case Configuration

The final CAMx meteorological inputs were based on the WRF/NAM simulations using the CMAQ-like Kv profiles as described in Chapters 2 and 5.

The 2014 emissions used in the 36-km and 12-km domains were the same as the WRAP-WAQS 2014v2 emissions. For the 4-km New Mexico domain, the WRAP 2014v2 emissions were processed by the SMOKE emissions model to generate the gridded hourly speciated emissions for CAMx. Chapter 4 describes the updates to the WRAP-WAQS 2014v2 emissions for New Mexico and the development of the emission inputs for the New Mexico 4-km domain.

Table 6-1 summarizes the CAMx configuration and options used for the CAMx 20114v2 base case simulation. Version 7.1 (v7.1) of CAMx released in January 2021 was used in the final 2014v2 base case simulation. CAMx was operated using the 36/12/4-km nested grid structure shown in Figure 1-1 using two-way grid nesting for all simulations. Boundary Conditions (BCs) for the CAMx most outer 36-km 36US modeling domain lateral boundaries were based on output from a 2014 simulation of the GEOS-Chem global chemistry conducted by WRAP for their 2014v2 modeling platform. CAMx was started on May 1, 2016 using the 36/12/4-km domains that allowed the model over two-weeks to initialize the model and wash out the initial concentrations before the first high ozone day on May 17, 2014.

Other CAMx model options and setup are defined in Table 6-1. The PPM advection solver (Colella and Woodward, 1984) was used for horizontal transport along with the spatially varying (Smagorinsky) horizontal diffusion approach. K-theory was used for vertical diffusion using the CMAQ-like Kv profiles from the WRFCAMx processing of the WRF/NAM output. The CB6r4 gas-phase chemical mechanism was selected because it includes the very latest chemical kinetic rates with halogen chemistry that affects ozone levels over the ocean. The latest aerosol mechanism was used in CAMx along with the

standard wet and dry deposition schemes. The Plume-in-Grid module was used to treat the near-source chemistry and dispersion of major NO_X emissions sources in the New Mexico 4-km domain for sources with greater than 5 tons per day NO_x emissions.

Table 6-1. Final CAMx model configuration for the 2014v2 base case simulation in NM OAI Study.

Science Options	CAMx	Comment
Model Codes	CAMx v7.1	Latest version of CAMx at time of study released in January 2020 (www.camx.com)
Horizontal Grid Mesh	36/12/4-km	
36-km grid	148 x 112 cells	36US domain
12-km grid	227 x 215 cells	12WUS2 domain. Includes buffer cells
4-km grid	245 x 227 cells	New Mexico 4-km domain. Includes buffer cells
Vertical Grid Mesh	25 vertical layers, defined by WRF	Layer 1 thickness ~20 m. Model top at 50 mb (~19 km). Layer collapsing from 35 vertical layers in WRF
Grid Interaction	36/12/4 km two-way nesting	
Initial Conditions	Start on May 1, 2014	First high ozone day is May 17, 2014
Boundary Conditions	WRAP 2014 GEOS-Chem	For 36US domain lateral boundaries
Emissions		
Baseline Emissions Processing	SMOKE, SMOKE-MOVES2014, BEIS v3.7	WRAP/WAQS 2014v2 emissions
Sub-grid-scale Plumes	Plume-in-Grid for major NO_X sources in New Mexico	Point sources with NO_x emission s greater than 5 tons per day
Chemistry		
Gas Phase Chemistry	CB6r4	Latest chemical reactions and kinetic rates with halogen chemistry (Yarwood et al., 2010)
Meteorological Processor	WRFCAMx	Compatible with CAMx v7.0
Horizontal Diffusion	Spatially varying	K-theory with Kh grid size dependence
Vertical Diffusion	CMAQ-like Kv	Evaluated YSU Kv scheme
Diffusivity Lower Limit	Kv-min = 0.1 to 1.0 m^2/s in lowest 100 m	Depends on urban land use fraction
Deposition Schemes		
Dry Deposition	Zhang dry deposition scheme	(Zhang et. al, 2001; 2003)
Wet Deposition	CAMx -specific formulation	rain/snow/graupel
Numerics		
Gas Phase Chemistry Solver	Euler Backward Iterative(EBI)	EBI fast and accurate solver
Vertical Advection Scheme	Implicit scheme w/ vertical velocity update	Emery et al., (2009a,b; 2011)
Horizontal Advection Scheme	Piecewise Parabolic Method (PPM) scheme	Colella and Woodward (1984)
Integration Time Step	Wind speed dependent	~0.5-1 min (4-km), 1-5 min (12-km), 5-15 min (36-km)

6.2 Ozone Model Performance Goals and Criteria

Emery and co-workers (2016) analyzed almost 100 PGM model applications and developed a set of PGM model performance goals and criteria based on the variability in the past PGM model performance. "Goals" indicate statistical values that approximately a third of the top performance past PGM applications have met and should be viewed as the best a model can be expected to achieve. "Criteria" indicates statistics values that about two thirds of past PGM applications have met and should be viewed as what a majority of the models have achieved. The CAMx revised 2014v2 and original 2014 base case simulations ozone model performance statistics for normalized mean bias (NMB) and normalized mean error (NME) are compared against the ozone model performance goals and criteria developed by Emery et al., (2016) that are given in Table 6-2.

Table 6-2. Recommended ozone benchmarks for photochemical model statistics (Source: Emery et al., 2016).

Species	NMB		NME		r	
	Goal	Criteria	Goal	Criteria	Goal	Criteria
1-hr & MDA8 Ozone	<±5%	<±15%	<15%	<25%	>0.75	>0.50

6.3 Spatial Ozone Model Performance

Figures 6-1 and 6-2 display the spatial distribution of bias (NMB) performance at monitoring sites in the 4-km NM domain for the revised 2014v2 and original 2014 CAMx base case simulation with and without using a 60 ppb observed ozone cutoff concentrations (i.e., only include predicted and observed MDA8 ozone pairs in the statistics when the observed MDA8 ozone is greater than 60 ppb). When the symbols are grey, they achieve the within ±5% ozone bias Performance Goal and when the symbols are the brightest green or yellow colors they are within the ozone bias Performance Criteria (i.e., between ±5% and ±15%).

With the exception of one monitoring site in El Paso, the NMB at all of the ozone sites in the 4-km domain achieve the ozone Performance Criteria using no cutoff in both CAMx base case simulations, although some sites have an overestimation bias greater than 5% Performance Goal (Figure 6-1). The CAMx 2014v2 and 2014 base case ozone bias performance looks nearly identical with the only noticeable differences being two sites (one in Doña Ana County and one in Luna County) that achieve the ozone bias Performance Goal in the revised 2014v2 CAMx base case (i.e., are colored grey in Figure 6-1, top) but have bias between the 5% and 15% in the original CAMx base case (Figure 6-1, bottom) so fall between the Performance Goal and Criteria (i.e., are colored bright yellow).

Whereas the CAMx base cases tend to have a small ozone overestimation bias when no observed ozone 60 ppb cutoff is used, when using a 60 ppb observed ozone cutoff both base cases tend to have a small underestimation bias (Figure 6-2). With one exception, when using the cutoff all sites achieve the ozone Performance Criteria and many sites achieve the ozone bias Performance Goal. The bias performance of the two base case simulations are nearly identical. The one exception is the Carlsbad site in Eddy County that is between the Performance Goal and Criteria (i.e., between -5% and -15%) in the

original 2014 base case (Figure 3-2, bottom), but has a NMB between -15% and -20% in the revised 2014v2 base case so fails to achieve the ozone bias Performance Criteria (Figure 3-2, top).

We also compared the spatial model performance of the two base cases for error (NME) and correlation (r), but the spatial maps were identical so did not provide any relevant information on the relative performance of the two base case simulations.

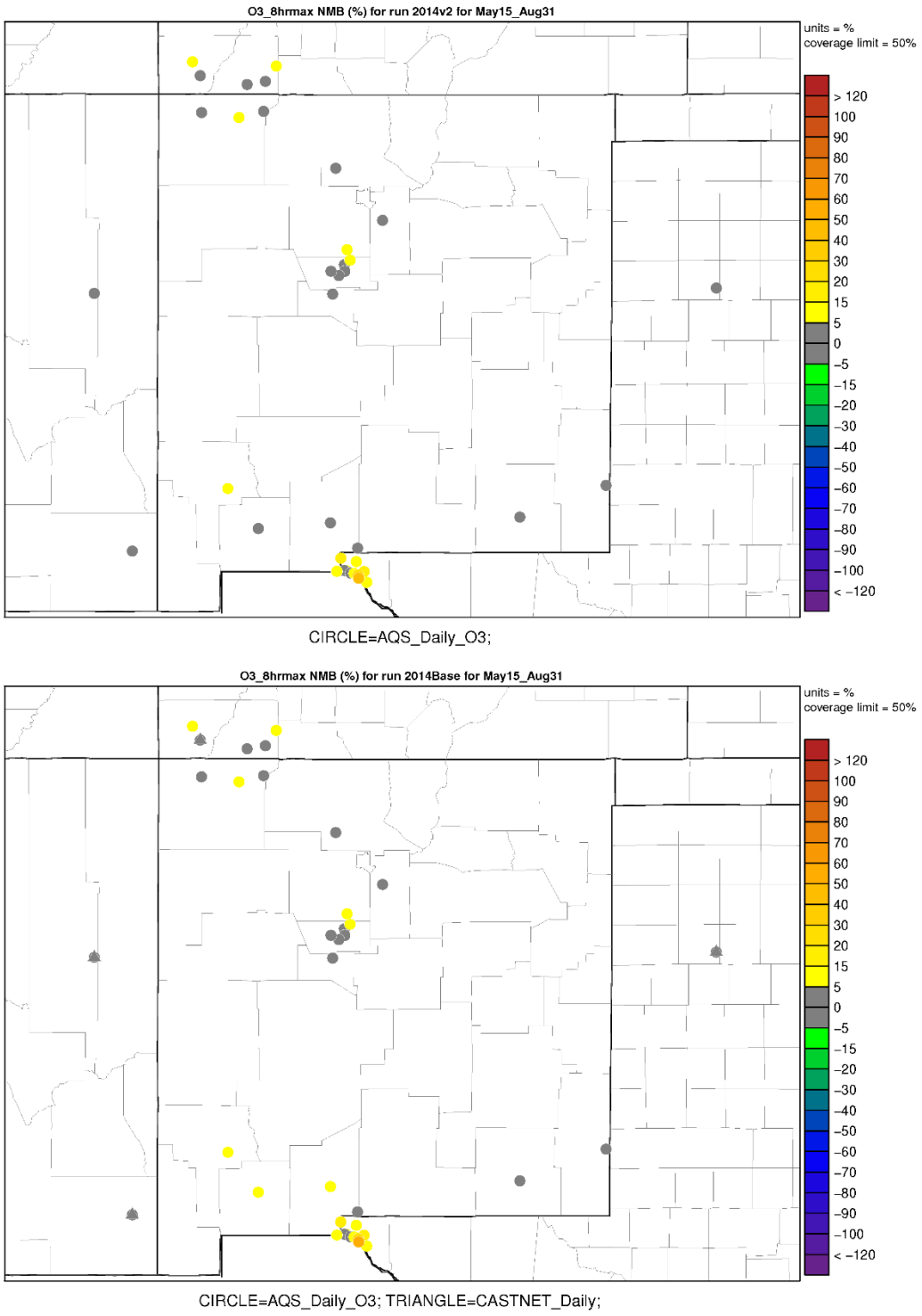

Figure 6-1. Normalized Mean Bias (NMB) for MDA8 ozone concentrations for the revised 2014v2 (top) and original 2014 (bottom) CAMx base case simulations with no ozone cutoff.

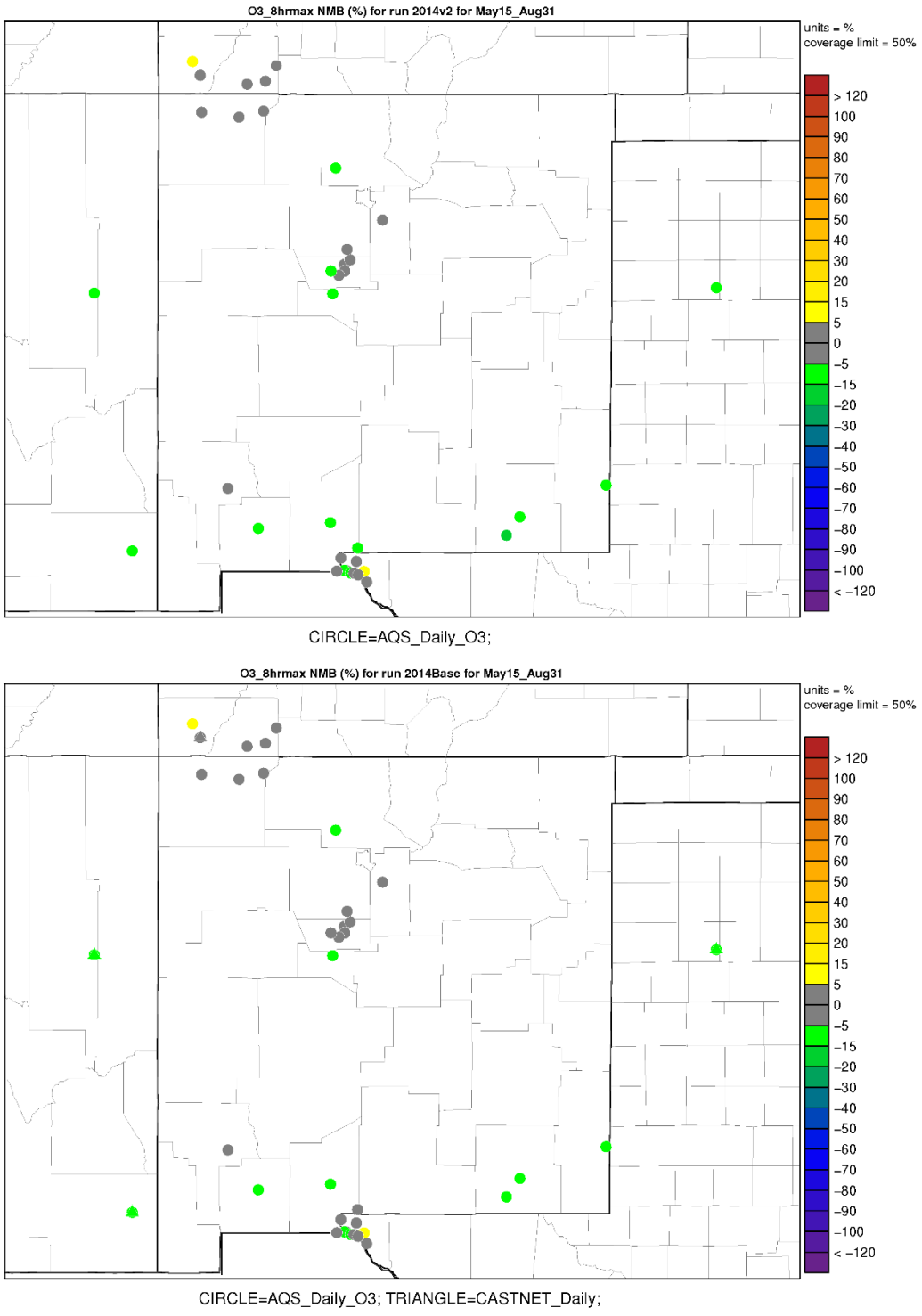

Figure 6-2. Normalized Mean Bias (NMB) for MDA8 ozone concentrations for the revised 2014v2 (top) and original 2014 (bottom) CAMx base case simulations with an observed 60 ppb ozone cutoff.

6.4 Scatter Plots of MDA8 Ozone

Figure 6-3 display scatter plots and summary statistics of MDA8 ozone across AQS or CASTNet sites in the 4-km domain for the revised 2014v2 and original 2014 CAMx base case simulations. The 2014v2 and 2014 MDA8 scatter plots look identical with the MDA8 performance at the AQS sites exhibiting a slight MDA8 ozone overestimation bias as indicated by the center density of the scatterplot being slightly above the 1:1 line of perfect agreement. This is in contrast to the CASTNet MDA8 scatterplots that are centered on the 1:1 line of perfect agreement so the two base case simulations are less biased.

The AQS performance statistics across the 4-km domain for the May-August 2014 modeling period show that the 2014v2 and 2014 MDA8 ozone performance is not exactly identical with the revised 2014v2 base case having a NMB of 4.4% that achieves the ozone bias Performance Goal, whereas the original 2014 base case has a NMB of 6.2% that falls between the ozone bias Performance Goal and Criteria. The 2014v2 NME (10.6%) is also slightly better than the original 2014 base case (10.9%).

Both CAMx base case simulations exhibit extremely good MDA8 ozone model performance across the CASTNet sites in the 4-km domain with near zero bias (-1.4% and +0.1%) and errors (8.1% and 7.9%) that are almost half the ozone error Performance Goal (<15%).

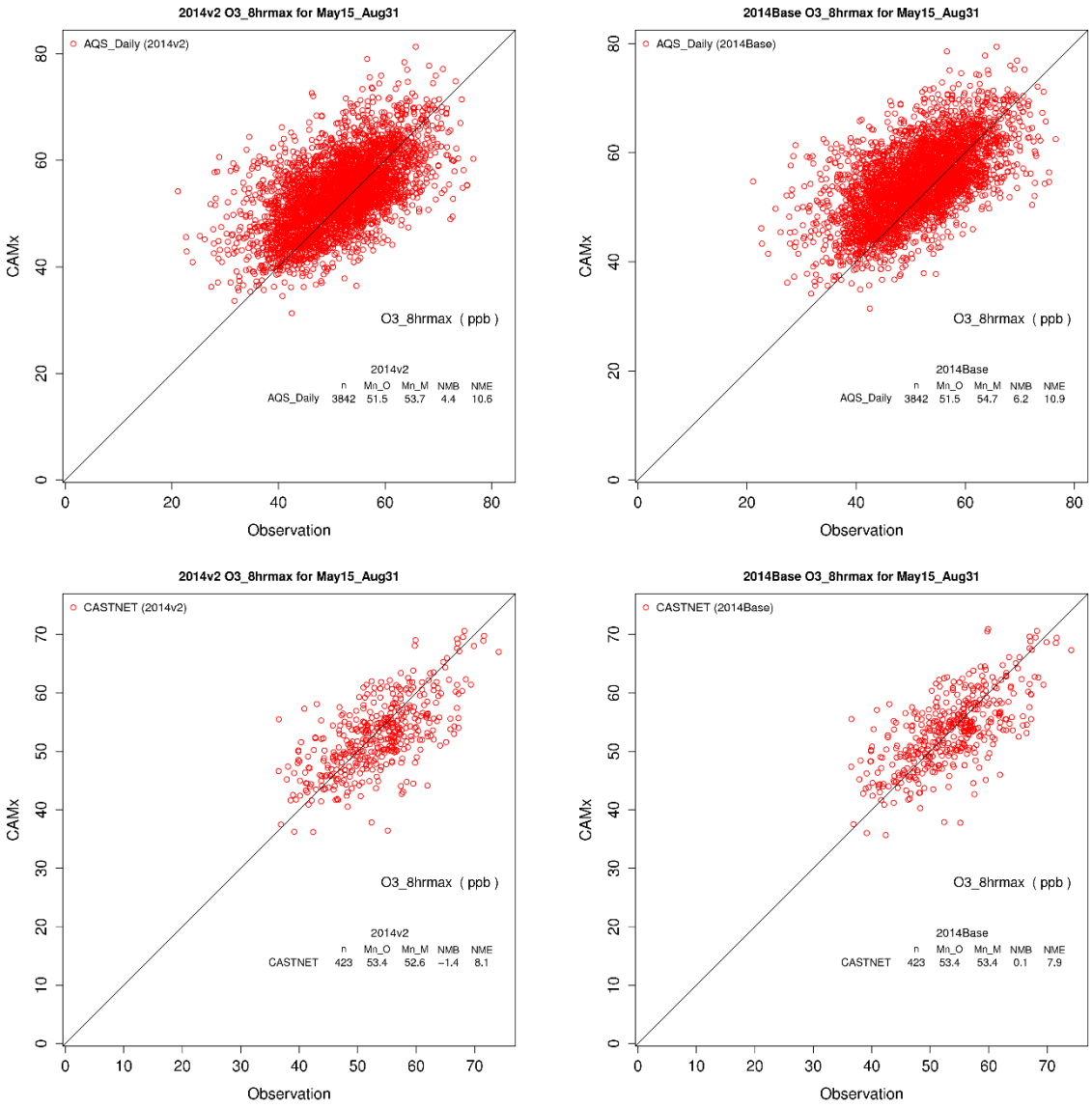

Figure 6-3. Scatter plots of predicted and observed MDA8 ozone concentrations for AQS (top) and CASTNet (bottom) monitoring sites within the 4-km New Mexico domain and the revised 2014v2 (left) and original 2014 (right) CAMx base case simulations.

6.5 MDA8 Ozone Time Series

Example predicted and observed MDA8 ozone time series at selected sites are presented below, with time series at all sites contained in the Appendix in Ramboll and WESTAR (2021). Figure 6-4 displays MDA8 ozone time series at the Desert View monitoring site in Doña Ana County in southern New Mexico. The CAMx MDA8 ozone predictions for the revised 2014v2 (blue) and original 2014 (green) base case simulations are almost on top of each other. In general, when they are a little different the revised 2014v2 MDA8 ozone is slightly lower, although that is not always the case as seen in the MDA8 ozone peaks in early June, mid-July, and end of August.

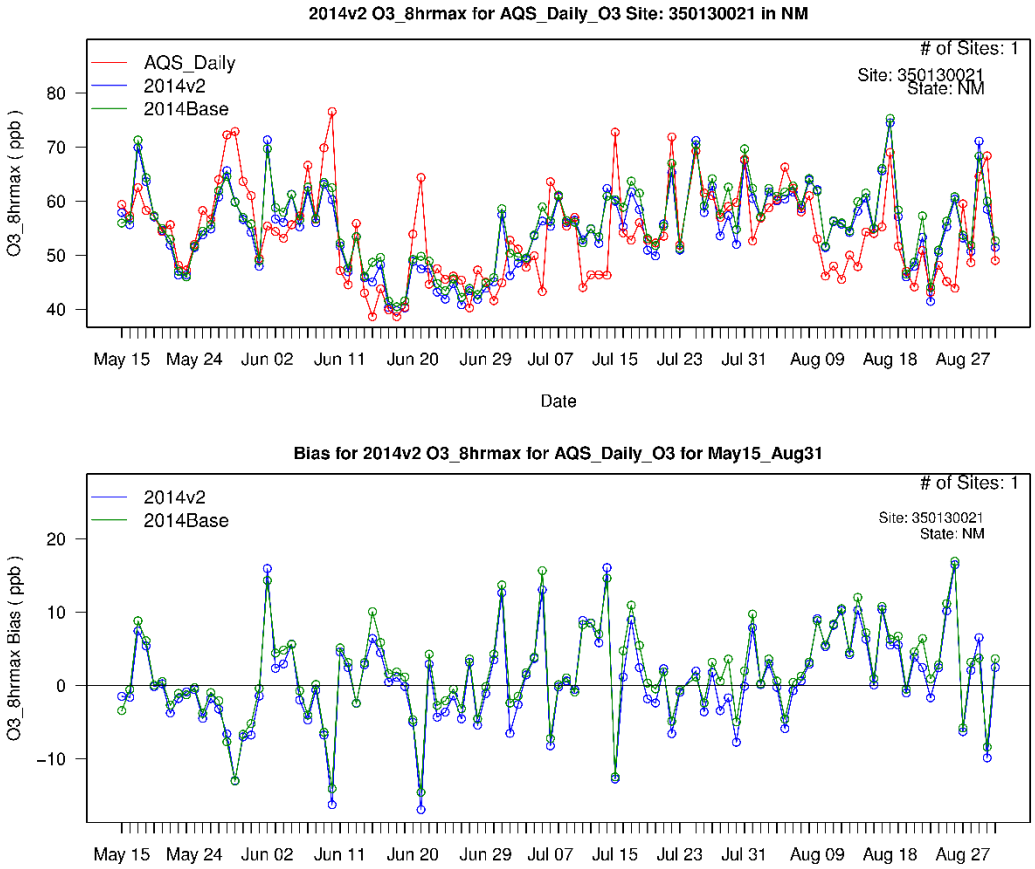

Figure 6-4. Time series of predicted and observed (red) MDA8 ozone at Desert View in Doña Ana County for the CAMx revised 2014v2 (blue) and original 2014 (green) CAMx base case simulations.

The MDA8 ozone time series comparison for the South East Heights monitoring site in Bernalillo County is shown in Figure 6-5. With the exception of a period in early July where the revised 2014v2 base case has a larger underestimation bias compared to the original 2014 base case, the two CAMx base case simulations are predicting nearly identical MDA8 ozone concentrations at this site.

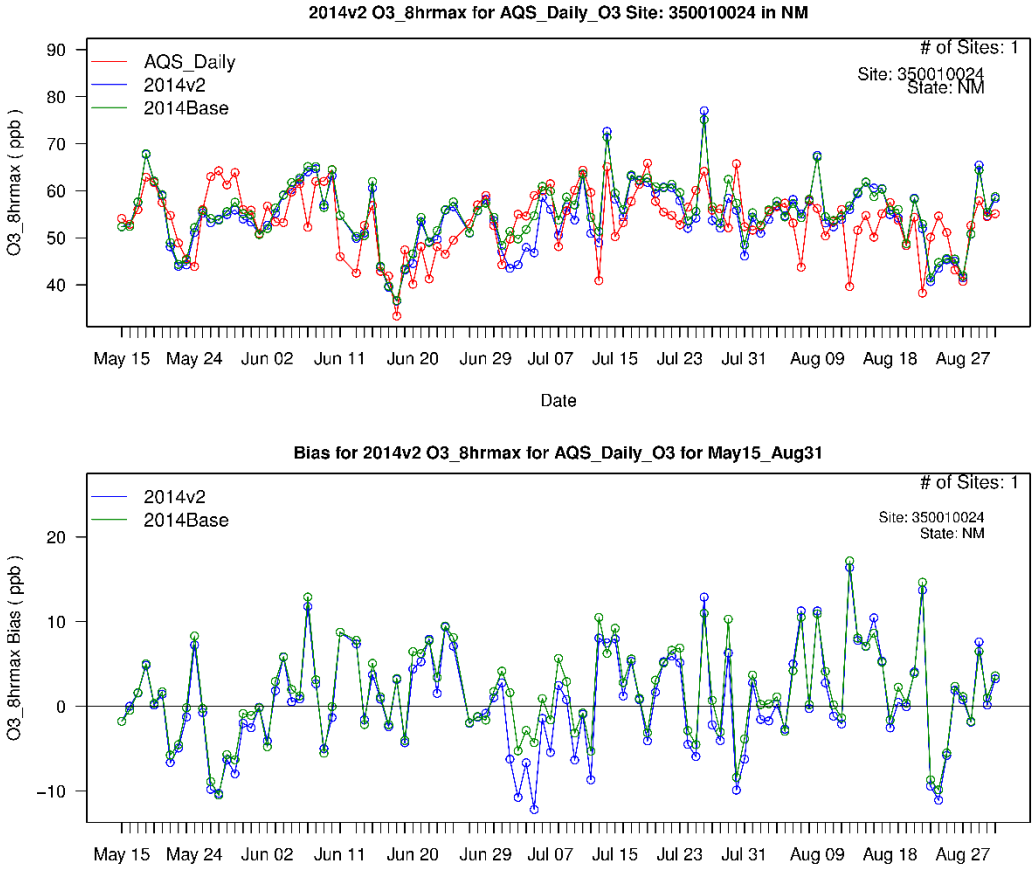

Figure 6-5. Time series of predicted and observed (red) MDA8 ozone at South East Heights in Bernalillo County for the CAMx revised 2014v2 (blue) and original 2014 (green) CAMx base case simulations.

The ozone time series at the Substation monitoring site in San Juan County is shown in Figure 6-6. Both CAMx base cases track the observed MDA8 ozone concentrations very well at the Substation monitoring site. Most of the time, the predicted MDA8 ozone are on top or nearly on top of each other and when different the revised 2014v2 MDA8 ozone is a little lower than the original CAMx 2014 base case.

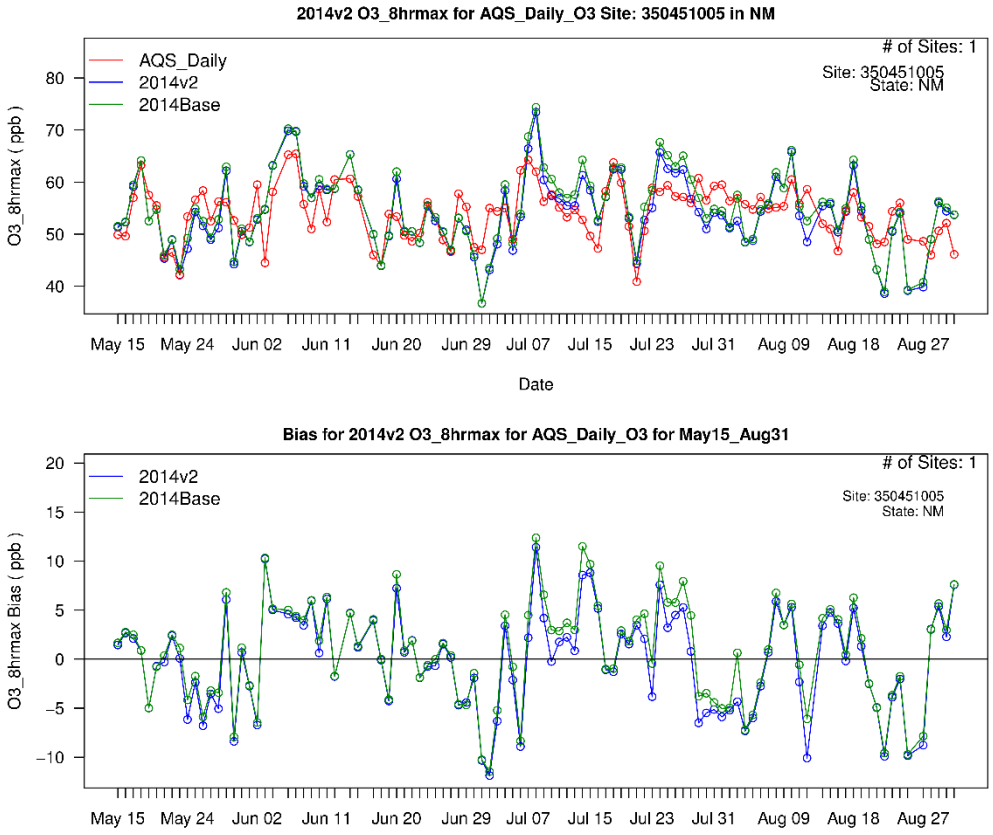

Figure 6-6. Time series of predicted and observed (red) MDA8 ozone at Sub Station in San Juan County for the CAMx revised 2014v2 (blue) and original 2014 (green) CAMx base case simulations.

6.6 Summary Ozone Model Performance Statistics in New Mexico

Ozone model performance statistics were calculated for three geographic regions in New Mexico. The central region was defined as all monitoring sites within Bernalillo County with the southern and northern regions defined as sites, respectively, south and north of Bernalillo County.

Tables 6-3 and 6-4 display the bias and error MDA8 ozone performance statistics with and without the observed MDA8 ozone 60 ppb cutoff for the three New Mexico subregions and the, respectively, original 2014 and revised 2014v2 CAMx base case simulations. The bias and error MDA8 ozone performance statistics are colored green when they achieve the Performance Goal, yellow when they lie between the Performance Goal and Criteria and red when they fail to achieve the Performance Criteria. The CAMx 2014 and 2014v2 base case performance statistics within the three New Mexico subregions are very good and very similar with the bias for the revised 2014v2 base case being 1-2 percentage points lower than the original 2014 CAMx base case simulation. Using no cutoff, when CAMx has a slight ozone overestimation tendency, the revised 2014v2 exhibits better performance statistics than the original 2014 base case. For example, the bias in the southern New Mexico region in original 2014 base case (5.8%) fails to achieve the ozone bias Performance Goal due to too high ozone overestimation, but achieves the ozone bias Performance Goal in the revised 2014v2 base case (3.5%). On the other hand, when an observed ozone 60 ppb cutoff is used the model tends to underestimate ozone a little so the revised 2014v2 base case ozone model performance is degraded a little compared to the original 2014 base case. For example, for the southern New Mexico subregion the original CAMx 2014 base case has a -6.1% NMB that is -7.8% for the revised CAMx 2014v2 base case, both of these NMB ozone performance statistics fall between the ozone bias Performance Goal and Criteria.

Table 6-3. Bias and error MDA8 ozone performance statistics for the original CAMx 2014 base case and the three subregions of New Mexico calculated with and without using an observed MDA8 ozone 60 ppb cutoff.

	Nocutoff		Withcutoff	
Region	NMB(%)	NME(%)	NMB(%)	NME(%)
North NM	4.3	9.1	0	6.4
Bernalillo	4.3	9.4	-2.8	7.1
South NM	5.8	10.5	-6.1	8.5

Table 6-4. Bias and error MDA8 ozone performance statistics for the revised CAMx 2014v2 base case and the three subregions of New Mexico calculated with and without using an observed MDA8 ozone 60 ppb cutoff.

	Nocutoff		Withcutoff	
Region	NMB(%)	NME(%)	NMB(%)	NME(%)
North NM	2.6	8.6	-1.0	6.6
Bernalillo	2.6	9.6	-4.3	8.5
South NM	3.5	10.2	-7.8	9.9

Tables 6-5 and 6-6 contain the bias performance statistics with and without a cutoff for each monitoring site in New Mexico and the, respectively, original CAMx 2014 and revised CAMx 2014v2 base case simulations. When not using the observed ozone cutoff, the original 2014 base case has 59% of the sites achieving the ozone bias Performance Goal with 36% of the sites falling between the Performance Goal and Criteria and one site failing to achieve the ozone bias Performance Criteria due to a 17.4% overestimation bias. The revised 2014v2 base case bias with no cutoff has 68% of the sites achieving the Performance Goal, 27% falling between the Performance Goal and Criteria and one site right at (15.0%) the Performance Criteria.

When an observed ozone cutoff is used, the number of sites achieving the ozone bias Performance Goal is flipped between the two base cases with 68% of the sites achieving the Performance Goal for the original 2014 base case and 59% of the sites achieving the Performance Goal for the revised 2014v2 base case with the remainder of the sites falling between the ozone bias Performance Goal and Criteria.

Table 6-5. Bias MDA8 ozone performance statistics with and without an observed ozone cutoff for each site in New Mexico and the original CAMx 2014 base case simulation.

2014Base (with MEGAN)			
SiteID	**SiteNames**	**NMB No Cutoff**	**NMB 60 ppb Cutoff**
350010023	Del Norte	1.7	-3.9
350010024	South East Heights	3.1	-2.4
350010029	South Valley	3.1	-2.8
350010032	Westside	1.1	-3.4
350011012	Foot Hills	13.6	2.0
350130008	La Union	17.4	-1.6
350130017	Sunland Park Yard	9.0	-3.6
350130020	Chaparral	4.8	-4.7
350130021	Desert View	3.2	-5.1
350130022	Santa Teresa	8.2	0.1
350130023	Solano	6.1	-6.5
350151005	Carlsbad	-1.1	-12.3
350171003	Chino Copper	9.1	-1.0
350250008	Hobbs Jefferson	2.1	-9.9
350290003	Deming Airport	6.2	-5.0
350390026	Coyote Ranger	3.3	-5.4
350431001	Bernalillo	8.1	3.8
350450009	Bloomfield	7.2	2.5
350450018	Navajo Lake	2.2	-0.6
350451005	Sub Station	1.4	3.3
350490021	Santa Fe Airport	3.8	-1.7
350610008	Los Lunas	0.8	-6.5

Table 6-6. Bias MDA8 ozone performance statistics with and without an observed ozone cutoff for each site in New Mexico and the revised CAMx 2014v2 base case simulation.

2014v2 (with BEIS)			
SiteID	**SiteNames**	**NMB No Cutoff**	**NMB 60 ppb Cutoff**
350010023	Del Norte	0.5	-4.9
350010024	South East Heights	1.3	-3.6
350010029	South Valley	0.9	-4.4
350010032	Westside	-1.0	-5.4
350011012	Foot Hills	11.9	0.8
350130008	La Union	15.0	-3.0
350130017	Sunland Park Yard	7.4	-4.1
350130020	Chaparral	2.8	-5.8
350130021	Desert View	1.4	-6.3
350130022	Santa Teresa	5.8	-1.8
350130023	Solano	3.9	-8.2
350151005	Carlsbad	-4.3	-14.5
350171003	Chino Copper	7.0	-1.8
350250008	Hobbs Jefferson	-1.2	-12.6
350290003	Deming Airport	3.8	-8.6
350390026	Coyote Ranger	1.2	-5.6
350431001	Bernalillo	6.4	3.3
350450009	Bloomfield	6.0	1.7
350450018	Navajo Lake	0.5	-3.6
350451005	Sub Station	-0.1	2.2
350490021	Santa Fe Airport	1.5	-2.5
350610008	Los Lunas	-1.7	-9.0

6.7 Conclusions of 2014 Base Case Modeling and Model Performance Evaluation

The evaluation of the NM OAI Study CAMx original 2014 and revised 2014v2 base case simulations focused on MDA8 ozone model performance across all sites within New Mexico, within three subregions in New Mexico (northern, Bernalillo County, and southern) and at individual sites in New Mexico. When examining MDA8 ozone performance across groups of sites, both CAMx 2014 base cases always achieves the ozone Performance Criteria and usually achieves the ozone Performance Goals. Except for one site (La Union in Doña Ana County) both CAMx base cases also achieve the ozone Performance Criteria at all monitoring sites and achieve the ozone Performance Goals as a majority of the sites in New Mexico. When examining MDA8 ozone performance across all observations, the model tended to have an ozone overestimation tendency but still always achieved the bias performance criteria (≤±15%) and usually achieved the bias performance goal (≤±5%). When comparing the model's ability to reproduce the highest observed ozone concentrations greater than 60 ppb, the model still always achieved the bias performance criteria and usually achieved the bias performance goal, albeit with an underestimation tendency. The

MDA8 ozone error essentially always achieves the performance goal whether examining all ozone observations or just those observations greater than 60 ppb.

In conclusion, the NM OAI Study original CAMx 2014 and revised CAMx 2014v2 base case simulations ozone model performance within New Mexico is as good or better than most recent PGM applications (e.g., WRAP-WAQS, EPA 2016v1 and Denver ozone SIP) and appears to be a reliable PGM modeling platform for evaluating emission reduction strategies for reducing ozone concentrations in New Mexico.

7. 2028 BASE CASE MODELING AND OZONE DESIGN VALUE PROJECTIONS

A CAMx v7.1 2028 36/12/4-km Base Case model simulation was conducted using the WRF/NAM meteorological, 2014 Boundary Conditions (BCs) and 2028 base case emission inputs described in, respectively, Chapters 2, 3 and 4. The CAMx 2028 base case simulation used the same model configuration as used in the CAMx v7.1 2014v2 revised base case simulations presented in Chapter 6 only with the 2028 Base Case anthropogenic emissions.

The CAMx 2014v2 and 2028 Base Case simulations were used to make 2028 future-year ozone design value (DVF) projections.

7.1 EPA Recommended Ozone Design Value Projection Procedure

EPA recommends using photochemical grid model (PGM) modeling results in a relative fashion to scale the observed current year ozone design value (DVC) to estimate the future year ozone design value (DVF). The model derived scaling factors are called Relative Response Factors (RRF) and are the ratio of future (2028) to base (2014v2) year ozone modeling results averaged over the 10 highest base year base case modeled Maximum Daily 8-hour Average (MDA8) ozone concentrations near the monitor:

$$RRF = \sum Model_{2028} / \sum Model_{2014}$$

$$DVF = DVC \times RRF$$

EPA guidance recommends that the DVC is calculated as the average of three-years of ozone design values (DV) centered on the base modeling year, which is 2014 in this case:

$$DVC_{2012\text{-}2016} = (DV_{2012\text{-}2014} + DV_{2013\text{-}2015} + DV_{2014\text{-}2016}) / 3$$

By near the monitor, EPA guidance recommends that the highest modeled base year MDA8 ozone is selected within a 3x3 array of grid cells centered on the monitor. For the future year, the future year MDA8 ozone is selected from the same grid cell in the 3x3 array centered on the monitor as used in the base year.

EPA guidance recommends using the 10 highest modeled base year MDA8 ozone concentrations days with MDA8 ozone greater than 60 ppb in the RRFs. If there are less than 10 modeled days with base year MDA8 ozone greater than 60 ppb, EPA guidance states that RRFs can still be calculated as long as there are at least 5 days with ozone greater than 60 ppb.

EPA has codified their recommended ozone DVF projection approach in the Software for the Modeled Attainment Test (SMAT[37]). The SMAT tool was used to make 2028 ozone DVF projections in the NM OAI Study. The default SMAT specification were used except

[37] https://www.epa.gov/scram/photochemical-modeling-tools

that the minimum number of days needed to calculated an RRF was lowered from 5 to 4 in order to obtain 2028 ozone DV projections at all sites in New Mexico.

7.1.1 Ozone DV Unmonitored Area Analysis (UAA)

SMAT includes an unmonitored area analysis (UAA) that examines projected future year ozone DVFs away from the monitoring sites. The first step in the UAA is the spatial interpolation of the monitor-based ozone DVCs ($DVC_{2012\text{-}2016}$) across the domain being analyzed, which is the 4-km New Mexico domain in this case. The SMAT spatial interpolation of the monitoring site ozone DVC can be performed with and without using the modeled ozone concentration gradients. As shown below, the SMAT UAA analysis was run for the NM OAI Study 2028 base case ozone DVC projections with and without using the modeled concentration gradients. We recommend using the interpolation without the modeled concentration gradients because of the influence of fires on UAA interpolated ozone DVCs that are uncertain, unverifiable, and not regulatory relevant.

The SMAT UAA procedure for projecting the spatially interpolated ozone DVCs is the same as used at the monitor described above, only instead of using the modeling results in the in a 3x3 array of grid cells with the highest 2014 modeled MDA8 ozone to define near the monitor, the value at the grid cell is used (i.e., 1x1 array).

7.2 2028 Base Case Ozone DVF Projections at Monitoring Sites

Table 7-1 displays the current year $DVC_{2012\text{-}2016}$ and projected 2028 ozone DVFs at monitoring sites in New Mexico for the 2028 Base Case simulation and their differences. There are two sites in Doña Ana County with current year $DVC_{2012\text{-}2016}$ above the 70 ppb 2015 ozone NAAQS, Desert View (72.0 ppb) and Santa Teresa (71.3 ppb). However, it should be noted that measured ozone concentrations in Southern New Mexico have been higher in more recent years, as shown in Table 1-1. This issue is examined in a DVC sensitivity analysis presented in Chapter 9.

The 2028 Base Case ozone DVFs at monitoring sites in northern New Mexico are projected to be -2.2 ppb to -5.6 ppb lower than the observed $DVC_{2012\text{-}2016}$. For the northern New Mexico sites, Navajo Lake has the highest ozone $DVC_{2012\text{-}2016}$ (67.0 ppb) and 2028 Base Case projected DVF (64.8) and is the site with the lowest reduction between the DVC and DVF (-2.2 ppb).

The current observed $DVC_{2012\text{-}2016}$ in Bernalillo County range from 65.0 to 68.0 ppb and are projected to be reduced by -4.4 ppb to -5.9 ppb by 2028 with all 2028 Base Case projected ozone DVFs in Bernalillo County below 63 ppb.

The current ozone $DVC_{2012\text{-}2016}$ at the southern New Mexico sites range from 62.0 to 72.0 ppb and are reduced by -2.0 ppb to -6.3 ppb in the 2028 Base Case. The sites in Doña Ana County have the largest ozone DV reductions between 2014 and 2028 (-4.7 to -6.3 ppb). While those monitoring sites in southeast New Mexico have the lowest ozone DVF reduction between 2014 and 2028 Base Cases, -2.3 ppb at Carlsbad and -2.0 ppb at Hobbs in, respectively, Eddy and Lea Counties. The lower reductions in 2028 Base Case ozone DVFs at the two southeastern New Mexico sites are due to increased oil and gas emissions in the Permian Basin between 2014 and 2028 that offset the effects due to emission reductions from other source sectors, such as mobile sources (see Chapter 4).

Table 7-1. Current year $DVC_{2012-2016}$ and projected 2028 Base Case ozone DVFs at New Mexico monitoring sites within the 4-km NM domain.

AQS_ID	2012-2016 DVC (ppb)	2028 Base DVF Base (ppb)	Difference 2028 DVF minus $DVC_{2012-16}$ (ppb)	Site Name	State	County
Northern New Mexico						
350390026	64.0	60.8	-3.2	Coyote Ranger District	NM	Rio Arriba
350431001	64.0	58.4	-5.6	Bernalillo (E Avenida)	NM	Sandoval
350450009	64.3	61.0	-3.3	Bloomfield	NM	San Juan
350450018	67.0	64.8	-2.2	Navajo Lake	NM	San Juan
350451005	63.7	60.8	-2.9	Substation	NM	San Juan
350490021	64.3	60.6	-3.7	Santa Fe Airport	NM	Santa Fe
Bernalillo County						
350010023	66.3	60.9	-5.4	Del Norte HS	NM	Bernalillo
350010024	68.0	62.3	-5.7	South East Heights	NM	Bernalillo
350010029	66.0	61.0	-5.0	South Valley	NM	Bernalillo
350010032	67.0	62.6	-4.4	Westside	NM	Bernalillo
350011012	65.0	59.1	-5.9	Foothills	NM	Bernalillo
Southern New Mexico						
350130008	66.3	60.0	-6.3	La Union	NM	Doña Ana
350130017	67.0	61.9	-5.1	Sunland Park City Yard	NM	Doña Ana
350130020	67.0	62.3	-4.7	Chaparral	NM	Doña Ana
350130021	72.0	67.0	-5.0	Desert View	NM	Doña Ana
350130022	71.3	66.1	-5.2	Santa Teresa	NM	Doña Ana
350130023	65.0	60.3	-4.7	Solano	NM	Doña Ana
350151005	69.0	66.7	-2.3	Carlsbad	NM	Eddy
350171003	62.0	59.0	-3.0	Chino Copper Smelter	NM	Grant
350250008	66.0	64.0	-2.0	Hobbs Jefferson	NM	Lea
350290003	66.0	62.7	-3.3	Deming Airport	NM	Luna
350610008	66.3	62.2	-4.1	Los Lunas (Los Lentes)	NM	Valencia

The current year $DVC_{2012\text{-}2016}$ and projected 2028 Base Case ozone DVFs at monitoring sites within the 4-km NM domain but outside of New Mexico are shown in Table 7-2. The El Paso UTEP site is the only site in Table 7-2 that has a $DVC_{2012\text{-}2016}$ that exceeds (71.0 ppb) the 2015 ozone NAAQS. Design values at monitoring sites in El Paso are projected to go down between -3.2 ppb to -5.2 ppb with projected 2028 Base Case ozone DVFs ranging from 62.5 ppb to 66.2 ppb.

The sites in Arizona and Colorado have current year $DVC_{2012\text{-}2016}$ that are 68 ppb or lower and are reduced from -1.6 ppb to -5.2 ppb with the smallest reductions occurring in La Plata County, Colorado and the largest reductions occurring in El Paso.

Table 7-2. Current year $DVC_{2012\text{-}2016}$ and projected 2028 Base Case ozone DVFs at monitoring sites within the 4-km NM domain but outside of New Mexico.

AQS_ID	2012-2016 DVC (ppb)	2028 Base DVF Base (ppb)	Difference 2028 DVF minus $DVC_{2012\text{-}16}$ (ppb)	Site Name	State	County
Arizona, Colorado and Texas						
40038001	68.0	64.0	-4.0	Chiricahua NM	AZ	Cochise
40170119	66.7	61.9	-4.8	Petrified Forest	AZ	Navajo
80677001	67.7	66.1	-1.6	UTE 1	CO	La Plata
80677003	66.7	64.4	-2.3	UTE 3	CO	La Plata
80830006	63.0	59.7	-3.3	Cortez - Health Dept	CO	Montezuma
80830101	66.0	62.4	-3.6	Mesa Verde NP	CO	Montezuma
481410029	61.0	58.0	-3.0	Ivanhoe	TX	El Paso
481410037	71.0	66.2	-4.8	El Paso UTEP	TX	El Paso
481410044	67.7	62.5	-5.2	El Paso Chamizal	TX	El Paso
481410055	62.7	59.2	-3.5	Ascarate Park SE	TX	El Paso
481410057	66.5	63.3	-3.2	Socorro Hueco	TX	El Paso
481410058	68.0	63.4	-4.6	Skyline Park	TX	El Paso
483819991	66.7	62.4	-4.3	Palo Duro	TX	Randall

7.3 2028 Base Case Ozone DVF Unmonitored Area Analysis

SMAT was run using output the 2014v2 and 2028 Base Case CAMx simulations to obtain the spatial distribution of interpolated current year ozone $DVC_{2012\text{-}2016}$ and projected 2028 ozone DVF throughout the 4-km NM domain using the Unmonitored Area Analysis (UAA) feature. SMAT UAA was run with and without using modeled concentration gradients in the spatial interpolation of the observed ozone $DVC_{2012\text{-}2016}$ at the monitoring sites to each grid cell in the 4-km NM domain.

Figure 7-1 displays the spatial distribution of the SMAT UAA ozone $DVC_{2012\text{-}2016}$ and DVF across the 4-km NM domain calculated using CAMx modeled ozone concentrations gradients in the spatial interpolation of the $DVC_{2012\text{-}2016}$. Although the highest $DVC_{2012\text{-}2016}$ at a monitoring site is 72.0 ppb at Desert View, using modeled concentration

gradients produces an interpolated $DVC_{2012\text{-}2016}$ as high as 89.5 ppb that occurs in Arizona on the border with New Mexico that is reduced to 84.0 ppb for the maximum 2028 Base Case UAA DVF. These high MDA8 ozone concentrations in eastern Arizona and southwestern New Mexico are due to elevated ozone concentrations from wildfire emissions that are used in the SMAT UAA $DVC_{2012\text{-}2016}$ spatial interpolation when the option to use modeled concentration gradients is selected. Because they occur away from any monitoring sites, whether actual elevated ozone occurred in these wildfire ozone plumes is not known. Away from these wildfire ozone plumes, the SMAT UAA $DVC_{2012\text{-}2016}$ range from 60 to 71 ppb that are reduced to the 50 to 65 ppb range in for the SMAT UAA 2028 ozone DVF with small patches in the 65-71 ppb range scattered across New Mexico.

The SMAT UAA ozone $DVC_{2012\text{-}2016}$ and 2028 Base Case projections obtained without using the modeled concentrations gradients are shown in Figure 7-2. When doing the SMAT UAA spatial interpolation of the $DVC_{2012\text{-}2016}$ without including the concentrations gradients the ozone $DVC_{2012\text{-}2016}$ across the 4-km NM modeling domain are constrained by the $DVC_{2012\text{-}2016}$ values at the monitoring sites (i.e., Tables 7-1 and 7-2), which range from 61.4 to 71.0 ppb (10 ppb range; Figure 7-2). This is in contrast when the modeled concentrations gradients are used in the SMAT UAA interpolation and the $DVC_{2012\text{-}2016}$ range from 58.2 to 89.5 ppb across the domain (31 ppb range; Figure 7-1).

Figure 7-3 displays a spatial map of the differences in ozone $DVC_{2012\text{-}2016}$ and 2028 base case DVF (DVF – DVC) from the SMAT UAA with the top panel shown the differences with and the bottom panel showing the differences without using the modeled spatial gradients in the interpolation. Using the modeled concentration gradients in the interpolation has a significant effect on the DVC/DVFs, but has little effect on the differences in the SMAT UAA DVF and DVC. In fact, the only perceptible change in the ozone DVF and DVC differences is near the location of the modeled wildfire ozone plume in eastern Arizona.

The largest differences in current year ozone DVC and the 2028 Base Case DVF occurs in the eastern part of the domain with reductions of -4 to-11 ppb that are coming in from east Texas where there are larger emission reductions due to larger population centers. Over most of New Mexico, there are small reductions in the -1 to -4 ppb range with reductions in the -4 to -6 ppb range near Albuquerque. However, within the Permian and San Juan Basins there are small areas of ozone DVF increases with the largest increase of +3 ppb.

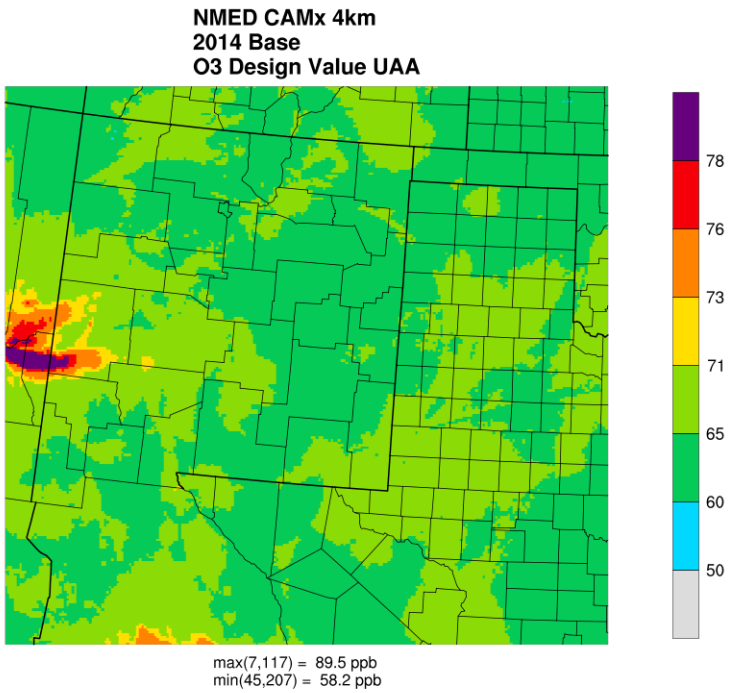

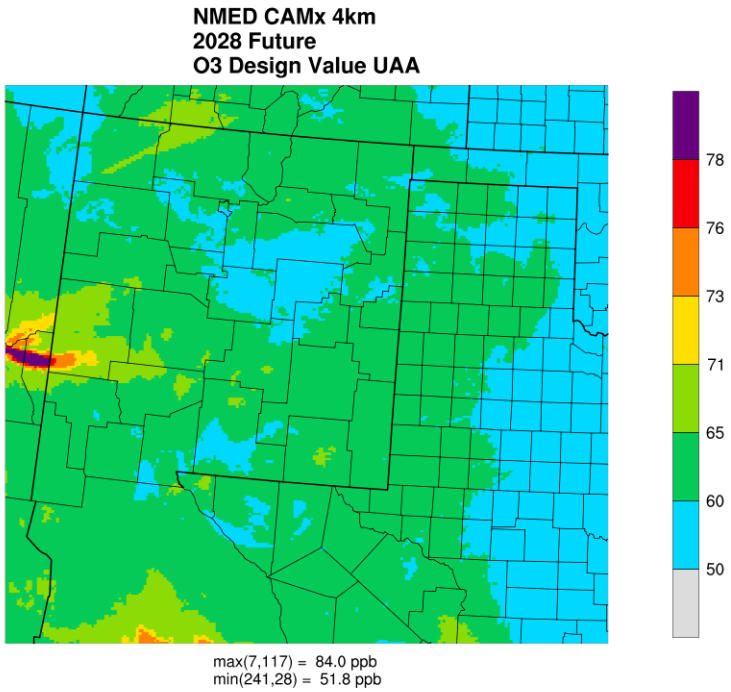

Figure 7-1. SMAT UAA current year ozone $DVC_{2012\text{-}2016}$ and projected 2028 future year ozone DVF for the 2028 Base Case using spatial interpolation with concentration gradients.

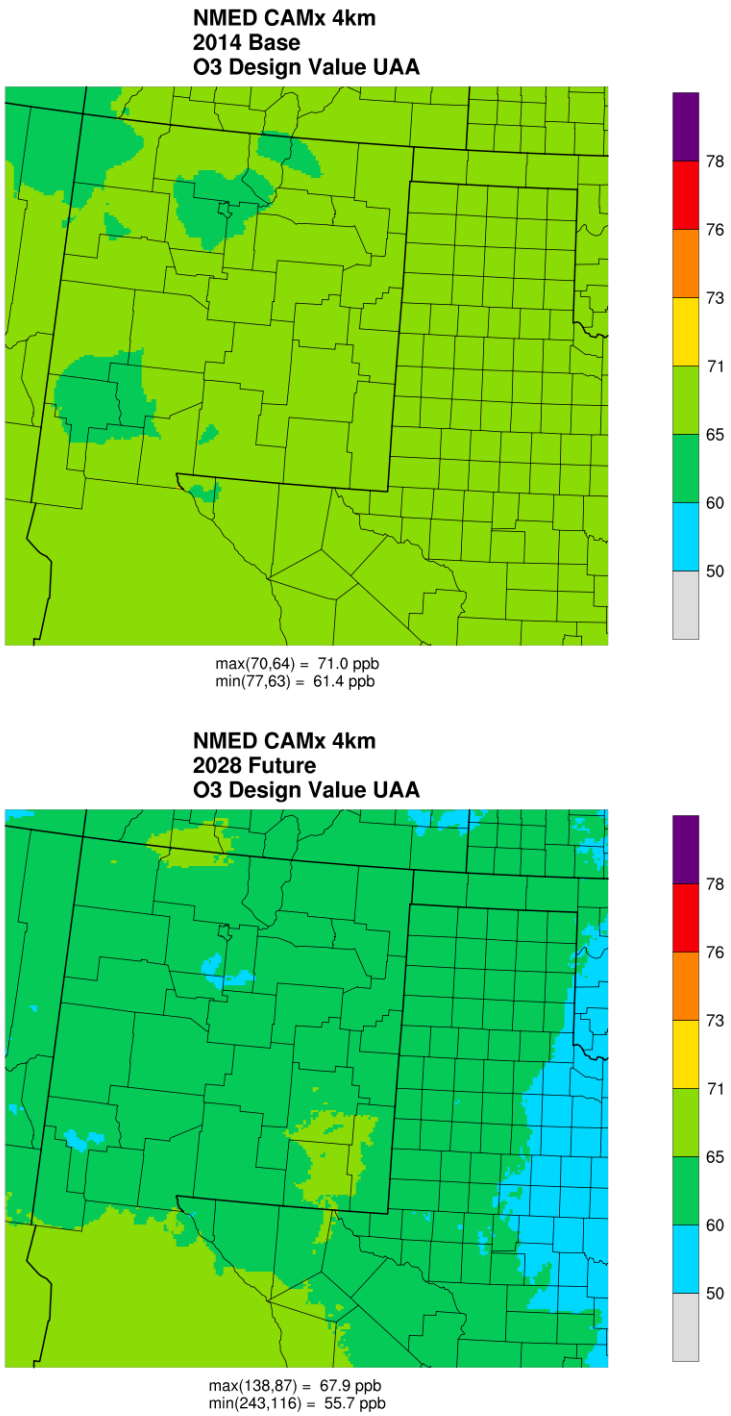

Figure 7-2. SMAT UAA current year ozone $DVC_{2012\text{-}2016}$ (top) and projected 2028 future year ozone DVF for the 2028 Base Case using spatial interpolation without concentration gradients.

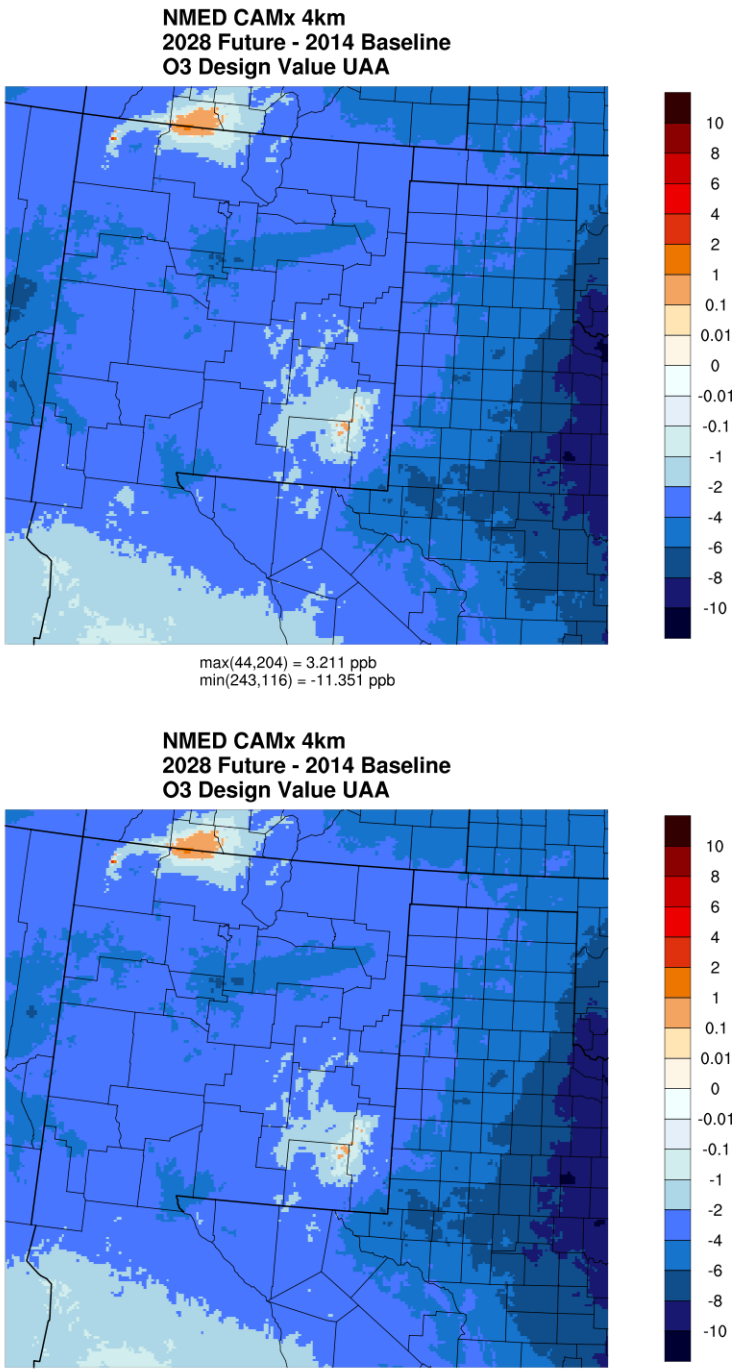

Figure 7-3. Differences between SMAT UAA current year ozone $DVC_{2012\text{-}2016}$ and projected 2028 future year ozone DVF for the 2028 Base Case using spatial interpolation with (top) and without (bottom) concentration gradients.

7.4 2014v2 and 2028 MDA8 Ozone Concentrations

In this section we present spatial maps of daily MDA8 ozone and the differences in MDA8 ozone for the 2014v2 and 2028 Base Case CAMx simulations for six example days. MDA8 ozone concentration and difference plots were generated for all ~100 days of the modeling episode, most of which were fairly low ozone concentration days so are of less interest.

7.4.1 Daily 2014v2 and 2028 Base Case MDA8 Ozone Concentrations

Figures 7-4 through 7-9 display example spatial maps of MDA8 ozone concentrations for the CAMx 2014v2 and 2028 Base Case simulations and their differences for six example days.

The most prominent features in the estimated MDA8 ozone concentrations on May 17, 2014 are locations of very high (> 80 ppb) ozone concentrations in eastern Arizona and southwest New Mexico (Figure 7-4). These high ozone concentrations have a signature of ozone from wildfires with the largest being an ozone plume being transported into western New Mexico from a wildfire in eastern Arizona. Although there are no ozone monitors located in the center of these model-estimated highly elevated ozone plumes, the Chino Copper Smelter site in Grant County is within the edge of the plume where the model estimates MDA8 ozone concentrations in the 65-71 ppb range that match the observed concentrations at this site extremely well for the May-June 2014 portion of the episode (see Appendix A in Ramboll and WESTAR, 2020c; 2021). Over most of New Mexico, the 2028 Base Case has lower MDA8 ozone concentrations with reductions as high as -11 ppb in southwest Torrance County. However, the 2028 Base Case has MDA8 ozone increases in the San Juan and Permian Basins with a maximum MDA8 ozone increase of +5 ppb in Eddy County.

On June 5, 2014, the 2014v2 Base Case has CAMx-estimated MDA8 ozone concentrations in the 65-71 ppb range in northwest New Mexico and in Doña Ana County with even a small location of MDA8 ozone exceeding the 2015 ozone NAAQS in the northeast corner of San Juan County and a modeled peak MDA8 ozone concentration of 72.9 ppb occurring in El Paso just over the border from Doña Ana County (Figure 7-5). Although the emission changes from 2014v2 to 2028 reduce the intrusion of elevated ozone entering Doña Ana County from El Paso, the elevated ozone in northwest New Mexico is increased. The area of estimated MDA8 ozone in San Juan County that is above the 2015 ozone NAAQS is larger in the 2028 Base Case than the 2014v2 Base Case and stretches into Rio Arriba County with a peak ozone value of 74 ppb in Colorado at the border with New Mexico. As shown in the MDA8 ozone difference plot in Figure 7-5, increases in MDA8 ozone concentrations in the 2028 Base Case are due to increased O&G emissions within the Permian and San Juan Basins.

Although the 2014v2 and 2028 Base Case estimated MDA8 ozone on July 12, 2014 is well below the NAAQS (mostly < 60 ppb with small pockets in the 60-65 ppb range), the 2028 Base Case has increases MDA8 ozone in the San Juan and Permian Basins with a maximum increase of +11.4 ppb (Figure 7-6). The maximum decrease in MDA8 ozone is -7.6 ppb near Albuquerque.

On July 24, 2014, the CAMx 2014v2 Base Case estimates elevated MDA8 ozone concentrations in northwest New Mexico with values even exceeding the 2015 ozone

NAAQS in San Juan County and a peak value of 74.7 ppb in Colorado at the border with New Mexico (Figure 7-7). The 2028 Base Case has lower ozone than the 2014v2 Base Case across New Mexico with only small areas of ozone increases. The area of MDA8 ozone in San Juan County that was above the 2015 ozone NAAQS in the 2014v2 Base Case is reduced to below the NAAQS in the 2028 Base Case, although the peak MDA8 ozone in Colorado at the border of New Mexico still exceeds the NAAQS (71.3 ppb).

The CAMx 2014v2 Base Case estimates a high peak MDA8 ozone concentration of 78.4 ppb in Albuquerque with several additional areas of high ozone above the NAAQS occurring in other northern New Mexico Counties on July 26, 2014 (Figure 7-8). Although the 2028 Base Case has reduced almost all of the areas with 2014v2 MDA8 ozone above the NAAQS, there is still an estimate ozone peak above the NAAQS (72.3 ppb) just west of Albuquerque in northeast Cibola County. Ozone increases are seen in the Permian and San Juan Basins on July 26 with the highest increase of +5.7 ppb occurring in the San Juan Basin.

An ozone peak of 74.1 ppb occurs on August 14 on the border of Doña Ana County and El Paso with ozone in excess of the NAAQS stretching into Doña County (Figure 7-9). The emission reductions in the 2028 Base Case appear reduce the estimated ozone in Doña County to below the NAAQS, although the peak ozone (71.2 ppb) just over the border in El Paso still exceeds the NAAQS. Ozone increases in the Permian and San Juan Basins are mostly less than +1 ppb and fairly isolated on this day.

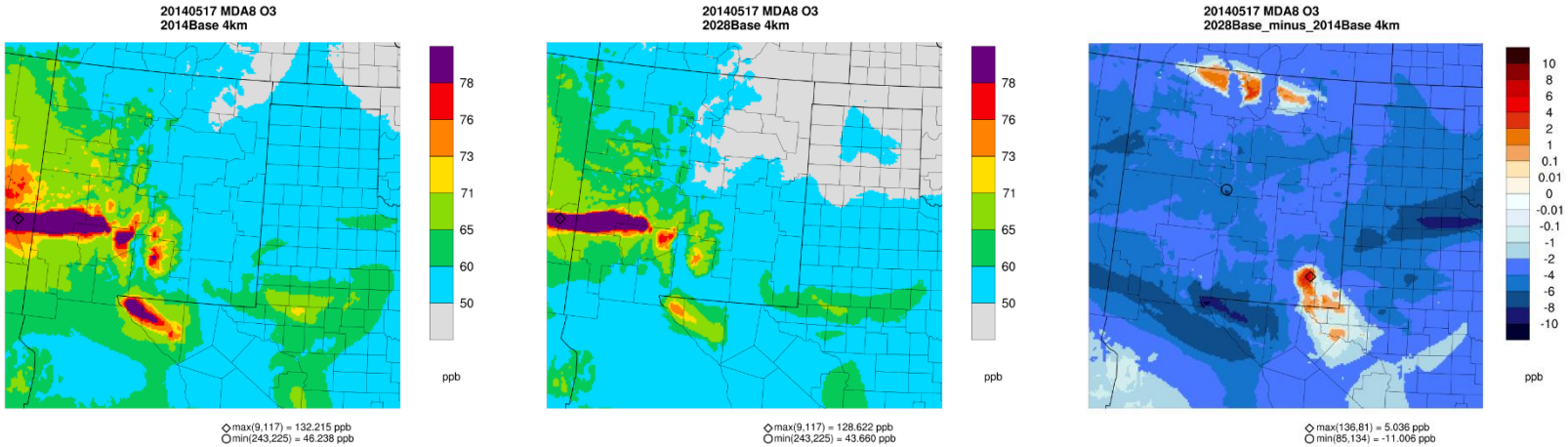

Figure 7-4. CAMx estimated MDA8 ozone concentrations (ppb) on May 17, 2014 for the 2014v2 Base Case (left), 2028 Base Case (middle) and their difference (right).

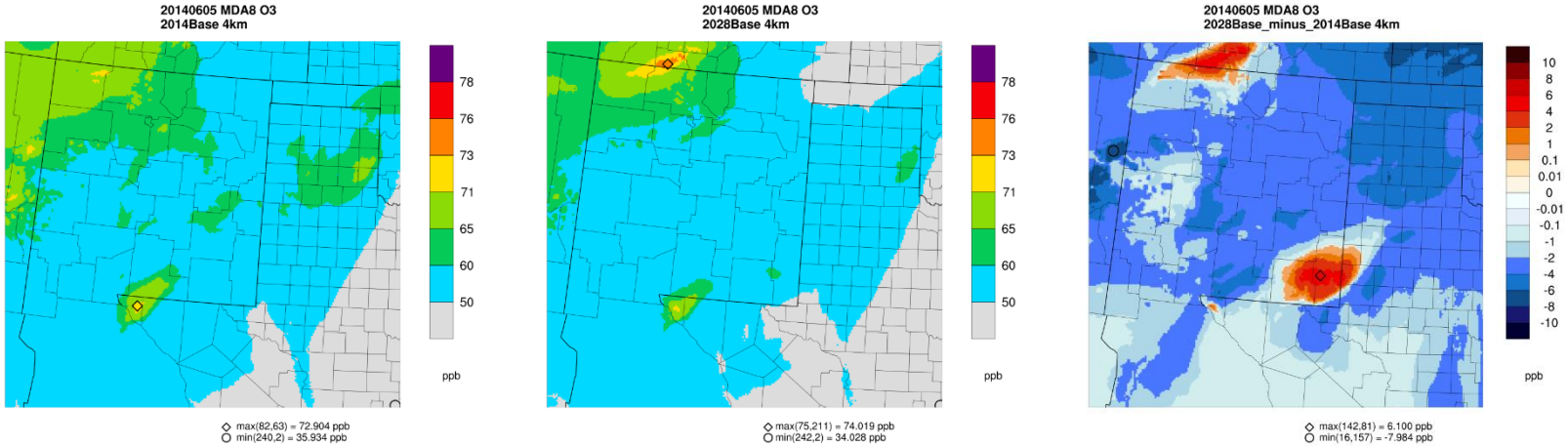

Figure 7-5. CAMx estimated MDA8 ozone concentrations (ppb) on June 5, 2014 for the 2014v2 Base Case (left), 2028 Base Case (middle) and their difference (right).

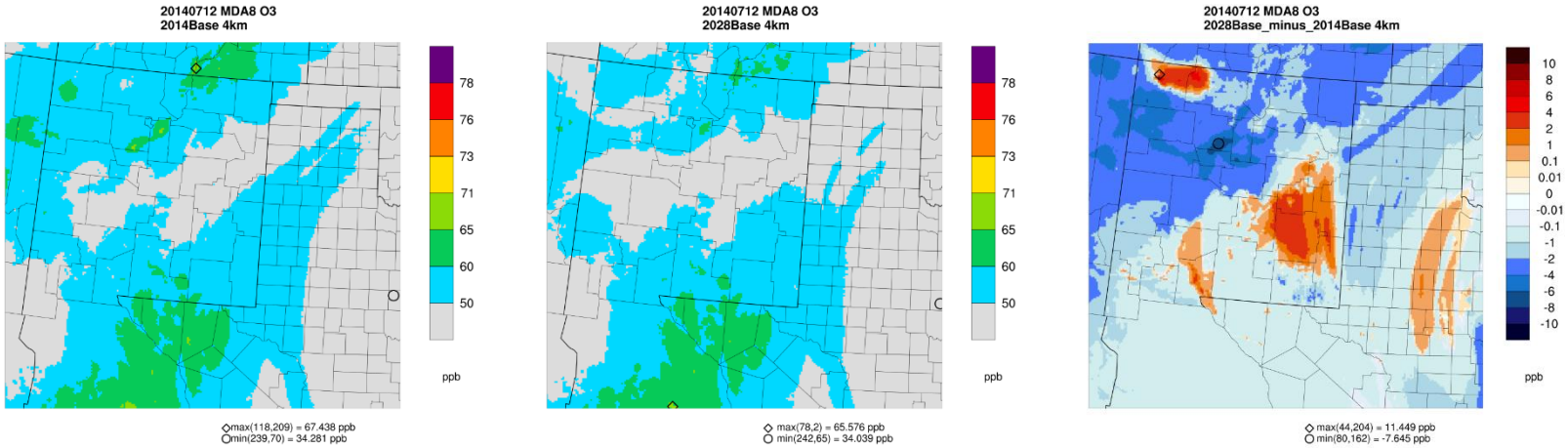

Figure 7-6. CAMx estimated MDA8 ozone concentrations (ppb) on July 12, 2014 for the 2014v2 Base Case (left), 2028 Base Case (middle) and their difference (right).

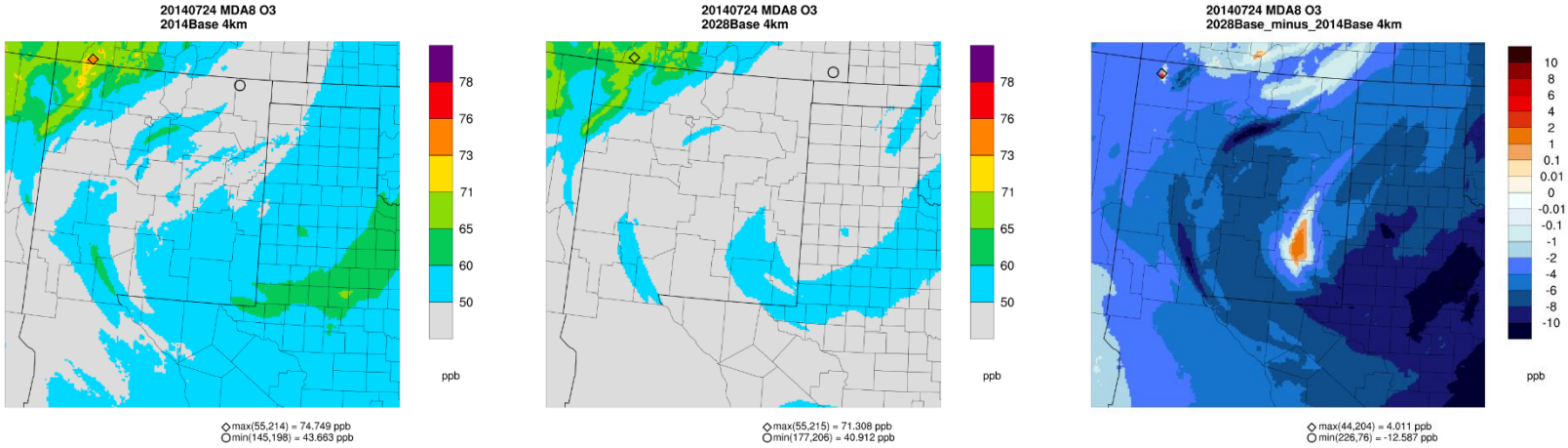

Figure 7-7. CAMx estimated MDA8 ozone concentrations (ppb) on July 24, 2014 for the 2014v2 Base Case (left), 2028 Base Case (middle) and their difference (right).

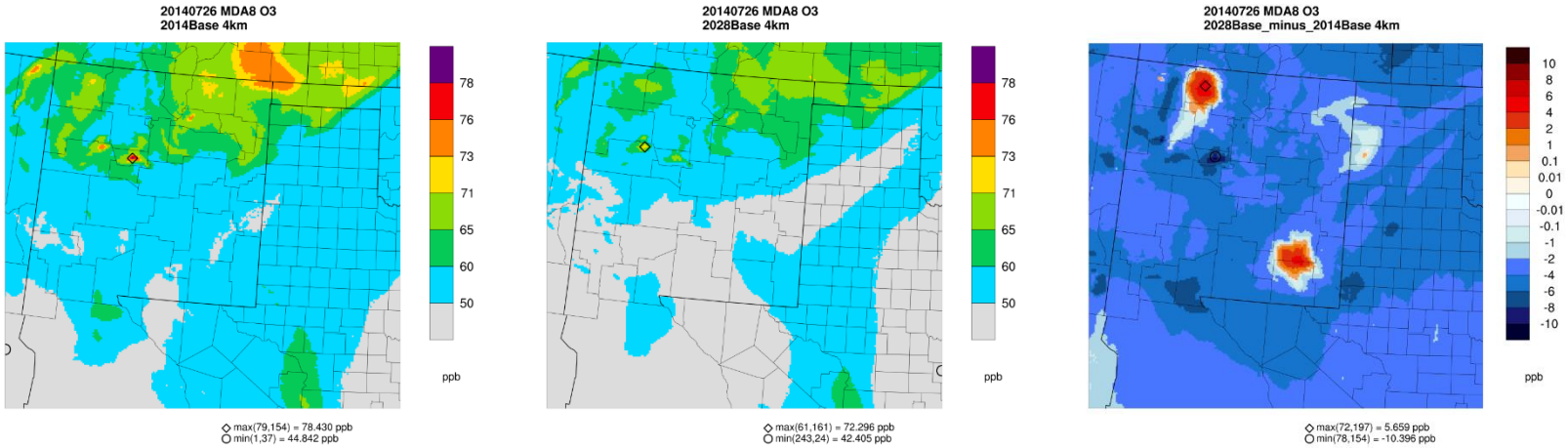

Figure 7-8. CAMx estimated MDA8 ozone concentrations (ppb) on July 26, 2014 for the 2014v2 Base Case (left), 2028 Base Case (middle) and their difference (right).

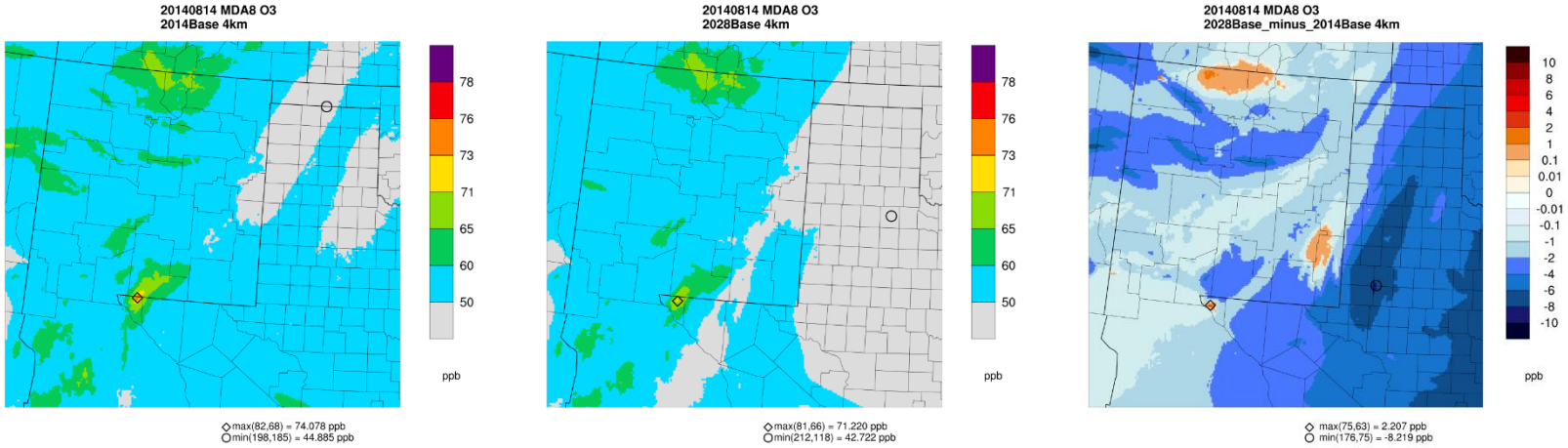

Figure 7-9. CAMx estimated MDA8 ozone concentrations (ppb) on August 14, 2014 for the 2014v2 Base Case (left), 2028 Base Case (middle) and their difference (right).

7.4.2 Comparison of Episode Maximum MDA8 and SMAT UAA Ozone DVF Differences

Figure 7-10 compare the differences in episode maximum MDA8 ozone concentrations and SMAT UAA ozone DVs between the 2014v2 and 2028 Base Case simulations (the SMAT UAA ozone DV differences are without using concentration gradients and was shown previously in the bottom panel of Figure 7-3). Not surprisingly, since the SMAT UAA DVs represents an average across several modeling days, the episode maximum MDA8 ozone differences have higher changes than the SMAT UAA ozone differences with a maximum increase of +5 ppb vs. +3 ppb and maximum decrease of -12 ppb vs. -11 ppb for the, respectively, episode maximum MDA8 ozone and UAA DVs. The largest decreases occur in Albuquerque and in southern Doña Ana County on the border with El Paso. The largest increases in ozone occur in the San Juan and Permian Basin.

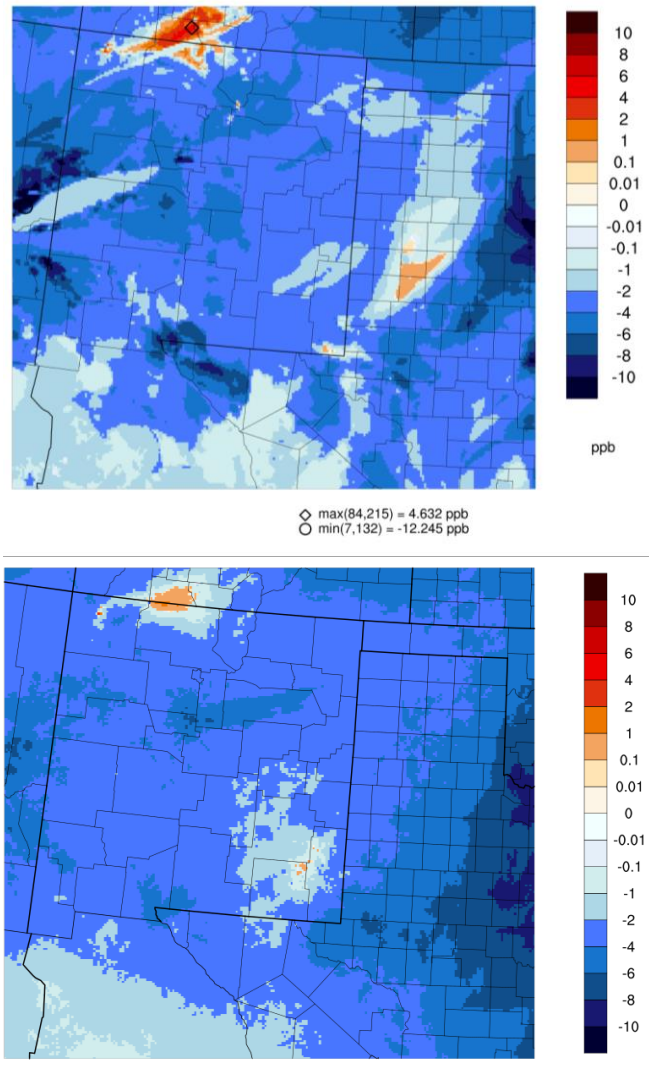

Figure 7-10. Differences in episode maximum MDA8 ozone concentrations (top) and SMAT UAA ozone DVs (bottom) between the 2014v2 and 2028 CAMx Base Case simulations.

8. 2028 OIL AND GAS CONTROL STRATEGY MODELING AND OZONE DESIGN VALUE PROJECTIONS

The implementation of the proposed New Mexico oil and gas (O&G) ozone precursor control strategy reduces VOC and NO_x emissions in the New Mexico portions of the San Juan and Permian Basins, as discussed in Section 4.5. Most of the O&G emission reduction in the San Juan Basin occur in northeastern San Juan and northwestern Rio Arriba Counties. While most of the emission reductions in the Permian Basin occur in Eddy and Lea Counties.

8.1 2028 Ozone Design Value Comparisons

The same procedures as used to project 2028 ozone DVFs for the CAMx 2028 Base Case (DVF_{Base}) were used to project the 2028 ozone DVFs for the 2028 O&G Control Strategy scenario (DVF_{Cntl}). These procedures start with an observed current year design value that is an average of 3 design values over 5-years ($DVC_{2012\text{-}2016}$) that is scaled by Relative Response Factors (RRFs) based on the ratio of the 2028 O&G Control Strategy over the 2014v2 Base Case CAMx ozone results to obtained a projected 2028 ozone DVF_{Cntl} for the 2028 O&G Control Strategy.

8.1.1 Ozone Design Values at the Monitoring Sites

Table 8-1 list the current year ozone $DVC_{2012\text{-}2016}$ and the projected 2028 ozone DVFs for the 2028 Base Case and 2028 O&G Control Strategy and the differences in the two 2028 ozone DVFs (DVF_{Cntl} – DVF_{Base}).

At monitoring sites in northern New Mexico, the 2028 ozone DVF_{Base} values are estimated to be reduced by -0.2 to -1.5 ppb due to the 2028 O&G Control Strategy with the largest reductions occurring at the Navajo Lake (-1.5 ppb) and Substation (-1.2 ppb) monitoring sites in San Juan County. After implementation of the 2028 O&G Control Strategy, the projected 2028 ozone DVF_{Cntl} in northern New Mexico range from 58.1 to 63.3 ppb.

Although not as close to the 2028 O&G emission reductions, the 2028 projected ozone DVF_{Cntl} in Bernalillo County see benefits of the 2028 O&G Control Strategy with ozone DVF reductions of -0.2 to -0.5 ppb. After implementation of the 2028 O&G Control Strategy, the projected 2028 ozone DVF_{Cntl} range from 58.8 to 62.1 ppb in Bernalillo County.

The 2028 ozone DVF reductions due to the 2028 O&G Control Strategy at the southern New Mexico monitoring sites range from -0.2 to -0.7 ppb with the largest reductions occurring at the Hobbs (-0.7 ppb) and Carlsbad (-0.3 ppb) monitoring sites in, respectively, Eddy and Lea Counties that lie within the Permian Basin. The other monitoring sites in southern New Mexico are farther away from the Permian Basin so have much more modest reductions in ozone DVFs (-0.1 to -0.2 ppb) due to the controls on oil and gas sources. After implementation of the 2028 O&G Control Strategies, the projected 2028 ozone DVF_{Cntl} at southern New Mexico sites range from 58.9 ppb to 66.8 ppb.

Table 8-1. Observed ozone $DVC_{2012-2016}$ and projected 2028 ozone DVFs for the 2028 Base Case and 2028 O&G Control strategy and differences in the 2028 ozone DVFs ($DVF_{Cntl} - DVF_{Base}$).

AQS_ID	2012-16	Projected 2028 DVF			Site Name	State	County
	DVC (ppb)	Base (ppb)	Cntl (ppb)	Cntl - Base			
Northern New Mexico							
350390026	64.0	60.8	60.0	-0.8	Coyote Ranger District	NM	Rio Arriba
350431001	64.0	58.4	58.1	-0.3	Bernalillo (E Avenida)	NM	Sandoval
350450009	64.3	61.0	60.2	-0.8	Bloomfield	NM	San Juan
350450018	67.0	64.8	63.3	-1.5	Navajo Lake	NM	San Juan
350451005	63.7	60.8	59.6	-1.2	Substation	NM	San Juan
350490021	64.3	60.6	60.4	-0.2	Santa Fe Airport	NM	Santa Fe
Bernalillo County							
350010023	66.3	60.9	60.7	-0.2	Del Norte HS	NM	Bernalillo
350010024	68.0	62.3	62.0	-0.3	South East Heights	NM	Bernalillo
350010029	66.0	61.0	60.5	-0.5	South Valley	NM	Bernalillo
350010032	67.0	62.6	62.1	-0.5	Westside	NM	Bernalillo
350011012	65.0	59.1	58.8	-0.3	Foothills	NM	Bernalillo
Southern New Mexico							
350130008	66.3	60.0	59.8	-0.2	La Union	NM	Doña Ana
350130017	67.0	61.9	61.8	-0.1	Sunland Park City Yard	NM	Doña Ana
350130020	67.0	62.3	62.2	-0.1	Chaparral	NM	Doña Ana
350130021	72.0	67.0	66.8	-0.2	Desert View	NM	Doña Ana
350130022	71.3	66.1	66.0	-0.1	Santa Teresa	NM	Doña Ana
350130023	65.0	60.3	60.2	-0.1	Solano	NM	Doña Ana
350151005	69.0	66.7	66.4	-0.3	Carlsbad	NM	Eddy
350171003	62.0	59.0	58.9	-0.1	Chino Copper Smelter	NM	Grant
350250008	66.0	64.0	63.3	-0.7	Hobbs Jefferson	NM	Lea
350290003	66.0	62.7	62.5	-0.2	Deming Airport	NM	Luna
350610008	66.3	62.2	62.0	-0.2	Los Lunas (Los Lentes)	NM	Valencia

Table 8-2 list the observed ozone $DVC_{2012\text{-}2016}$ and projected 2028 ozone DVFs for monitoring sites outside of New Mexico but within the 4-km NM modeling domain. There are small reductions in projected ozone DVFs in Arizona (0.0 and -0.1 ppb) and El Paso, Texas (0.0 to -0.2 ppb) due to the New Mexico 2028 O&G Control Strategy. However, there are more substantial reductions in projected 2028 ozone DVFs at sites in La Plata (-0.7 and -0.9 ppb) and Montezuma (-0.5 ppb) counties in southwestern Colorado that are adjacent to the New Mexico portion of the San Juan Basin where some of the 2028 O&G Control Strategy emission reductions occur.

Table 8-2. Observed ozone $DVC_{2012\text{-}2016}$ and projected 2028 ozone DVFs for the 2028 Base Case and 2028 O&G Control strategy and differences in the 2028 ozone DVFs ($DVF_{Cntl} - DVF_{Base}$).

AQS_ID	2012-16	Projected 2028 DVF			Site Name	State	County
	DVC (ppb)	Base (ppb)	Cntl (ppb)	Cntl - Base			
Arizona, Colorado and Texas							
40038001	68.0	64.0	63.9	-0.1	Chiricahua NM	AZ	Cochise
40170119	66.7	61.9	61.9	0.0	Petrified Forest	AZ	Navajo
80677001	67.7	66.1	65.2	-0.9	UTE 1	CO	La Plata
80677003	66.7	64.4	63.7	-0.7	UTE 3	CO	La Plata
80830006	63.0	59.7	59.2	-0.5	Cortez - Health Dept	CO	Montezuma
80830101	66.0	62.4	61.9	-0.5	Mesa Verde NP	CO	Montezuma
481410029	61.0	58.0	57.9	-0.1	Ivanhoe	TX	El Paso
481410037	71.0	66.2	66.1	-0.1	El Paso UTEP	TX	El Paso
481410044	67.7	62.5	62.4	-0.1	El Paso Chamizal	TX	El Paso
481410055	62.7	59.2	59.1	-0.1	Ascarate Park SE	TX	El Paso
481410057	66.5	63.3	63.2	-0.1	Socorro Hueco	TX	El Paso
481410058	68.0	63.4	63.4	0.0	Skyline Park	TX	El Paso
483819991	66.7	62.4	62.2	-0.2	Palo Duro	TX	Randall

8.1.2 2028 O&G Control Strategy Ozone DVF Unmonitored Area Analysis

The SMAT Unmonitored Area Analysis (UAA) was applied to estimate the spatial distribution of projected 2028 ozone DVF_{Cntl} throughout the 4-km NM modeling domain. Figure 8-1 displays the spatial distribution of the SMAT UAA ozone DVFs for the 2028 Base Case and 2028 O&G Control Strategy where the SMAT UAA was applied without using concentration gradients in the spatial interpolation of the $DVC_{2012\text{-}2016}$. Within New Mexico, the projected 2028 DVF_{Base} tends to be mostly in the 60-71 ppb range, with a few small locations with the values dropping below 60 ppb. The highest ozone concentrations (65-71 ppb) in New Mexico for the 2028 ozone DVF_{Base} occur in the San Juan and Permian Basin as indicated by the lighter green shading (Figure 8-1, top panel). When the O&G Control Strategy is applied, the ozone DVF_{Cntl} in the San Juan Basin is lower (i.e., in the 60-65 ppb with the light green shading completely gone) and the area of ozone DVF_{Base} in the 65-71 ppb range is greatly reduced for the ozone DVF_{Cntl} case.

Figure 8-2 shows a spatial map of the differences in SMAT UAA projected 2028 ozone DVFs between the 2028 Base Case and 2028 O&G Control Strategy (DVF_{Cntl} – DVF_{Base}) where the top and bottom panels represent ozone DVF differences without and with using the modeled concentration gradients in the SMAT UAA spatial interpolation. As shown in Chapter 7, use of concentration gradients has a large effect on the projected 2028 ozone DVFs, but it has no material effect on the differences in the ozone DVFs for the two 2028 emission scenarios as the plots appear almost identical.

Within the Permian Basin, the 2028 O&G Control Strategy reduces the ozone DVF by -0.5 to -1.5 ppb with most of the largest reductions (-1.0 to -1.5 ppb) occurring in Lea County. The 2028 O&G Control Strategy has a larger effect on the 2028 ozone DVF in the San Jun Basin with reductions of -1.0 to -3.0 ppb with the largest reductions (-2.0 to -3.0 ppb) straddling the New Mexico/Colorado state line at Rio Arriba/Archuleta Counties.

There are also isolated grid cells of SMAT UAA ozone DVF increases in the Permian and San Juan Basins due to the 2028 O&G Control Strategy. These ozone DVF increases appear to be several isolated 4-km grid cells and are likely due to highly localized ozone increases at the locations of O&G point source NO_x emission reductions due to the O&G Control Strategy. Most (e.g., 90-95%) fresh emissions of oxides of nitrogen (NO_x) are in the form of nitric oxide (NO) that is converted fairly quickly to nitrogen dioxide (NO_2). The NO-O_3 titration reaction ($NO + O_3 \rightarrow NO_2 + O_2$) occurs very quickly and can locally deplete ozone concentrations due to the fresh NO emissions while forming NO_2 that can form ozone further downwind during photochemistry. This can result in localized ozone increases when NO_x emissions are reduced in high NO_x emission areas, such as large urban areas or within NO_x point source plumes. The so called "NO_x Disbenefits" effects (i.e., local ozone increases due to NO_x emission reductions) has been verified in numerous measurement and modeling studies and has been one reason that in the past Los Angeles was more likely to have higher ozone on weekend days than weekdays because of the lower morning NO_x emissions on weekend days (the "weekend effect"). Over the years as NO_x emissions have been controlled, the effects of "NO_x Disbenefits" has been lessening but can still occur in major urban areas and in NO_x point source plumes.

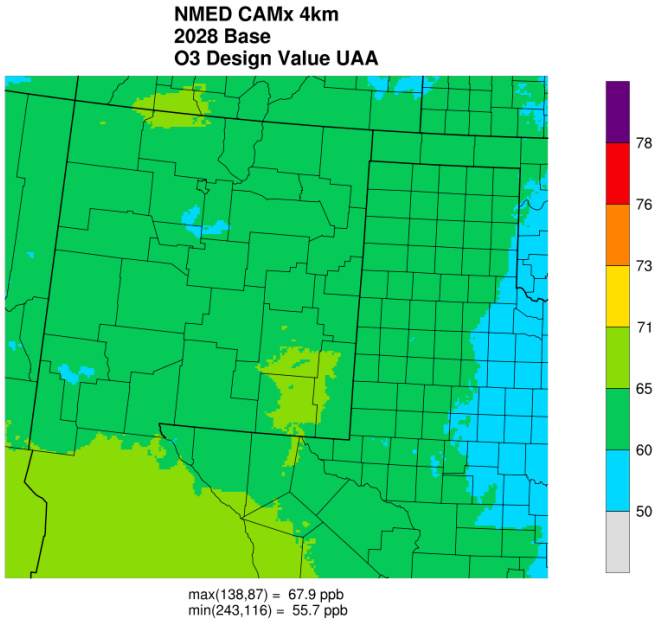

Figure 8-1. SMAT UAA spatial distribution of projected 2028 ozone DVF_{Base} (top) and DVF_{Cntl} (bottom).

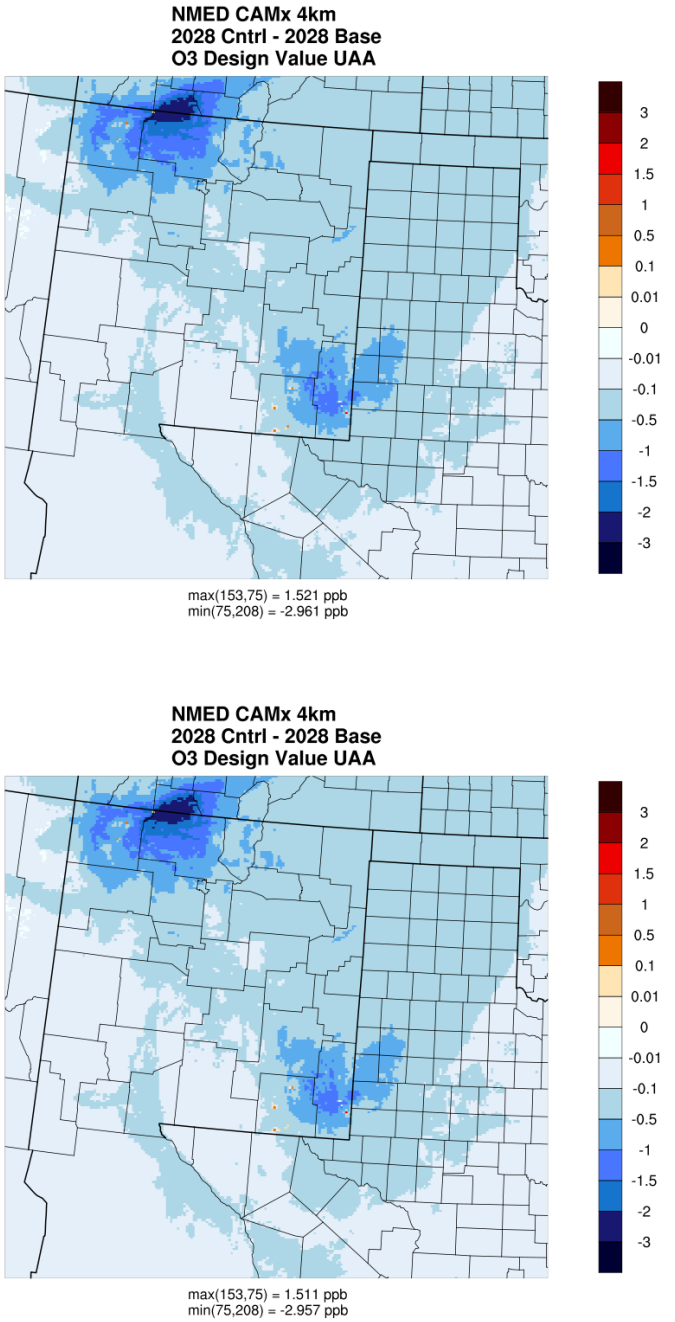

Figure 8-2. Differences in SMAT UAA projected 2028 ozone DVFs (ppb) for the 2028 Base Case and 2028 O&G Control Strategy (DVF_{Cntl} – DVF_{Base}) running SMAT without (top) and with (bottom) using modeled concentration gradients in the $DVC_{2012\text{-}2016}$ spatial interpolation.

8.2 2028 Base Case and 2028 O&G Control Strategy MDA8 Ozone Concentrations

In this section we present spatial maps of modeled MDA8 ozone and the differences in MDA8 ozone for the 2028 Base Case and O&G Control Strategy emission scenarios for several example days.

8.2.1 Daily 2014v2 and 2028 Base Case MDA8 Ozone Concentrations

Figures 8-3 through 8-8 display example spatial maps of MDA8 ozone concentrations and their differences for the two CAMx 2028 emission scenarios for the same six days that were used to compare the 2014v2 and 2028 Base Case results that were presented in Figures 7- through 7-9. However, in the MDA8 difference plots for the two 2028 emission scenarios, a finer scale is used to better illustrate the 2028 MDA8 ozone differences due to the implementation of the O&G Control Strategy in 2028.

As discussed in Chapter 7, CAMx estimates very high MDA8 ozone concentrations on May 17, 2014 that are due to emissions from wildfires (Figure 8-3). The 2028 O&G Control Strategy scenario reduces the MDA8 ozone within the San Juan and Permian Basins by from -1 to -3 ppb on May 17th, with ozone reductions of -0.1 to -0.5 ppb spanning the area between the two Basins. There are areas of MDA8 ozone increases around the western edges of the O&G control area in the San Juan Basin with ozone increases as high as +1.4 ppb.

On June 5, 2014, the 2028 Base Case has CAMx-estimated MDA8 ozone concentrations in excess of the 70 ppb 2015 ozone NAAQS in northeast San Juan and northwest Rio Arriba Counties with a peak MDA8 ozone of 74 ppb on the border with and just inside of Colorado (Figure 8-4). The 2028 O&G Control Strategy is very effectively reducing these high MDA8 ozone exceedances in the San Juan Basin with ozone reductions of up to -4.6 ppb that reduce the MDA8 ozone to below the 2015 ozone NAAQS in San Juan and Rio Arriba Counties. MDA8 ozone is also reduced in the Permian Basin, although not nearly as great as in the San Juan Basin on this day. There are very small areas of ozone increases due to the 2028 O&G Control Strategy within New Mexico that are less than 0.1 ppb, although they are as high as 0.4 ppb near the Four Corners location.

The 2028 Base Case MDA8 ozone on July 12, 2014 in New Mexico is mostly below 60 ppb (blue) with some isolated areas slightly above that (green; Figure 8-5). The 2028 O&G Control Strategy results in MDA8 ozone reductions of more than -0.5 ppb over large areas expanding out of the two O&G Basins with reductions as high as -4.6 ppb in the San Juan Basin and as high as -1.0 to -1.5 ppb reduction in the Permian Basin. In the Permian Basin in the southeast corner of New Mexico, there are ozone increases due to the 2028 O&G Control Strategy that appear to be mostly in the +0.1 to +0.5 ppb range, with a peak increase of +1.6 ppb.

Elevated MDA8 ozone concentrations approaching, but below, the 2015 ozone NAAQS are estimated to occur in San Juan County on July 24, 2014 with a peak value of 71.3 ppb that is above the NAAQS occurring right across the border in Colorado (Figure 8-6). Although the 2028 O&G Control Strategy reduces the MDA8 ozone on this day across wide areas of New Mexico, with ozone reductions as high as -2.8 ppb in the Permian Basin, there are estimated increases in MDA8 ozone in San Juan County. These MDA8 ozone increases in San Juan County due to the 2028 O&G Control Strategy and are as high as +6.4 ppb. These increased in MDA8 ozone concentrations in San Juan County

due to the 2028 O&G Control Strategy are sufficient to increase the MDA8 ozone concentration in one grid cell to 71.0 ppb, which exceeds the 2015 ozone NAAQS.

On July 26th there are patches of elevated MDA8 ozone in the 2028 Base Case in the 65-71 ppb range in northern New Mexico with a peak MDA8 ozone concentration of 72.3 ppb in the northeast corner of Cibola County that exceeds the ozone NAAQS (Figure 8-7). The 2028 O&G Control Strategy reduces the MDA8 ozone Peak in Cibola County by -0.4 ppb to 71.9 ppb, which still exceeds the NAAQS. The 2028 O&G Control Strategy results in reductions in MDA8 ozone concentrations in excess of -3.0 ppb in the San Juan and Permian Basins with a maximum reduction 0f -5.4 ppb. The ozone reductions in the San Juan Basin are sufficient to reduce MDA8 ozone concentrations that were in the 65-71 ppb range in the 2028 Base Case to below 65 ppb.

On August 14, 2014, there are small areas of MDA8 ozone concentrations in the 65-71 ppb range in New Mexico on the northern border with Colorado and in southern border in Doña Ana County with the domain-wide peak ozone of 71.2 ppb just over the border from Doña Ana County in El Paso (Figure 8-8). The 2028 O&G Control Strategy has little effects on the MDA8 ozone peak in El Paso that remains at 71.2 ppb. The 2028 O&G Control Strategy reduces MDA8 ozone in the San Juan and Permian Basins by as much as -1.8 ppb; the ozone reductions in San Juan County reduce the size of the elevated ozone in the 65-71 ppb range. There are also areas of ozone increases to the west and northeast of the San Juan Basin due to the 2028 O&G Control Strategy that are as much as +1.6 ppb.

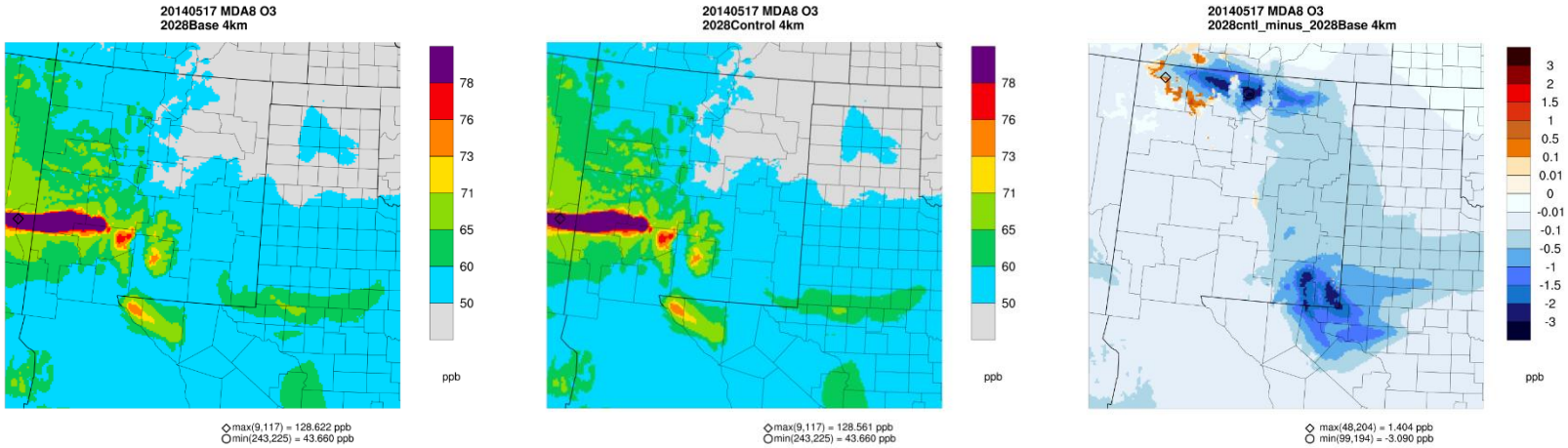

Figure 8-3. CAMx estimated MDA8 ozone concentrations (ppb) on May 17, 2014 for the 2028 Base Case (left), 2028 O&G Control Strategy Case (middle) and their difference (right).

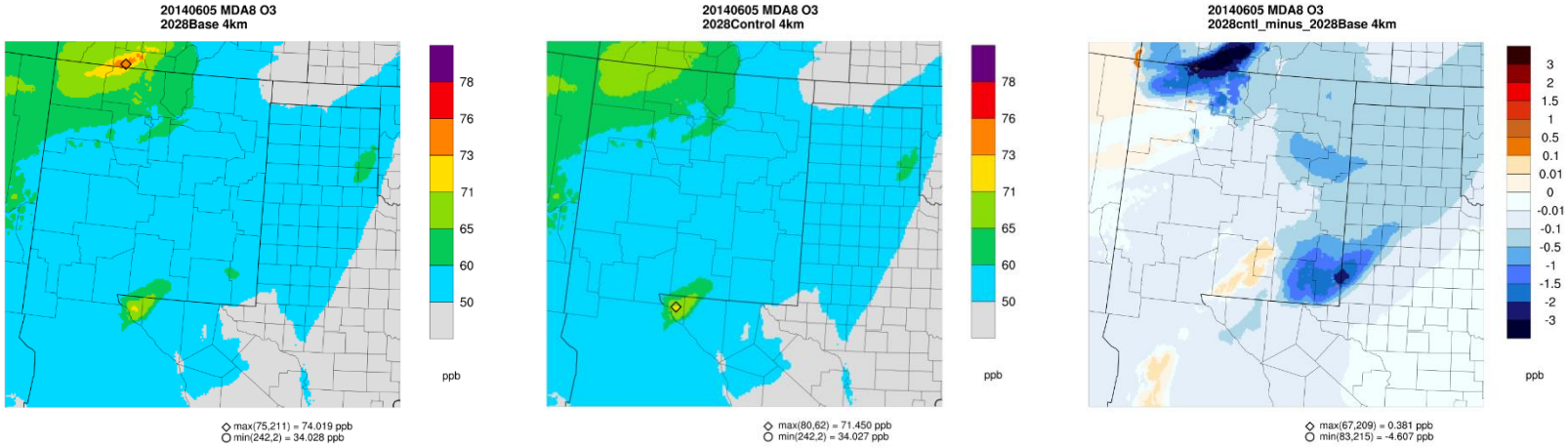

Figure 8-4. CAMx estimated MDA8 ozone concentrations (ppb) on June 5, 2014 for the 2028 Base Case (left), 2028 O&G Control Strategy (middle) and their difference (right).

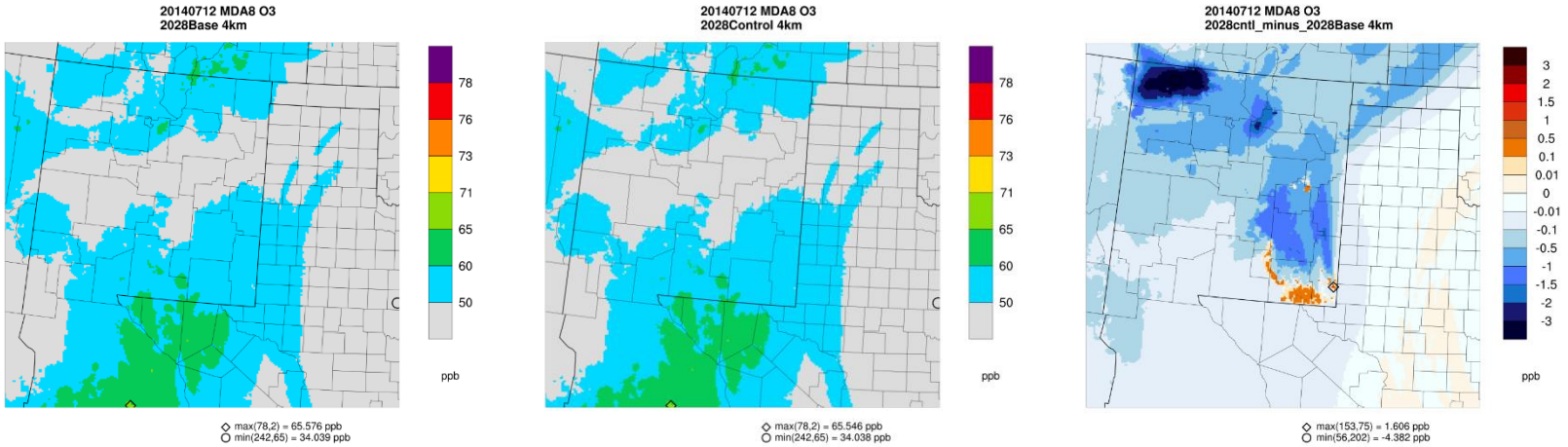

Figure 8-5. CAMx estimated MDA8 ozone concentrations (ppb) on July 12, 2014 for the 2028 Base Case (left), 2028 O&G Control Strategy (middle) and their difference (right).

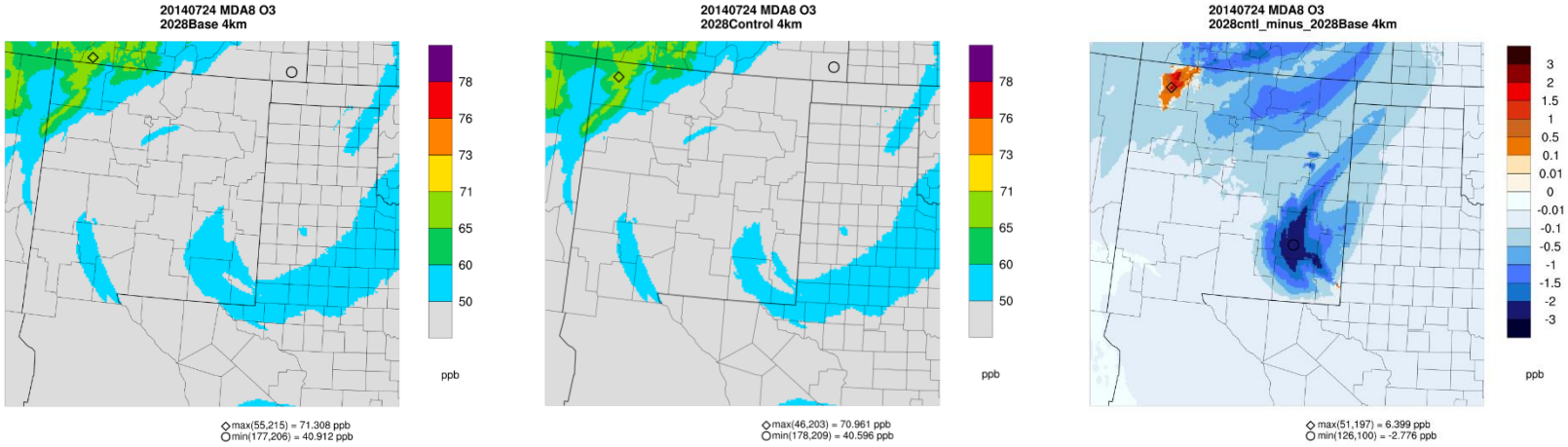

Figure 8-6. CAMx estimated MDA8 ozone concentrations (ppb) on July 24, 2014 for the 2028 Base Case (left), 2028 O&G Control Strategy (middle) and their difference (right).

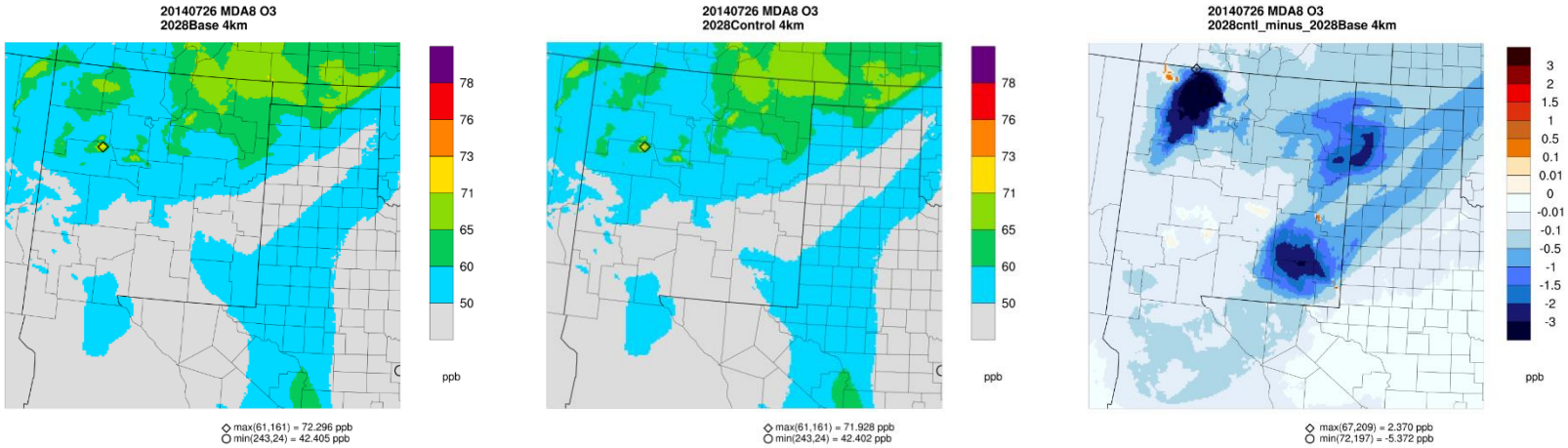

Figure 8-7. CAMx estimated MDA8 ozone concentrations (ppb) on July 26, 2014 for the 2014v2 Base Case (left), 2028 Base Case (middle) and their difference (right).

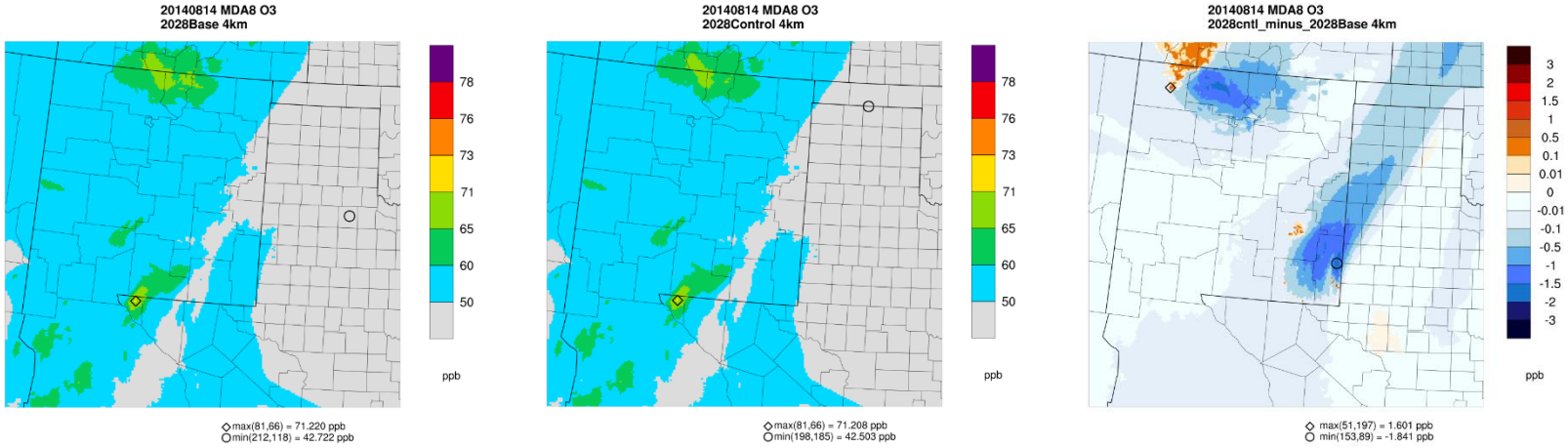

Figure 8-8. CAMx estimated MDA8 ozone concentrations (ppb) on August 14, 2014 for the 2014v2 Base Case (left), 2028 Base Case (middle) and their difference (right).

8.3 Conclusions of the 2028 Base and 2028 O&G Control Strategy Modeling

The O&G Control Strategy results in wide areas of reductions in 2028 Base Case MDA8 ozone concentrations and SMAT UAA projected 2028 ozone DVFs across large portions of New Mexico, with the largest ozone reductions occurring in the San Juan and Permian Basins. There are also areas of increases in MDA8 ozone and SMAT UAA projected 2028 ozone DVFs due to the O&G Control Strategy that usually occur in isolated locations within and near the San Juan and Permian Basin. The ozone increases in the SMAT UAA projected DFVs across New Mexico due to the O&G Control Strategy occur in a few isolated grid cells in the San Juan and Permian Basins; the projected 2028 ozone DVFs at all the monitoring sites saw only ozone reductions with no ozone increases due to the O&G Control Strategy. The size of the areas and magnitudes of the ozone reductions due to the 2028 O&G Control Strategy scenario were much greater than the ozone increases.

Using the current year ozone design value from 2012-2016 ($DVC_{2012\text{-}2016}$), the projected 2028 ozone DVFs for both the 2028 Base Case and 2028 O&G Control Strategy are below the 70 ppb 2015 ozone NAAQS with the highest values for the 2028 Base and O&G Control Cases occurring at the Desert View (67.0 and 66.8 ppb) monitoring site in Doña Ana County and the Carlsbad (66.7 and 66.4 ppb) monitoring site in Eddy County. However, as noted in Chapter 1 (Table 1-1), more recent observed DVs at Desert View and Carlsbad are much higher than the observed current year $DVC_{2012\text{-}2016}$ used in the 2028 ozone DVF projections presented in Chapters 7 and 8. The sensitivity of the choice of current year DVC on the projected 2028 ozone DVFs is analyzed in Chapter 9.

9. SENSITIVITY OF PROJECTED 2028 OZONE DESIGN VALUES TO CURRENT YEAR OZONE DESIGN VALUES

Following EPA photochemical grid modeling guidance ozone projection procedures, the projected 2028 future year ozone design values (DVFs) were below the 70 ppb 2015 ozone NAAQS at all monitoring sites in New Mexico. EPA's guidance uses as a starting point for the future year ozone projections an average of three current year design values centered on the base modeling year (i.e., $DVC_{2012\text{-}2016}$). However, at many sites in New Mexico, the current year $DVC_{2012\text{-}2016}$ is lower than the most recent 2017-2019 ozone design values ($DV_{2017\text{-}2019}$). For example, at the Desert View site in Doña Ana County the most recent $DV_{2017\text{-}2019}$ is 77 ppb that is 5 ppb higher than the $DVC_{2012\text{-}2016}$ (72.0 ppb). And the most recent $DV_{2017\text{-}2019}$ at the Carlsbad site in Eddy County (79 ppb) is 7.7 ppb higher than the $DVC_{2012\text{-}2016}$ (71.3 ppb) used in the 2028 ozone DVF projections presented in Chapters 7 and 8.

In this Chapter we examine the sensitivity of the 2028 ozone DVF projections to the observed current year ozone design value (DVC) used as the starting point for the 2028 ozone DVF projections. Instead of using the $DVC_{2012\text{-}2016}$ as the starting point for the 2028 ozone DVF projections, we use the average of three ozone design values from 2015-2019 5-year period (i.e., $DVC_{2015\text{-}2019}$) and also conduct 2028 ozone DVF projections using the latest ozone $DV_{2017\text{-}2019}$ as the DVC. Note that we are still using the CAMx 2014v2 Base Case modeling results for the denominator of the RRFs used to make the 2028 ozone DVF projections that will not account for the changes in emissions between 2014 and the more current years that affect the magnitude of the ozone $DVC_{2015\text{-}2019}$ and $DV_{2017\text{-}2019}$. This includes emission reductions from mobile sources as well as emission increases from O&G sources. Thus, the 2028 ozone DVF projection sensitivity analysis to base year ozone DVC has uncertainties and will likely overstate 2028 ozone DVFs in and near the Permian Basin where the more current year O&G emissions are higher than they were in 2014 and understate the DVFs in areas not affected by O&G emissions from the Permian Basin.

9.1 2028 Ozone Design Value Sensitivity Analysis using $DVC_{2015\text{-}2019}$

Table 9-1 presents the current year ozone design value from 2015-2019 ($DVC_{2015\text{-}2019}$) and the projected 2028 ozone DVFs using the $DVC_{2015\text{-}2019}$ as the ozone projection DVC starting point. The $DVC_{2015\text{-}2019}$ are higher than the EPA-recommended (EPA, 2018) $DVC_{2012\text{-}2016}$ used as the ozone DVF projection starting point in Chapters 7 and 8. For example, there are four monitoring sites with $DVC_{2015\text{-}2019}$ above the NAAQS with Desert View (74.3 ppb), Santa Teresa (74.0 ppb), and Carlsbad (73.7 ppb) having $DVC_{2015\text{-}2019}$ of, respectively, 2.3, 2.7 and 4.7 ppb higher than the corresponding $DVC_{2012\text{-}2016}$. Note that the $DVC_{2015\text{-}2019}$ at Carlsbad Caverns NP (71.0 ppb) also exceeds the NAAQS, however it was not in operation for the $DVC_{2012\text{-}2016}$ period and the $DVC_{2015\text{-}2019}$ is based on just 3-years of data (2016-2018), so is actually based on just one design value, $DV_{2016\text{-}2018}$.

The 2028 projected ozone DVFs for the 2028 Base Case using the current year $DVC_{2015\text{-}2019}$ has one monitoring site that exceeds the 2015 ozone NAAQS, 71.2 ppb at Carlsbad. The next highest 2028 ozone DVFs for the 2028 Base Case are 69.3 ppb at Carlsbad Caverns NP and 69.1 ppb at Desert View.

The emissions controls in the 2028 O&G Control Strategy are sufficient to reduce the 2028 Base Case ozone DVF at Carlsbad (71.2 ppb) to below the ozone NAAQS (70.9 ppb) when $DVC_{2015\text{-}2019}$ current year design value is used in the 2028 ozone DVF projections.

Table 9-1. Projected 2028 ozone DVFs for the 2015-2019 current year design value $DVC_{2015\text{-}2019}$ sensitivity analysis.

AQS_ID	2015-19	Projected 2028 DVF			Site Name	County
	DVC (ppb)	Base (ppb)	Cntl (ppb)	Cntl - Base		
350010023	69.0	63.4	63.1	-0.3	Del Norte HS	Bernalillo
350010029	66.0	61.0	60.5	-0.5	South Valley	Bernalillo
350011012	69.0	62.7	62.4	-0.3	Foothills	Bernalillo
350130008	68.7	62.1	62.0	-0.1	La Union	Doña Ana
350130020	70.7	65.7	65.7	0.0	Chaparral	Doña Ana
350130021	74.3	69.1	68.9	-0.2	Desert View	Doña Ana
350130022	74.0	68.6	68.5	-0.1	Santa Teresa	Doña Ana
350130023	67.7	62.9	62.7	-0.2	Solano	Doña Ana
350151005	73.7	71.2	70.9	-0.3	Carlsbad	Eddy
350153001	71.0	69.3	69.3	0.0	Carlsbad Caverns NP	Eddy
350250008	69.3	67.2	66.5	-0.7	Hobbs Jefferson	Lea
350390026	66.3	63.0	62.2	-0.8	Coyote Ranger Dist	Rio Arriba
350431001	67.0	61.2	60.9	-0.3	Bernalillo (E Avenida)	Sandoval
350450009	67.0	63.6	62.8	-0.8	Bloomfield	San Juan
350450018	69.0	66.7	65.2	-1.5	Navajo Lake	San Juan
350451005	67.3	64.2	62.9	-1.3	Substation	San Juan
350490021	65.0	61.2	61.0	-0.2	Santa Fe Airport	Santa Fe
350610008	66.7	62.6	62.3	-0.3	Los Lunas (Los Lentes)	Valencia

9.2 2028 Ozone Design Value Sensitivity Analysis using $DVC_{2017\text{-}2019}$

Table 9-2 shows the results of the 2028 ozone DVF projection current year ozone design value sensitivity analysis using the latest 2017-2019 ozone design value as the starting point for the 2028 ozone projections. There are three monitors in New Mexico with $DV_{2015\text{-}2019}$ above the NAAQS: Desert View (77.0 ppb), Santa Teresa (76.0 ppb) and Carlsbad (79 ppb). These $DV_{2017\text{-}2019}$ values are, respectively, 5.0, 4.7 and 10.0 ppb higher than the $DVC_{2012\text{-}2016}$ used as the

ozone projection starting point in the 2028 ozone DVF projections presented in Chapters 7 and 8.

For the 2028 Base Case, there are two sites with projected 2028 ozone DVFs in the $DV_{2017\text{-}2019}$ current year design value sensitivity test that have DVF values above the 2015 ozone NAAQS: 71.6 ppb at Desert View and 76.4 ppb at Carlsbad. The 76.0 ppb $DV_{2017\text{-}2019}$ at Santa Teresa is reduced to 70.5 ppb under the 2028 Base Case so attains the ozone NAAQS.

The projected 2028 ozone DVF using the $DV_{2017\text{-}2019}$ as the current year DVC under the O&G Control Strategy are 71.4 ppb at Desert View and 76.0 at Carlsbad so still exceed the 2015 ozone NAAQS. In fact, the Carlsbad 76.0 ppb ozone DVF even exceeds the 2008 ozone NAAQS.

Table 9-2. Projected 2028 ozone DVFs for the 2017-2019 current year design value $DV_{2017\text{-}2019}$ sensitivity analysis.

AQS_ID	2017-19	Projected 2028 DVF			Site Name	County
	DVC (ppb)	Base (ppb)	Cntl (ppb)	Cntl - Base		
350010023	70.0	64.3	64.0	-0.3	Del Norte HS	Bernalillo
350010029	67.0	61.9	61.4	-0.5	South Valley	Bernalillo
350011012	71.0	64.5	64.2	-0.3	Foothills	Bernalillo
350130008	70.0	63.3	63.2	-0.1	La Union	Doña Ana
350130020	73.0	67.8	67.8	0.0	Chaparral	Doña Ana
350130021	77.0	71.6	71.4	-0.2	Desert View	Doña Ana
350130022	76.0	70.5	70.3	-0.2	Santa Teresa	Doña Ana
350130023	70.0	65.0	64.8	-0.2	Solano	Doña Ana
350151005	79.0	76.4	76.0	-0.4	Carlsbad	Eddy
350250008	71.0	68.9	68.1	-0.8	Hobbs Jefferson	Lea
350390026	67.0	63.6	62.8	-0.8	Coyote Ranger Dist	Rio Arriba
350431001	68.0	62.1	61.8	-0.3	Bernalillo (E Avenida)	Sandoval
350450009	68.0	64.6	63.7	-0.9	Bloomfield	San Juan
350450018	69.0	66.7	65.2	-1.5	Navajo Lake	San Juan
350451005	69.0	65.8	64.5	-1.3	Substation	San Juan
350490021	66.0	62.2	62.0	-0.2	Santa Fe Airport	Santa Fe
350610008	68.0	63.8	63.5	-0.3	Los Lunas (Los Lentes)	Valencia

10. 2028 SOURCE SECTOR APCA OZONE SOURCE APPORTIONMENT MODELING

Ozone source apportionment modeling was conducted to determine the contributions of Source Sectors within New Mexico to 2028 ozone concentrations and projected future year ozone design values (DVF) under the 2028 New Mexico oil and gas (O&G) control strategy emissions scenario. The Anthropogenic Precursor Culpability Assessment (APCA) version of the CAMx ozone source apportionment tool was used and the modeling also obtained contributions from Colorado, Texas and the remainder of U.S. states as well as international anthropogenic emissions.

10.1 Versions of Ozone Source Apportionment

CAMx includes two ozone source apportionment tools: the Ozone Source Apportionment Technology (OSAT) and the Anthropogenic Precursor Culpability Assessment (APCA). Both use tagged tracer species that track ozone formation from VOC (V_i) and NO_x (NIT_i + RGN_i) emissions from each user-specified Source Group (i). A Source Group can consist of a Source Region and/or Source Category. A typical OSAT/APCA application will use a Source Region map that divides the modeling domain into geographic regions and separate emission files of different Source Categories are provided as input to CAMx; ozone source apportionment is obtained for Source Groups that are defined as the intersection of the Source Regions with the Source Categories (e.g., on-road mobile sources from New Mexico). The ozone source apportionment tool runs in parallel to the CAMx host model and extracts information on ozone formation and assigns it to the user-defined Source Groups.

There are 10 reactive tracers used to track ozone formation for each user-defined Source Group as follows:

V_i	VOC emissions
NIT_i	Nitric oxide (NO) and nitrous acid (HONO) emissions
RGN_i	Nitrogen dioxide (NO_2), nitrate radical (NO_3) and dinitrogen pentoxide (N_2O_5)
TPN_i	Peroxyl acetyl nitrate (PAN), analogues of PAN and peroxy nitric acid (PNA)
NTR_i	Organic nitrates (RNO_3)
$HN3_i$	Gaseous nitric acid (HNO_3)
$O3N_i$	Ozone formed under NOx sensitive conditions
$O3V_i$	Ozone formed under VOC sensitive conditions
OON_i	Odd-oxygen in NO_2 formed from O3Ni
OOV_i	Odd-oxygen in NO_2 formed from O3Vi

For each time step and grid cell, when ozone is formed in the host model OSAT determines whether the ozone formation was more VOC sensitive or NO_x sensitive and apportions the ozone formed to Source Groups based on the relative contribution of the limiting precursor to the total precursor (e.g., under VOC sensitive conditions $V_i/ \sum V_i$). APCA differs from OSAT in that it will only allocate ozone formed to natural (e.g., biogenic) emissions Source Groups when the ozone formed is due to natural VOC interacting with natural NO_x. So when ozone is formed due to biogenic VOC emissions interacting with anthropogenic NO_x emissions under VOC sensitive ozone formation conditions, a case OSAT would assign to the natural Source Group $O3V_i$ tracer, APCA redirects the ozone formed to the anthropogenic Source Group $O3N_i$ tracer. APCA was designed to provide more control strategy relevant information than OSAT and is used in identifying ozone contributions in emissions culpability assessments (e.g., CSAPR[38]). However, OSAT has to be used to obtain information on whether ozone formation is more VOC or NO_x sensitive. Details on the CAMx OSAT and APCA source apportionment tools are provided in Chapter 7 of the CAMx user's guide.[39] Since we are running CAMx v7.1, it uses the third version of OSAT3 and corresponding version of APCA.

As the main focus of the 2028 Source Sector ozone source apportionment modeling is to identify the contributions of anthropogenic emission source sectors and regions to elevated MDA8 ozone concentrations in New Mexico, the APCA version of ozone source apportionment tool was used.

10.2 2028 Source Sector APCA Ozone Source Apportionment Specifications

Details on the design and specifications of the 2028 Source Sector APCA ozone source apportionment simulate are provide below.

10.2.1 2028 O&G Control Strategy Emissions Scenario

The 2028 Source Sector APCA ozone source apportionment was conducted using the 2028 New Mexico O&G Control Strategy emissions scenario.

10.2.2 Definition of Source Groups

The 2028 Source Sector APCA ozone source apportionment simulation used a Source Region map to define geographic regions of emission areas to be tracked. Separate source contributions were also obtained for 9 emission Source Categories as well as contributions due to Boundary Conditions (BCs) around the lateral edges of the 36-km grid resolution domain.

10.2.2.1 Boundary Conditions

The CAMx v7 source apportionment tool has a new capability to provide separate contributions due to stratified BCs. Typically, these stratifications will be different source sectors from outside of the CAMx modeling domain. WRAP conducted 2014 GEOS-Chem modeling for a base case (BASE), a 2014 GEOS-Chem no

[38] https://www.epa.gov/csapr
[39] http://www.camx.com/files/camxusersguide_v7-10.pdf

international anthropogenic emissions case (i.e., Zero-out Rest of World or ZROW) and a no global anthropogenic emissions case (i.e., just natural emissions). Output from the three 2014 GEOS-Chem runs were processed to generate lateral BCs for the CAMx 36-km 36US1 North America modeling domain that contained: (1) the contributions of international anthropogenic emissions (BC_{Intl}); (2) the contributions of U.S. anthropogenic emissions (BC_{US}); and (3) the contributions of natural sources ($BC_{Natural}$). Details on the WRAP 2014 GEOS-Chem base, ZROW and Natural modeling are contained in a Run Specification Sheet[40] and the WRAP/WAQS 2014v2 model performance evaluation webpage.[41]

This results in the 2028 Source Sector APCA ozone source apportionment simulation tracking ozone contributions from three Source Groups for the lateral boundaries ($BC_{Natural}$, BC_{Intl} and BC_{US}). Contributions due to the top BC concentration as well as Initial Concentrations (IC) were also separately tracked resulting in 5 Source Groups used to track the contributions of BC and IC.

10.2.2.2 Source Regions

Five source regions were used in the 2028 Source Sector APCA ozone source apportionment simulation as shown in Figure 10-1:

1. New Mexico;
2. Texas;
3. Colorado;
4. Remainder U.S. states plus coastal water out to 200 nautical miles (nmi) from the U.S. coast; and
5. International, which included Mexico, Canada and waters off their coasts plus waters more than 200 nmi off the U.S. coast.

[40] https://views.cira.colostate.edu/docs/iwdw/platformdocs/WRAP_2014/Run_Spec_WRAP_2014_Task1-7_NAT-ZROW_v4.pdf
[41] https://views.cira.colostate.edu/iwdw/docs/WRAP_WAQS_2014v2_MPE.aspx

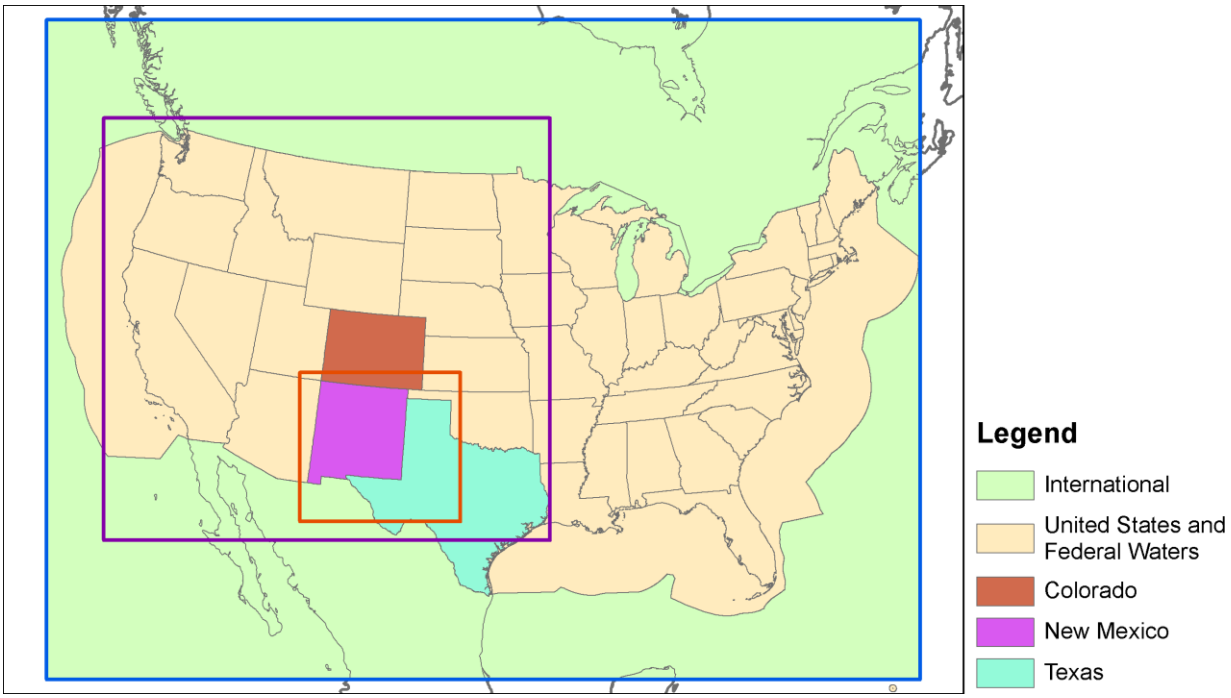

Figure 10-1. Source regions used in the 2028 Source Sector APCA ozone source apportionment simulation.

10.2.2.3 Source Categories

The emissions inventory was divided up into 9 Source Categories in the 2028 Source Sector APCA ozone source apportionment modeling as follows:

1. Natural (biogenic, lightning NO_x, windblown dust and oceanic [sea salt and dimethyl sulfide]);
2. Fires (U.S. wildfires, wildland prescribed burns and agricultural burning and other [Mexico/Canada] fires);
3. Oil and gas point sources (surrogate for midstream O&G);
4. Oil and gas non-point sources (surrogate for upstream O&G);
5. EGU point;
6. Non-EGU point;
7. On-road mobile;
8. Non-road mobile; and
9. Remainder anthropogenic.

Since the APCA version of the CAMx ozone source apportionment tool is being utilized, Natural emissions has to be the first Source Category so APCA knows which Source Category is uncontrollable.

10.2.2.4 Source Groups

With 5 Source Regions and 9 Source Categories, plus 5 Source Groups for IC/BC, there is a total of 50 Source Groups that separate ozone source contributions are obtained (50 = 5 x 9 + 5).

10.3 2028 Source Sector APCA Ozone Source Apportionment Modeling Results

The 2028 Source Sector APCA ozone source apportionment modeling results were analyzed to obtain the contributions of the different Source Sectors within New Mexico to projected future year 2028 ozone design values (DVFs) as well as contributions to Maximum Daily Average 8-hour (MDA8) ozone concentrations. The 2028 ozone DVF and modeled MDA8 ozone concentrations were analyzed at the monitoring sites as well as across the 4-km New Mexico domain. Figure 10-2 shows the locations of the monitoring sites within the 4-km New Mexico domain.

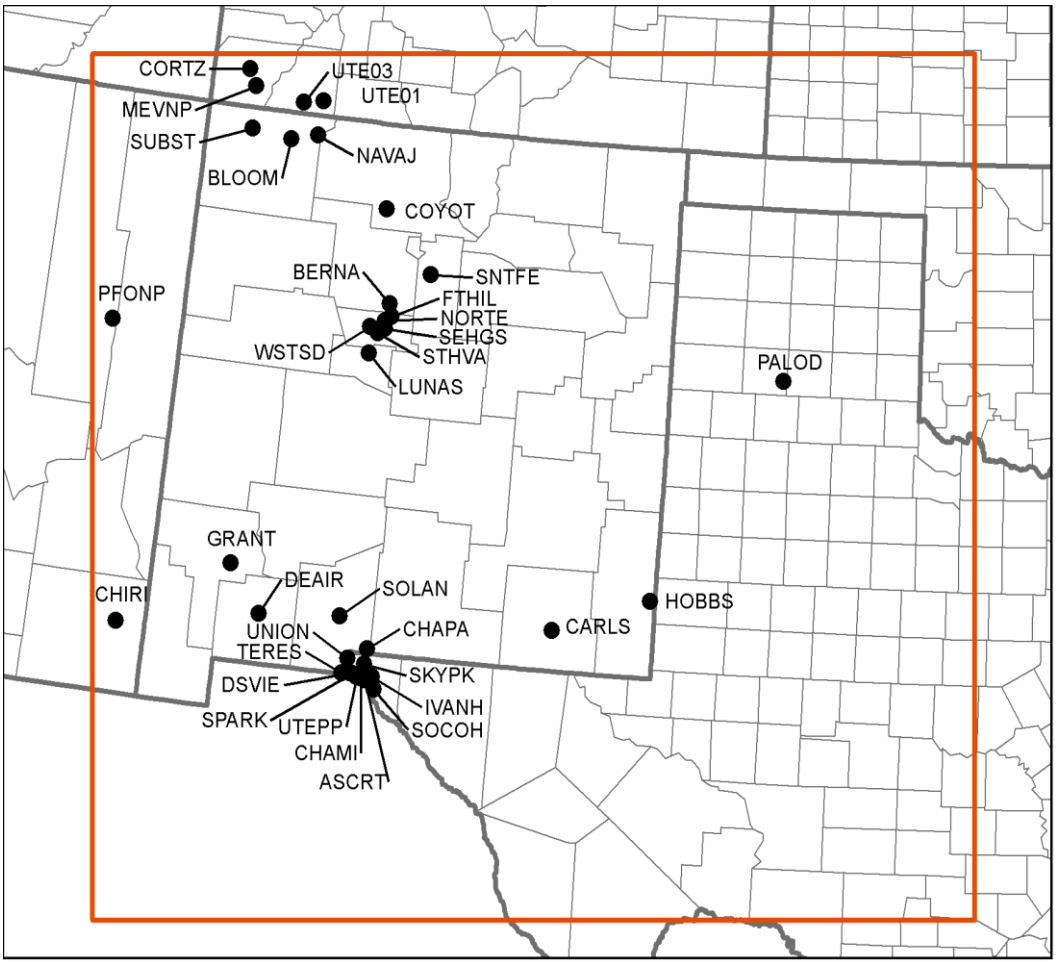

Figure 10-2. Locations of ozone monitoring sites within the 4-km New Mexico modeling domain.

10.3.1 Source Sector Contributions to Projected 2028 Ozone DVFs

In this section, the contributions of Source Sector emissions within New Mexico and the entire United States to future year projected 2028 ozone design values (DVF) at New Mexico monitoring sites and across the 4-km New Mexico domain are analyzed.

10.3.1.1 New Mexico Source Sector 2028 Ozone DVF Contributions

Table 10-1 displays the current year 2012-2016 DVC, the projected 2028 ozone DVF for the 2028 O&G Control Scenario and the reductions in the 2028 ozone DVF due to the removal of anthropogenic emissions in New Mexico for each of the 7 anthropogenic emissions Source Sectors at all monitoring sites in New Mexico. The incremental ozone contributions in the 2028 ozone DVF due to New Mexico emissions from the 7 Source Sectors are shown for several New Mexico monitoring sites in Figures 10-3 through 10-18.

At the three monitoring sites in San Juan County, New Mexico emissions from EGU and O&G Source Sectors contribute the most to the 2028 ozone DVF (Table 10-1). The largest ozone contribution is 3.1 ppb for the New Mexico EGU Source Sector at the SUBST site (Figure 10-5) due to its close proximity to the Four Corners Power Plant (FCPP) that is assumed to have Units 4 and 5 operating in 2028. The EGU ozone contributions fall off with distance from the FCPP as seen at the BLOOM (1.9 ppb; Figure 10-4), NAVAJ (1.7 ppb; Figure 10-3) and COYOT (0.5 ppb; Figure 10-6) monitoring sites. New Mexico O&G Point contributes 0.2 to 0.9 ppb and O&G Non-Point contributes 0.5 to 2.1 ppb to 2028 ozone DVFs at the four northern New Mexico monitoring sites in San Juan and Rio Arriba Counties. All other Source Sectors have contributions of 0.5 ppb or less at the northern New Mexico sites.

Sites in Central New Mexico include those in Bernalillo County (Figures 10-7 through 10-10) as well as two sites in neighboring counties (Figures 10-11 and 10-12). Ozone concentrations in Bernalillo County are highly influenced by emissions from Albuquerque, which is by far the largest city in New Mexico. So, Source Sectors associated with population centers (e.g., on-road, non-road and other anthropogenic) tend to have the highest contributions to the 2028 ozone DVFs at these sites. Although they have different magnitudes of ozone contributions, the rankings of the Source Sector contributions are very similar at the Bernalillo County sites with Other Anthropogenic being highest followed by On-Road and Non-Road mobile with the other four Source Sectors being half or less of the top three Source Sectors. On-Road mobile is the highest followed by Other Anthropogenic and Non-Road at the Santa Fe (Figure 10-11) and Sandoval County (Figure 10-12) sites, with all other Source Sector contributions being much lower.

Sites in the southern New Mexico (Figures 10-13 through 10-18) include those in southern Doña Ana County on the border with Texas that tend to have mostly small contributions from New Mexico Source Sectors with the exception of EGU (0.7 to 0.9 ppb), due to the close proximity of the Rio Grande Power Plant to some of the sites, and On-Road mobile (0.4-0.5 ppb) due to population centers along I-25 (e.g., Sunland Park, Santa Teresa, etc.). The Solano monitor (Figure 10-16) has higher ozone contributions due to On-Road (1.2 ppb) and Non-Road (0.7 ppb) mobile sources because of the higher mobile emissions from the City of Las Cruces, which is the second largest city in New Mexico.

New Mexico emissions from the O&G Point and Non-Point Sources sectors have the highest ozone contribution at the Carlsbad (0.5 and 0.5 ppb) and Hobbs (0.9 and 1.1 ppb) monitoring sites in southeastern New Mexico (Figures 10-17 and 10-18). These two southeastern New Mexico monitors are essentially within the Permian Basin. The contribution of On-Road to the 2028 ozone DVF at Carlsbad and Hobbs sites is 0.3 ppb, with all other Source Sector contributions being lower.

Table 10-1. Reduction in 2028 ozone DVF due to the elimination of emissions from 7 Source Sectors in New Mexico.

AQS_ID	Site_ID	DVC	DVF	O&GPT	O&GNP	EGU	NonEGU	OnRoad	NonRoad	OAnth
Northern New Mexico										
350390026	COYOT	64.0	60.0	-0.2	-0.5	-0.5	0.0	-0.2	-0.1	0.0
350450009	BLOOM	64.3	60.2	-0.7	-1.4	-1.9	0.0	-0.4	-0.1	-0.1
350450018	NAVAJ	67.0	63.3	-0.9	-2.1	-1.7	-0.1	-0.4	-0.2	-0.1
350451005	SUBST	63.7	59.6	-0.6	-1.5	-3.1	-0.1	-0.5	-0.2	-0.2
Central New Mexico										
350010023	NORTE	66.3	60.7	-0.2	-0.3	-0.5	-1.0	-2.7	-2.0	-3.6
350010024	SEHGS	68.0	62.0	-0.2	-0.3	-0.5	-1.1	-2.5	-1.9	-3.2
350010029	STHVA	66.0	60.5	-0.3	-0.5	-0.5	-1.0	-2.2	-1.7	-2.4
350010032	WSTSD	67.0	62.1	-0.2	-0.4	-0.4	-0.4	-1.6	-1.2	-1.8
350011012	FTHIL	65.0	58.8	-0.2	-0.3	-0.5	-0.7	-2.5	-2.0	-3.0
350431001	BERNA	64.0	58.1	-0.1	-0.2	-0.4	-0.4	-2.1	-1.5	-1.9
350490021	SNTFE	64.3	60.4	-0.2	-0.3	-0.2	-0.3	-1.2	-0.7	-0.8
Southern New Mexico										
350130008	UNION	66.3	59.8	-0.2	-0.2	-0.7	0.0	-0.5	-0.3	-0.1
350130017	SPARK	67.0	61.8	-0.2	-0.2	-0.9	0.0	-0.4	-0.2	-0.2
350130020	CHAPA	67.0	62.2	-0.1	-0.1	-0.3	0.0	-0.2	-0.1	-0.1
350130021	DSVIE	72.0	66.8	-0.2	-0.3	-0.9	-0.1	-0.5	-0.3	-0.2
350130022	TERES	71.3	66.0	-0.3	-0.3	-0.7	-0.1	-0.5	-0.3	-0.2
350130023	SOLAN	65.0	60.2	-0.2	-0.2	-0.2	-0.2	-1.2	-0.7	-0.3
350151005	CARLS	69.0	66.4	-0.5	-0.5	-0.2	-0.1	-0.3	-0.2	-0.1
350171003	GRANT	62.0	58.9	0.0	0.0	0.0	0.0	-0.1	-0.1	0.0
350250008	HOBBS	66.0	63.3	-0.9	-1.1	-0.2	0.0	-0.3	-0.2	-0.1
350290003	DEAIR	66.0	62.5	-0.2	-0.1	-0.2	0.0	-0.6	-0.4	0.0

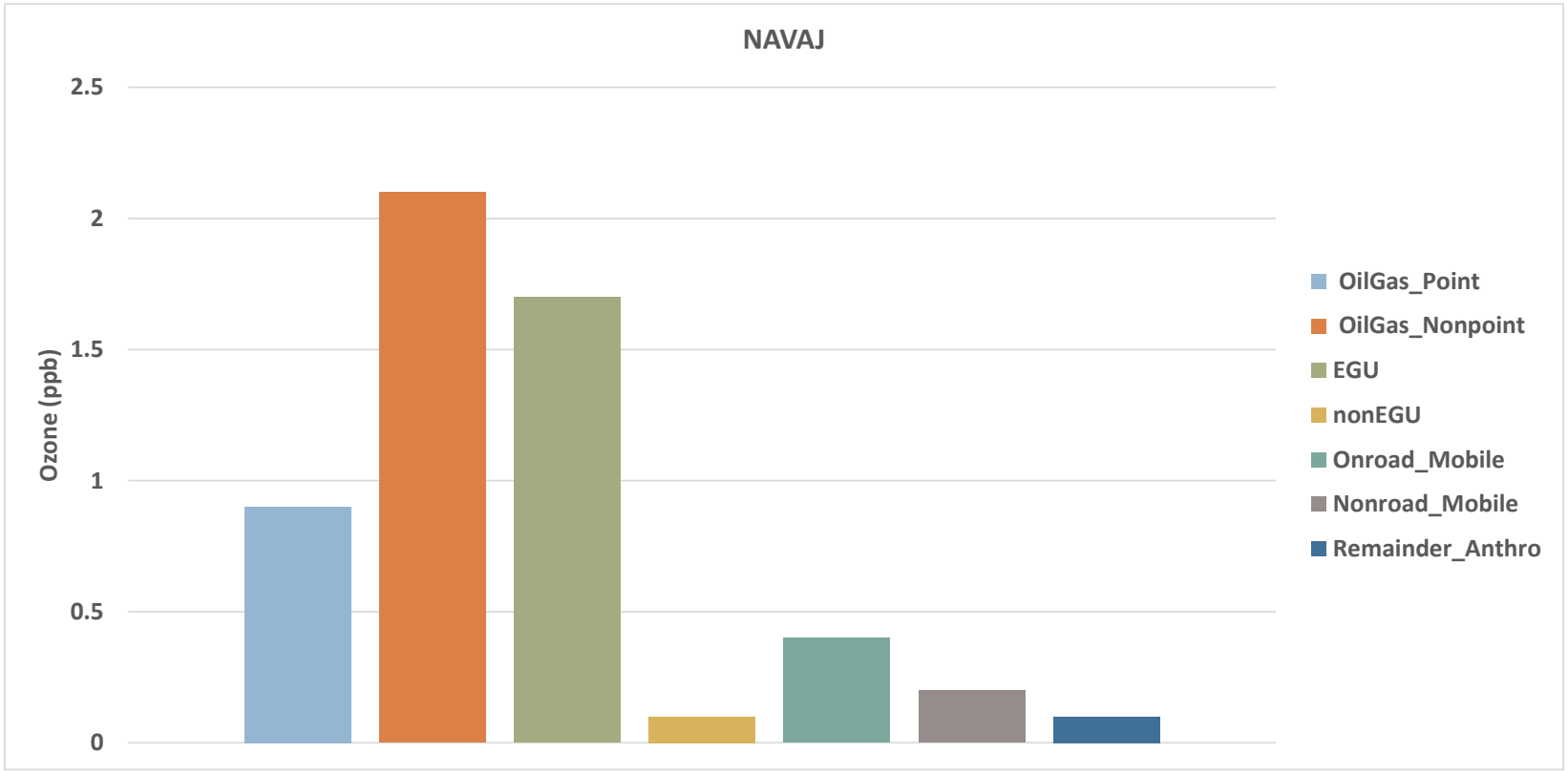

Figure 10-3. Contributions of New Mexico anthropogenic emissions from 7 Source Sectors to projected 2028 ozone DVFs at Navajo Lake in San Juan County.

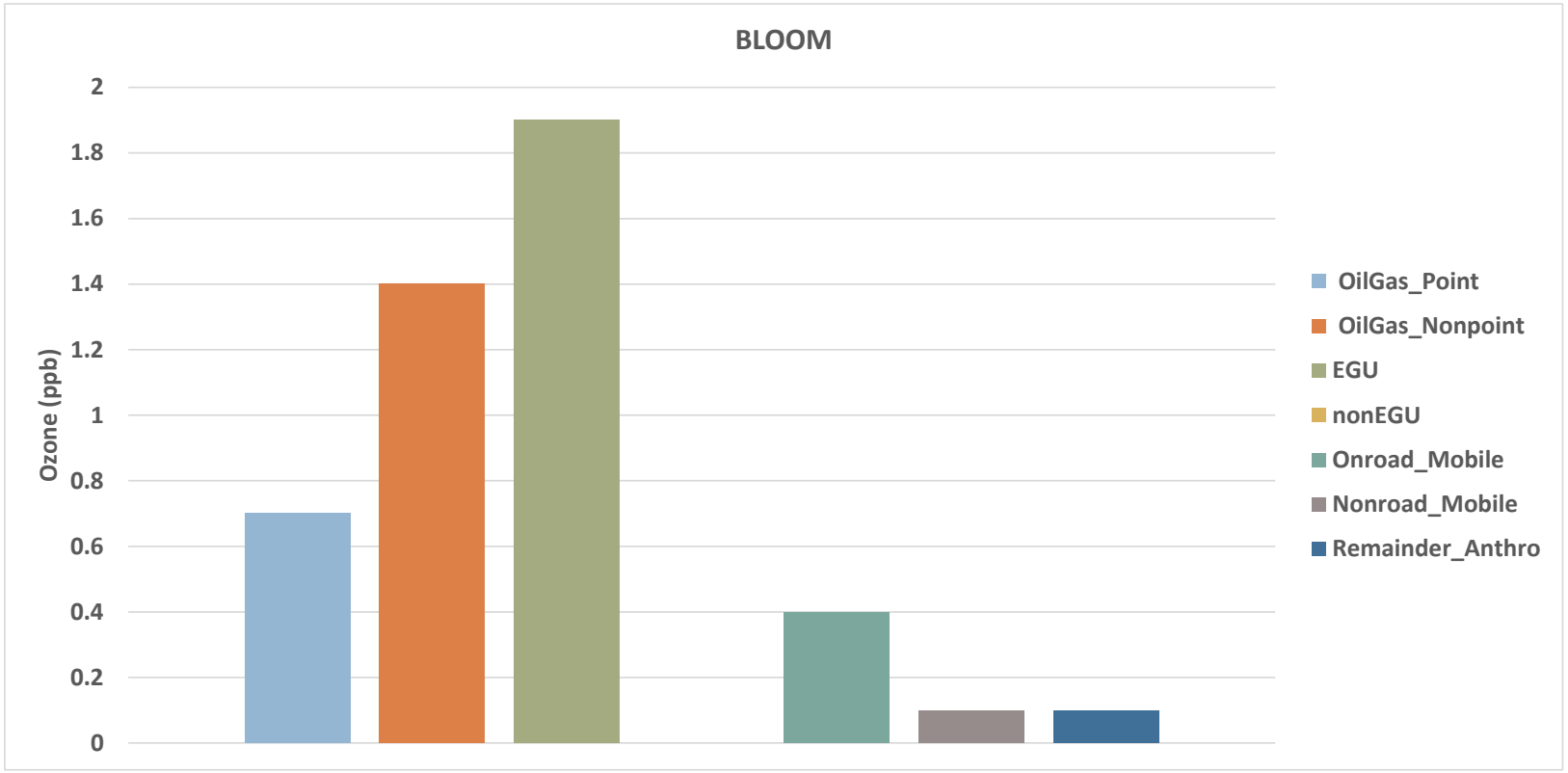

Figure 10-4. Contributions of New Mexico anthropogenic emissions from 7 Source Sectors to projected 2028 ozone DVFs at Bloomfield in San Juan County.

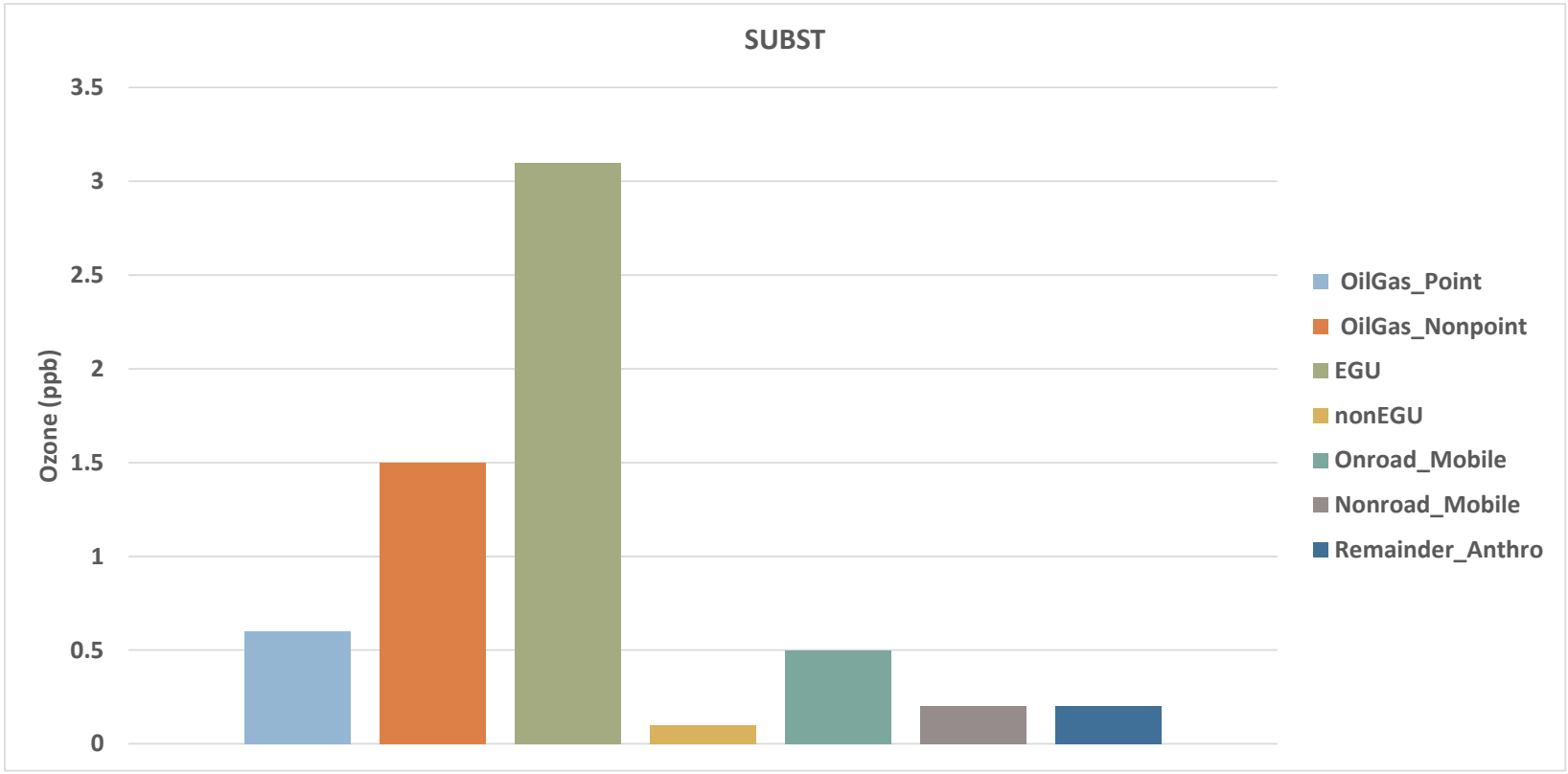

Figure 10-5. Contributions of New Mexico anthropogenic emissions from 7 Source Sectors to projected 2028 ozone DVFs at Substation in San Juan County.

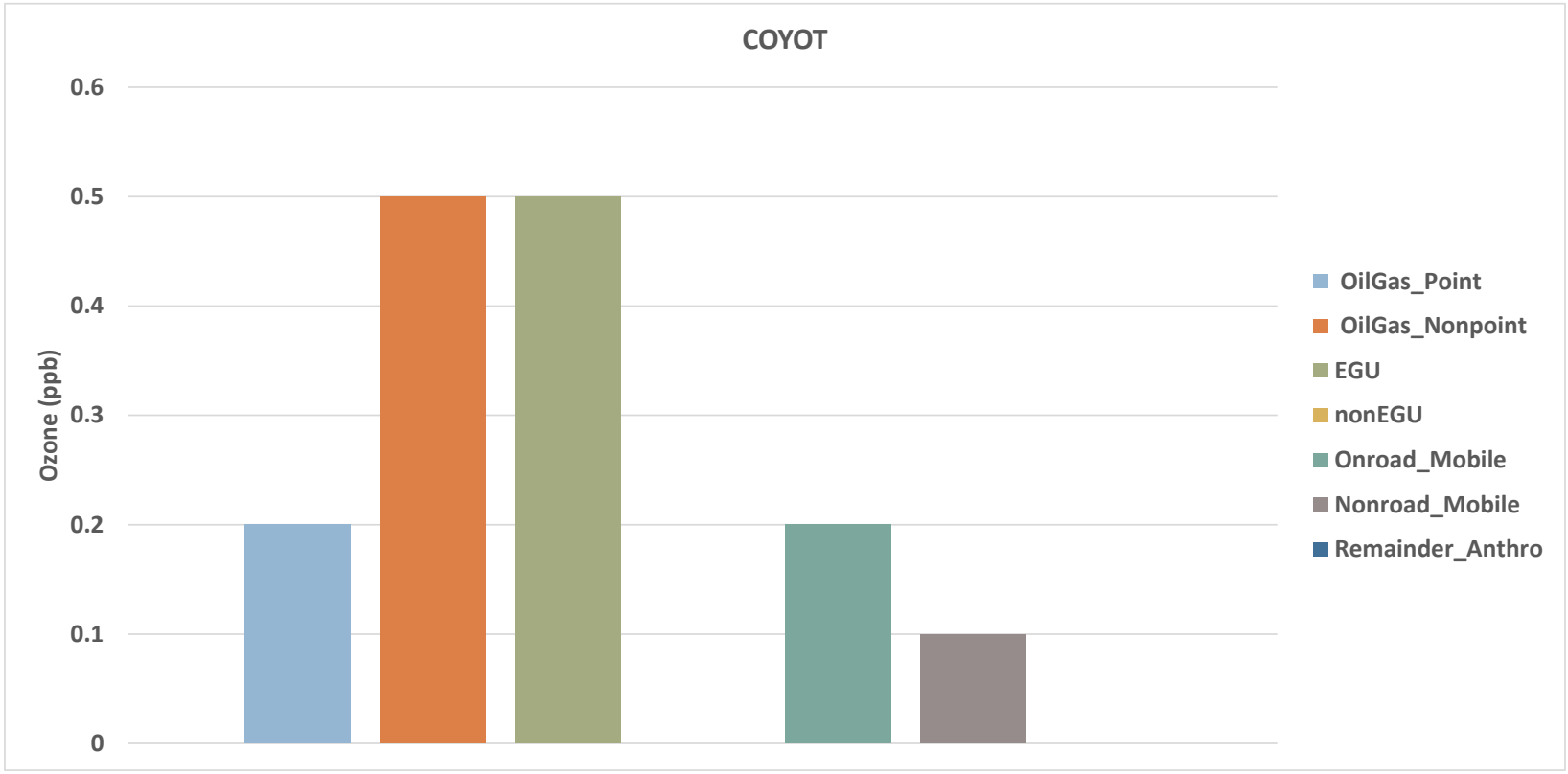

Figure 10-6. Contributions of New Mexico anthropogenic emissions from 7 Source Sectors to projected 2028 ozone DVFs at Coyote Ranger District in Rio Arriba County.

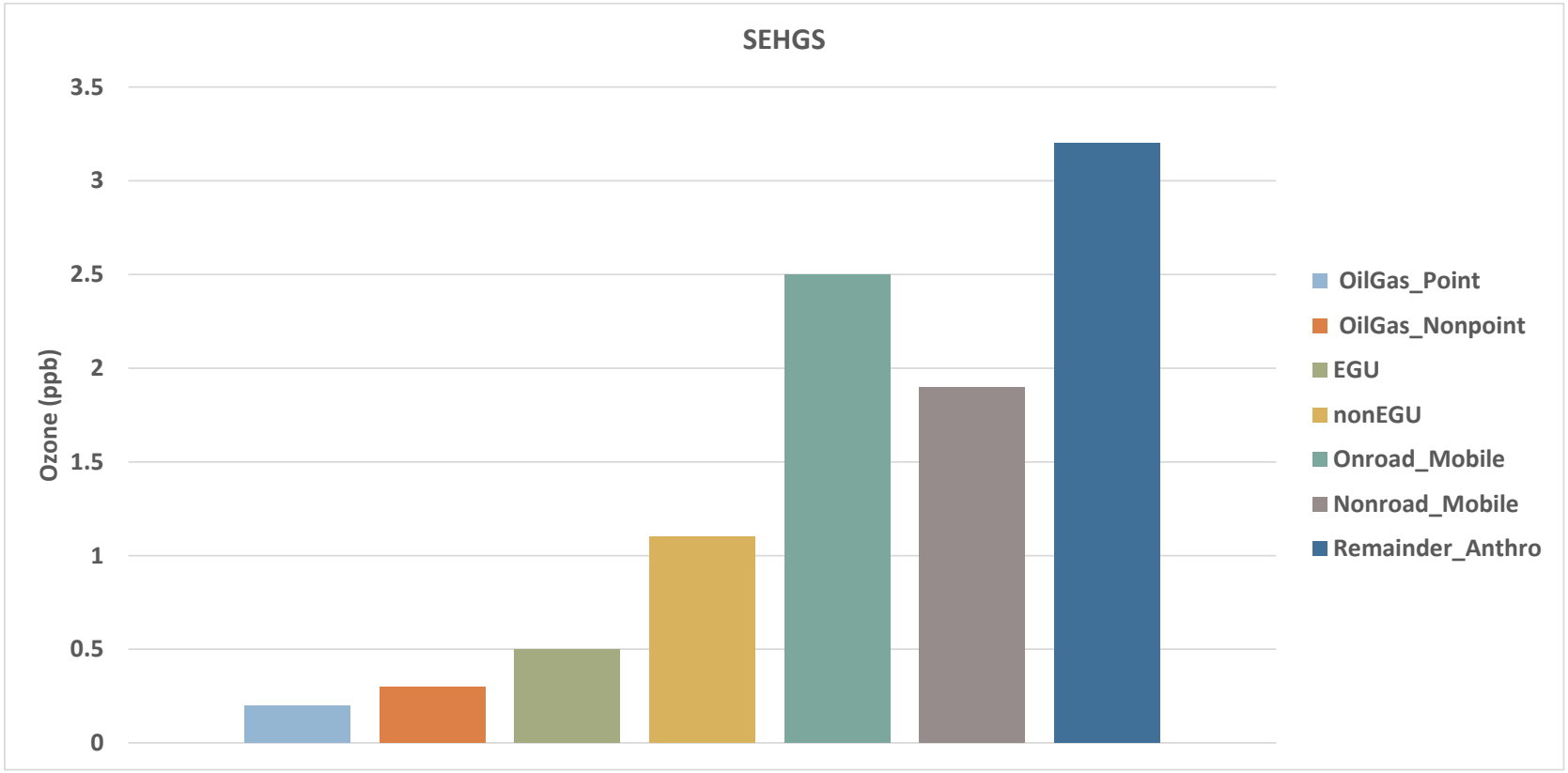

Figure 10-7. Contributions of New Mexico anthropogenic emissions from 7 Source Sectors to projected 2028 ozone DVFs at Southeast Heights in Bernalillo County.

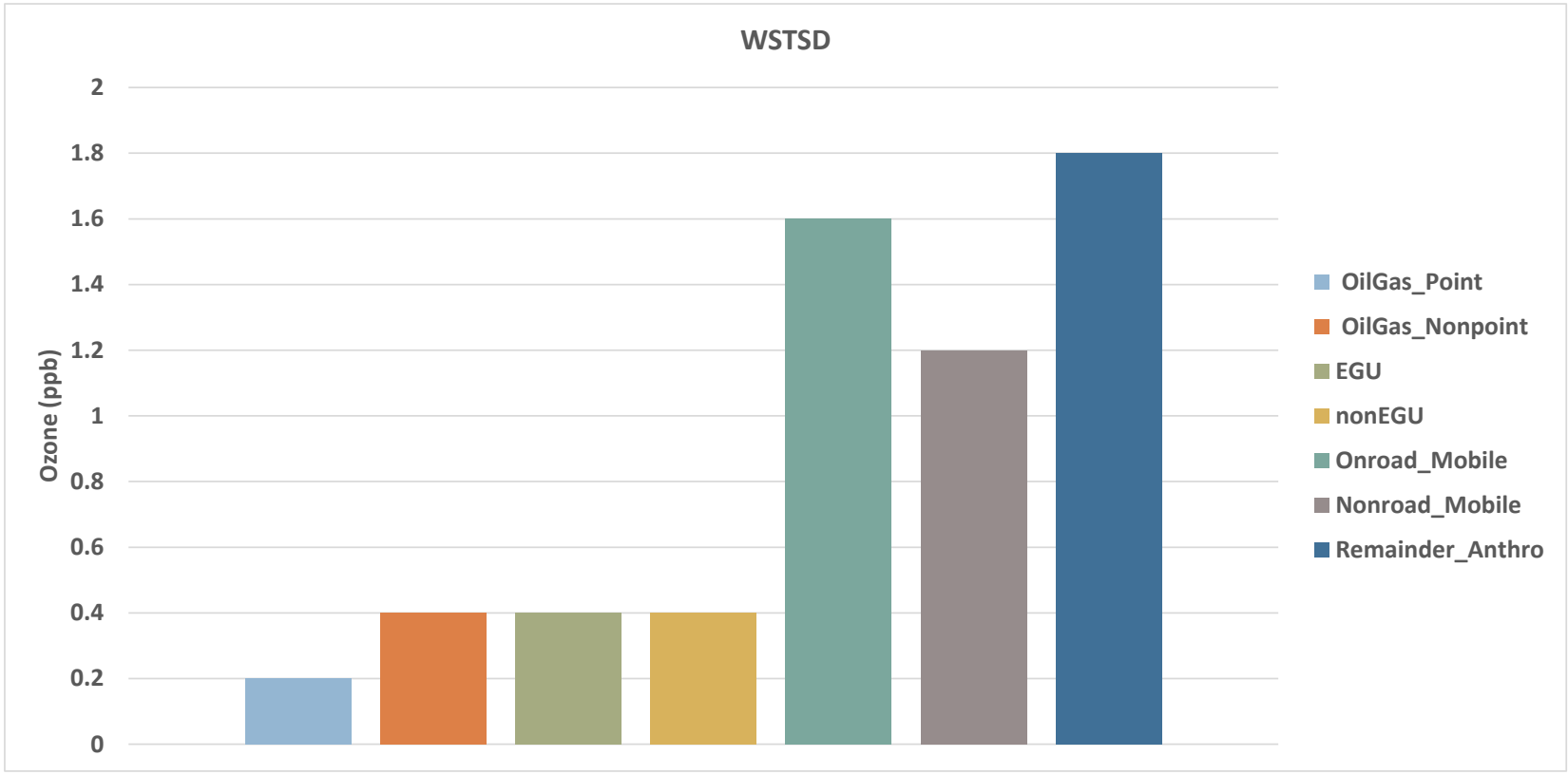

Figure 10-8. Contributions of New Mexico anthropogenic emissions from 7 Source Sectors to projected 2028 ozone DVFs at Westside in Bernalillo County.

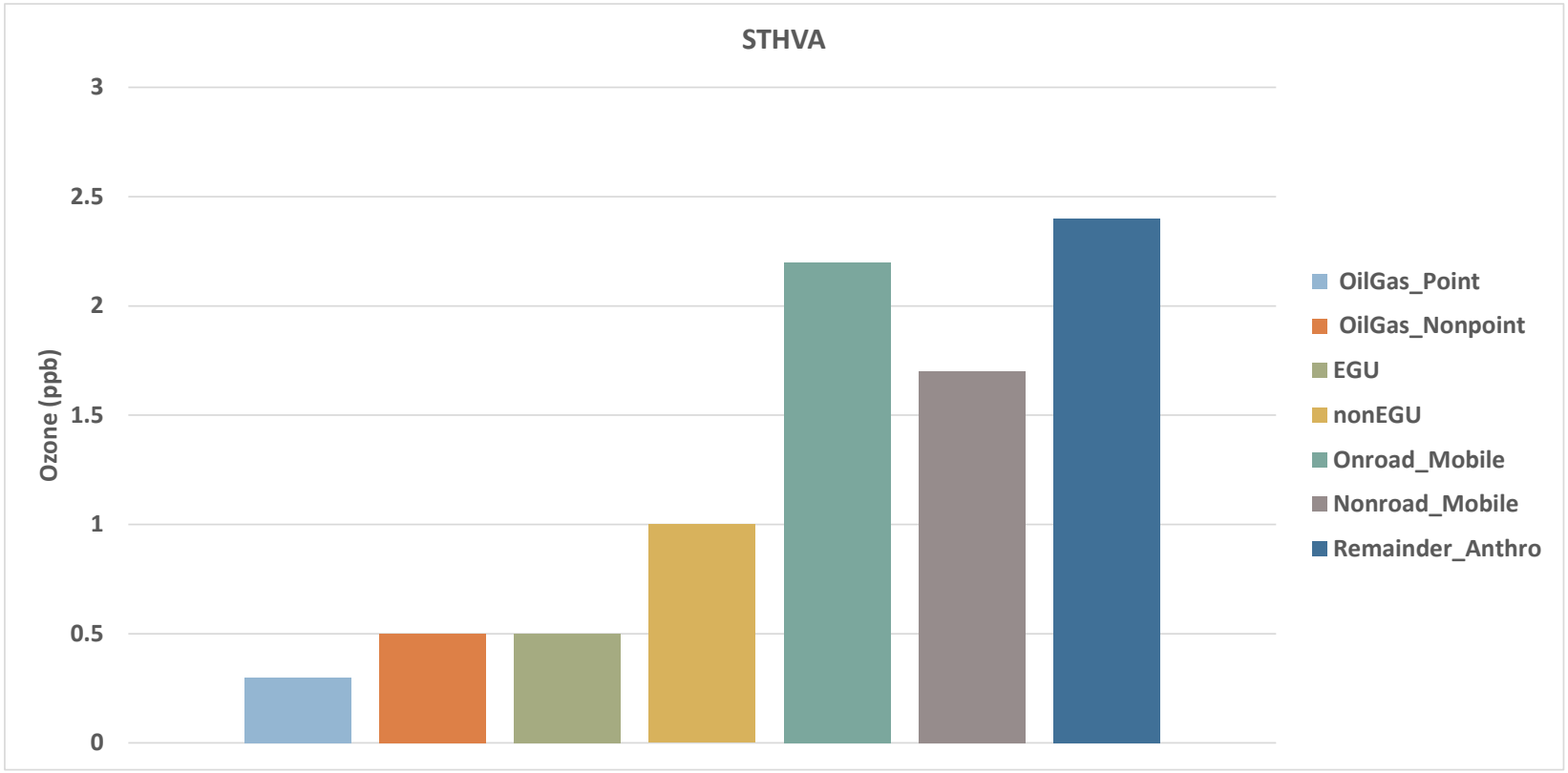

Figure 10-9. Contributions of New Mexico anthropogenic emissions from 7 Source Sectors to projected 2028 ozone DVFs at South Valley in Bernalillo County.

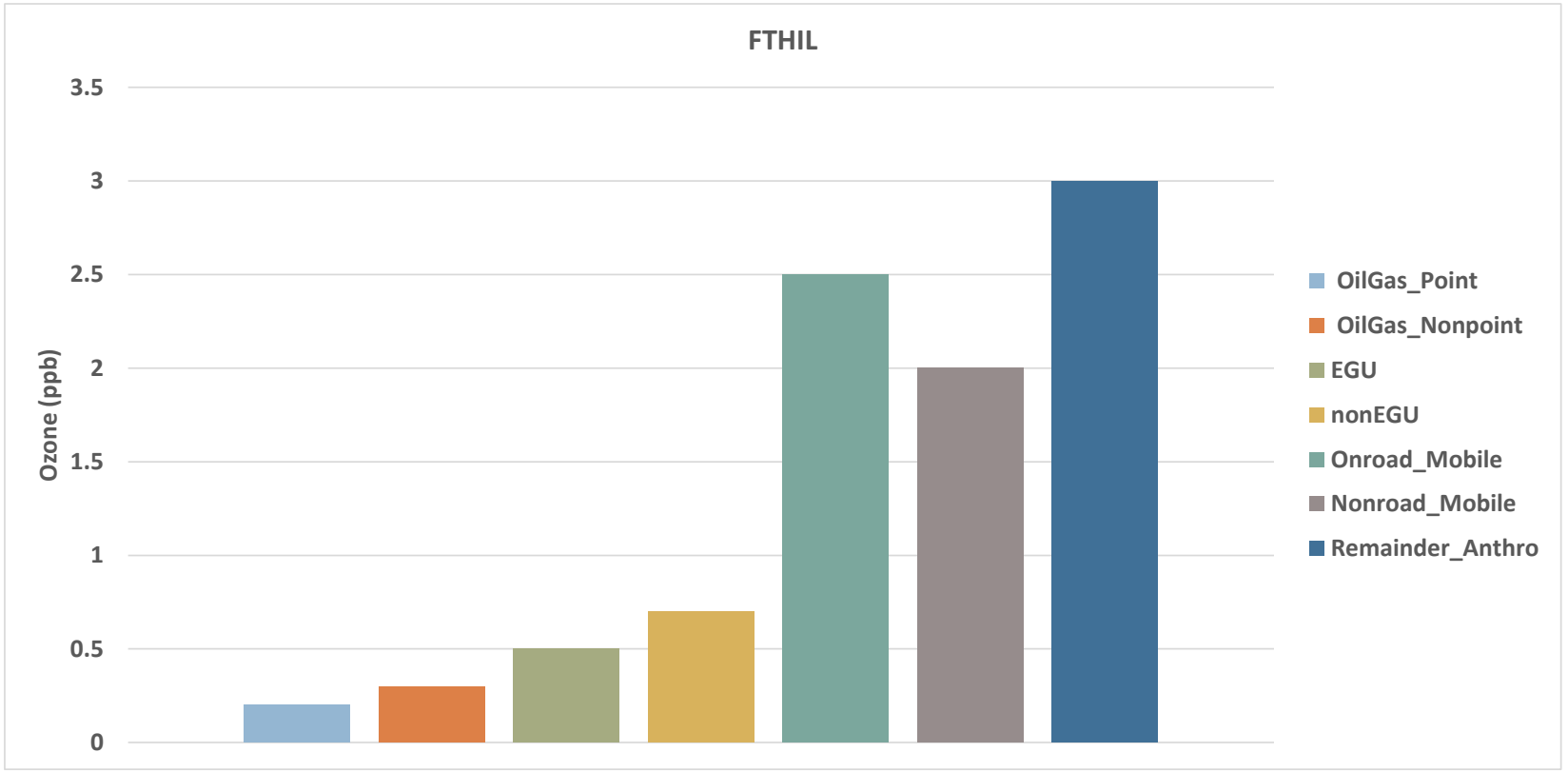

Figure 10-10. Contributions of New Mexico anthropogenic emissions from 7 Source Sectors to projected 2028 ozone DVFs at Foothills in Bernalillo County.

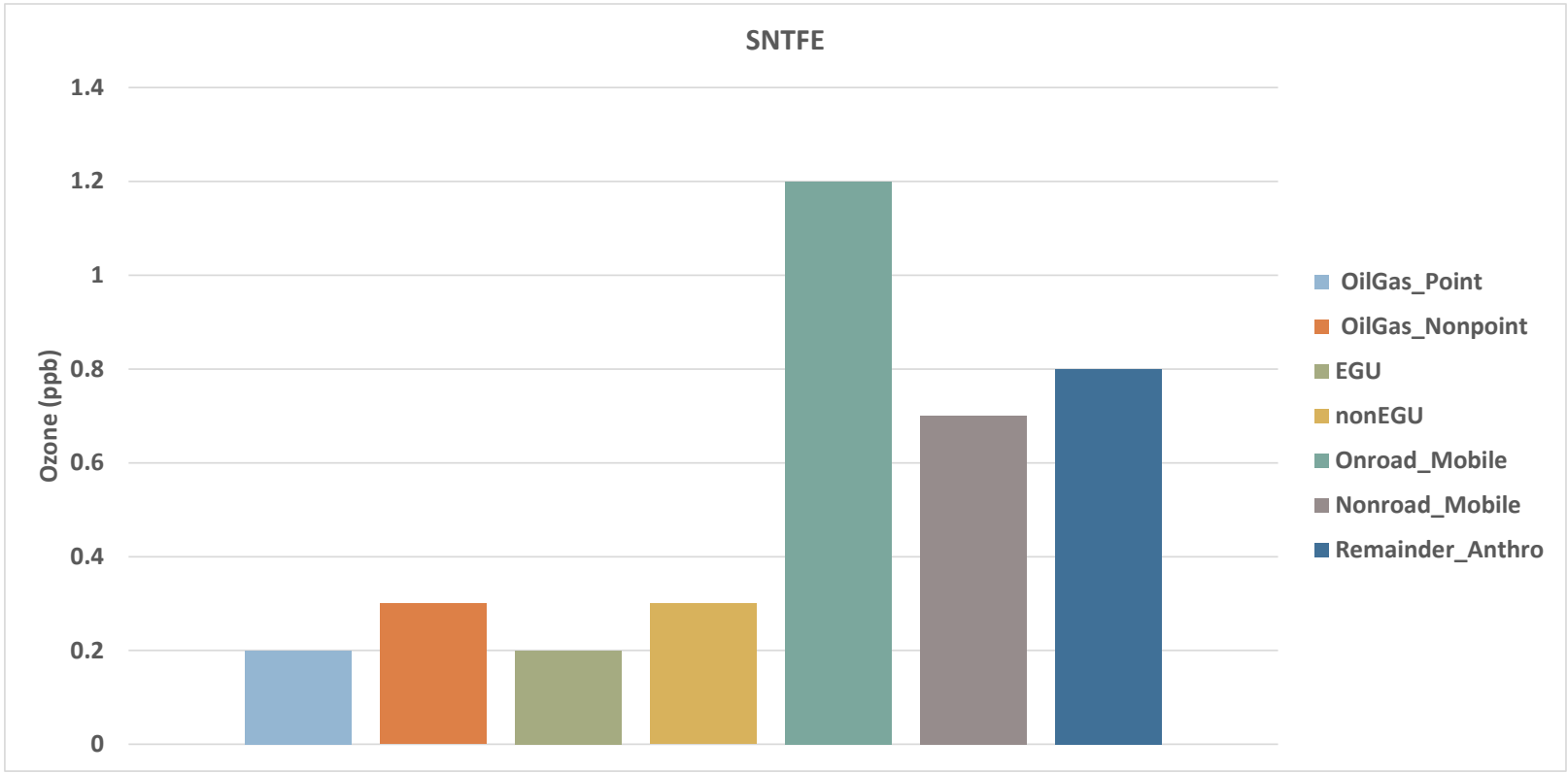

Figure 10-11. Contributions of New Mexico anthropogenic emissions for 7 Source Sectors to projected 2028 ozone DVFs at Santa Fe in Santa Fe County.

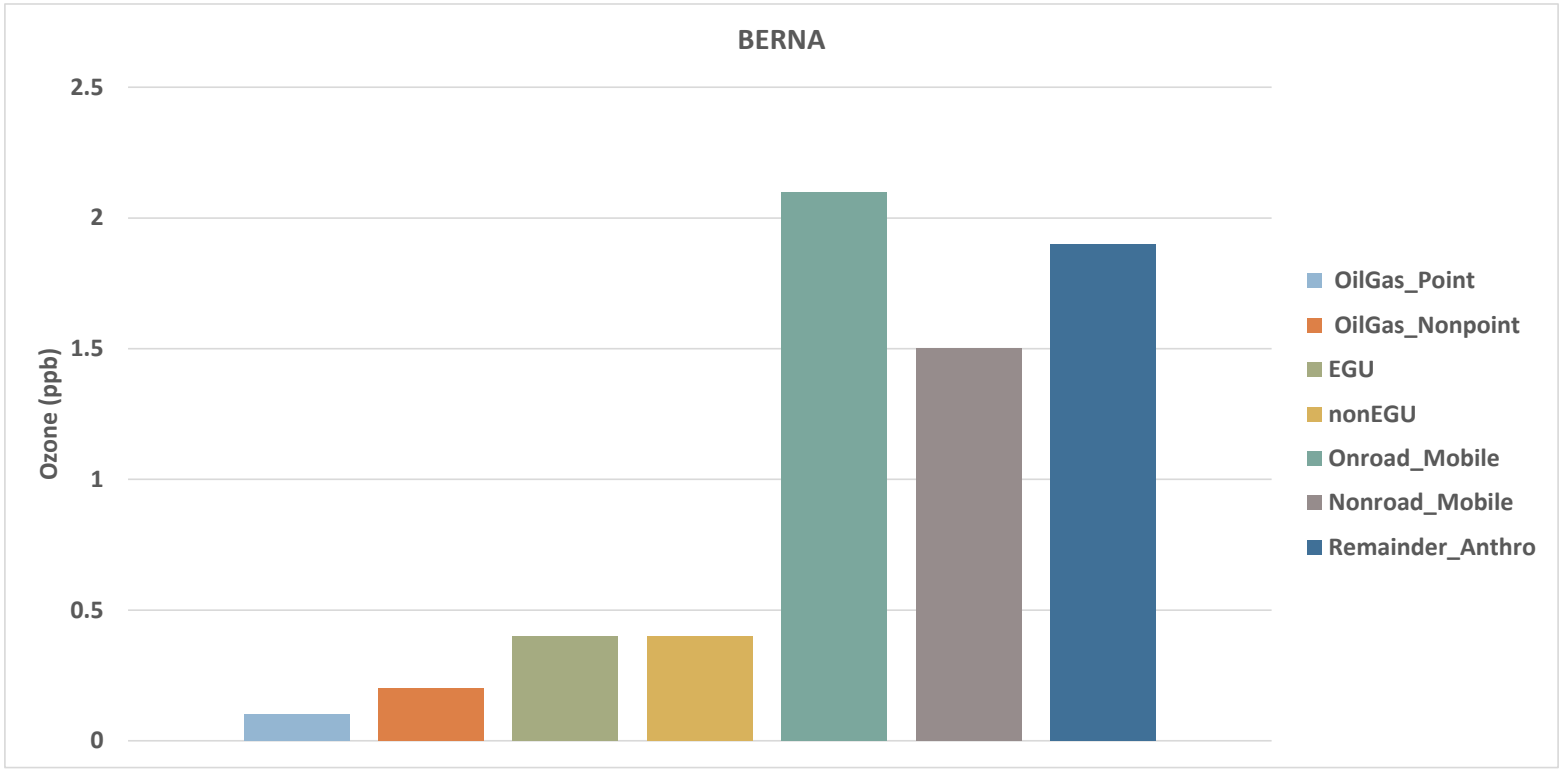

Figure 10-12. Contributions of New Mexico anthropogenic emissions from 7 Source Sectors to projected 2028 ozone DVFs at Bernalillo in Sandoval County.

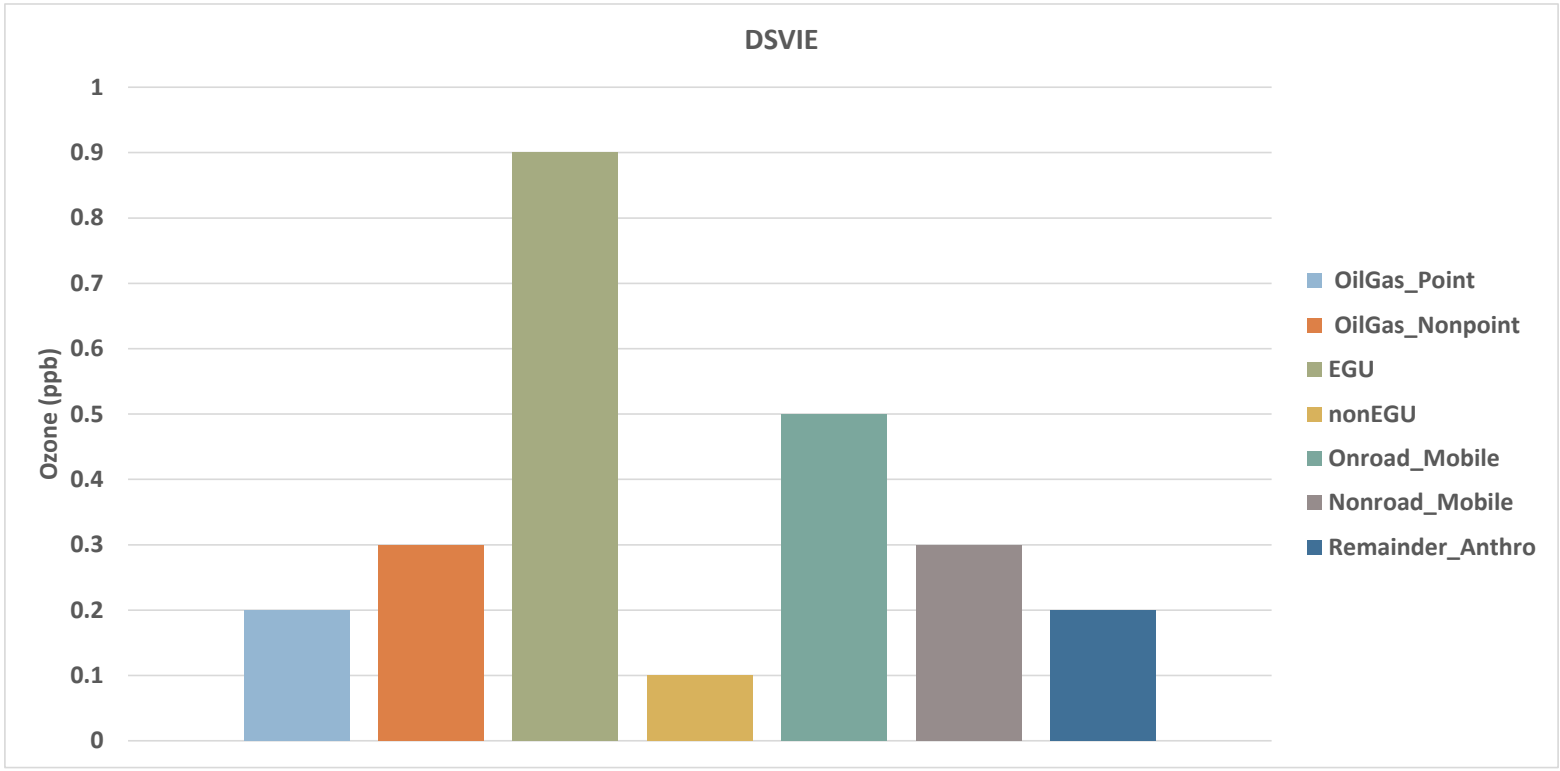

Figure 10-13. Contributions of New Mexico anthropogenic emissions from 7 Source Sectors to projected 2028 ozone DVFs at Desert View in Doña Ana County in southern New Mexico.

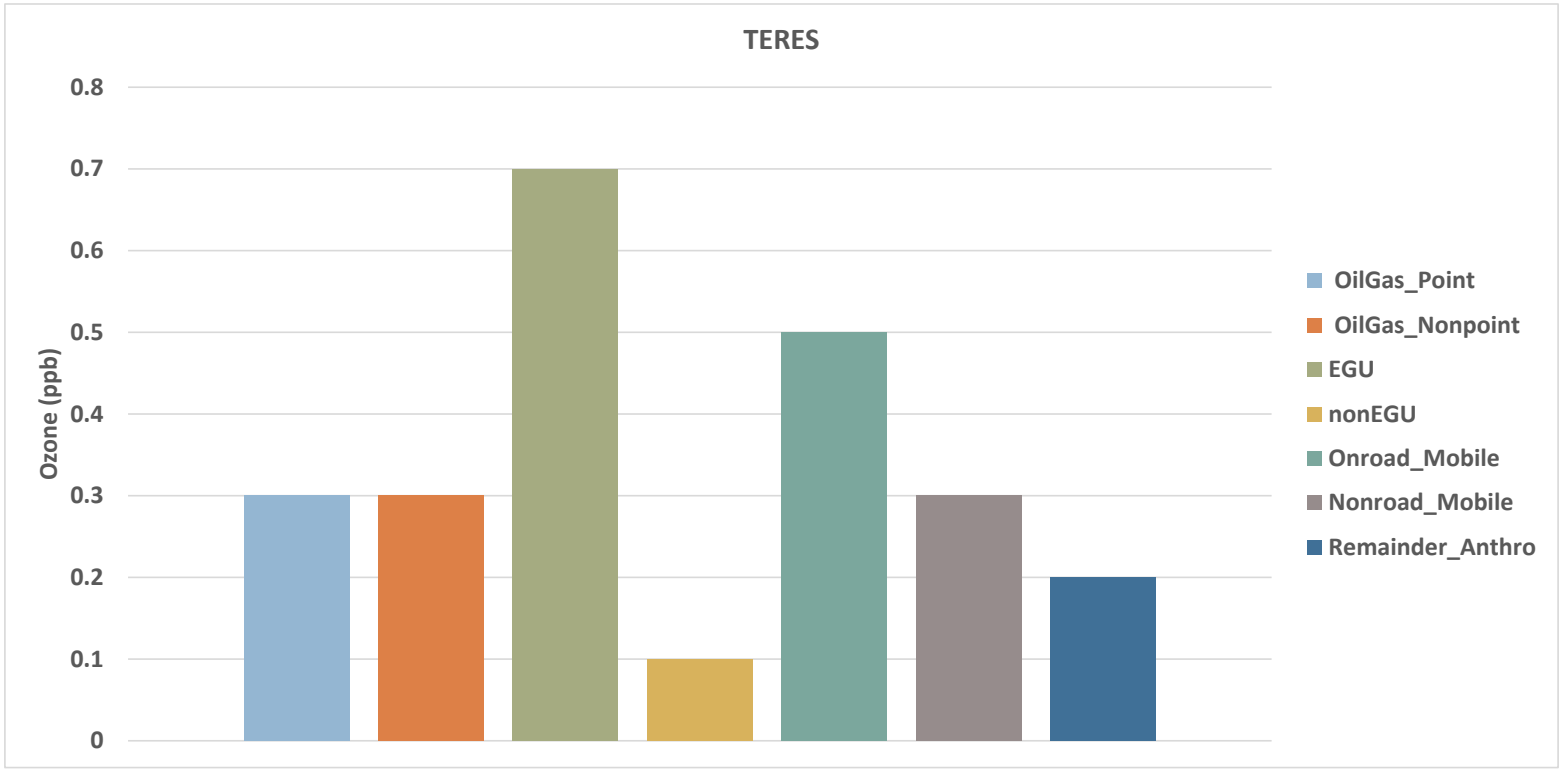

Figure 10-14. Contributions of New Mexico anthropogenic emissions for 7 Source Sectors to projected 2028 ozone DVFs at Santa Teresa in Doña Ana County in southern New Mexico.

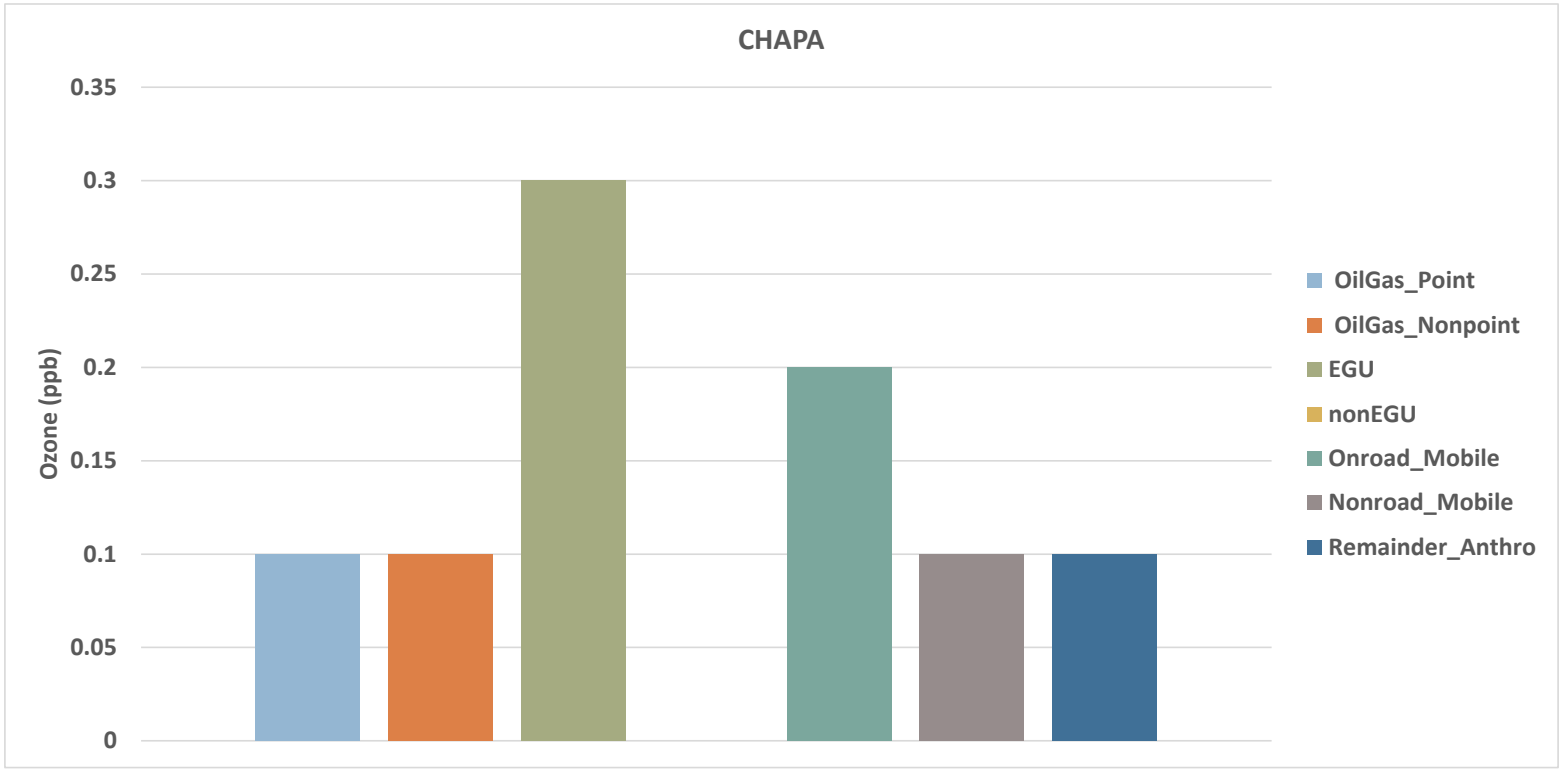

Figure 10-15. Contributions of New Mexico anthropogenic emissions for 7 Source Sectors to projected 2028 ozone DVFs at Chaparral in Doña Ana County in southern New Mexico.

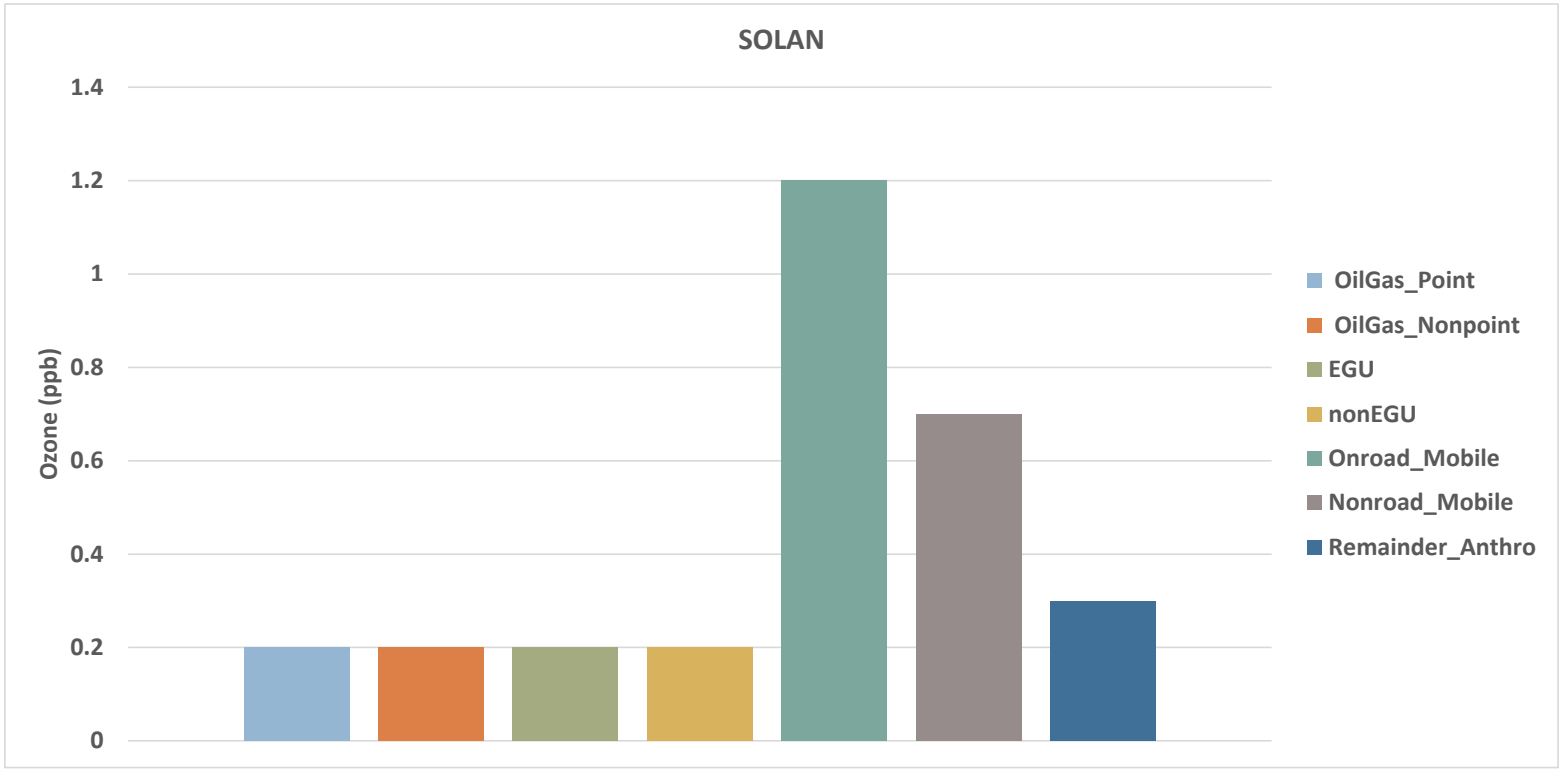

Figure 10-16. Contributions of New Mexico anthropogenic emissions for 7 Source Sectors to projected 2028 ozone DVFs at Solano in Doña Ana County in southern New Mexico.

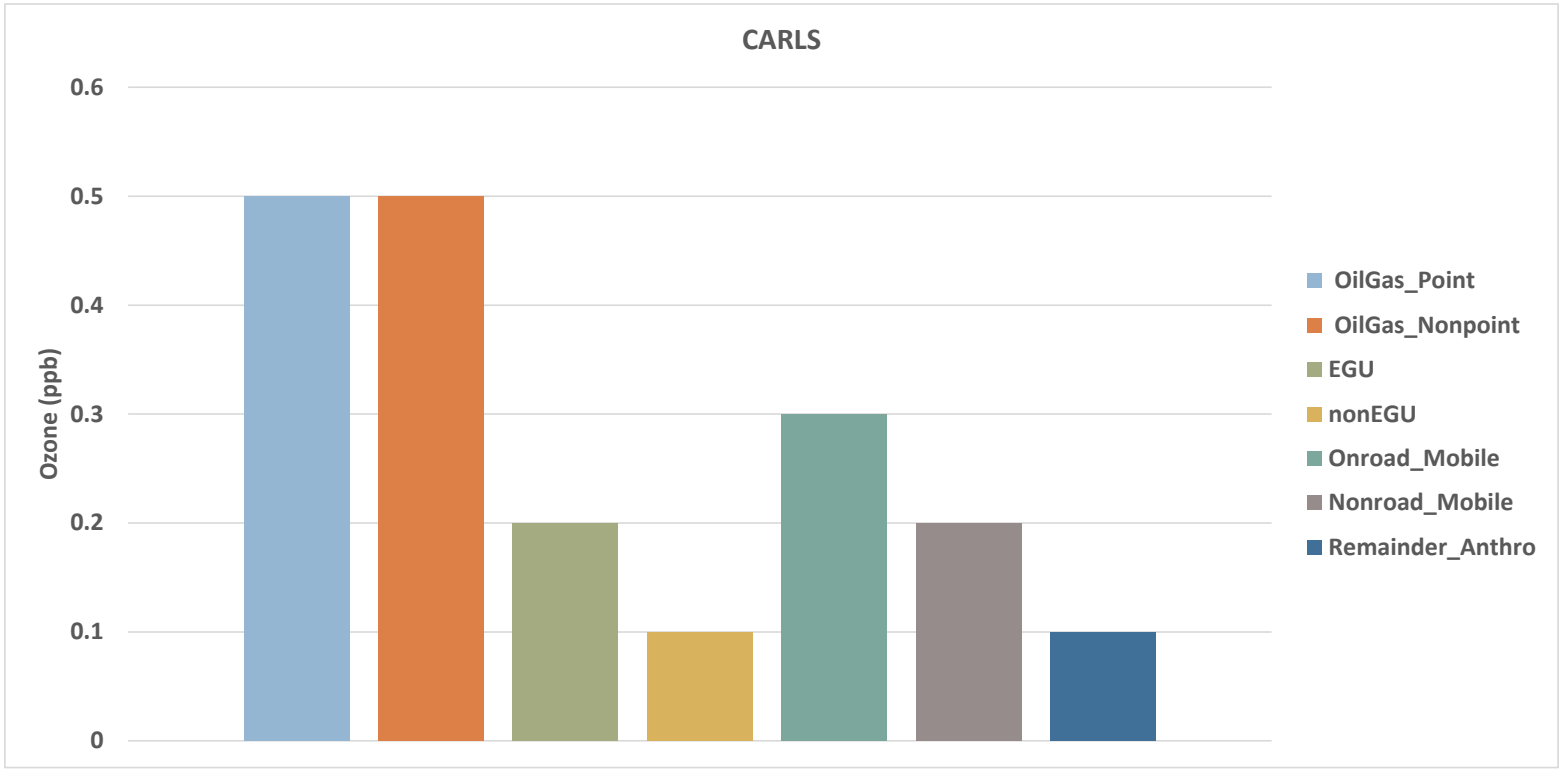

Figure 10-17. Contributions of New Mexico anthropogenic emissions for 7 Source Sectors to projected 2028 ozone DVFs at Carlsbad in Eddy County in southeastern New Mexico.

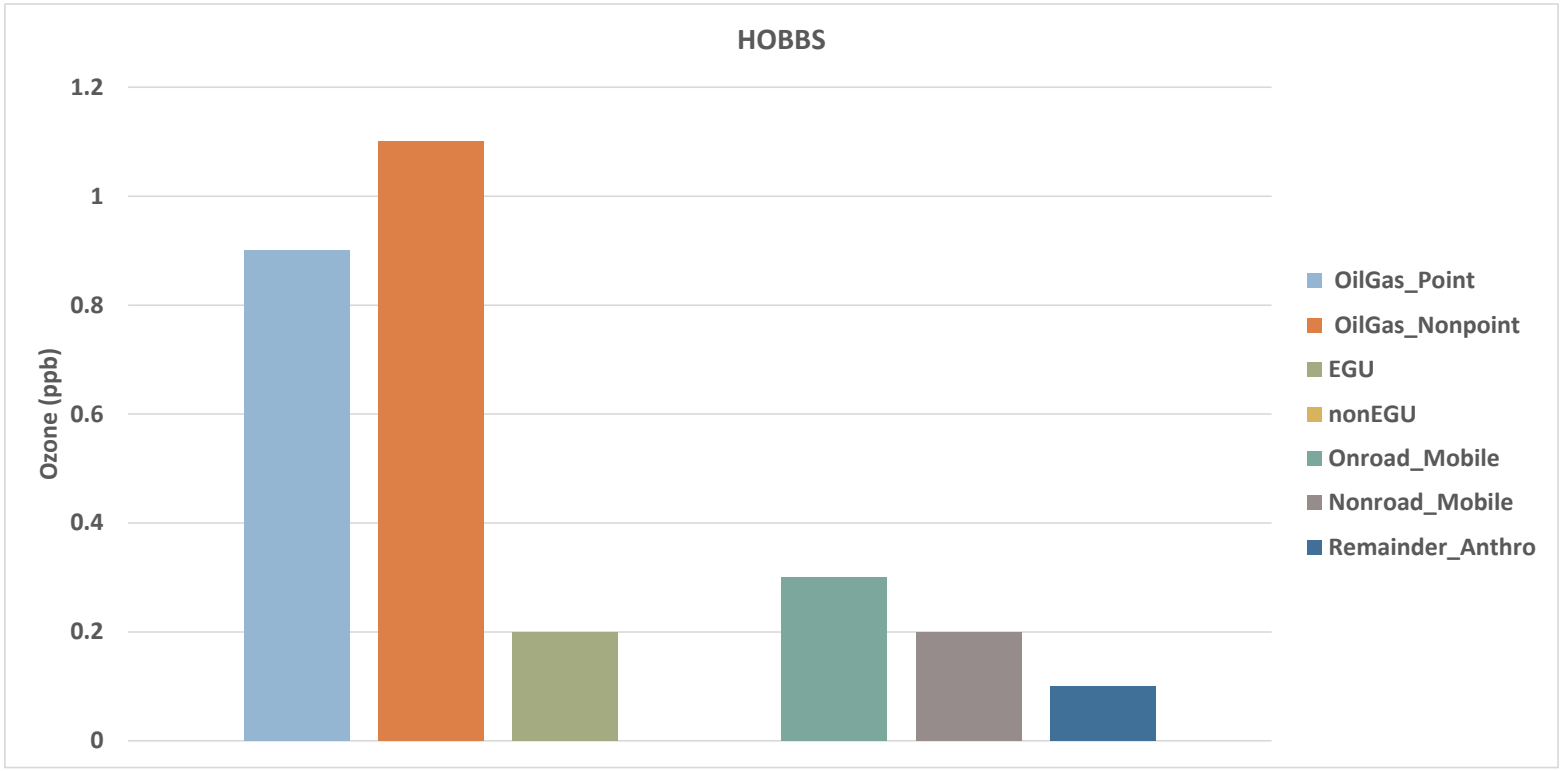

Figure 10-18. Contributions of New Mexico anthropogenic emissions for 7 Source Sectors to projected 2028 ozone DVFs at Hobbs in Lea County in southeastern New Mexico.

The SMAT Unmonitored Area Analysis (UAA) feature was used to estimate the spatial distribution 2028 ozone DVFs across the 4-km New Mexico domain for the 2028 O&G Control Scenario without New Mexico emissions from each of the 7 anthropogenic emission Source Sectors. Figures 10-19 and 10-20 display the reduction in 2028 ozone DVFs across the New Mexico 4-km domain due to the removal of New Mexico emissions for the 7 Source Sectors. Removing New Mexico EGU emissions reduces the 2028 ozone DVF by as much as 3.1 ppb in San Juan County with ozone reductions of 0.1 to 1.0 ppb in the upper half of New Mexico and from Doña Ana to Lea Counties in southern New Mexico (Figure 10-19a). The removal of New Mexico Non-EGU Point emissions results in a reduction of 1.3 ppb in eastern Bernalillo County and reductions of 0.1 to 1.0 in adjacent counties, with little effect over the rest of New Mexico away from Bernalillo County (Figure 10-19b).

New Mexico On-Road mobile contributes as much as 2.6 ppb to the 2028 ozone DVF with reductions of 1-2 ppb stretching from Albuquerque to Santa Fe and in Las Cruces (Figure 10-19c). New Mexico Non-Road mobile contributes as much as 2.1 ppb in Bernalillo County (Figure 10-19d).

New Mexico Non-Point O&G has large (> 2 ppb) contributions to the 2028 ozone DVF in the San Juan and Permian Basins (Figure 10-20a). Whereas, New Mexico Point O&G contributes as much as 1-2 ppb in the Permian Basin but less than 1 ppb in the San Juan Basin (Figure 10-20b). The Other Anthropogenic Source Sector contributions has a similar distribution as the two mobile Source Sectors with the highest ozone contributions centered on Bernalillo County (Figure 10-20c).

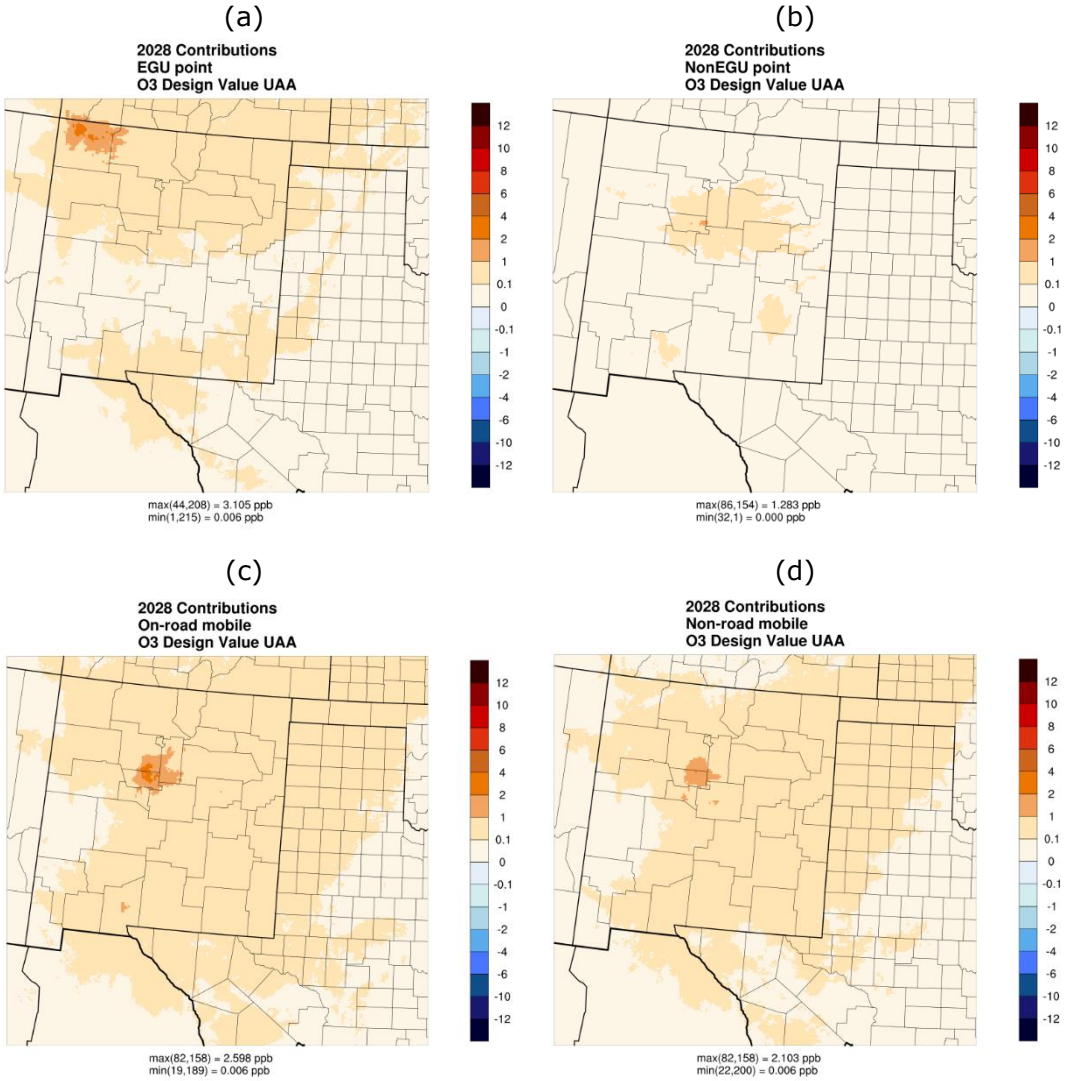

Figure 10-19. Reduction in 2028 ozone DVF due to removal of New Mexico Source Sector emissions for: (a) EGU Point; (b) Non-EGU Point; (c) On-Road Mobile; and (d) Non-Road Mobile.

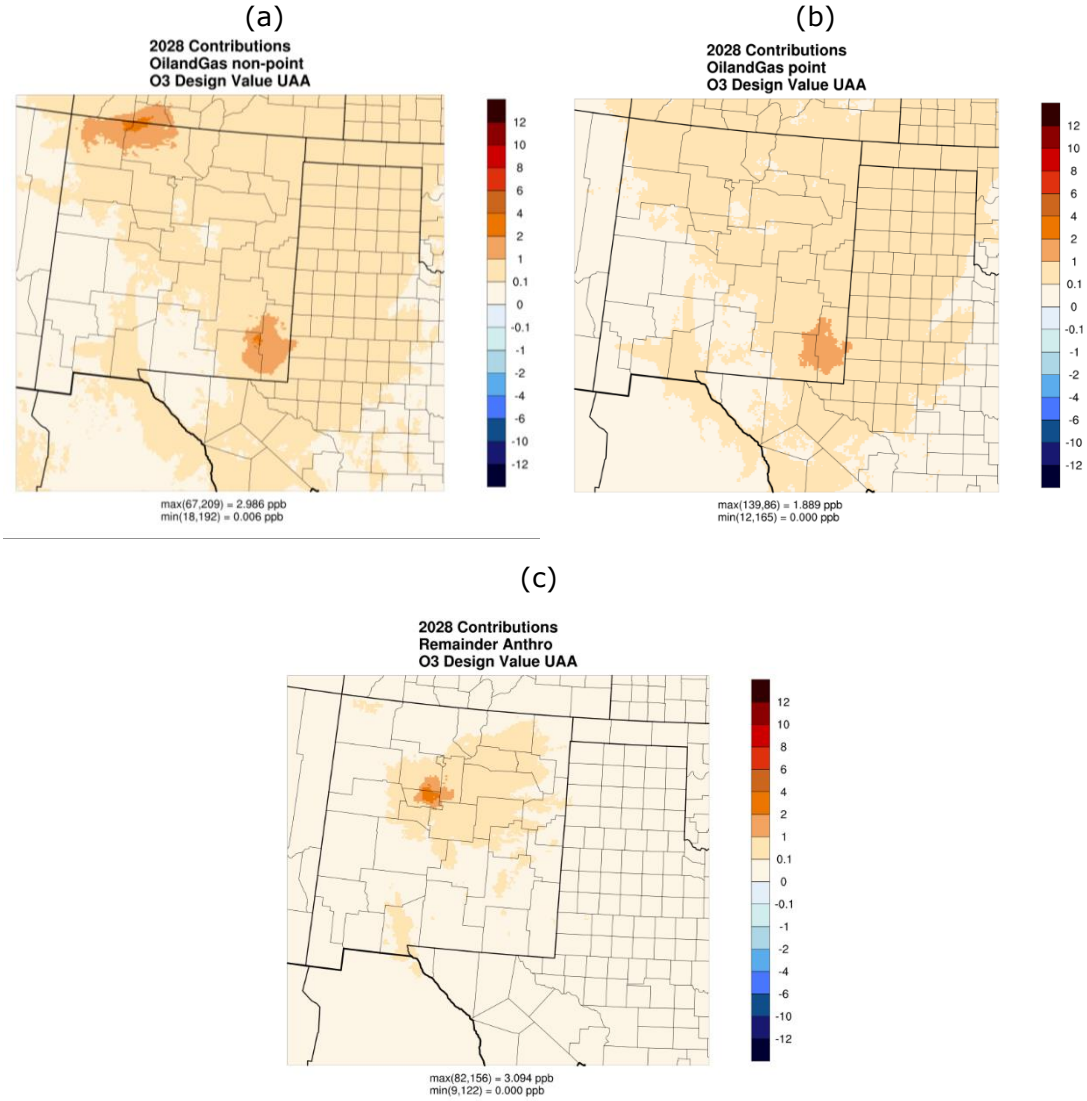

Figure 10-20. Reduction in 2028 ozone DVF due to removal of New Mexico Source Sector emissions for: (a) Non-Point O&G; (b) Point O&G; and (c) Other Anthropogenic.

10.3.1.2 United States Source Sector 2028 Ozone DVF Contributions

Table 10-2 displays the reductions in 2028 ozone DVFs due to the elimination of Source Sector emissions throughout the United States. Table 10-3 shows the percent of the all U.S. Source Sector ozone reduction that was due to just the Source Sector emissions in New Mexico (i.e., the percent the ozone reductions in Table 10-1 are of the ozone reductions in Table 10-2). At the three San Juan County sites, O&G non-point contributes the most (2-3 ppb) with approximately 60-78% coming from O&G non-point sources in New Mexico. Oil and gas point contributes 1.1 to 1.3 ppb at the three San Juan County sites with 55-69% coming from sources in New Mexico. The U.S. EGU Source Sector contributes 2.0 to 3.6 ppb to the 2028 ozone DVF at the three San Juan County sites with a vast majority (~85%) coming from New Mexico. On the other hand, the U.S. On-Road (1.7 ppb) and Non-Road (1.2 ppb) contribution at the three San Juan County sites comes mostly from outside of New Mexico (10-30%).

For sites in Bernalillo County in central New Mexico, 40% to 86% of the U.S. Source Sector contributions come from sources within New Mexico. The largest U.S. Source Sector contributions are for On-Road (3-4 ppb) and Non-Road (2-3 ppb) for which 60-70% of the contribution is due to sources from New Mexico.

At the Doña Ana County monitoring sites, approximately 25% (13-38%) of the U.S. O&G and 22-50% of the U.S. EGU Source Sector is from New Mexico. However, only 9-17% of the U.S. On-Road ozone contribution is from New Mexico sources with the exception of Solano that has 44% of the U.S. on-road mobile ozone contribution due to New Mexico on-road emissions. .

The Carlsbad and Hobbs monitors in southeast New Mexico have approximately half of their U.S. O&G ozone contributions from New Mexico sources, with only ~20% of U.S. mobile contribution coming from New Mexico.

The Grant monitor in southwest New Mexico has almost no ozone contributions from sources in New Mexico.

Table 10-2. Reduction in 2028 ozone DVF due to the elimination of emissions from 7 Source Sectors in United States.

AQS_ID	Site_ID	DVC	DVF	O&GPT	O&GNP	EGU	NonEGU	On-Road	Non-Road	OAnth
Northern New Mexico										
350390026	COYOT	64.0	60.0	-0.5	-0.9	-0.8	-0.7	-1.5	-1.0	-0.7
350450009	BLOOM	64.3	60.2	-1.1	-2.1	-2.3	-0.7	-1.7	-1.1	-0.6
350450018	NAVAJ	67.0	63.3	-1.3	-2.7	-2.0	-0.8	-1.7	-1.2	-0.8
350451005	SUBST	63.7	59.6	-1.1	-2.5	-3.6	-0.8	-1.7	-1.2	-0.7
Central New Mexico										
350010023	NORTE	66.3	60.7	-0.5	-0.7	-1.1	-1.7	-3.9	-3.0	-4.2
350010024	SEHGS	68.0	62.0	-0.5	-0.7	-1.0	-1.7	-3.6	-2.8	-3.7
350010029	STHVA	66.0	60.5	-0.6	-0.9	-1.0	-1.6	-3.3	-2.5	-2.9
350010032	WSTSD	67.0	62.1	-0.4	-0.7	-0.9	-1.0	-2.7	-2.0	-2.4
350011012	FTHIL	65.0	58.8	-0.5	-0.7	-1.1	-1.4	-3.8	-3.0	-3.7
350431001	BERNA	64.0	58.1	-0.4	-0.6	-0.8	-1.1	-3.4	-2.5	-2.6
350490021	SNTFE	64.3	60.4	-0.5	-0.7	-0.7	-0.7	-2.0	-1.4	-1.3
Southern New Mexico										
350130008	UNION	66.3	59.8	-0.8	-0.9	-1.6	-1.5	-3.2	-2.3	-1.5
350130017	SPARK	67.0	61.8	-0.7	-1.0	-1.8	-1.5	-3.0	-2.1	-1.7
350130020	CHAPA	67.0	62.2	-0.6	-0.8	-1.3	-1.4	-2.3	-1.7	-1.3
350130021	DSVIE	72.0	66.8	-0.8	-1.1	-1.8	-1.6	-3.1	-2.2	-1.8
350130022	TERES	71.3	66.0	-0.8	-1.1	-1.6	-1.5	-2.9	-2.1	-1.5
350130023	SOLAN	65.0	60.2	-0.7	-1.0	-0.9	-1.1	-2.7	-1.8	-1.1
350151005	CARLS	69.0	66.4	-0.8	-1.1	-0.5	-0.8	-1.3	-0.9	-0.7
350171003	GRANT	62.0	58.9	-0.2	-0.3	-0.4	-0.7	-1.3	-1.0	-0.7
350250008	HOBBS	66.0	63.3	-1.6	-2.2	-0.7	-0.6	-1.4	-1.0	-0.7
350290003	DEAIR	66.0	62.5	-0.4	-0.5	-0.6	-0.7	-1.7	-1.2	-0.7

Table 10-3. Percent contribution of New Mexico Source Sectors to All United Source Sectors reduction in 2028 ozone DVF.

AQS_ID	Site_ID	O&GPT	O&GNP	EGU	NonEGU	On-Road	Non-Road	OAnth
Northern New Mexico								
350390026	COYOT	40%	56%	63%	0%	13%	10%	0%
350450009	BLOOM	64%	67%	83%	0%	24%	9%	17%
350450018	NAVAJ	69%	78%	85%	13%	24%	17%	13%
350451005	SUBST	55%	60%	86%	13%	29%	17%	29%
Central New Mexico								
350010023	NORTE	40%	43%	45%	59%	69%	67%	86%
350010024	SEHGS	40%	43%	50%	65%	69%	68%	86%
350010029	STHVA	50%	56%	50%	63%	67%	68%	83%
350010032	WSTSD	50%	57%	44%	40%	59%	60%	75%
350011012	FTHIL	40%	43%	45%	50%	66%	67%	81%
350431001	BERNA	25%	33%	50%	36%	62%	60%	73%
350490021	SNTFE	40%	43%	29%	43%	60%	50%	62%
Southern New Mexico								
350130008	UNION	25%	22%	44%	0%	16%	13%	7%
350130017	SPARK	29%	20%	50%	0%	13%	10%	12%
350130020	CHAPA	17%	13%	23%	0%	9%	6%	8%
350130021	DSVIE	25%	27%	50%	6%	16%	14%	11%
350130022	TERES	38%	27%	44%	7%	17%	14%	13%
350130023	SOLAN	29%	20%	22%	18%	44%	39%	27%
350151005	CARLS	63%	45%	40%	13%	23%	22%	14%
350171003	GRANT	0%	0%	0%	0%	8%	10%	0%
350250008	HOBBS	56%	50%	29%	0%	21%	20%	14%
350290003	DEAIR	50%	20%	33%	0%	35%	33%	0%

10.3.2 Source Sector Contributions to Modeled MDA8 Ozone Concentrations

The contributions of the Source Sector emissions to the absolute CAMx modeling results 2028 daily MDA8 ozone concentrations are analyzed in this section. We first present spatial maps of the episode maximum MDA8 ozone contributions across the 4-km New Mexico domain for each Source Region. The contributions of all and New Mexico Source Sectors to MDA8 ozone concentrations are then presented at four example New Mexico monitoring sites for the 10 days used to make the 2028 ozone DVF projections (i.e., the 10 SMAT days). Finally, the spatial maps of New Mexico and all United States Source sector contributions to daily MDA8 ozone concentrations are presented for six example days during the May-August 2014 modeling episode.

10.3.2.1 Episode Maximum Source Sector MDA8 Ozone Contributions by Source Region

Figures 10-21 and 10-22 display the episode maximum MDA8 ozone contributions due to Source Sector emissions from New Mexico. The maximum New Mexico EGU MDA8 ozone contribution is 10.9 ppb and occurs at the location of the Four Corners Power Plan in San Juan County (Figure 10-21a). Elevated ozone due to emissions from New Mexico EGUs is also seen in Lea County at the location of the Hobbs, Cunningham and Maddox EGUs and in southern Doña Ana County at the location of the Rio Grande EGU (Figure 10-21a). The highest New Mexico Non-EGU Point source contribution is 3.1 ppb in eastern Bernalillo County with the Non-EGU Point contribution mostly less than 1 ppb away from Bernalillo County (Figure 10-21b). The maximum New Mexico On-Road (4.7 ppb) and Non-Road (4.0 ppb) ozone contributions both occur in Albuquerque, with a secondary ozone maximum occurring in Las Cruces (Figure 10-21c and d). The On-Road ozone spatial patterns follow the major freeways, including east-west I-40 and north-south I-25, with even I-10 evident in Luna County in southwest New Mexico (Figure 10-21c).

The highest New Mexico O&G Non-Point (7.6 ppb) and O&G Point (5.4 ppb) both occur at the same location in the Permian Basin (Figure 10-22a and b). The O&G Non-Point ozone contributions exceed 5 ppb over large portions of the Permian and San Juan Basins (Figure 10-22a). The O&G Point source ozone contributions are lower, exceeding 3 ppb over large portions of the Permian Basin with much lower ozone contributions in the San Juan Basin (Figure 10-22b). The Other Anthropogenic ozone contribution has a bull’s eye centered on Albuquerque with a maximum of 6.2 ppb (Figure 10-22c). Fires are highly episodic with four distinct fire ozone plumes present in New Mexico with episode maximum exceeding 20 ppb (Figure 10-22d).

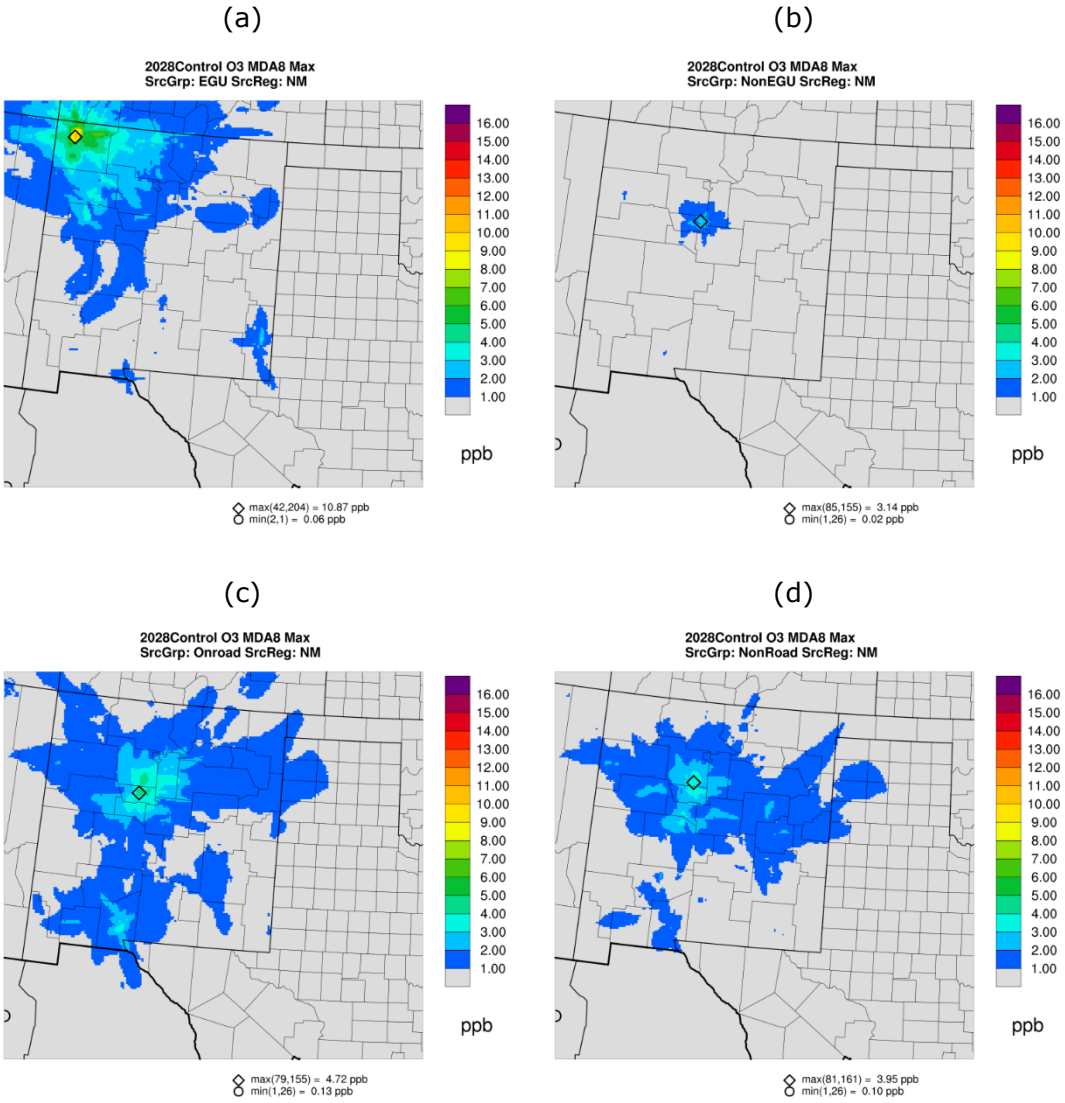

Figure 10-21. Episode maximum daily MDA8 ozone contributions from Source Sectors in New Mexico for: (a) EGU Point; (b) Non-EGU Point; (c) On-Road Mobile; and (d) Non-Road Mobile.

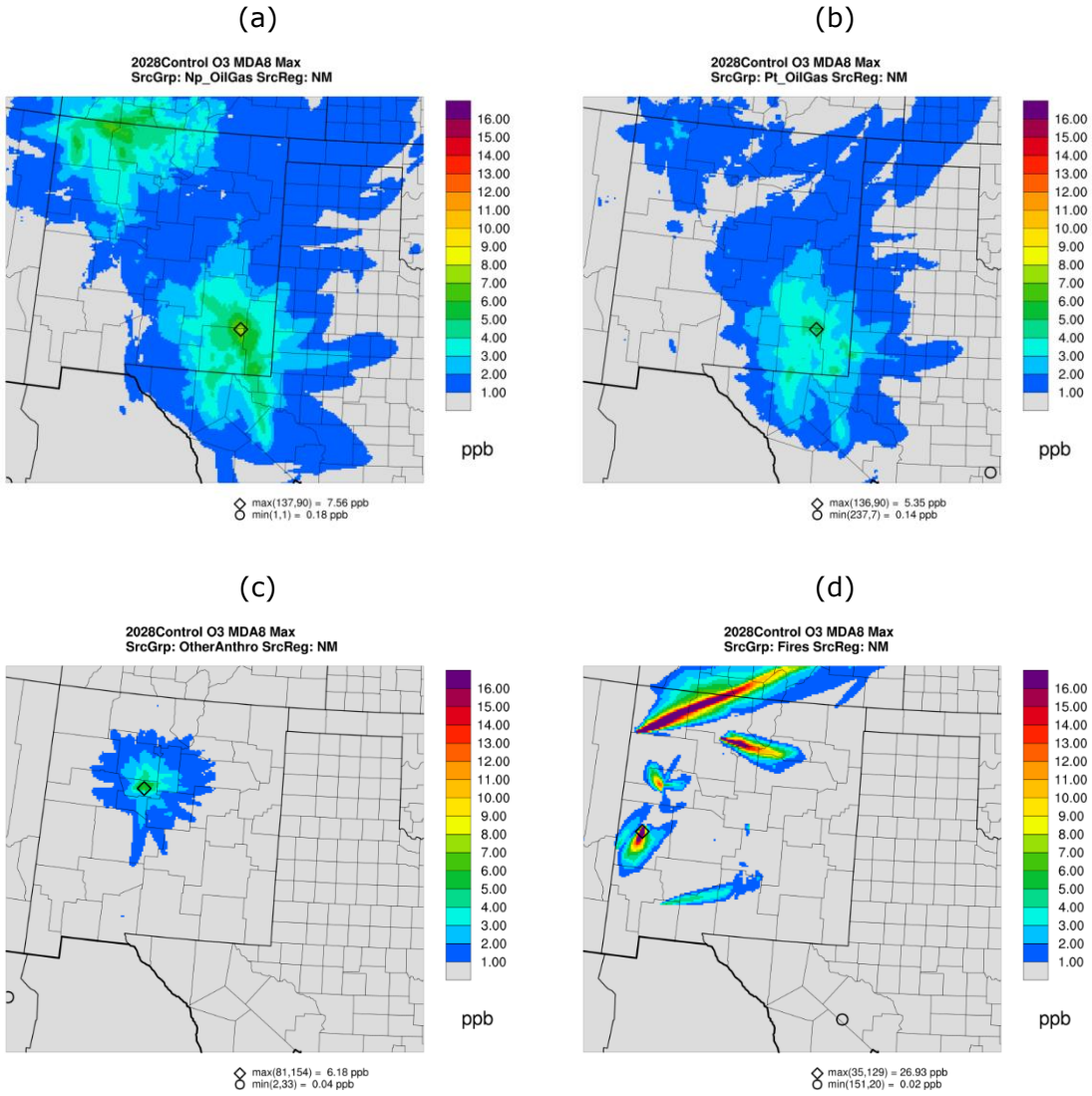

Figure 10-22. Episode maximum daily MDA8 ozone contributions from Source Sectors in New Mexico for: (a) Non-Point O&G; (b) Point O&G; (c) Other Anthropogenic; and (d) Fires.

Figure 10-23 displays the episode maximum MDA8 ozone contributions due to emissions from Texas for 9 Source Sectors (7 anthropogenic Source Sectors plus fires and natural). The presence of EGUs in the Texas Panhandle is clearly evident (e.g., 1,100 MW Tolk coal EGU) that produce ozone in excess of 2 ppb entering eastern New Mexico (Figure 10-23, top left). Elevated ozone due to Texas Non-EGU Point, On-Road, Non-Road, and Other Anthropogenic is seen in El Paso with elevated ozone concentrations entering Doña Ana County. The Texas anthropogenic Source Sector that contributes the most to ozone in New Mexico is O&G. Texas O&G Non-Point (Figure 10-23, middle right) produces ozone above 4 ppb in Lea County and ozone in excess of 2 ppb as far north as Santa Fe and San Miguel Counties. Within the New Mexico portion of the Permian Basin, the maximum Texas O&G Non-Point ozone contribution exceeds 3 ppb and the maximum Texas O&G Point contribution exceeds 2 ppb.

The Colorado Source Sector with the largest contribution to New Mexico ozone concentrations is O&G Non-Point that has a peak ozone contribution in the 4-km domain of 7 ppb that occurs in Colorado just north of the border of San Juan and Rio Arriba Counties (Figure 10-24, middle right). Colorado O&G Non-Point contributes ozone in excess of 4 ppb in the northern portion of the two northwest New Mexico counties and ozone in excess of 1.5-2.0 ppb stretching south to Bernalillo County. Other Colorado anthropogenic emissions Source Sectors contribute ozone in excess of 0.5 ppb across large portions of New Mexico with O&G Point contributing ozone in excess of 1 ppb in San Juan County.

The highest Source Sector ozone contributions in the 4-km New Mexico domain due to all emissions in the U.S. are shown in Figure 10-25. The peak U.S. EGU ozone contribution is 11.5 ppb at the same locations as the New Mexico EGU peak ozone contribution with most of the U.S. EGU contribution at this location due to the FCPP in New Mexico (10.9 ppb, see Figure 10-21a). In addition to the EGU ozone hotspots in the Texas panhandle discussed above (Figure 10-23), there are also all U.S. EGU ozone hotspots in eastern Arizona at the locations of the Springerville and Coronado Generating Stations (Figure 10-25, top left). The U.S. On-Road, Non-Road and Other Anthropogenic ozone contributions (Figure 10-25) look similar to the New Mexico alone ozone contributions (Figures 10-21 and 10-22) with the addition of an incremental ozone concentrations across the 4-km domain due to the U.S. Source Sector emissions from outside New Mexico.

The peak U.S. O&G Non-Point ozone contribution is 10.5 ppb (Figure 10-25, middle right) and occurs at the same location in Colorado on the border with New Mexico as where the Colorado O&G Non-Point peak ozone (7.0 ppb) occurred (Figure 10-24, middle right). The additional 4.5 ppb ozone comes mainly from New Mexico O&G Non-Point emissions (Figure 10-22a). Ozone due to U.S. O&G Non-Point exceeds 8 ppb in the New Mexico portions of the San Juan and Permian Basins. Ozone due to U.S. O&G Point sources exceeds 4 ppb over a wide area in the Permian Basin, whereas U.S. O&G Point rarely exceeds 4 ppb in the San Juan Basin.

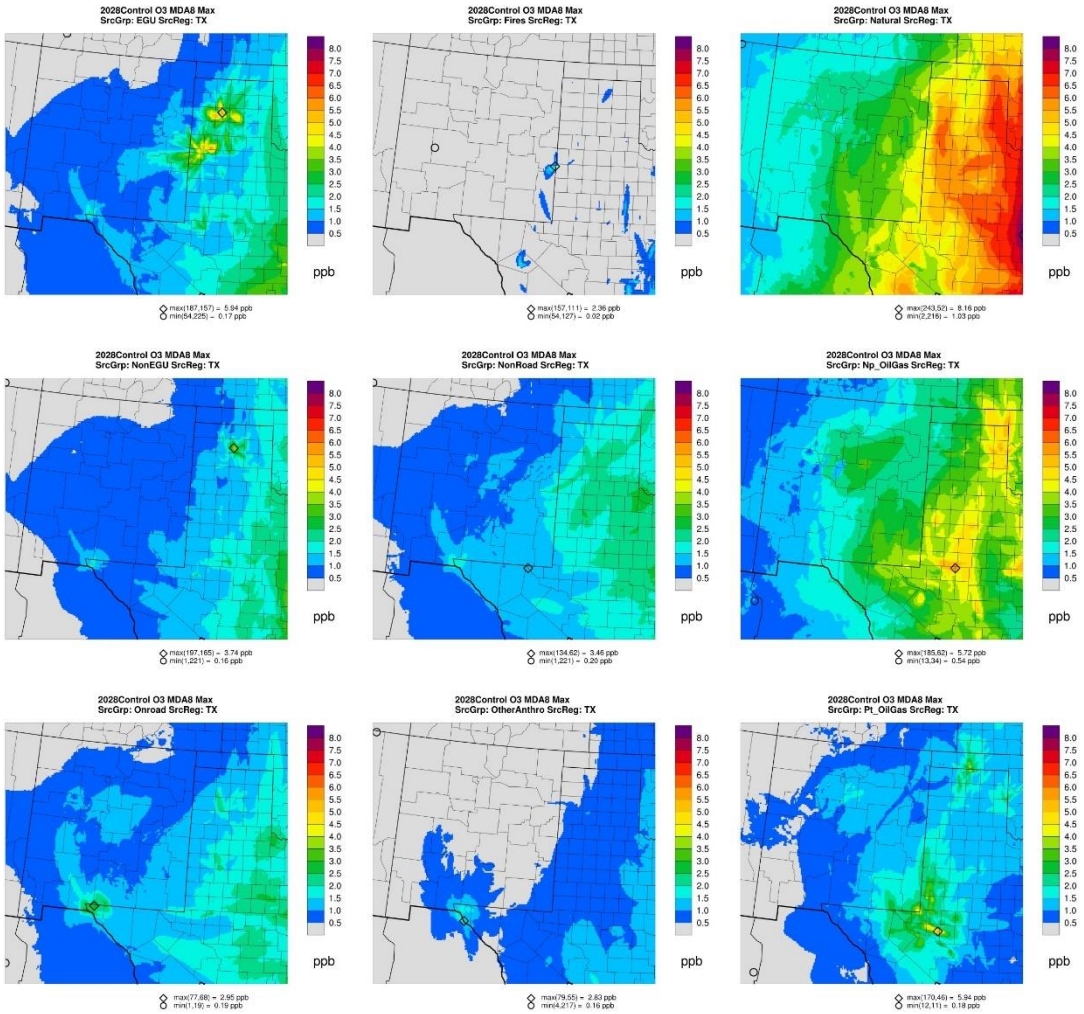

Figure 10-23. Episode maximum MDA8 ozone contributions from Source Sectors in Texas for EGU Point (top left), Fires (top middle), Natural (top right), Non-EGU Point (middle left), Non-Road (middle middle), O&G Non-Point (middle right), On-Road (bottom left), Other Anthropogenic (bottom middle) and O&G Point (bottom right) from the 2028 O&G Control Strategy emissions scenario.

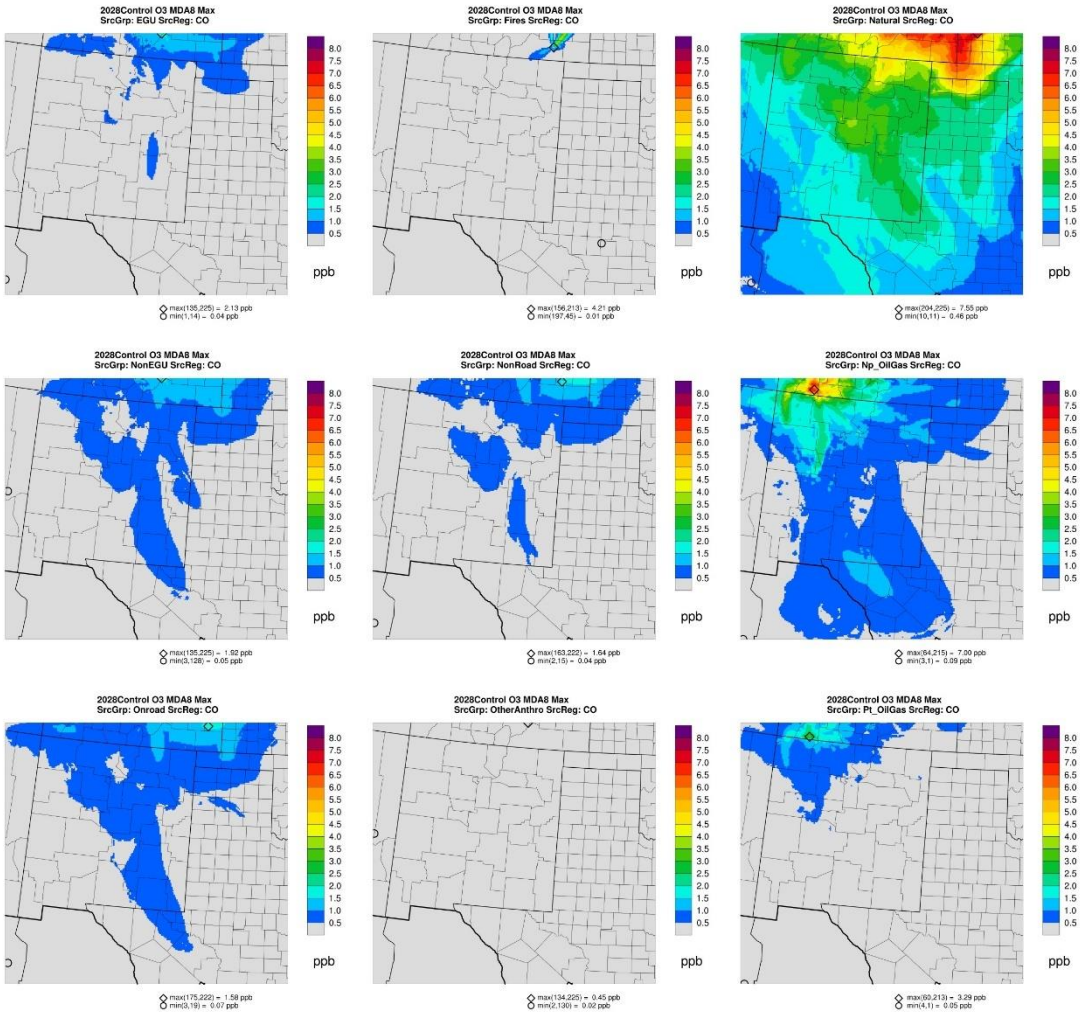

Figure 10-24. Episode maximum MDA8 ozone contributions from Source Sectors in Colorado for EGU Point (top left), Fires (top middle), Natural (top right), Non-EGU Point (middle left), Non-Road (middle middle), O&G Non-Point (middle right), On-Road (bottom left), Other Anthropogenic (bottom middle) and O&G Point (bottom right) from the 2028 O&G Control Strategy emissions scenario.

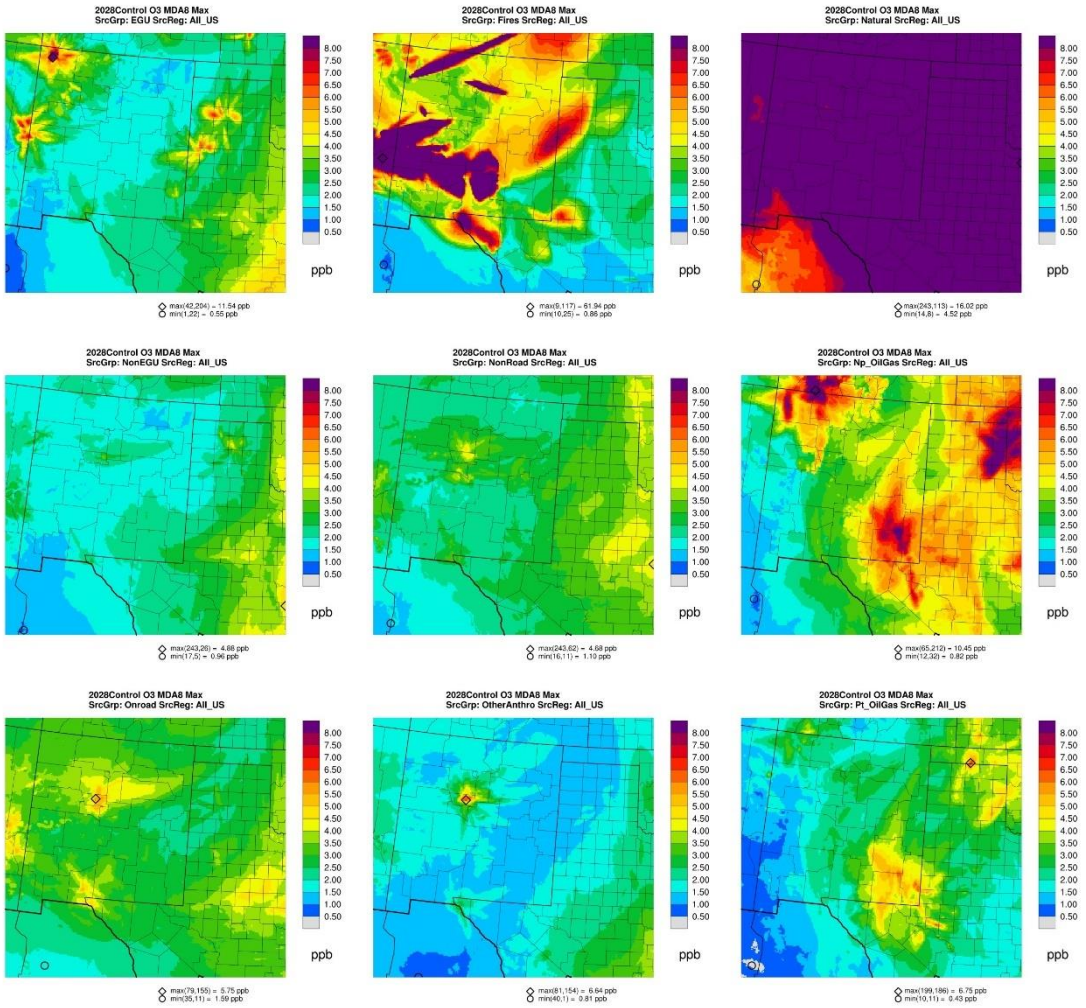

Figure 10-25. Episode maximum MDA8 ozone contributions from Source Sectors in United States for EGU Point (top left), Fires (top middle), Natural (top right), Non-EGU Point (middle left), Non-Road (middle middle), O&G Non-Point (middle right), On-Road (bottom left), Other Anthropogenic (bottom middle) and O&G Point (bottom right) from the 2028 O&G Control Strategy emissions scenario.

The top two panels in Figure 10-26 display the episode maximum MDA8 ozone contributions due to international anthropogenic emissions that are either within the CAMx 36/12/4-km modeling domain (i.e., mainly from in-domain Mexico emissions) or coming through the BCs (BC_{Intl}) from international emissions from outside of the CAMx modeling domains that were generated from 2014 GEOS-Chem simulations. The in-domain international anthropogenic emissions contribute high ozone concentrations in southern New Mexico with values exceeding 16 ppb stretching into Doña Ana, Luna and Otero Counties. The southeastern half of New Mexico has ozone contributions in excess of 8 ppb due to in-domain international emissions. Although the ozone peaks are not as high as the in-domain international anthropogenic emissions, the BC_{Intl} ozone contributions exceed 10 ppb across all of New Mexico and are as high as 13 ppb

(Figure 10-26b). The $BC_{Natural}$ ozone contributions is as high as 49 ppb in San Juan County (Figure 10-26c), while the BC_{US} ozone contributions ranges from 3-4 ppb across New Mexico (Figure 10-26d).

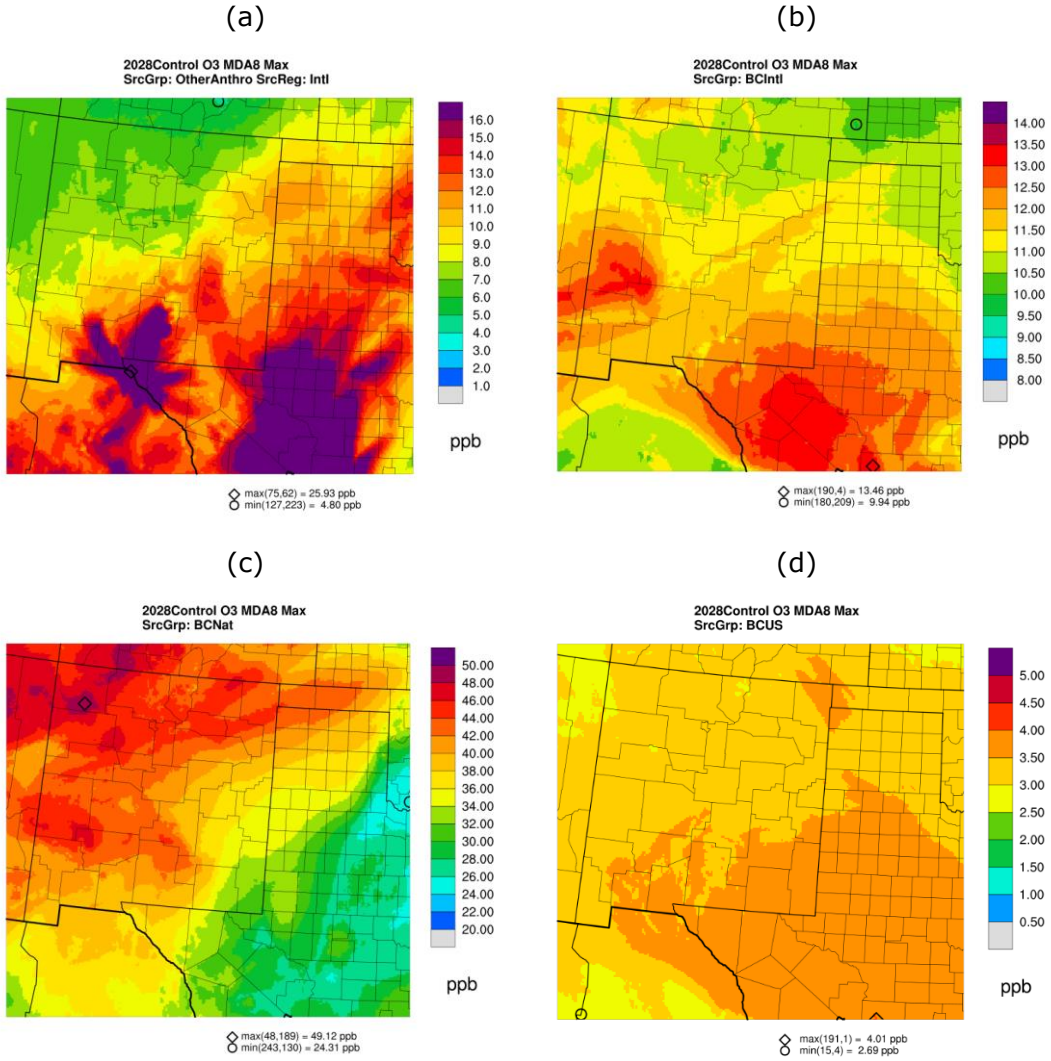

Figure 10-26. Episode maximum MDA8 ozone contributions from: (a) International Anthropogenic Emissions within CAMx 36/12/4-km domains; (b) BCs due to International Anthropogenic Emissions (BC_{Intl}); (c) BCs due to Natural sources ($BC_{Natural}$); and (d) BCs due to U.S. Anthropogenic Emissions (BC_{US}).

10.3.2.2 Source Sector Ozone Contributions to MDA8 Ozone Concentrations on Modeled High Ozone Days

The daily CAMx 2028 Source Sector APCA ozone source apportionment modeling results were extracted at the locations of the New Mexico ozone monitoring sites and loaded into an Excel Dashboard to visualize the source contributions using stacked bar, pie and tree charts. The Dashboard displays modeled 2028 MDA8 ozone concentrations at a user-selected monitoring site in groups of 10 high ozone days, and the average across the 10 days. These 10 days include the 10 days used in the SMAT 2028 ozone DVF projections, as well as the modeled 2028 first and second highest group of 10 days.

Figures 10-27 through 10-34 display results from the Dashboard for 5 monitoring sites representing different locations in New Mexico. Figures 10-27 and 10-28 display the modeled 2028 ozone results at the Navajo Lake monitor in northwest New Mexico for the 10 SMAT days. The top panel in Figure 10-27 shows stacked bar charts of daily MDA8 ozone contributions by Source Region and BCs for the 10 SMAT days at Navajo Lake. The total MDA8 ozone concentrations are 60-70 ppb and the BCs (grey bar) contribute by far the most with contributions ranging from 26 to 60 ppb. The New Mexico contribution ranges from near zero to 10.9 ppb. The bottom panel in Figure 10-27 shows a Tree Chart and breaks down each Source Region's contribution by Source Category averaged across the 10 SMAT days at Navajo Lake. The Natural category dominates the BC contribution followed by the BC International Anthropogenic Emissions category.

Figure 10-28 focuses on contributions due to emissions from New Mexico Source Categories to MDA8 ozone on the 10 SMAT days at Navajo Lake showing day by day results in the top panel and a pie chart of New Mexico contributions averaged across the 10 days in the bottom panel. For the Navajo Lake site, New Mexico O&G Non-Point is always the largest contributor (38% on average) followed by EGU (29% on average) and then O&G Point (16% on average). Next most important is either On-Road or Natural, depending on the day (6-7% on average). The other two San Juan County sites have higher EGU contributions, with EGU being the highest New Mexico Source Category accounting for 50% and 32% of the New Mexico ozone contribution at, respectively, Substation and Bloomfield.

Figures 10-29 and 10-30 show ozone contribution results for the 10 SMAT days at the Foothills monitoring site and represents typical contributions for sites in Bernalillo County. There is a wide-range of variation in the New Mexico ozone contribution to the 10 SMAT days at Foothills, from near zero to 15 ppb. BCs contribute the most, 27 to 47 ppb. The remaining U.S. and in-domain international emissions also contribute a fair amount. The three most important New Mexico Source Categories contributing to modeled MDA8 ozone at Foothills averaged across the 10 SMAT days are Other Anthropogenic (27%), On-Road (35%) and Non-Road (20%) (Figure 10-30).

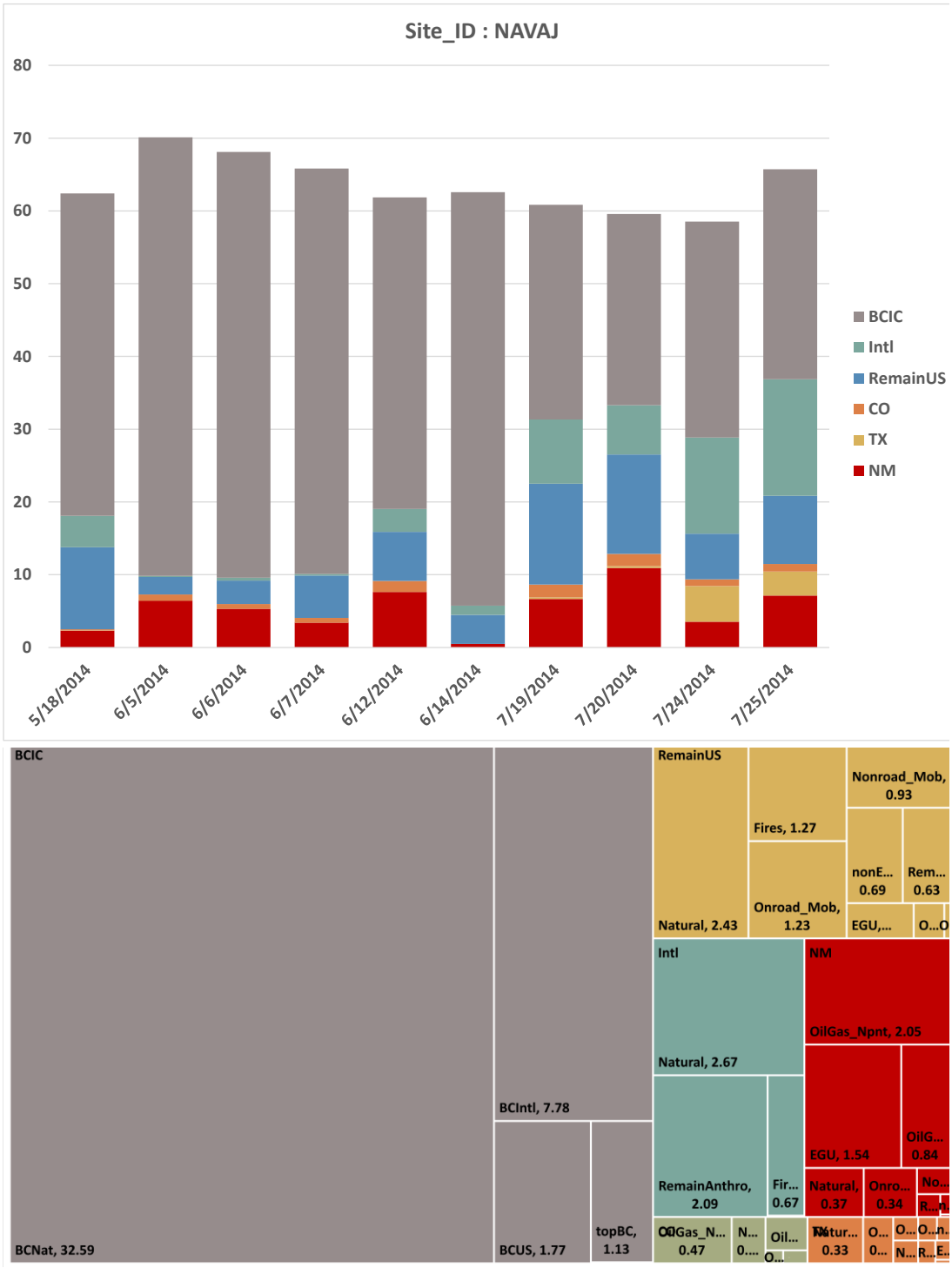

Figure 10-27. Contributions of all Source Groups to total MDA8 ozone concentrations at Navajo Lake for the 10 high SMAT ozone days (top) and average across the 10 SMAT days (bottom).

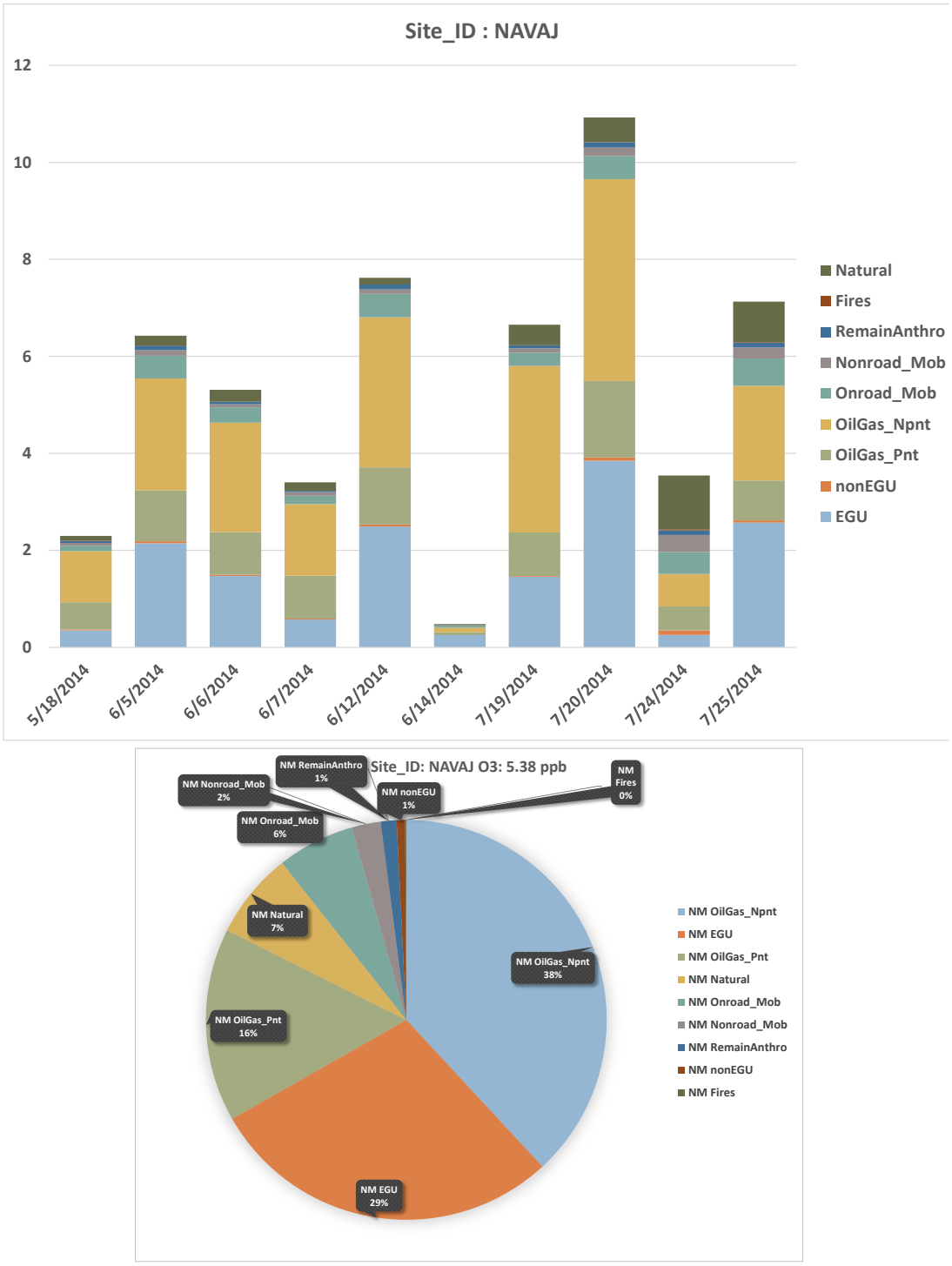

Figure 10-28. Contributions of New Mexico Source Groups to MDA8 ozone concentrations from New Mexico at Navajo Lake for the 10 high SMAT ozone days (top) and average across the 10 SMAT days (bottom).

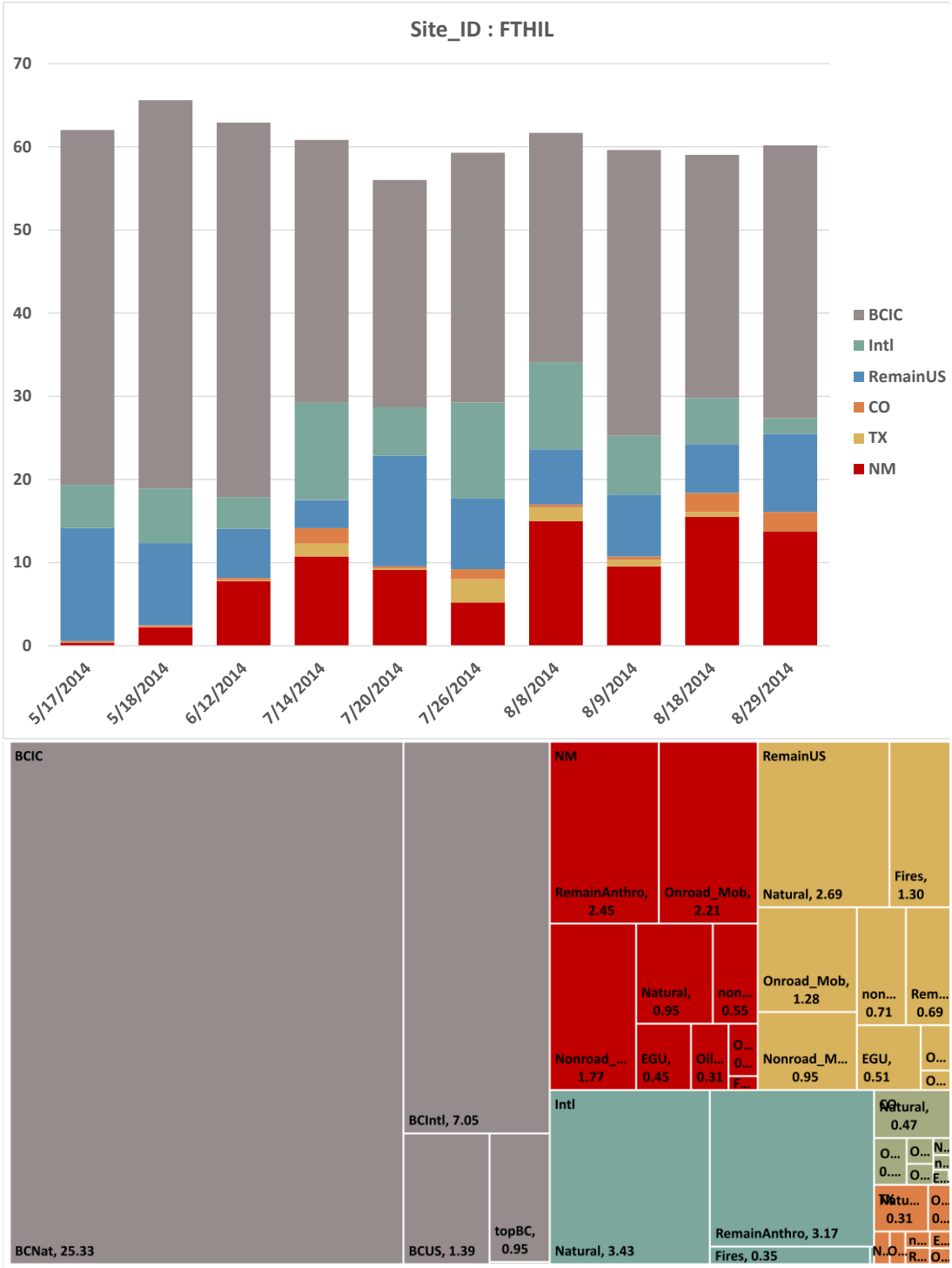

Figure 10-29. Contributions of all Source Groups to total MDA8 ozone concentrations at Foothills for the 10 high SMAT ozone days (top) and average across the 10 SMAT days (bottom).

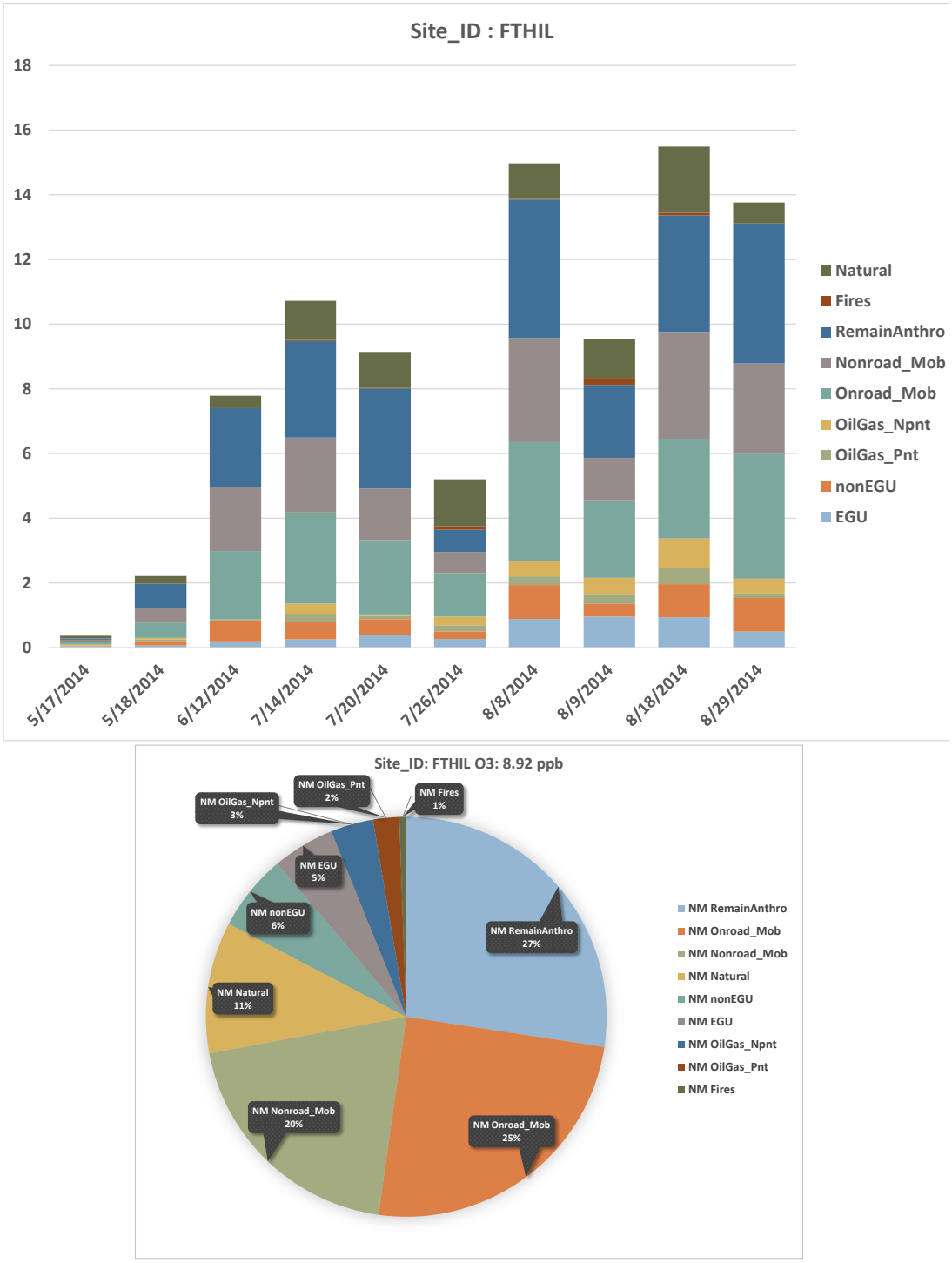

Figure 10-30. Contributions of New Mexico Source Groups to MDA8 ozone concentrations from New Mexico at Foothills for the 10 high SMAT ozone days (top) and average across the 10 SMAT days (bottom).

Ozone contributions for the 10 SMAT days at the Desert View monitor in Doña Ana County are shown in Figures 10-31 and 10-32. BCs from outside the 36-km North American domain is the largest contributor (45% on average), followed by in-domain international emissions (27%), Remainder US (14%) and Texas (8%). Emissions from New Mexico only contribute 4% of the total ozone averaged across the 10 SMAT days at Desert View. International anthropogenic emissions from BCs (5.8 ppb) and in-domain (i.e., Mexico) sources (13.0 ppb) contribute a combined 18.8 ppb (30%) of the average ozone across the 10 SMAT days at Desert View (Figure 10-31, bottom). As shown in Figure 10-32, the contributions from sources in New Mexico contributes from 1.3 to 4.4 ppb to the total MDA8 ozone on the 10 SMAT days, with an average contribution of 2.8 ppb. The largest New Mexico contributing Source Sector is EGU (29%), followed by Natural (18%), On-Road (15%) with 10% contribution coming from Non-Road and Remaining Anthropogenic (Figure 10-32, bottom).

Figures 10-33 and 10-34 displays the 10 SMAT day ozone contributions at the Carlsbad monitoring site. BC and in-domain international emissions contribute the most to ozone at Carlsbad. There is a lot of variation in the day-to-day contributions from New Mexico (0.2 to 5 ppb) with an average contribution of 2.0 ppb. Similar results are seen for Texas (0.5 to 9 ppb with an average of 2.5 ppb). Non-Point O&G and then Point O&G are the two largest anthropogenic Source Sector contributors from both New Mexico and Texas.

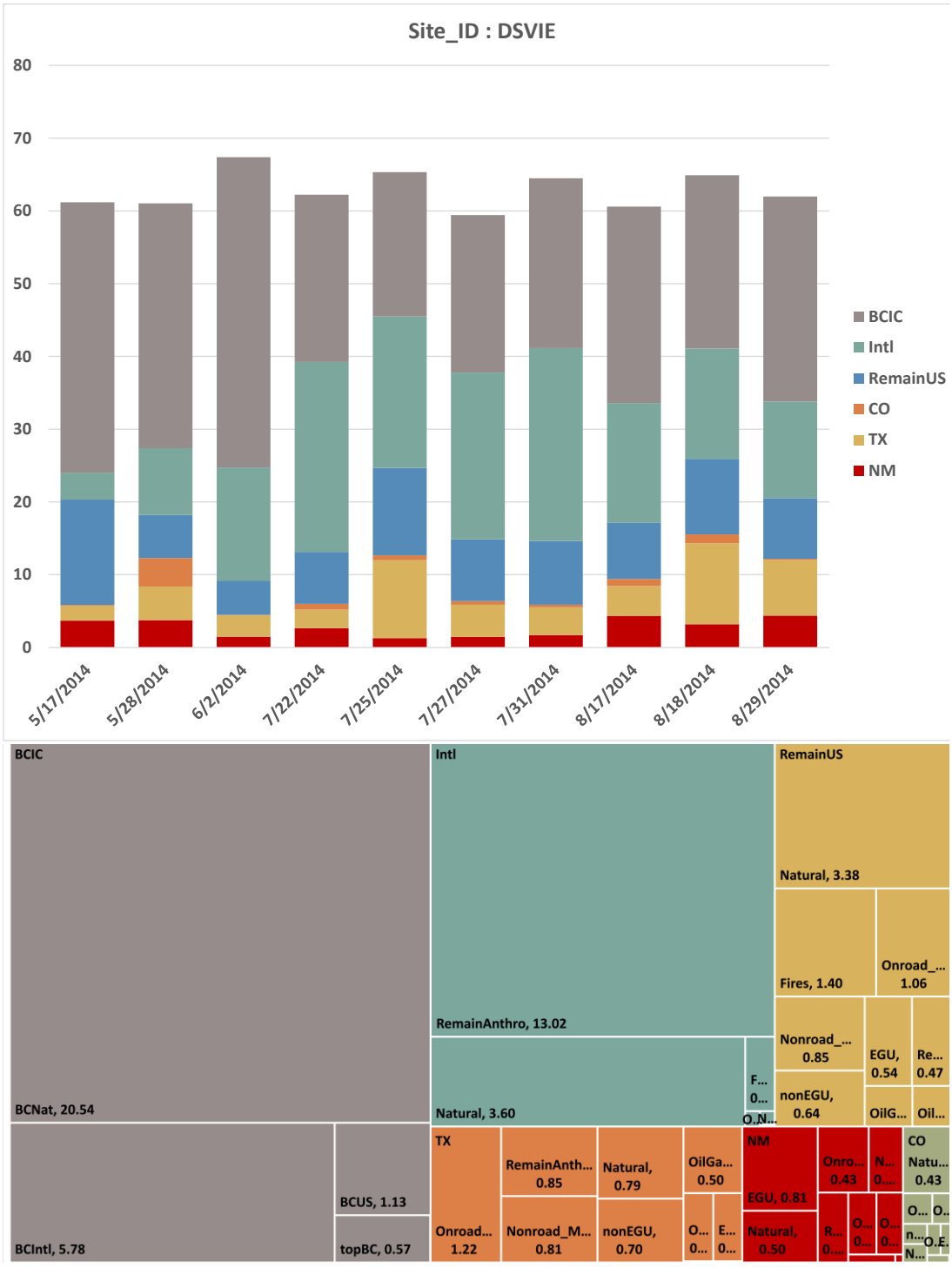

Figure 10-31. Contributions of all Source Groups to total MDA8 ozone concentrations at Desert View for the 10 high SMAT ozone days (top) and average across the 10 SMAT days (bottom).

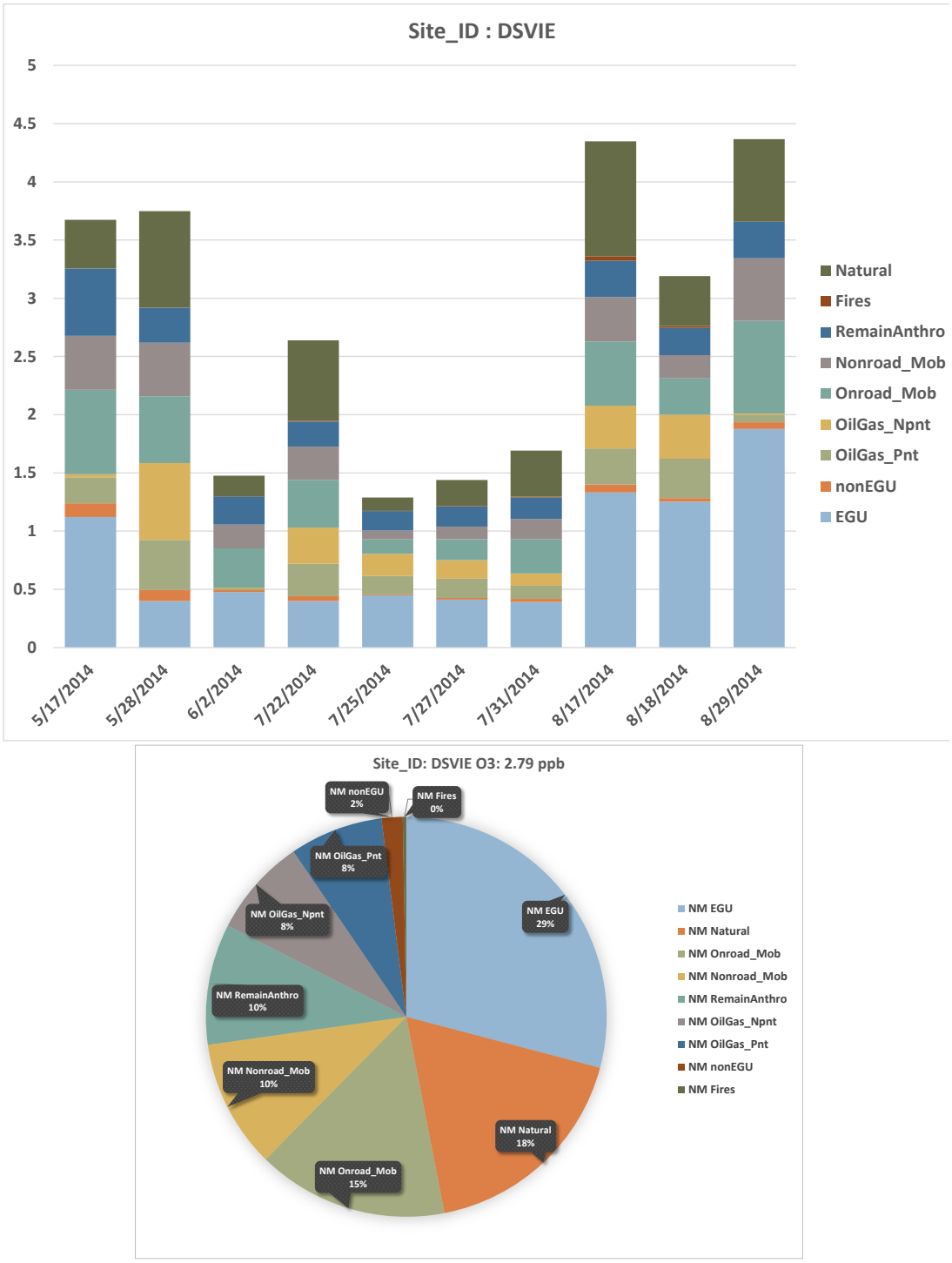

Figure 10-32. Contributions of New Mexico Source Groups to MDA8 ozone concentrations at Desert View for the 10 high SMAT ozone days (top) and average across the 10 SMAT days (bottom).

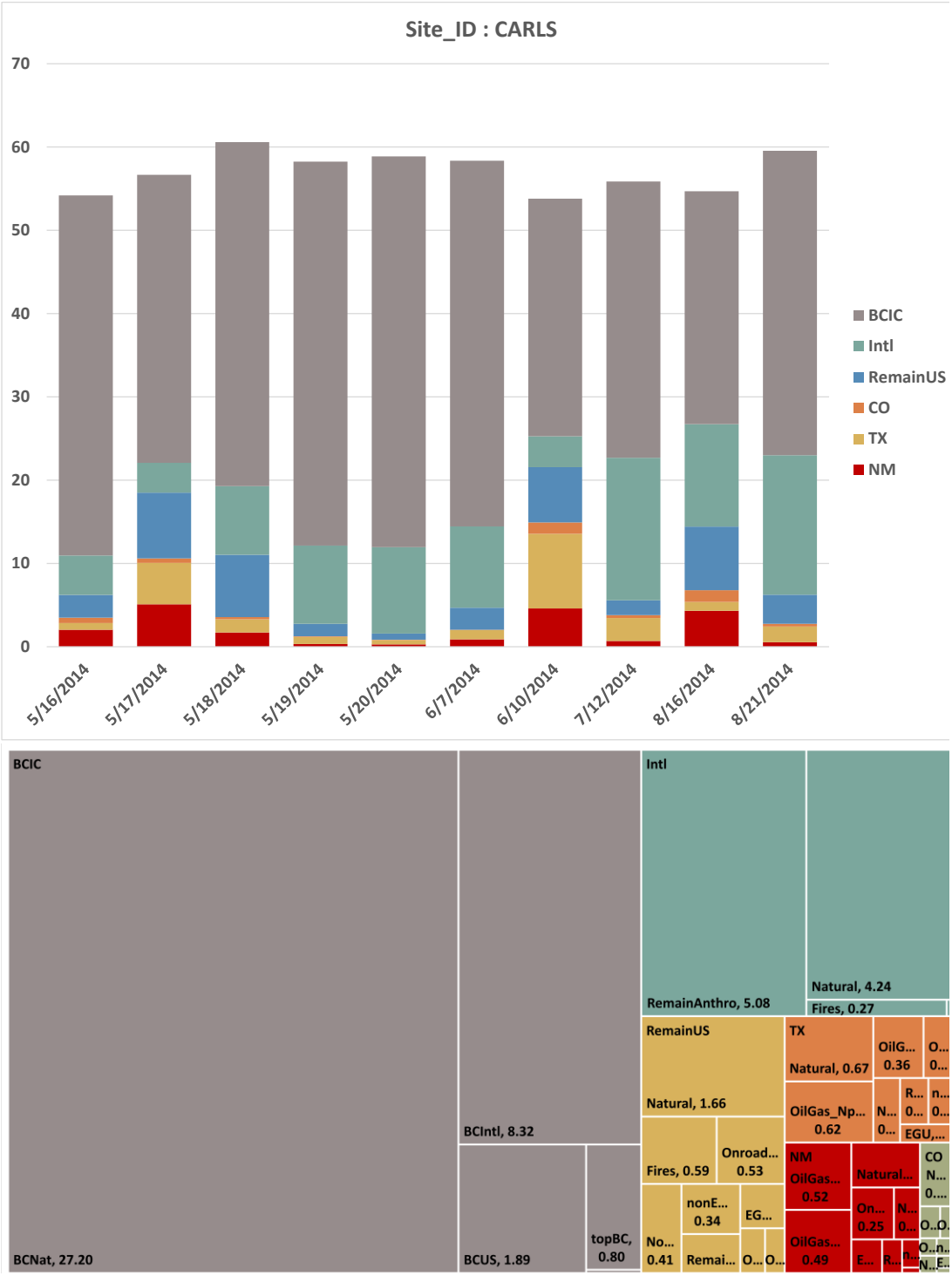

Figure 10-33. Contributions of all Source Groups to total MDA8 ozone concentrations at Carlsbad for the 10 high SMAT ozone days (top) and average across the 10 SMAT days (bottom).

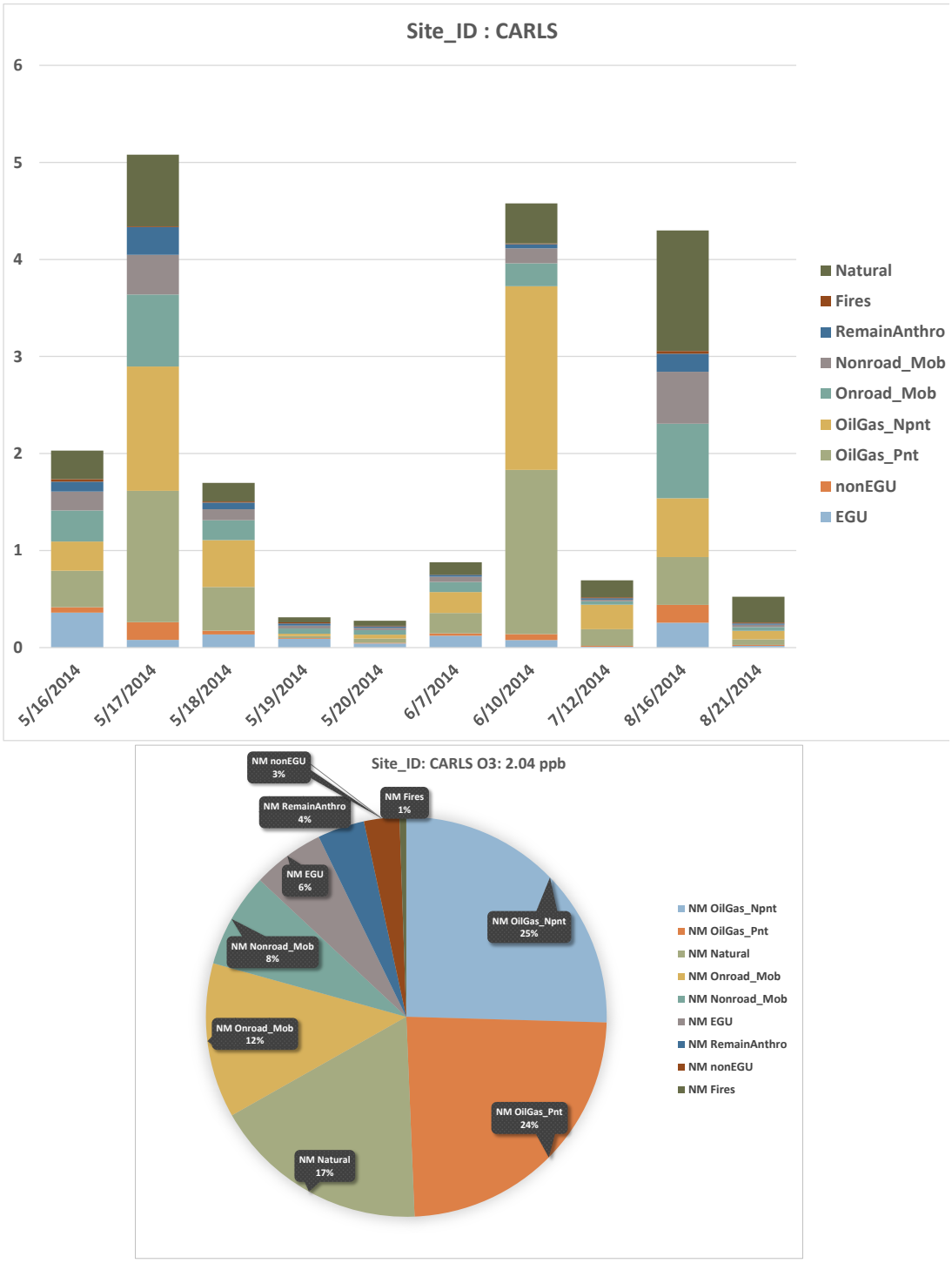

Figure 10-34. Contributions of New Mexico Source Groups to MDA8 ozone concentrations at Carlsbad for the 10 high SMAT ozone days (top) and average across the 10 SMAT days (bottom).

10.3.3 International Anthropogenic Emissions Contributions to Projected 2028 ozone DVFs

The SMAT ozone DVF projection tool was run using the CAMx 2028 O&G Control Strategy output with the contributions of international anthropogenic emissions removed. The ozone concentrations due to the BC_{Intl} and in-domain international emissions (i.e., Mexico, Canada and CMV_{Intl}) were removed from the CAMx 2028 O&G Control Strategy output and SMAT was run to obtain projected 2028 ozone DVFs without any contributions of international anthropogenic emissions. SMAT was run using three different current year ozone design values: $DVC_{2012\text{-}2016}$, $DVC_{2015\text{-}2019}$ and $DVC_{2017\text{-}2019}$ using the same procedures as used in the 2028 ozone DVF projection DVC sensitivity analysis discussed in Chapter 9. Tables 10-4 through 10-6 display the projected 2028 ozone DVFs for the 2028 O&G Control Strategy and 2028 no international anthropogenic emissions scenarios using the three sets of DVCs.

The elimination of the international anthropogenic emissions reduces the projected 2028 ozone DVFs by 13 to 25 ppb with the smallest reductions at the northern and largest reductions at the southern sites in New Mexico. For all DVC scenarios, the projected 2028 ozone DVFs at all monitoring sites in New Mexico are below the 2015 70 ppb ozone NAAQS when ozone contributions due to international anthropogenic emissions are removed. The highest projected 2028 ozone DVF under the no international anthropogenic emissions scenario is 52.8 ppb at the Carlsbad monitoring site when the $DVC_{2017\text{-}2019}$ current year design value is used in the 2028 ozone DVF projection.

Figure 10-35 displays the spatial distribution of the current year ozone DVC and the projected 2028 ozone DVF for the 2028 O&G Control Strategy using the SMAT UAA tool and the three definitions of DVCs. Using the $DVC_{2012\text{-}2016}$ and $DVC_{2015\text{-}2019}$, the SMAT projected 2028 ozone DVFs are all below the 2015 ozone NAAQS under the 2028 O&G Control Strategy emissions scenario. However, when the $DVC_{2017\text{-}2019}$ is used, the SMAT UAA estimates projected 2028 ozone DVFs in excess of the 2015 ozone NAAQS across all of Eddy County in southeast New Mexico.

The spatial distribution of the projected 2028 ozone DVF with no international anthropogenic emissions and its differences with the 2028 O&G Control Strategy 2028 ozone DVF using the three DVC definitions are shown in Figure 10-36. The removal of the international anthropogenic emission contributions reduces the 2028 ozone DVFs in New Mexico by 10-30 ppb. The highest 2028 ozone DVF in the 4-km New Mexico domain are 52.5, 55.2 and 56.4 ppb for the, respectively, $DVC_{2012\text{-}2016}$, $DVC_{2015\text{-}2019}$ and $DVC_{2017\text{-}2019}$ current year design value sensitivity scenarios, which are well below the 2015 70 ppb ozone NAAQS.

Table 10-4. Projected 2028 ozone DVFs for the 2028 O&G Control Strategy (2028OGCS) and 2028 no international anthropogenic emissions (2028INTL) scenarios using the $DVC_{2012\text{-}2016}$ current year ozone DVC.

AQS_ID	2012-16 DVC (ppb)	2028OGCS DVF (ppb)	2028INTL DVF (ppb)	2028 DVF Difference OGCS–INTL (ppb)	Site Name	County
350010023	66.3	60.7	47.2	-13.5	Del Norte HS	Bernalillo
350010024	68.0	62.0	48.5	-13.5	South East Heights	Bernalillo
350010029	66.0	60.5	47.1	-13.4	South Valley	Bernalillo
350010032	67.0	62.1	48.5	-13.6	Westside	Bernalillo
350011012	65.0	58.8	45.7	-13.1	Foothills	Bernalillo
350130008	66.3	59.8	39.9	-19.9	La Union	Doña Ana
350130017	67.0	61.8	38.4	-23.4	Sunland Park	Doña Ana
350130020	67.0	62.2	39.6	-22.6	Chaparral	Doña Ana
350130021	72.0	66.8	42.6	-24.2	Desert View	Doña Ana
350130022	71.3	66.0	42.2	-23.8	Santa Teresa	Doña Ana
350130023	65.0	60.2	41.5	-18.7	Solano	Doña Ana
350151005	69.0	66.4	46.1	-20.3	Carlsbad	Eddy
350171003	62.0	58.9	43.0	-15.9	Chino Copper Smelt	Grant
350250008	66.0	63.3	44.9	-18.4	Hobbs Jefferson	Lea
350290003	66.0	62.5	43.3	-19.2	Deming Airport	Luna
350390026	64.0	60.0	47.4	-12.6	Coyote Ranger Dist	Rio Arriba
350431001	64.0	58.1	44.4	-13.7	Bernalillo (E Avenida)	Sandoval
350450009	64.3	60.2	46.4	-13.8	Bloomfield	San Juan
350450018	67.0	63.3	50.2	-13.1	Navajo Lake	San Juan
350451005	63.7	59.6	48.5	-11.1	Substation	San Juan
350490021	64.3	60.4	47.9	-12.5	Santa Fe Airport	Santa Fe
350610008	66.3	62.0	47.5	-14.5	Los Lunas (Los Lentes)	Valencia

Table 10-5. Projected 2028 ozone DVFs for the 2028 O&G Control Strategy (2028OGCS) and 2028 no international anthropogenic emissions (2028INTL) scenarios using the $DVC_{2015\text{-}2019}$ current year ozone DVC.

AQS_ID	2015-19 DVC (ppb)	2028OGCS DVF (ppb)	2028INTL DVF (ppb)	2028 DVF Difference OGCS–INTL (ppb)	Site Name	County
350010023	69.0	63.1	49.2	-13.9	Del Norte HS	Bernalillo
350010029	66.0	60.5	47.1	-13.4	South Valley	Bernalillo
350011012	69.0	62.4	48.5	-13.9	Foothills	Bernalillo
350130008	68.7	62.0	41.3	-20.7	La Union	Doña Ana
350130020	70.7	65.7	41.8	-23.9	Chaparral	Doña Ana
350130021	74.3	68.9	43.9	-25.0	Desert View	Doña Ana
350130022	74.0	68.5	43.8	-24.7	Santa Teresa	Doña Ana
350130023	67.7	62.7	43.3	-19.4	Solano	Doña Ana
350151005	73.7	70.9	49.2	-21.7	Carlsbad	Eddy
350153001	71.0	69.3	44.1	-25.2	Carlsbad NP	Eddy
350250008	69.3	66.5	47.1	-19.4	Hobbs Jefferson	Lea
350390026	66.3	62.2	49.1	-13.1	Coyote Ranger Dist	Rio Arriba
350431001	67.0	60.9	46.5	-14.4	Bernalillo (E Avenida)	Sandoval
350450009	67.0	62.8	48.3	-14.5	Bloomfield	San Juan
350450018	69.0	65.2	51.7	-13.5	Navajo Lake	San Juan
350451005	67.3	62.9	51.2	-11.7	Substation	San Juan
350490021	65.0	61.0	48.4	-12.6	Santa Fe Airport	Santa Fe
350610008	66.7	62.3	47.8	-14.5	Los Lunas (Los Lentes)	Valencia

Table 10-6. Projected 2028 ozone DVFs for the 2028 O&G Control Strategy (2028OGCS) and 2028 no international anthropogenic emissions (2028INTL) scenarios using the $DVC_{2017\text{-}2019}$ current year ozone DVC.

AQS_ID	2017-19 DVC (ppb)	2028OGCS DVF (ppb)	2028INTL DVF (ppb)	2028 DVF Difference OGCS–INTL (ppb)	Site Name	County
350010023	70.0	64.0	49.9	-14.1	Del Norte HS	Bernalillo
350010029	67.0	61.4	47.8	-13.6	South Valley	Bernalillo
350011012	71.0	64.2	49.9	-14.3	Foothills	Bernalillo
350130008	70.0	63.2	42.1	-21.1	La Union	Doña Ana
350130020	73.0	67.8	43.1	-24.7	Chaparral	Doña Ana
350130021	77.0	71.4	45.5	-25.9	Desert View	Doña Ana
350130022	76.0	70.3	45.0	-25.3	Santa Teresa	Doña Ana
350130023	70.0	64.8	44.7	-20.1	Solano	Doña Ana
350151005	79.0	76.0	52.8	-23.2	Carlsbad	Eddy
350250008	71.0	68.1	48.3	-19.8	Hobbs Jefferson	Lea
350390026	67.0	62.8	49.6	-13.2	Coyote Ranger Dist	Rio Arriba
350431001	68.0	61.8	47.2	-14.6	Bernalillo (E Avenida)	Sandoval
350450009	68.0	63.7	49.1	-14.6	Bloomfield	San Juan
350450018	69.0	65.2	51.7	-13.5	Navajo Lake	San Juan
350451005	69.0	64.5	52.5	-12.0	Substation	San Juan
350490021	66.0	62.0	49.1	-12.9	Santa Fe Airport	Santa Fe
350610008	68.0	63.5	48.7	-14.8	Los Lunas (Los Lentes)	Valencia

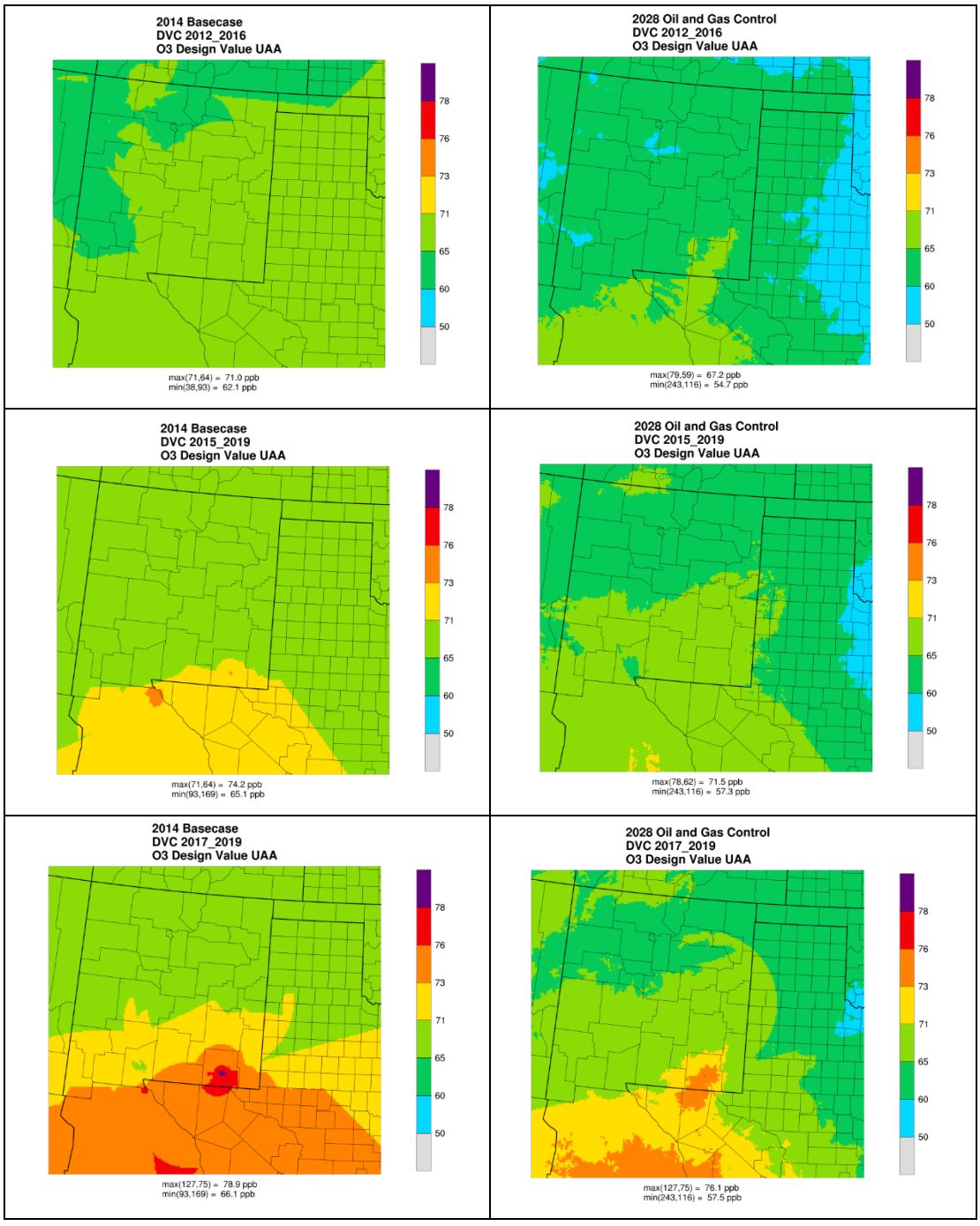

Figure 10-35. SMAT UAA ozone design values (ppb) for the current year ozone DVC (left) and projected 2028 ozone DVF for the 2028 O&G Control Strategy (right) using current year DVCs based on 2012-2016 (top), 2015-2019 (middle) and 2017-2019 (bottom) ozone design values.

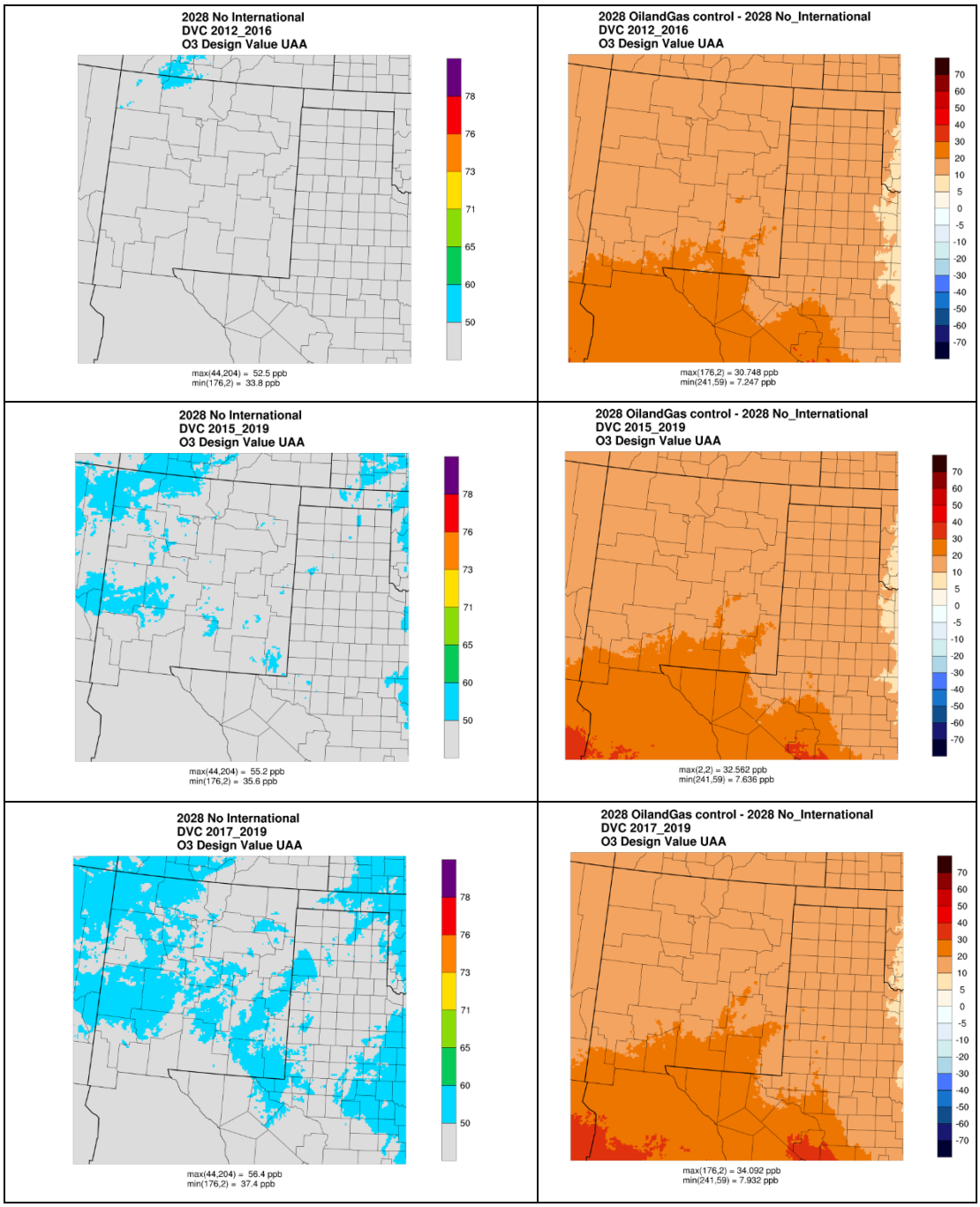

Figure 10-36. SMAT UAA ozone design values (ppb) for the projected 2028 ozone DVF from the 2028 No International Anthropogenic Emissions scenario (left) and differences in 2028 ozone DVFs between the 2028 No International Emissions and 2028 O&G Control Strategy scenarios (right) using current year DVCs based on 2012-2016 (top), 2015-2019 (middle) and 2017-2019 (bottom) ozone design values.

11. 2028 VOC AND NOX SENSITIVITY OSAT OZONE SOURCE APPORTIONMENT MODELING

A second CAMx 2028 ozone source apportionment model simulation was performed to estimate whether ozone formation that leads to elevated ozone concentrations in New Mexico occurs under conditions that are more sensitive to VOC or NO_x emissions. The VOC/NO_x emissions sensitivity ozone source apportionment simulation used the Ozone Source Apportionment Technology (OSAT) version of the CAMx ozone source apportionment tools. As discussed in Section 10.1, when using OSAT, the relative amounts of the O3V and O3N ozone source apportionment tracers provide an indication of whether ozone formation is more sensitive to VOC or NO_x emissions.

11.1 2028 OSAT Ozone Source Apportionment Design

The CAMx 2028 OSAT VOC/ NO_x sensitivity ozone source apportionment simulation used the 36/12/4-km nested domain structure, summer of 2014 meteorology and the 2028 O&G Control Strategy emissions scenario. The same five Source Regions as used in the 2028 Source Sector APCA ozone source apportionment simulation were used (See Figure 10-1):

1. New Mexico;
2. Texas;
3. Colorado;
4. Remainder U.S. states plus coastal water out to 200 nautical miles (nmi) of the U.S. coast; and
5. International, which include Mexico, Canada and waters off their coasts, plus waters more than 200 nmi off the U.S. coast.

Three Source Categories were specified in the 2028 OSAT ozone source apportionment modeling:

1. Anthropogenic emissions;
2. Fires; and
3. Natural emissions.

Fires include U.S. wildfires (WF), wildland prescribed burns (Rx) and agricultural burning (Ag), and other fires from Mexico and Canada. Natural emissions include biogenic, lightning NO_x (LNO_x), windblown dust (WBD) and oceanic (sea salt and DMS) sources.

With 5 Source Regions and 3 Source Categories, plus separate Source Groups for Initial Concentrations (IC) and Boundary Conditions (BC), that results in a total of 17 Source Groups for which separate ozone source contributions will be obtained in the 2028 OSAT ozone source apportionment modeling (17 = 5 x 3 + 2).

11.2 Spatial Distribution of VOC/NO_x Ozone Formation Sensitivity

The sensitivity of ozone formation to VOC and NO_x emissions is obtained for each of the 15 emission Source Groups that consist of emissions from 3 source categories (i.e., anthropogenic, fires and natural) emitting from 5 Source Regions. The percent contribution of NO_x sensitive ozone formation metric is used to display the ozone formation sensitivity that is defined as follows:

$$\text{Percent } NO_x \text{ Sensitive Ozone (\%NOxSens)} = 100 \times \sum O3N_i \,/\, \sum (O3V_i + O3N_i)$$

Where the sum is performed over the 15 different emissions Source Groups (i) that consist of the three emission Source Categories emitting from the 5 Source Regions. The Percent VOC Sensitive Ozone will be 100 minus the Percent NO_x Sensitive Ozone metric.

Note that the O3V and O3N tracers for the IC and BC Source Groups are not used in the Percent NO_x Sensitive Ozone metric since they were defined from the 2014 simulation of the 2014 GEOS-Chem global chemistry model and the CAMx GEOS2CAMx processor arbitrarily assigns half of the GEOS-Chem total ozone to the O3V and O3N tracers each so do they not have accurate information on whether such IC/BC ozone concentrations are more VOC or NO_x sensitive.

Spatial displays of the Percent NO_x Sensitive Ozone metric were generated for Maximum Daily Average 8-hour (MDA8) ozone concentrations and several combinations of Source Groups for each day of the May-August 2014 modeling episode. When presenting the Percent NO_x Sensitive Ozone metric for a combination of Source Groups, it is also important to know the total MDA8 ozone due to the same combination of Source Groups in order to interpret the significance of the %NOxSens metric; if the MDA8 ozone concentrations due to the combination of Source Groups is very small (e.g., < 0.01 ppb), whether the ozone formed was more sensitive to VOC or NO_x emissions is inconsequential. Spatial maps across the New Mexico 4-km modeling domains were generated for total MDA8 ozone and Percent NO_x Sensitive Ozone for the following combinations of Source Groups:

- All emissions based Source Groups (i.e., anthropogenic, fires and natural emissions emitted from the 5 Source Regions in the CAMx modeling domain).
- All anthropogenic emissions based Source Groups across the CAMx modeling domain.
- The New Mexico anthropogenic emissions Source Group.

The Percent NO_x Sensitive Ozone for the New Mexico anthropogenic emissions Source Group provides information on whether New Mexico VOC or NO_x emissions may be more important to ozone formation.

Figures 11-1 through 11-8 display the total MDA8 ozone and Percent NO_x Sensitive ozone metric for eight example days during the episode that tended to have relatively higher ozone concentrations and included the six example days displayed in previous Chapters.

11.2.1 Percent NO_x Sensitive Ozone on May 17, 2014

Figure 11-1 displays the 2028 OSAT source apportionment results for the May 17, 2014 day that was dominated by ozone concentrations from a fire in eastern Arizona that caused modeled elevated ozone concentrations in southwestern New Mexico. Figure 11-1a displays the MDA8 ozone concentrations from all Source Groups, including IC/BC, and is the modeled total MDA8 ozone on this day. The modeled peak MDA8 ozone on May 17th is 129 ppb and occurs within the fire ozone plume in eastern Arizona. The Percent NO_x Sensitive Ozone due to all emissions based source groups indicates ozone formation across the 4-km NM domain is more NO_x sensitive than VOC sensitive with the color scale going from green (%NOxSens > 65%) to red/orange (%NOxSens > 85%) (Figure 11-1b). Although, it is interesting to note that at the locations of the higher total MDA8 ozone concentrations, the amount of %NOxSens ozone is less, with the lowest value (%NOxSens = 64%) occurring at the same location as the peak modeled MDA8 ozone concentration in eastern Arizona.

Figure 11-1c and d show the MDA8 ozone and %NOxSens metric for all anthropogenic emissions on May 17th, with the anthropogenic emissions %NOxSens metric being mostly orange and red (%NOxSens > 90%), indicating mostly NO_x sensitive ozone formation. There are areas of high MDA8 ozone due to anthropogenic emissions in west Texas (peak of 23 ppb) where %NOxSens ozone is a little lower (80-90%), as well as a small area on the Colorado side of the San Juan Basin with lower %NOxSens metric. Figure 11-1e and f show the MDA8 ozone and %NOxSens metric for New Mexico anthropogenic emissions on May 17th. The highest contribution of New Mexico anthropogenic emissions to MDA8 ozone is 9 ppb and occurs in the Permian Basin with ozone formation being very NO_x sensitive (%NOxSens > 85%). The lowest New Mexico NO_x sensitive ozone is in the San Juan Basin with a minimum value of 32%, indicating a VOC sensitive ozone formation value of 68% (Figure 11-1f). The New Mexico anthropogenic emissions ozone contribution in the San Juan Basin is less than 3 ppb (Figure 11-1e).

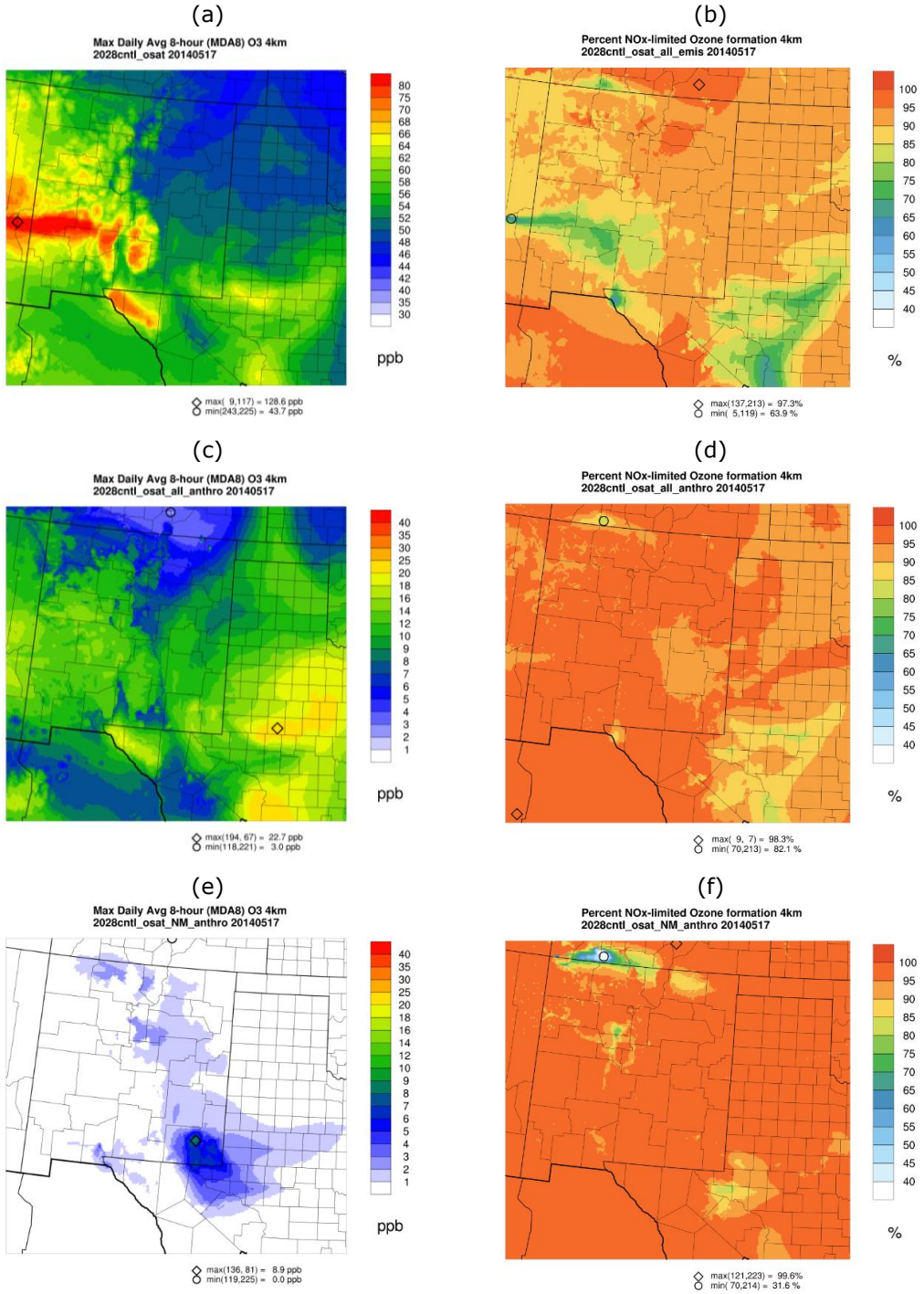

Figure 11-1. 2028 MDA8 ozone (left) and Percent NO_X Sensitive Ozone (right) on May 17, 2014 for: (a) total MDA8 ozone; (c) ozone due to anthropogenic emissions; (e) ozone due to New Mexico anthropogenic emissions; (b) %NOxSens for all emissions; (d) %NOxSens for all anthropogenic emissions; and (f) %NOxSens for New Mexico anthropogenic emissions.

11.2.2 Percent NO_x Sensitive Ozone on May 26, 2014

On May 26th, the peak modeled MDA8 ozone concentrations is 58 ppb and occurs in San Juan County (Figure 11-2a). Ozone formation from all emissions is mostly NO_x sensitive across New Mexico (Figure 11-2b). Although the lowest %NOxSens due to all emissions on May 26 (68%) occurs at the location of the peak MDA8 ozone in San Juan County. When looking at just anthropogenic emissions, the %NOxSens ozone is mostly greater than 90% across most of New Mexico on May 26th with the exception of San Juan County and stretching south into McKinley County with a %NOxSens minimum of 69% (Figure 11-2d) occurring at the same location as the modeled 58 ppb peak. The maximum MDA8 ozone due to New Mexico anthropogenic emissions on May 26th is 7 ppb and occurs at the same location as the 58 ppb total MDA8 ozone peak in San Juan County. Ozone formation due to New Mexico emissions at the location of this MDA8 ozone peak in San Juan County is split approximately equally between VOC and NO_x sensitive ozone formation (%NOxSens = 45%; Figure 11-2f).

11.2.3 Percent NO_x Sensitive Ozone on May 28, 2014

May 28th has elevated ozone concentrations in southern New Mexico, including southern Doña Ana County and the Permian Basin, as well as within the Albuquerque urban plume (Figure 11-3a). Ozone formation across New Mexico due to anthropogenic emission tends to be mostly NO_x sensitive on May 28th with the lowest NO_x sensitive ozone of 73% occurring at almost the exact same location in southern Doña Ana County as the ozone peak (Figure 11-3b). When just looking at the sensitivity of anthropogenic emissions, the %NOxSens value at the location of the peak in southern Doña Ana County increases from 73% to 81% (Figure 11-3d). Finally, the contributions of New Mexico anthropogenic emissions to the ozone peak in southern Doña Ana County is 2-4 ppb and is very NO_x sensitive (%NOxSens > 90%) (Figure 11-3e and f). The highest MDA8 ozone due to New Mexico anthropogenic emissions on May 28th is 9 ppb in the Albuquerque urban plume where %NOxSens is slightly lower than the surrounding areas (85-90%), with the lowest New Mexico anthropogenic emissions %NOxSens being 75% in a high ozone area in the Permian Basin.

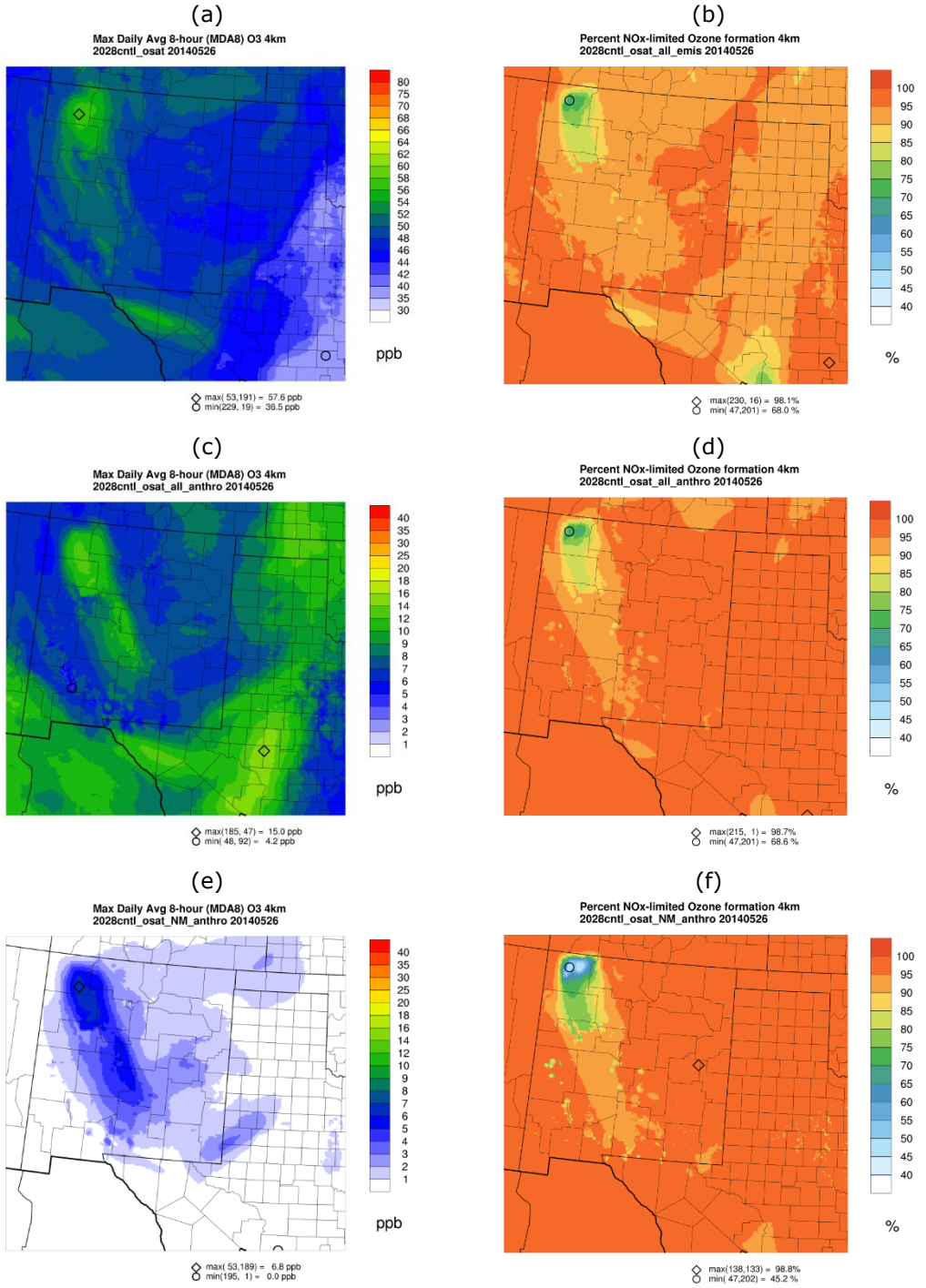

Figure 11-2. 2028 MDA8 ozone (left) and Percent NO_X Sensitive Ozone (right) on May 26, 2014 for: (a) total MDA8 ozone; (c) ozone due to anthropogenic emissions; (e) ozone due to New Mexico anthropogenic emissions; (b) %NOxSens for all emissions; (d) %NOxSens for all anthropogenic emissions; and (f) %NOxSens for New Mexico anthropogenic emissions.

.

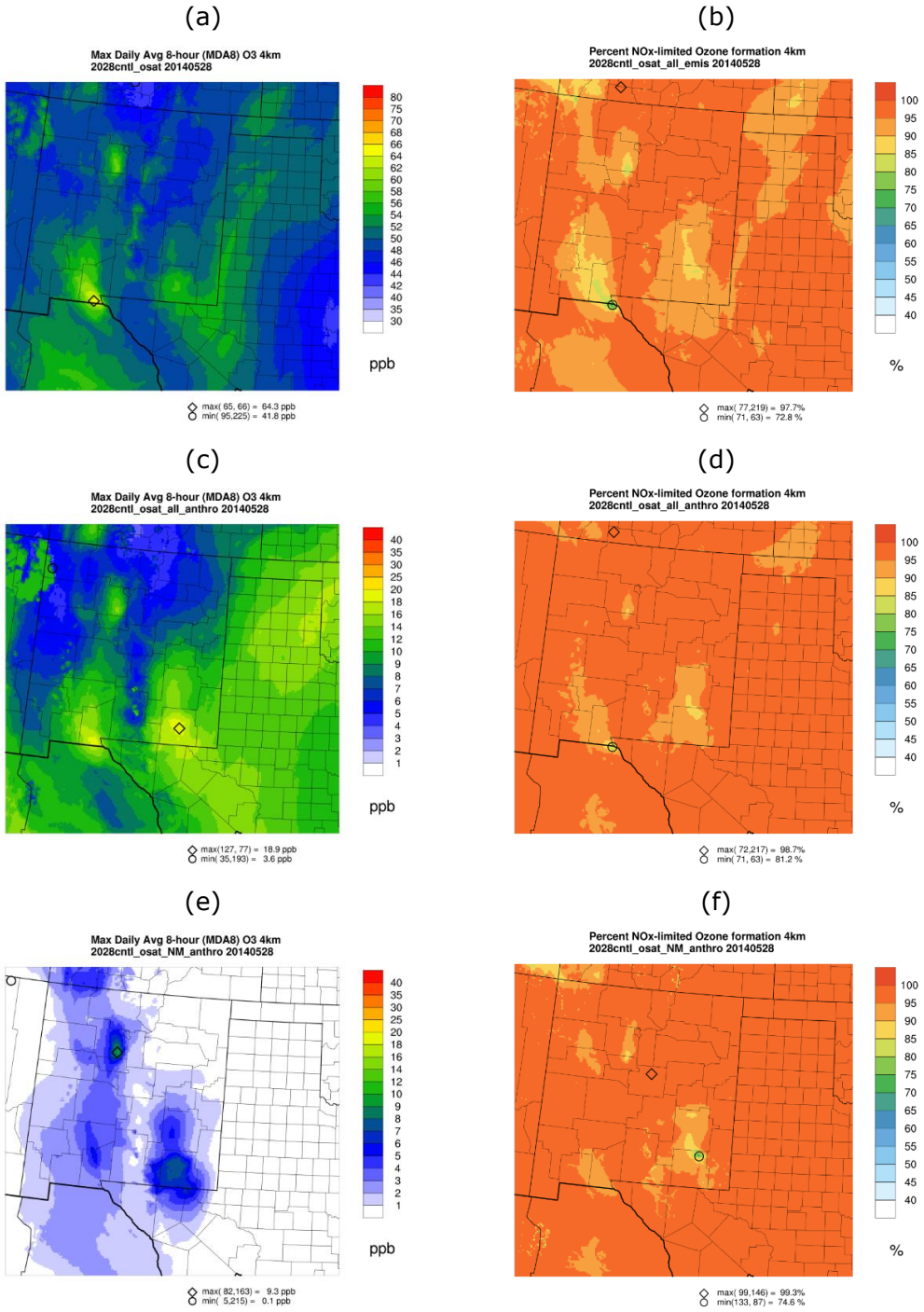

Figure 11-3. 2028 MDA8 ozone (left) and Percent NO_X Sensitive Ozone (right) on May 28, 2014 for: (a) total MDA8 ozone; (c) ozone due to anthropogenic emissions; (e) ozone due to New Mexico anthropogenic emissions; (b) %NOxSens for all emissions; (d) %NOxSens for all anthropogenic emissions; and (f) %NOxSens for New Mexico anthropogenic emissions .

11.2.4 Percent NO_x Sensitive Ozone on June 5, 2014

CAMx estimates 2028 high MDA8 ozone concentrations in excess of the 70 ppb ozone NAAQS on June 5, 2014 in the San Juan Basin and El Paso (Figure 11-4a). In these high ozone locations, ozone formation is split approximately 50%/50% between VOC and NO_x sensitive ozone formation conditions (Figure 11-4b). When looking at just anthropogenic emissions, ozone formation tends to be more NO_x sensitive with %NOxSens ranging from 60-85% in El Paso and 70-85% in San Juan Basin (Figure 11-4d). Ozone from New Mexico anthropogenic emissions is mainly NO_x sensitive in El Paso on June 5th, but in the San Juan Basin there is more VOC sensitive ozone formation with New Mexico anthropogenic emissions ozone contribution ranging from 1 to 4 ppb (Figure 11-4e and f). In particular, there are large areas of blue shaded %NOxSens ozone in San Juan County due to New Mexico anthropogenic emissions that indicates that New Mexico VOC and NO_x anthropogenic emissions are equally important to ozone formation in San Juan County on this day. On the other hand, ozone formation within the Permian Basin appears to be more NO_x sensitive on June 5th.

11.2.5 Percent NO_x Sensitive Ozone on July 12, 2014

The total MDA8 ozone on July 12th has elevated ozone concentrations entering New Mexico from the south that appears to have originated in Mexico (Figure 11-5a). Ozone formation from anthropogenic emissions on this day is estimated to occur primarily under NO_x sensitive conditions (%NOxSens of 86% to 100%; Figure 11-5d). Ozone formation from New Mexico anthropogenic emissions is primarily NO_x sensitive on July 12th with a relative larger amount of VOC sensitive ozone in the south where elevated ozone concentrations occur, but New Mexico's anthropogenic emissions ozone contribution is less than 1 ppb (Figure 11-5e and f).

11.2.6 Percent NO_x Sensitive Ozone on July 24, 2014

On July 24th, the peak MDA8 ozone in the 4-km domain is above the NAAQS (71.1 ppb) and occurs in San Juan County (Figure 11-6a). Although ozone formation is primarily NO_x sensitive across the 4-km NM domain, the largest VOC sensitive ozone due to all emissions (23% or %NOxSens = 77%) occurs at the location of the peak ozone in San Juan County (Figure 11-6b). However, the amount of VOC sensitive ozone at this location due to anthropogenic emissions is 13% (Figure 11-6d), and less than that (~10%) for anthropogenic emission from New Mexico (Figure 11-6f).

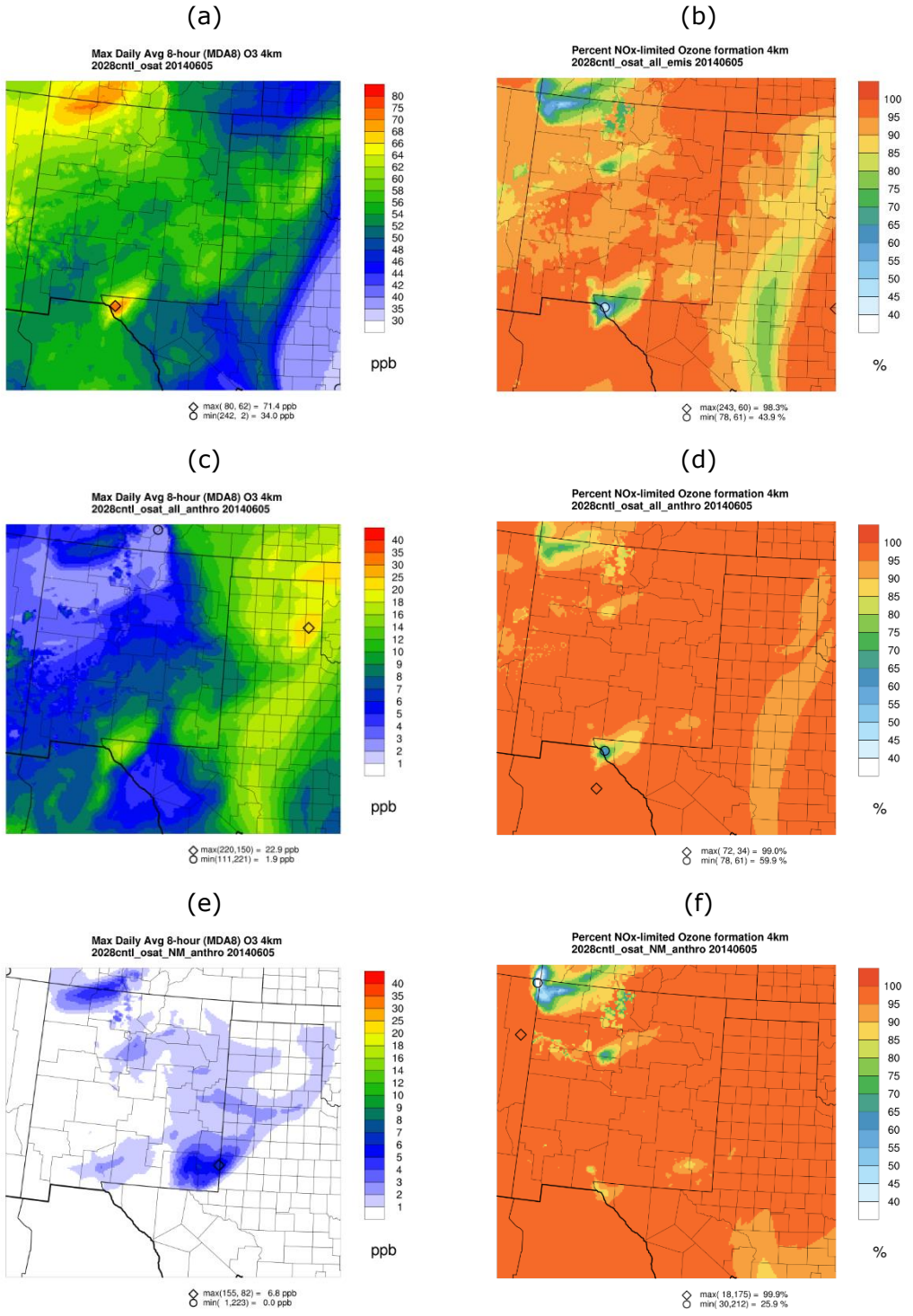

Figure 11-4. 2028 MDA8 ozone (left) and Percent NO_X Sensitive Ozone (right) on June 5, 2014 for: (a) total MDA8 ozone; (c) ozone due to anthropogenic emissions; (e) ozone due to New Mexico anthropogenic emissions; (b) %NOxSens for all emissions; (d) %NOxSens for all anthropogenic emissions; and (f) %NOxSens for New Mexico anthropogenic emissions .

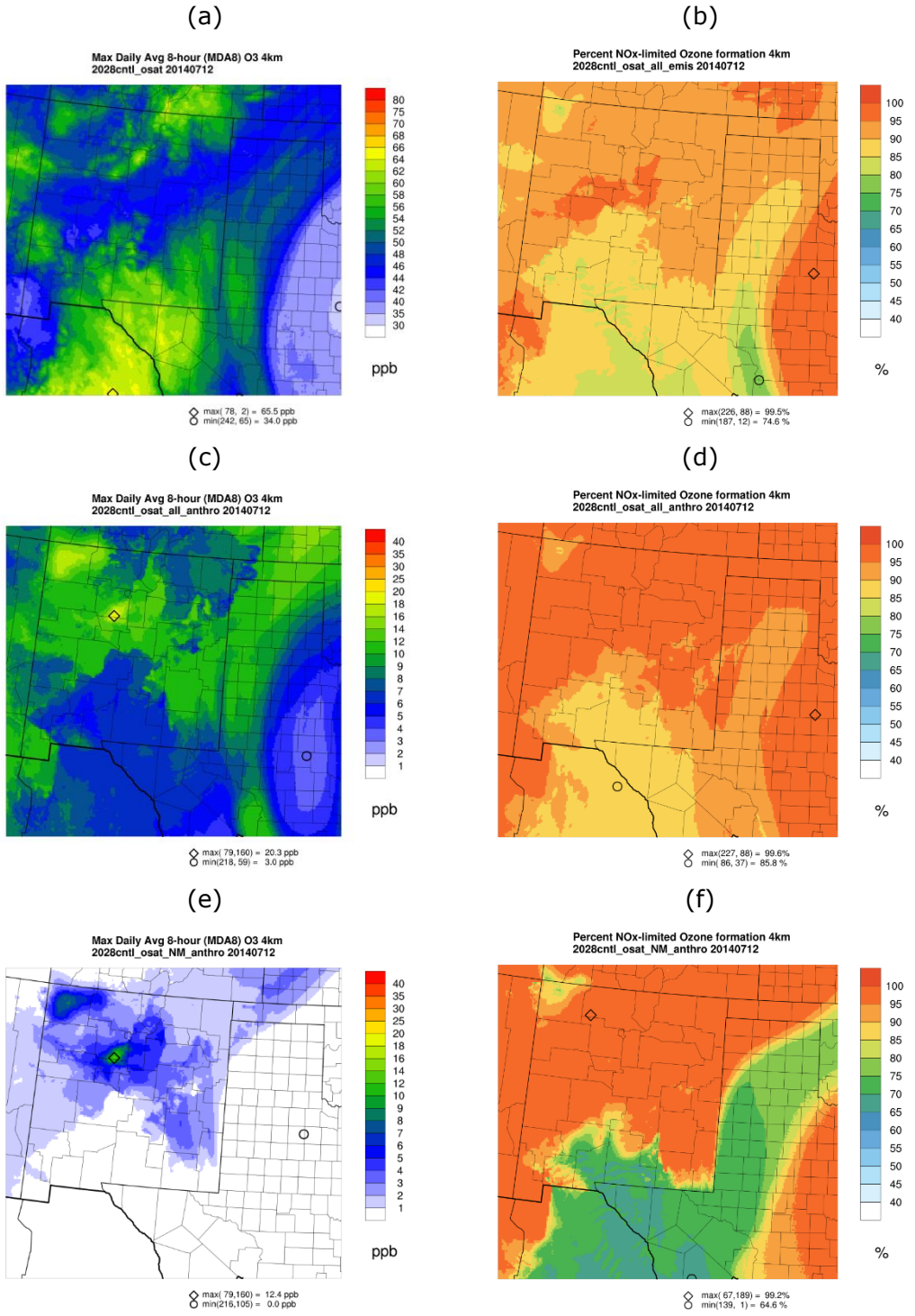

Figure 11-5. 2028 MDA8 ozone (left) and Percent NO_X Sensitive Ozone (right) on July 12, 2014 for: (a) total MDA8 ozone; (c) ozone due to anthropogenic emissions; (e) ozone due to New Mexico anthropogenic emissions; (b) %NOxSens for all emissions; (d) %NOxSens for all anthropogenic emissions; and (f) %NOxSens for New Mexico anthropogenic emissions.

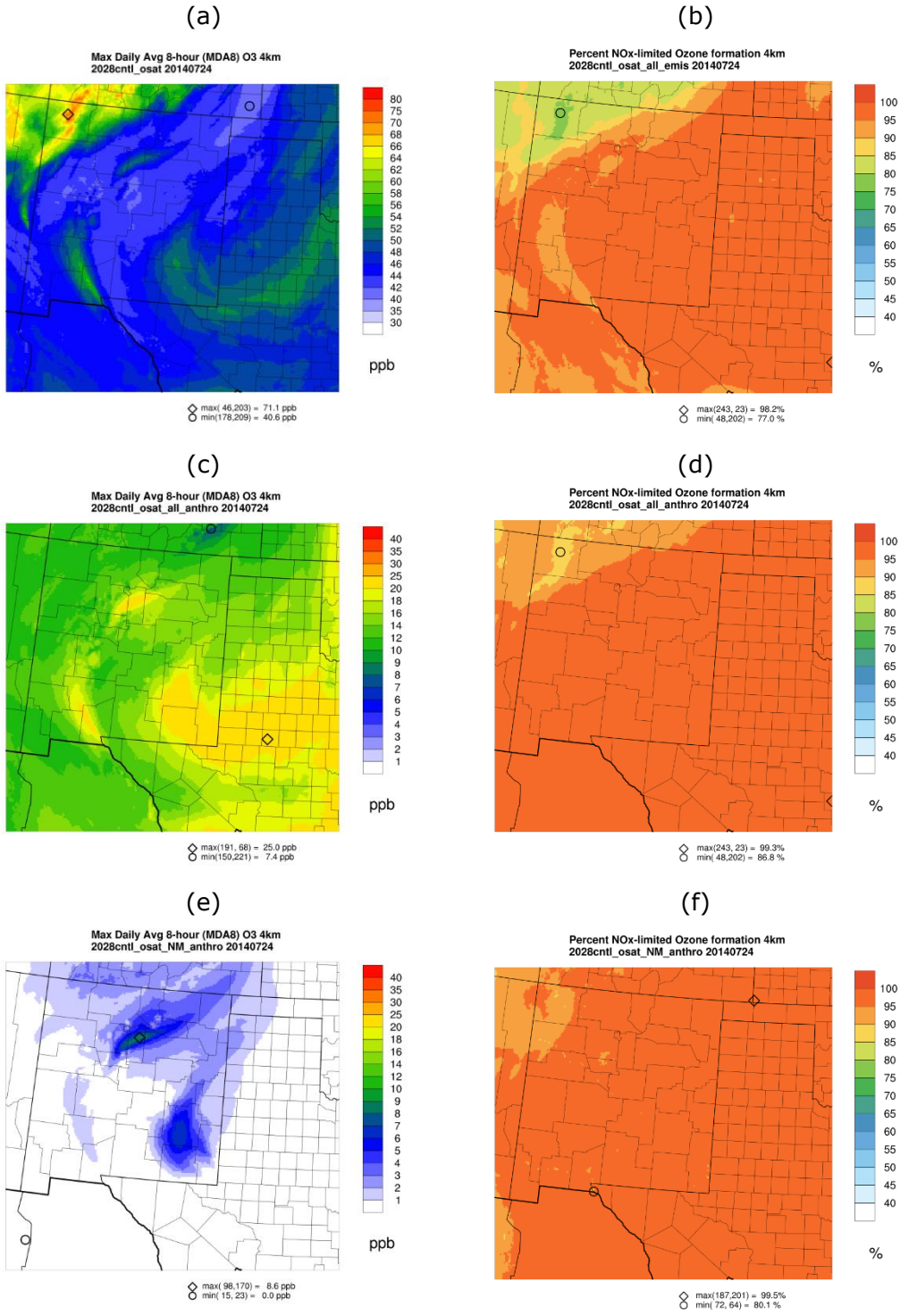

Figure 11-6. 2028 MDA8 ozone (left) and Percent NO_X Sensitive Ozone (right) on July 24, 2014 for: (a) total MDA8 ozone; (c) ozone due to anthropogenic emissions; (e) ozone due to New Mexico anthropogenic emissions; (b) %NOxSens for all emissions; (d) %NOxSens for all anthropogenic emissions; and (f) %NOxSens for New Mexico anthropogenic emissions.

11.2.7 Percent NO_x Sensitive Ozone on July 26, 2014

Modeled elevated MDA8 ozone concentrations occur in northern New Mexico on July 26th with a maximum value above the NAAQS (72 ppb) in northeast Cibola County, west of Albuquerque (Figure 11-7a). Ozone formation is primarily NO_x sensitive across northern New Mexico on this day (%NOxSens > 85%) with the lowest NO_x sensitivity occurring at the location of the 72 ppb ozone peak in Cibola County (78%; Figure 11-7b). However, the NO_x sensitive ozone formation due to anthropogenic emissions at this location is 88% (Figure 11-7d) with a similar value estimated for anthropogenic emission from New Mexico (Figure 11-7f). New Mexico anthropogenic emissions contribute a significant amount (14 ppb) of the 72 ppb ozone peak in northeast Cibola County (Figure 11-7e). Ozone formation due to New Mexico anthropogenic emissions in the San Juan Basin is more VOC sensitive than the rest of New Mexico on July 26th.

11.2.8 Percent NO_x Sensitive Ozone on August 14, 2014

On August 14th there is modeled elevated MDA8 ozone concentrations in northern Rio Arriba County in the San Juan Basin as well as in southern New Mexico with a peak MDA8 ozone in the 4-km domain of 71.2 ppb in El Paso (Figure 11-8a). Although ozone formation is primarily (85-95%) NO_x sensitive across New Mexico on this day, at the locations of the highest MDA8 ozone concentrations, there is relatively more VOC sensitive ozone formation (Figure 11-8b). At the location of the 71.2 ppb ozone peak in El Paso, the CAMx OSAT simulation estimates that ozone formation due to anthropogenic emissions is ~75% NO_x sensitive and ~25% VOC sensitive. Anthropogenic emissions from New Mexico contribute approximately 1 ppb to the ozone peak in El Paso that is primarily formed under NO_x sensitive conditions (Figure 11-8e and f).

11.2.9 Percent NO_x Sensitive Ozone due to New Mexico Anthropogenic Emissions

Figure 11-9 displays the spatial distribution of the Percent NO_x Sensitive Ozone metric due to New Mexico anthropogenic emissions for 15 example days from the May-August 2014 modeling episode, including the 8 days discussed above. As expected, given its mostly rural nature, the CAMx OSAT simulations estimates that ozone formation due to New Mexico anthropogenic emissions is primarily NO_x sensitive. However, there are several locations where ozone formation is estimated to have relatively higher VOC sensitive ozone formation conditions. The San Juan Basin consistently has higher VOC sensitive ozone formation conditions due to New Mexico anthropogenic emissions. Albuquerque also has higher VOC sensitive ozone formation conditions due to New Mexico anthropogenic emissions, and occasionally, ozone formation in the Permian Basin also has relatively higher VOC sensitive ozone formation. As discussed above, the highest MDA8 ozone conditions also have relatively higher VOC sensitive ozone formation conditions. For example, at the location of the relatively high (58 ppb) MDA8 ozone in San Juan County on May 26th the fraction of VOC sensitive ozone is 32% for all emissions, 31% for all anthropogenic emissions and 55% for New Mexico anthropogenic emissions (Figure 11-2). On May 28th the high ozone (64 ppb) in southern Dona Ana County on the border with Texas has a Percent VOC Sensitive Ozone of 27% for all emissions and 19% for all anthropogenic emissions with New Mexico anthropogenic emissions having Percent VOC

Sensitive Ozone for a secondary peak in the Permian Basin of 25% (Figure 11-3). June 5th is a day where there is high MDA8 ozone in the San Juan and Rio Arriba Counties that is approaching the NAAQS that is split approximately equally between VOC and NO_X sensitive ozone (Figure 11-4). On August 14th the modeled ozone peak exceeds the ozone NAAQS in El Paso and ~30% of the ozone was formed under VOC sensitive conditions (Figure 11-8).

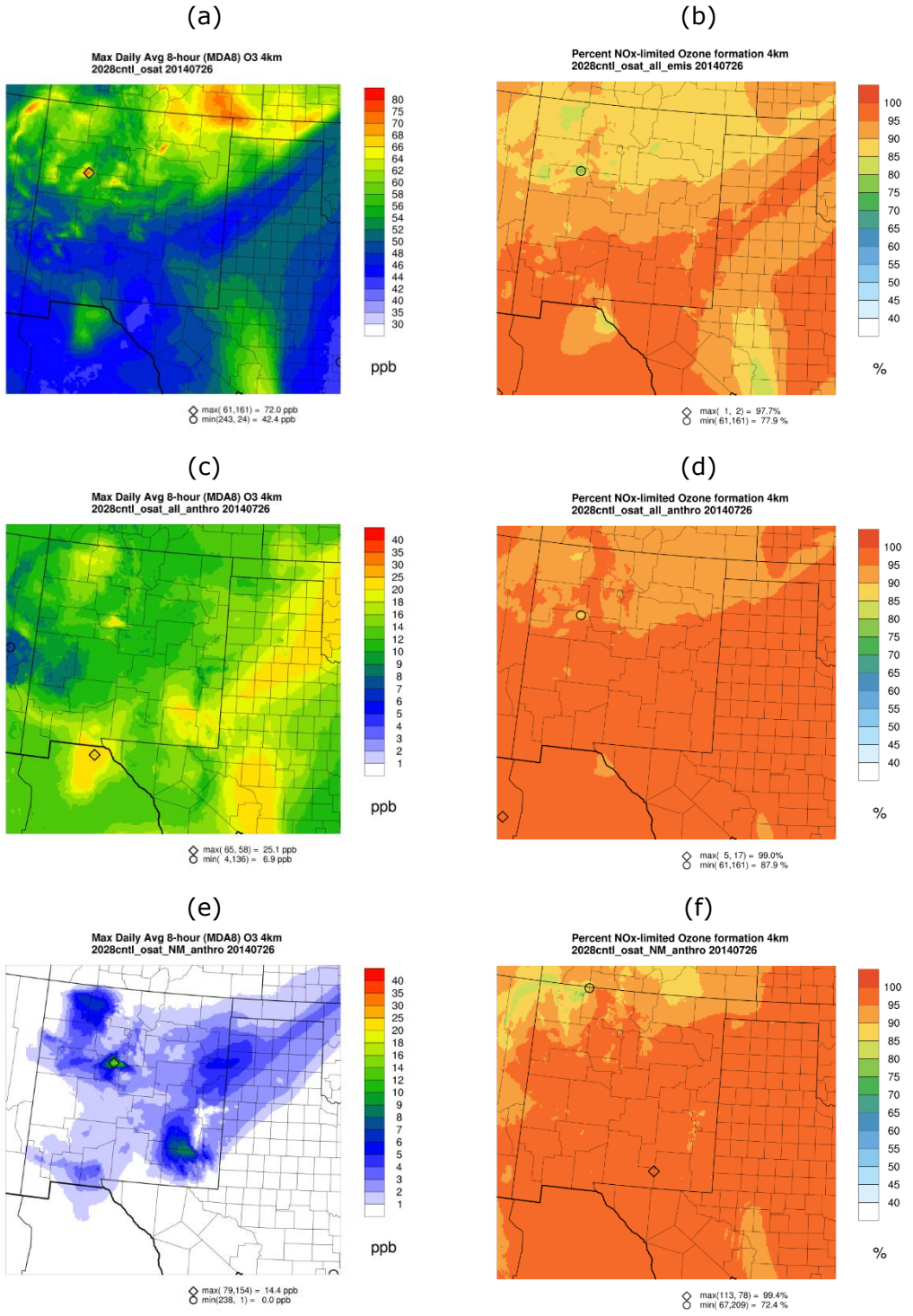

Figure 11-7. 2028 MDA8 ozone (left) and Percent NO_X Sensitive Ozone (right) on July 26, 2014 for: (a) total MDA8 ozone; (c) ozone due to anthropogenic emissions; (e) ozone due to New Mexico anthropogenic emissions; (b) %NOxSens for all emissions; (d) %NOxSens for all anthropogenic emissions; and (f) %NOxSens for New Mexico anthropogenic emissions.

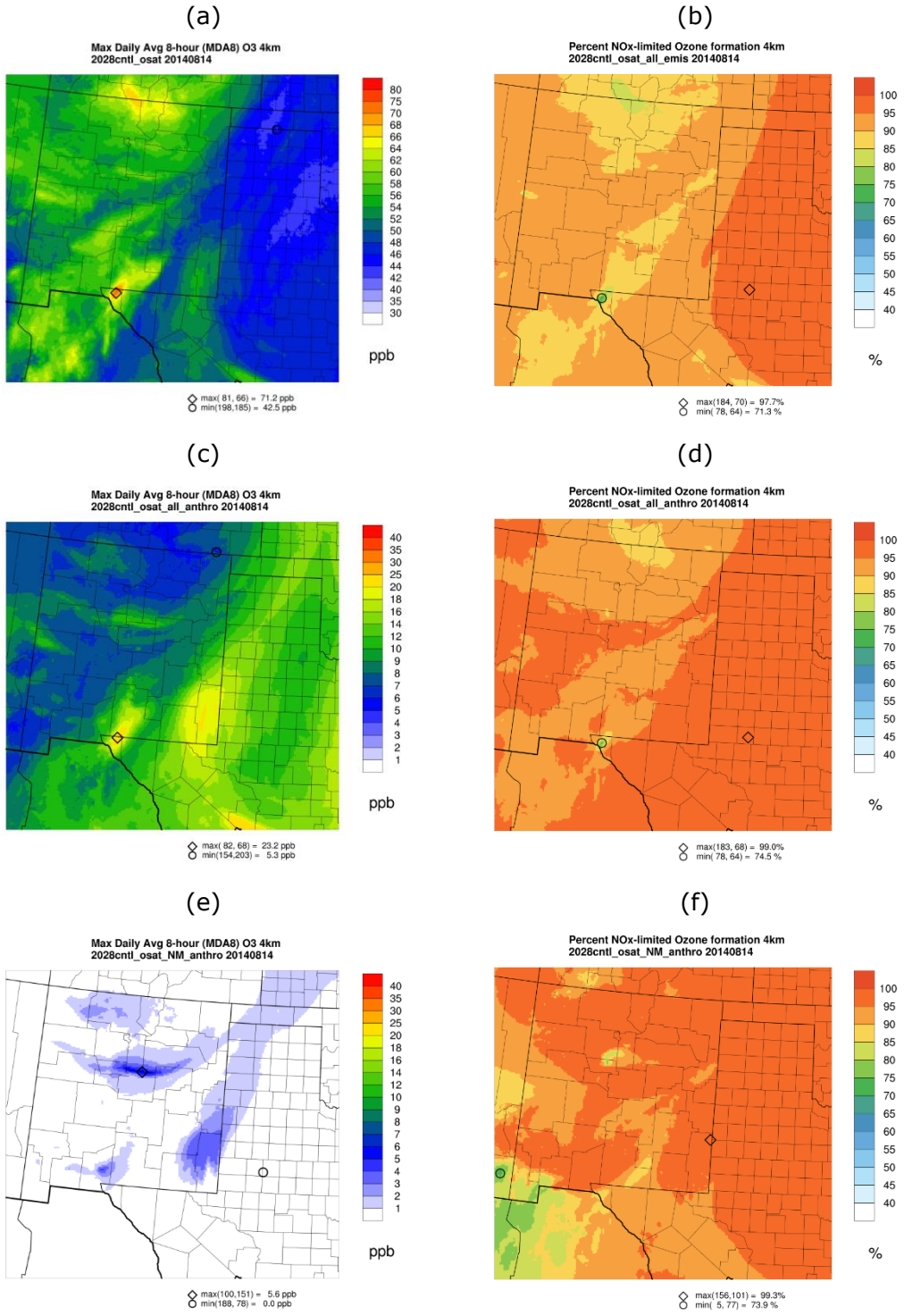

Figure 11-8. 2028 MDA8 ozone (left) and Percent NO_X Sensitive Ozone (right) on August 14, 2014 for: (a) total MDA8 ozone; (c) ozone due to anthropogenic emissions; (e) ozone due to New Mexico anthropogenic emissions; (b) %NOxSens for all emissions; (d) %NOxSens for all anthropogenic emissions; and (f) %NOxSens for New Mexico anthropogenic emissions.

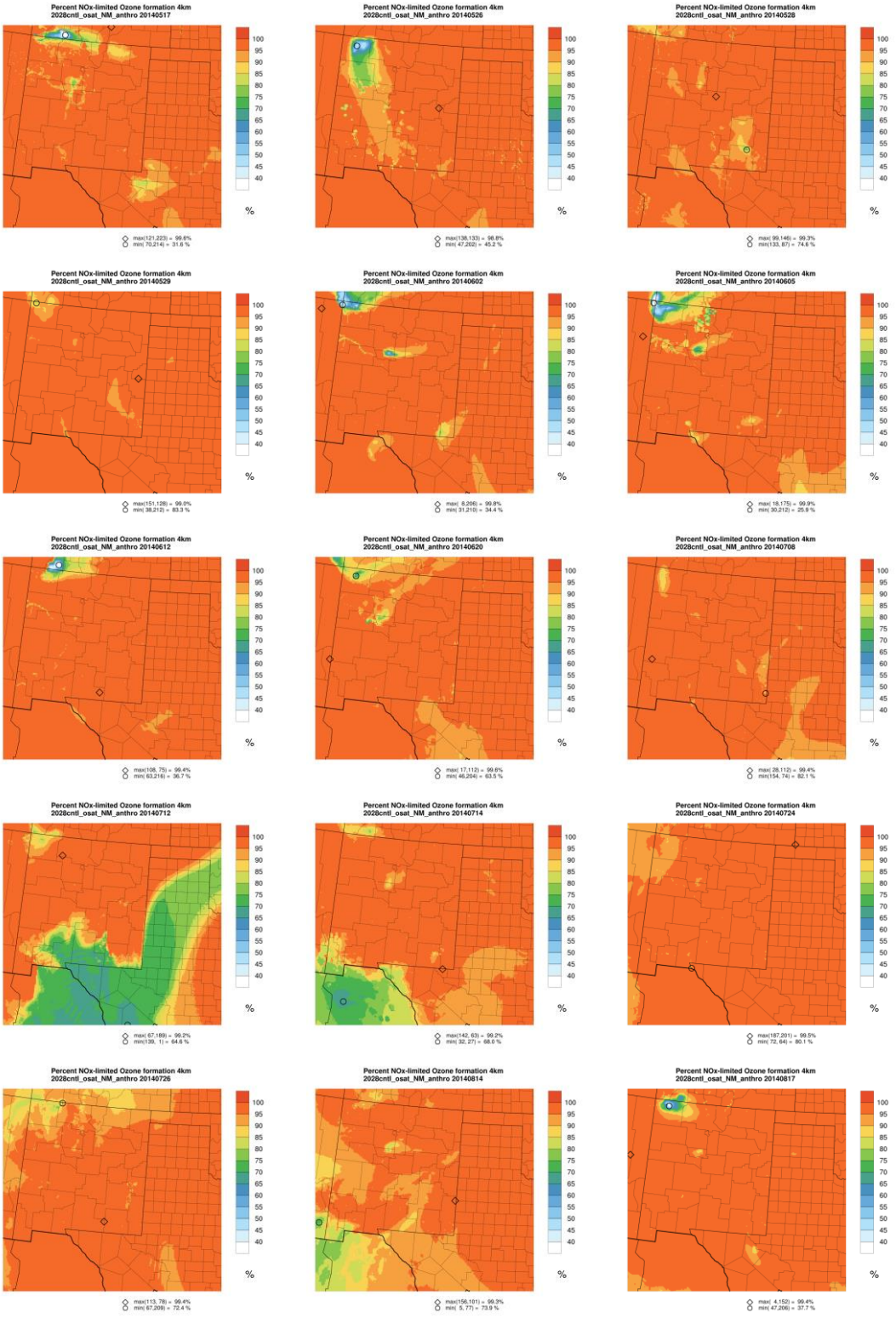

Figure 11-9. Spatial distribution of Percent NO_x Sensitive Ozone due to New Mexico anthropogenic emissions across the 4-km New Mexico domain for 15 days of relatively higher MDA8 ozone concentrations.

11.3 Analysis of VOC/NOx Ozone Formation Sensitivity at Monitoring Sites in New Mexico

The CAMx 2028 OSAT ozone source apportionment results were extracted at the locations of the New Mexico monitoring sites and loaded into an Excel Dashboard where the source apportionment contributions to daily MDA8 ozone concentrations can be visualized. The Dashboard displays the OSAT source apportionment O3V and O3N results for groups of 10 days and the average across the 10 days for different combinations of the 3 Source Categories and 5 Source regions within the CAMx modeling domain, with examples for several monitoring sites discussed below.

11.3.1 VOC/NO_x Sensitivity at Substation in San Juan County

Figure 11-10 displays the CAMx OSAT results at the Substation site in San Juan County using daily stacked bar charts of O3V and O3N for the 10 days used by SMAT to make the 2028 ozone DVF projections, along with a pie chart of the O3V and O3N results averaged across the 10 SMAT days. The Dashboard can also display results for the highest and second highest 10 modeled MDA8 ozone concentration days from the CAMx 2028 O&G Control Strategy simulation. As discussed in Chapter 7, the 10 SMAT days are selected as the 10 days with the highest modeled MDA8 ozone near the monitor in the CAMx 2014v2 Base Case, so there is a lot of overlap in days between the 10 SMAT days and the 10 highest modeled 2028 MDA8 ozone days.

The displays in Figure 11-10 use warmer colors (e.g., red) for the NO_x sensitive ozone O3N and cooler colors (e.g., blue) for the VOC sensitive ozone O3V. Emissions within the CAMx domain contribute from 6 to 36 ppb to the total MDA8 ozone across the 10 SMAT days at Substation, with a vast majority of the ozone formed being NO_x sensitive, whose daily variation ranges from approximately 70% to 90% of the SMAT 10 days daily MDA8 ozone concentrations due to emissions (Figure 11-10, top). Averaged across the 10 SMAT days, the total MDA8 ozone at Substation is 63.7 ppb with 67% of that due to BCs and the rest (21.1 ppb) due to in-domain emissions, of which 81% is NO_x sensitive and 19% is VOC sensitive (Figure 11-10, bottom). Since Figure 11-10 is for all emissions sources, the region-specific stacked bars and pie slices display the contributions of anthropogenic, fire and natural emissions from all of the Source Regions.

The Dashboard can be used to isolate the amount of VOC and NO_x sensitive ozone from the different Source Categories and Regions used in the CAMx OSAT simulation with two example pie charts averaged across the 10 SMAT days at Substation shown in Figure 11-11. The top pie chart in Figure 11-11 shows ozone contributions averaged across the 10 SMAT days for all anthropogenic emissions and all Source Regions. All emissions in the domain contributed 21.1 ppb to the average of the 10 SMAT days at Substation of which 11.4 is due to the anthropogenic emissions (Figure 11-11, top) so the remainder (9.7 ppb) is due to natural and fire emissions. Of the 11.4 ppb all anthropogenic emissions ozone contribution, 91% was formed under NOx sensitive and 9% was formed under VOC sensitive conditions. The bottom pie chart in Figure 11-11 shows the contributions to the average of the 10 SMAT days at Substation due to anthropogenic emissions from New Mexico and shows that New Mexico is

contributing 42% of the anthropogenic emissions contribution (4.7 of 11.4 ppb) at Substation with most of that (87%) being NO_x sensitive ozone.

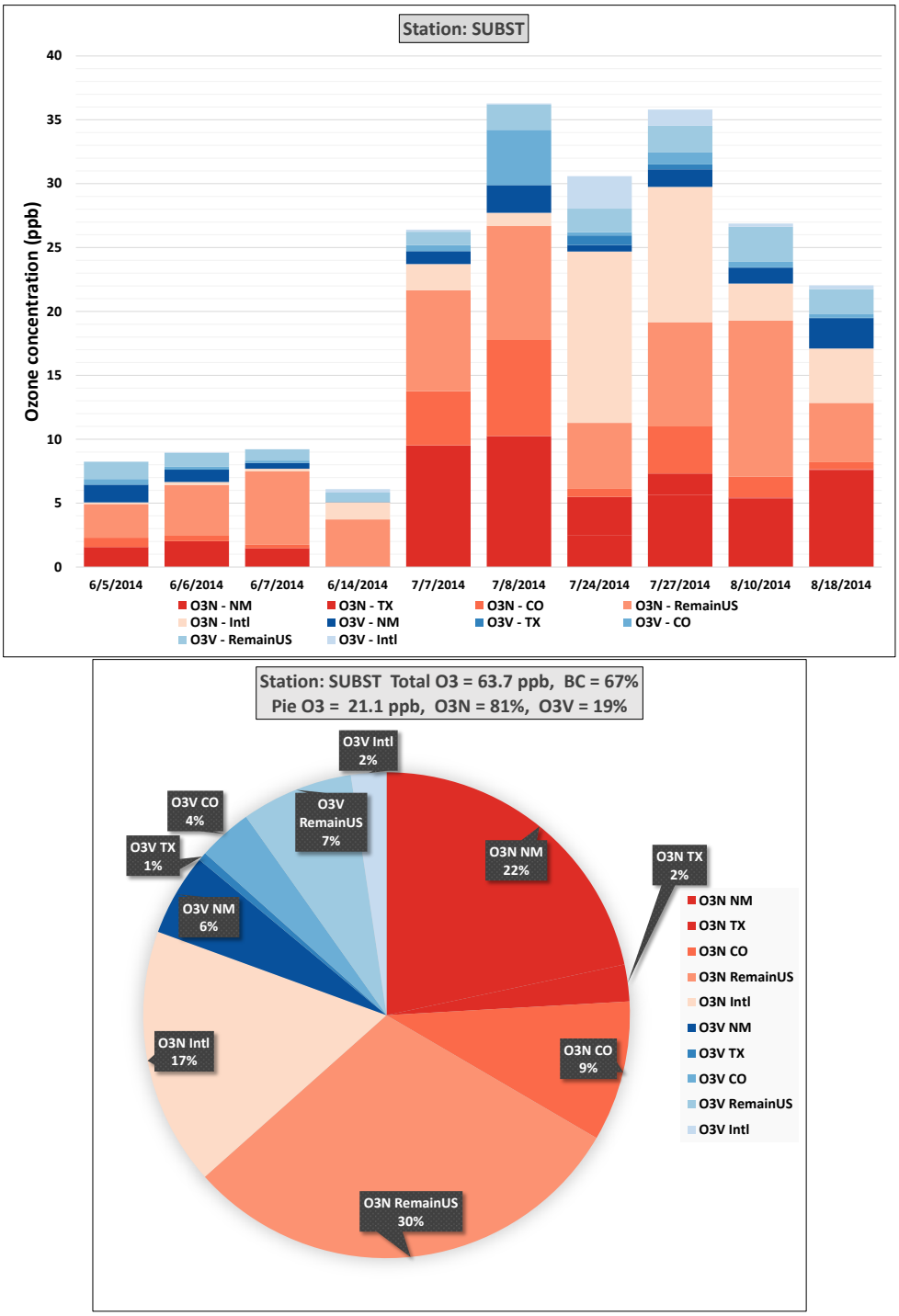

Figure 11-10. Bar Chart of daily O3V (blue) and O3N (red) contributions across the 10 days used by SMAT and pie chart of ozone contributions averaged across the 10 SMAT days for all Source Categories and Source Regions and the Substation monitor in San Juan County.

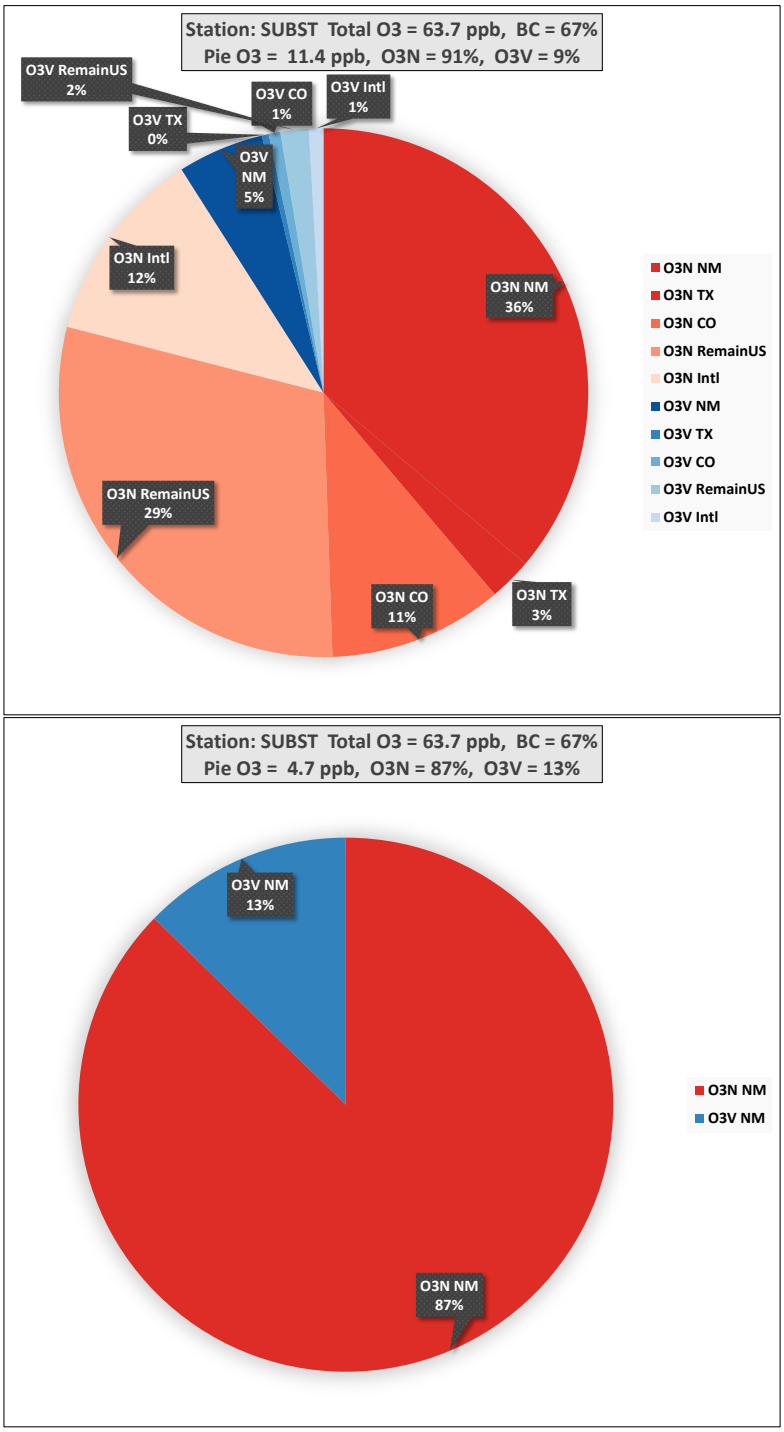

Figure 11-11. O3V and O3N contributions averaged across the 10 SMAT days at Substation for all anthropogenic emissions (top) and New Mexico anthropogenic emissions (bottom).

11.3.2 VOC/NO_x Sensitivity at South East Heights in Bernalillo County

The CAMx OSAT source apportionment results for the 10 SMAT days and all sources at the South East Heights monitoring in Bernalillo County are shown in Figure 11-12. There is a lot of day-to-day variability across the 10 SMAT days with in-domain emissions estimated to contribute from 10 to 40 ppb, with the remainder of the ozone coming from the BCs. On the two lowest in-domain emissions ozone days (June 7 and 8 with 10 and 11 ppb ozone from in-domain emissions), the ozone is almost completely (> 90%) NO_x sensitive, whereas on other days the VOC sensitive ozone can exceed 20% (e.g., August 29). This daily variation in VOC and NO_x sensitivity in Bernalillo County was also seen in the spatial maps (e.g., Figure 11-9). Averaged across the 10 SMAT days at South East Heights, in-domain emission sources contribute 25.4 ppb, of which 87% is NO_x sensitive ozone with the O3N from New Mexico (30%), remainder U.S. (26%) and international (25%) being the highest contributors.

A vast majority (93%) of the 14.5 ppb anthropogenic emissions ozone contribution at South East Heights was formed under NO_x sensitive conditions (Figure 11-12, top) with over half of that coming from New Mexico (7.4 ppb) that was also primarily (92%) NO_x sensitive ozone (Figure 11-13, bottom).

11.3.3 VOC/NO_x Sensitivity at Desert View in Doña Ana County

The CAMx OSAT results for the Desert View monitoring site in Doña Ana County are shown in Figures 11-14 and 11-15. Ozone from Texas and Mexico contributes greatly to ozone levels at Desert View. This includes ozone from El Paso that can have a higher fraction of VOC sensitive ozone (e.g., see Figure 11-4) that is seen on some days in the daily bar charts in Figure 11-14 (e.g., July 24, 2014). Emissions within the CAMx domain contribute 24 to 46 ppb of the daily MDA8 ozone on the 10 SMAT days at Desert View with 14 to 28 ppb of that being anthropogenic in origin. Across all emissions, the average of the 10 SMAT days is 81% NO_x sensitive, with the anthropogenic component of ozone being much more NO_x sensitive (90%) than the natural/fire component (69%). New Mexico anthropogenic emissions contribute 2 ppb (10%; Figure 11-15, bottom) of the 20.9 ppb anthropogenic ozone (Figure 11-15, top) at Desert View with emissions from Mexico contributing approximately half (10.6 ppb) and Texas (3.9 ppb), almost 20%.

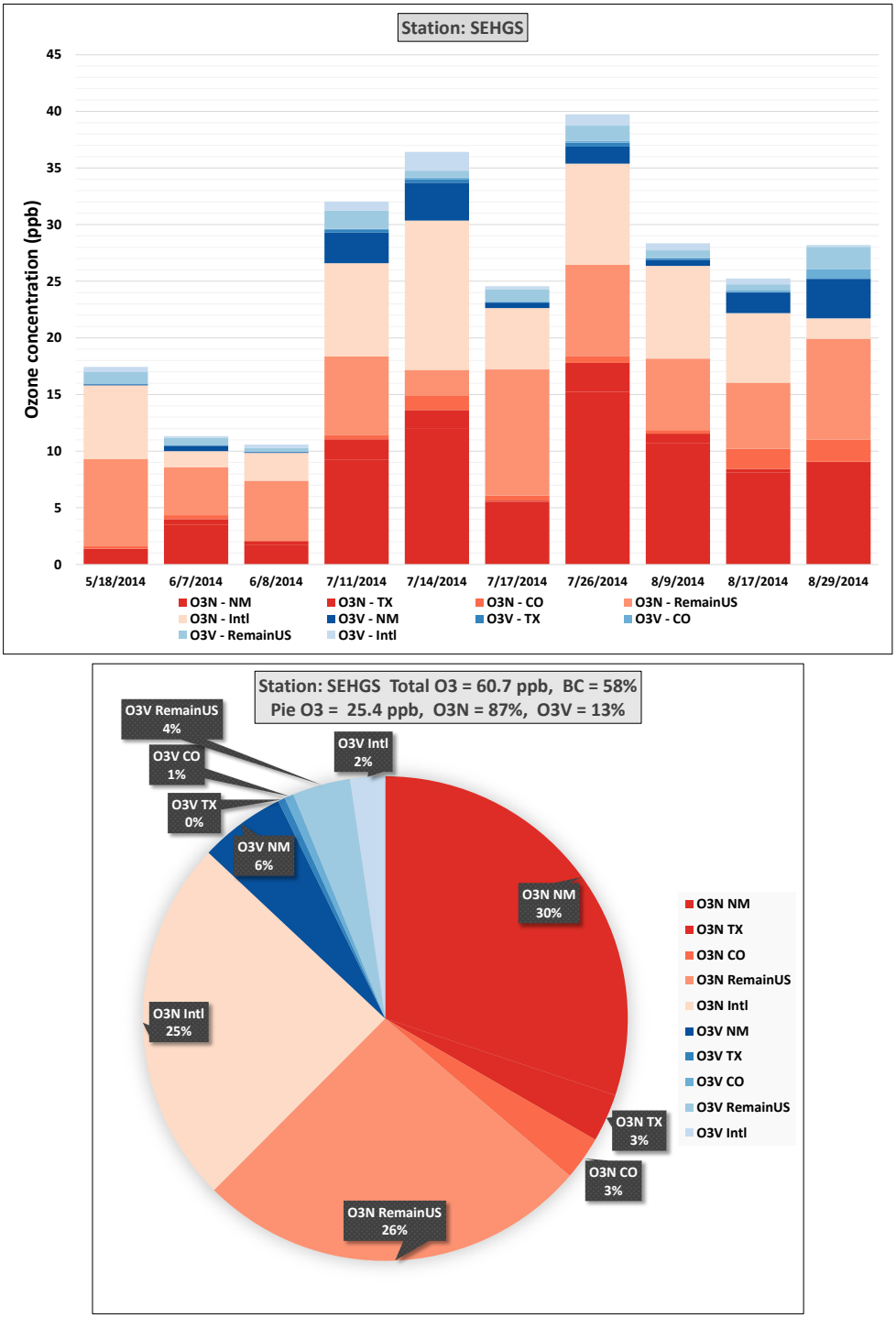

Figure 11-12. Bar Chart of daily O3V (blue) and O3N (red) contributions across the 10 days used by SMAT and pie chart of ozone contributions averaged across the 10 SMAT days for all Source Categories and Source Regions and the South East Heights monitor in Bernalillo County.

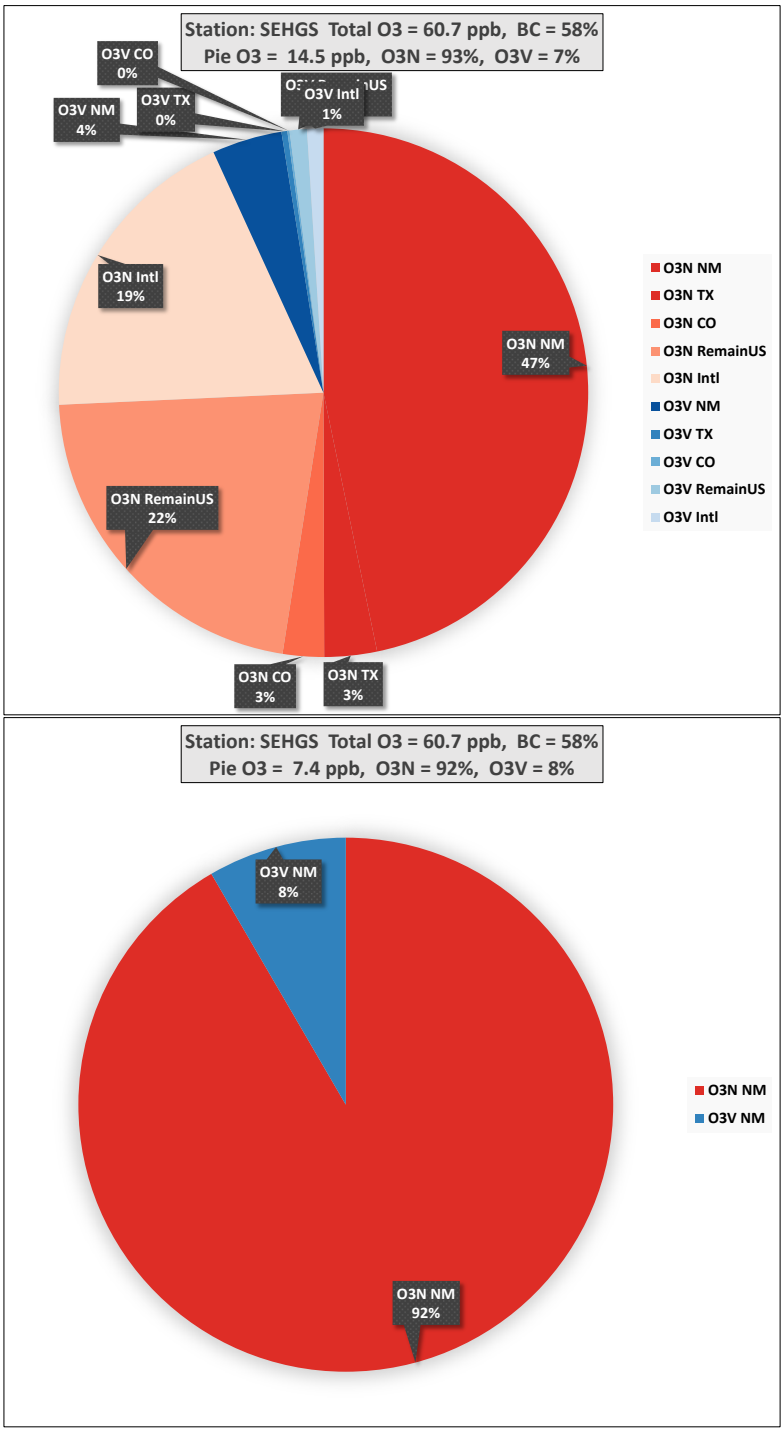

Figure 11-13. O3V and O3N contributions averaged across the 10 SMAT days at South East Heights monitoring site for all anthropogenic emissions (top) and New Mexico anthropogenic emissions (bottom).

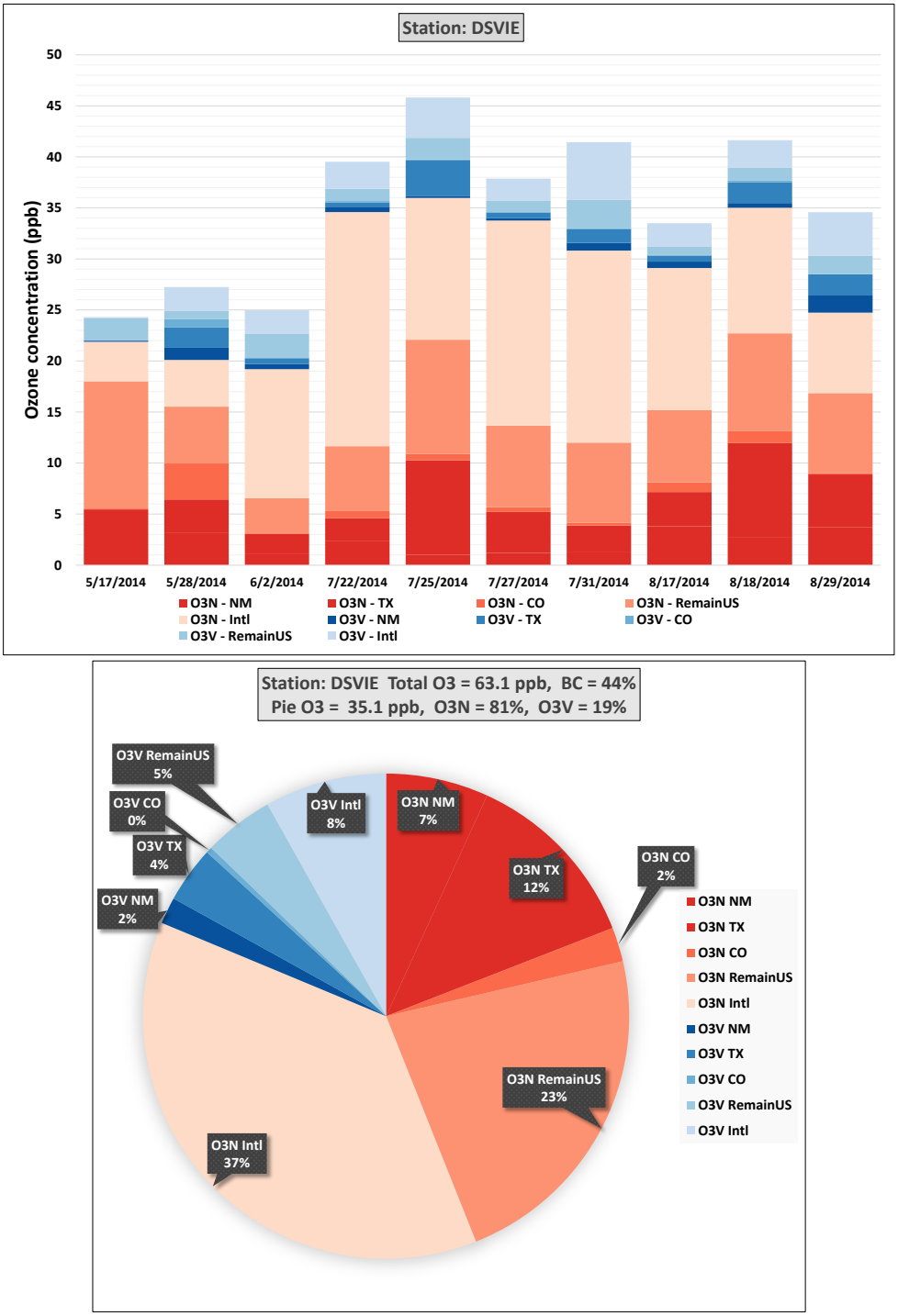

Figure 11-14. Bar Chart of daily O3V (blue) and O3N (red) contributions across the 10 days used by SMAT and pie chart of ozone contributions averaged across the 10 SMAT days for all Source Categories and Source Regions and the Desert View monitor in Doña Ana County.

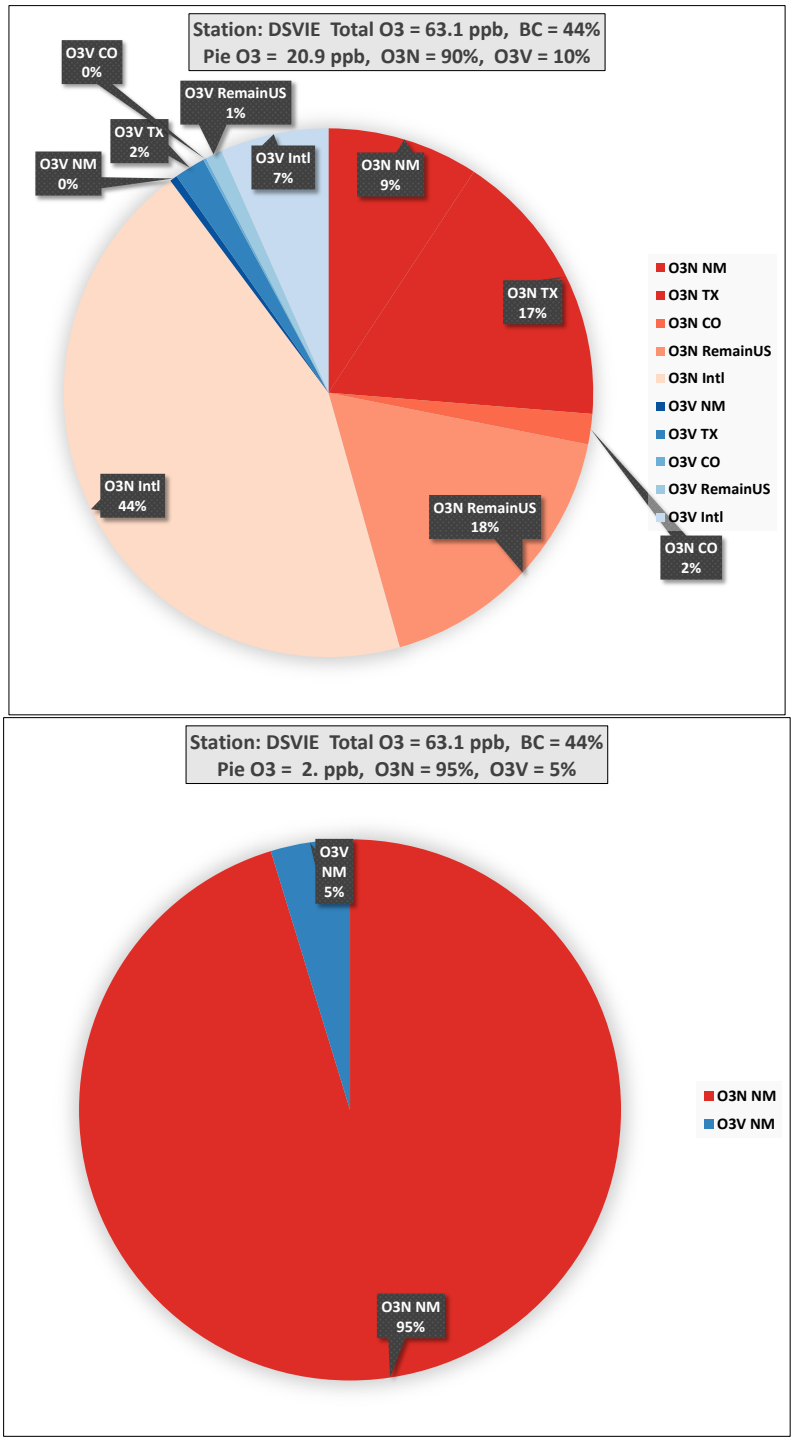

Figure 11-15. O3V and O3N contributions averaged across the 10 SMAT days at Desert View monitoring site for all anthropogenic emissions (top) and New Mexico anthropogenic emissions (bottom).

11.3.4 VOC/NO_x Sensitivity at Carlsbad in Eddy County

Figures 11-16 and 11-17 display the CAMx 2028 OSAT results at the Carlsbad monitor in Eddy County. Across the 10 SMAT days, emissions within the CAMx domain account for 11 to 27 ppb of the daily ozone at Carlsbad (Figure 11-16, top). The model estimates more NO_x sensitive ozone at Carlsbad (91% on average) than Desert View (81% on average). The ozone due to emissions averaged across the 10 SMAT days at Carlsbad is 19.1 ppb that is approximately equally split between anthropogenic (10.0 ppb) and natural/fire (9.1 ppb) sources, with the ozone from the anthropogenic emissions (94%) being more NO_x sensitive than the ozone from the natural/fire emissions (87%). Of the 10 ppb from anthropogenic emissions, almost half (4.7 ppb) is from international emissions with anthropogenic emissions from New Mexico and Texas both contributing 16% (1.6 ppb) each (Figure 11-17).

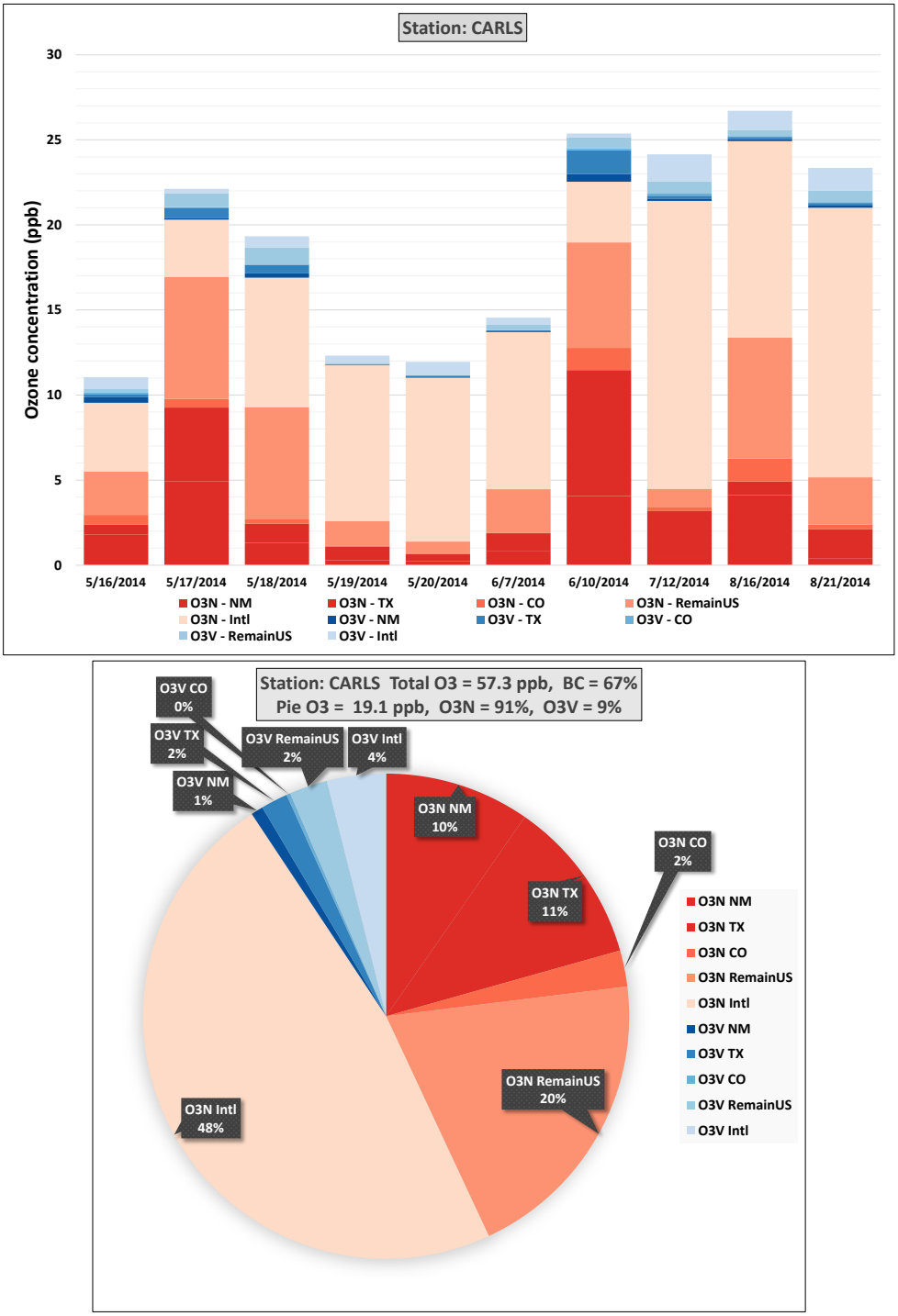

Figure 11-16. Bar Chart of daily O3V (blue) and O3N (red) contributions across the 10 days used by SMAT and pie chart of ozone contributions averaged across the 10 SMAT days for all Source Categories and Source Regions and the Carlsbad monitor in Eddy County.

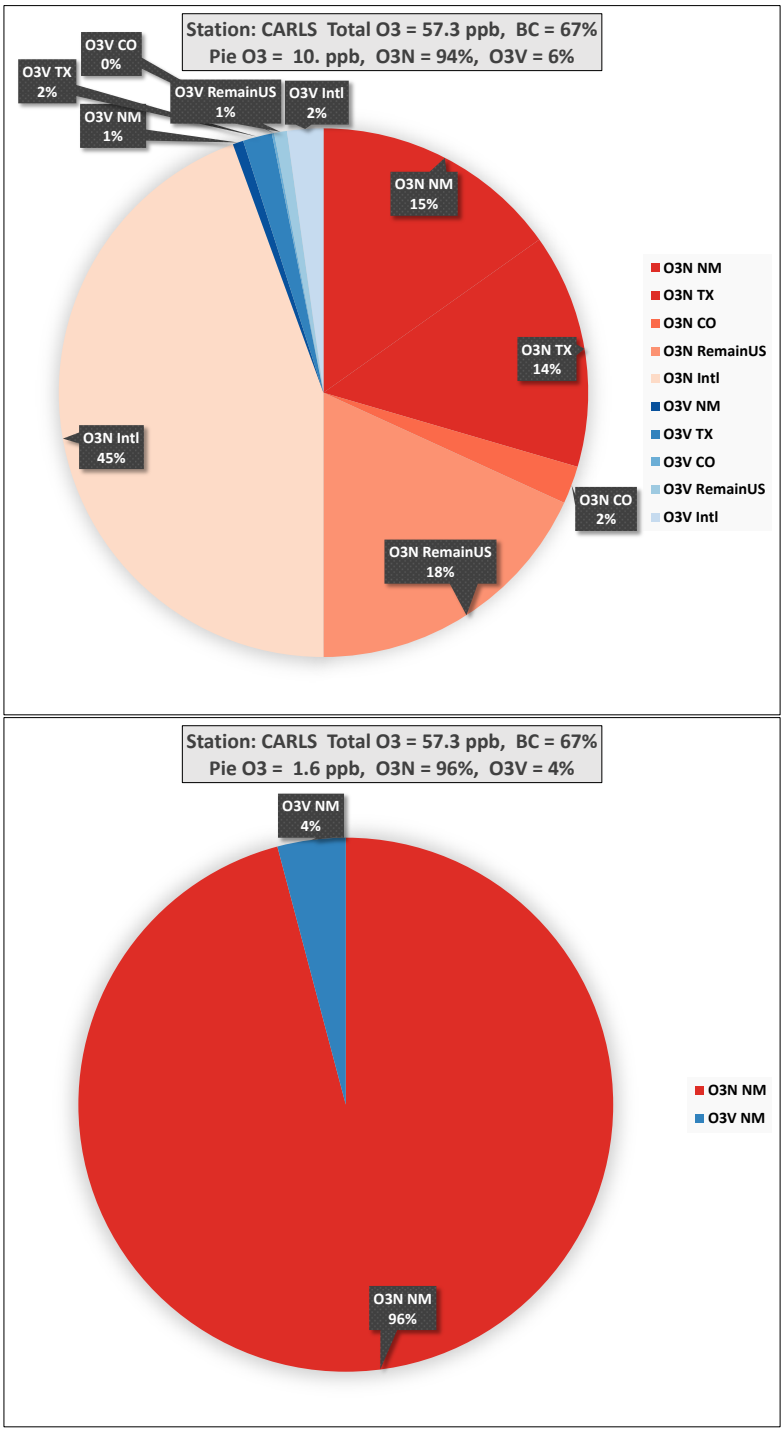

Figure 11-17. O3V and O3N contributions averaged across the 10 SMAT days at Carlsbad monitoring site for all anthropogenic emissions (top) and New Mexico anthropogenic emissions (bottom).

12. SUMMARY AND CONCLUSIONS

12.1 Summary of CAMx 2014 36/12/4-km Photochemical Model Platform Development

A CAMx 2014 36/12/4-km ozone modeling platform was developed with the 4-km domain focused on New Mexico and adjacent states. The CAMx 2014 36/12/4-km modeling platform was based on the Western Regional Air Partnership (WRAP), Western Air Quality Study (WAQS) CAMx 2014 36/12-km modeling platform. WRF meteorological modeling was conducted to generate CAMx meteorological inputs for the 36/12/4-km domains and summer of 2014. A model performance evaluation was conducted that compared CAMx 2014 estimated ozone concentrations with concurrent ozone observations that produced good ozone model performance. A revised CAMx 2014v2 base case was conducted with a newer version of the CAMx model and updated biogenic emissions that also produced very good ozone model performance.

SMOKE emission and CAMx ozone modeling was conducted for a 2014v2 Base Case, a 2028 Base Case and a 2028 O&G Control Strategy that implemented O&G controls on O&G sources in the New Mexico portions of the San Juan and Permian Basins. The proposed New Mexico O&G ozone precursor rule controls were implemented in the 2028 Base Case NM O&G emissions by Eastern Research Group (ERG) under separate contract with NMED.

12.2 Summary of 2028 Ozone Modeling Results and Ozone Design Value Projections

2028 projected future year ozone design values (DVF) were made using the CAMx 2014v2, 2028 Base Case and 2028 O&G Control Strategy modeling results following EPA's latest photochemical modeling guidance (EPA, 2018). EPA's modeling guidance recommends scaling the current year design value (DVC) using a Relative Response Factor (RRF) based on the ratio of the future to current year modeling results (i.e., RRF = CAMx $Ozone_{2028}$/CAMx $Ozone_{2014}$). The guidance recommends using a DVC based on an average of three ozone design values centered on the base modeling year, which in this case is 2014, so design values from 2012-2016 are used (i.e., $DVC_{2012\text{-}2016}$). Following EPA's ozone projection approach guidance, all 2028 projected ozone DVFs were below the 2015 ozone NAAQS at all monitoring sites in New Mexico using the $DVC_{2012\text{-}2016}$ observed ozone starting point for the projections.

A comparison of the CAMx absolute modeled daily MDA8 ozone concentrations for the 2028 Base Case and 2028 O&G Control Strategy found that the strategy resulted in MDA8 ozone reductions over large areas of New Mexico, with the largest ozone reductions occurring in the San Juan and Permian Basins. However, there were also isolated areas of ozone increases due to the 2028 O&G Control Strategy that usually occurred in or near the San Juan and Permian Basins that are likely due to "NO_x Disbenefits" where NO_x emission reductions can cause localized ozone increases. For at least one day (June 5, 2014) that CAMx 2028 Base Case had a large area with MDA8 ozone concentrations that exceeded the 70 ppb ozone NAAQS in San Juan County, the 2028 O&G Control Strategy was sufficient to reduce the MDA8 ozone concentrations to below the NAAQS. On

another day (July 24, 2014), the "NO_x Disbenefits" of the 2028 O&G Control Strategy was sufficient to increase the MDA8 ozone concentrations in one 4-km grid cell in San Juan County that was below the NAAQS in the 2028 Base Case to right at the threshold for exceeding the NAAQS (71.0 ppb) in the 2028 O&G Control Strategy.

12.3 Sensitivity of 2028 Ozone Design Value Projections to Current Year Ozone Design Value

Given the upward trend in ozone design values in southern New Mexico in recent years (see Table 1-1), the sensitivity of the 2028 future year ozone DVF projections to the current year ozone design value (DVC) was investigated by making 2028 ozone DVF projections using current year design values based on observations from 2015-2019 (i.e., $DVC_{2015\text{-}2019}$) and 2017-2019 (i.e., $DV_{2017\text{-}2019}$) instead of the $DVC_{2012\text{-}2016}$ current year design value recommended in EPA's ozone modeling guidance (EPA, 2018).

There were four monitoring sites with $DVC_{2015\text{-}2019}$ exceeding the 70 ppb ozone NAAQS, compared to two using the $DVC_{2012\text{-}2016}$. The Carlsbad site projected 2028 ozone DVF (71.2 ppb) still exceeded the ozone NAAQS for the 2028 Base Case when the $DVC_{2015\text{-}2019}$ current year design value was used in the projection. However, the emission reductions in the 2028 O&G Control Strategy were sufficient to bring the projected 2028 ozone DVF at the Carlsbad site (70.9 ppb) to below the ozone NAAQS in the $DVC_{2015\text{-}2019}$ current year design value sensitivity analysis.

Three monitors exceeded the 70 ppb ozone NAAQS using the most recent ozone design value ($DV_{2017\text{-}2019}$), but one of the sites that had their $DVC_{2015\text{-}2019}$ exceeding the NAAQS was no longer in operation in 2017-2019 (i.e., Carlsbad Caverns NP). Two of the sites were still estimated to have projected 2028 ozone DVFs that exceeded the ozone NAAQS for both the 2028 Base Case and 2028 O&G Control Strategy in the $DV_{2017\text{-}2019}$ current year DVC sensitivity analysis. Under the 2028 O&G Control Strategy, the projected 2028 ozone DVFs at Carlsbad and Desert View were, respectively, 76.0 and 71.4 ppb using the $DV_{2017\text{-}2019}$ as the current year DVC in the ozone projections.

There were significant increases in O&G emissions within the Permian Basin since 2014 that are not accounted for in the CAMx ozone modeling results in the $DVC_{2015\text{-}2019}$ and $DV_{2017\text{-}2019}$ current year design value sensitivity tests. If those additional O&G emissions were included in the CAMx base year base case simulations, the projected 2028 ozone DVFs would be lower in the vicinity of the Permian Basin because of the higher denominator in the RRF projections factors due to higher O&G emissions than occurred in 2014.

EPA recommends using the average of three years of design values for the DVC as it is more stable and has less year-to-year variability than a single design value period (EPA, 2018, pp. 101[42]). So, the 2028 ozone DVFs projection sensitivity test using the $DV_{2017\text{-}2019}$ has an additional caveat as it is less stable and more influenced by year-to-year variability in ozone concentrations.

[42] https://www.epa.gov/sites/production/files/2020-10/documents/o3-pm-rh-modeling_guidance-2018.pdf

12.4 2028 Source Sector APCA Ozone Source Apportionment Modeling

The 2028 O&G Control Strategy Source Sector APCA ozone source apportionment modeling found that approximately half to two-thirds of the ozone on high MDA8 ozone days in New Mexico is due to Boundary Conditions (BCs) that are mainly from international and natural emissions from outside of the CAMx 36-km North America modeling domain. The highest contributing New Mexico Source Sector varied by location. For sites in San Juan County in northwestern New Mexico, EGU and O&G Non-Point sources were the two highest contributing Source Sectors followed by O&G Point sources. For sites in Bernalillo County in the central part of New Mexico, Other Anthropogenic, On-Road and Non-Road were the highest contributing Source Sectors. In Doña Ana County in southern New Mexico, New Mexico EGU and On-Road were the highest contribution Source Sectors. O&G Non-Point and Point sources were the highest contributing New Mexico Source Sectors at the Carlsbad and Hobbs sites in southeastern New Mexico. Texas and Mexico had large contributions to ozone in southern New Mexico, whereas Colorado had large contributions in northwestern New Mexico.

International anthropogenic emissions contributed 13 to 26 ppb to the projected 2028 ozone DVFs at New Mexico sites, with larger international contributions at the southern New Mexico sites. The elimination of the contributions of international anthropogenic emissions reduced the projected 2028 ozone DVFs to below 60 ppb under all scenarios, even when the $DVC_{2017\text{-}2019}$ was used that produced a projected 2028 ozone DVF at Carlsbad that exceeded both the 2008 and 2015 ozone NAAQS.

12.5 2028 VOC/NO_x Sensitivity OSAT Ozone Source Apportionment Modeling

The 2028 VOC/NO_x Sensitivity OSAT ozone source apportionment simulation found that ozone formation across New Mexico was primarily NO_x sensitive. There were some areas that had relatively higher VOC sensitive ozone formation conditions on some days, including the San Juan Basin, Albuquerque, the Texas part of El Paso, and to a lesser extent, the Permian Basin. There are even days (e.g., June 5th) where elevated MDA8 ozone concentrations in San Juan Basin that approached the ozone NAAQS and ozone formation was approximately evenly split between NO_x and VOC sensitive ozone formation conditions. But overall, ozone formation was more NO_x sensitive than VOC sensitive. The highest modeled ozone concentrations tend to have relatively higher VOC sensitive ozone concentrations. Thus, although ozone formation appears to be mainly NO_x sensitive, VOC controls will also have benefits in reducing some of the highest ozone concentrations in New Mexico.

13. REFERENCES

Air Sciences. 2020. Fire Emission Inventories for Regional Haze Planning: Methods and Results. Air Sciences, Inc., Portland, Oregon. Prepared for Western Regional Air Partnership. April. (https://www.wrapair2.org/pdf/fswg_rhp_fire-ei_final_report_20200519_FINAL.PDF).

Appel, W., R. Gilliam, N. Davis, A. Zubrow, and S. Howard. 2011. Overview of the atmospheric model evaluation tool (AMET) v1.1 for evaluating meteorological and air quality models. Environmental Modeling & Software. 26. 434-443. 10.1016/j.envsoft.2010.09.007.

Coats, C.J. 1995. Sparse Matrix Operator Kernel Emissions (SMOKE) Modeling System, MCNC Environmental Programs, Research Triangle Park, NC.

Colella, P., and P.R. Woodward. 1984. The Piecewise Parabolic Method (PPM) for Gas-dynamical Simulations. *J. Comp. Phys.*, **54**, 174201.

Daley, C., M. Halbleib, J. Smith, W. Gibson, M. Doggett, G. Taylor, J. Curtis and P. Pasteris. 2008. Physiographically sensitive mapping of climatological temperature and precipitation across the conterminous United States. *Intl. J. Climate*. (http://prism.oregonstate.edu/documents/Daly2008_PhysiographicMapping_IntJnlClim.pdf).

Emery, C., E. Tai, and G. Yarwood. 2001. Enhanced Meteorological Modeling and Performance Evaluation for Two Texas Episodes, report to the Texas Natural Resources Conservation Commission, prepared by ENVIRON, International Corp, Novato, CA.

Emery, C.E., Z. Liu, A.G. Russell, M.T. Odman, G. Yarwood and N. Kumar. 2016. Recommendations on statistics and benchmarks to assess photochemical model performance. J. of the Air and Waste Management Assoc., Vol. 67, Issue 5. DOI: 10.1080/10962247.2016.1265027. (https://www.tandfonline.com/doi/full/10.1080/10962247.2016.1265027).

EPA. 2018. Modeling Guidance for Demonstrating Air Quality Goals for Ozone, PM2.5, and Regional Haze. U.S. Environmental Protection Agency, Office of Air Quality Planning and Standards, Air Quality Assessment Division. Research Triangle Park, NC. EPA 454/R-18-009. November 29. (https://www3.epa.gov/ttn/scram/guidance/guide/O3-PM-RH-Modeling_Guidance-2018.pdf).

EPA. 2019. Meteorological Model Performance for Annual 2016 Simulation WRF v3.8. U.S. Environmental Protection Agency, Office of Air Quality Planning and Standards, Air Quality Assessment Division. Research Triangle Park, NC. EPA 454/R-19-010. July. (https://www.epa.gov/sites/production/files/2020-10/documents/met_model_performance-2016_wrf.pdf).

Guenther, A., X. Jiang, T. Duhl, T. Sakulyanontvittaya, J. Johnson and X. Wang. 2014. MEGAN version 2.10 User's Guide. Washington State University, Pullman, WA. May 12. (http://lar.wsu.edu/megan/docs/MEGAN2.1_User_GuideWSU.pdf).

Heath, N., J. Pleim, R. Gillian, D. Kang, M. Woody, K. Foley and W. Appel. 2016. Impacts of WRF Lightning Assimilation on Offline CMAQ Simulations.

Presented at 2016 CMAS Conference, Chapel Hill, NC. October 24-26. (https://cfpub.epa.gov/si/si_public_record_report.cfm?dirEntryId=335757&Lab=NERL).

Kalnay, E. et al. 1996. The NCEP/NCAR 40-Year Reanalysis Project. *Bull. Am. Meteorol. Soc.*, 77(3), 437-471. (https://rda.ucar.edu/datasets/ds090.0/docs/bams/bams1996mar/bams1996mar.pdf).

Michalakes, J., J. Dudhia, D. Gill, J. Klemp and W. Skamarock. 1998. Design of a Next-Generation Regional Weather Research and Forecast Model. Mesoscale and Microscale Meteorological Division, National Center for Atmospheric Research, Boulder, CO. (http://www.mcs.anl.gov/~michalak/ecmwf98/final.html).

Michalakes, J., S. Chen, J. Dudhia, L. Hart, J. Klemp, J. Middlecoff and W. Skamarock. 2001. Development of a Next-Generation Regional Weather Research and Forecast Model. Developments in Teracomputing: Proceedings of the 9th ECMWF Workshop on the Use of High Performance Computing in Meteorology. Eds. Walter Zwieflhofer and Norbet Kreitz. World Scientific, Singapore. Pp. 269-276. (http://www.mmm.ucar.edu/mm5/mpp/ecmwf01.htm).

Michalakes, J., J. Dudhia, D. Gill, T. Henderson, J. Klemp, W. Skamarock and W. Wang. 2004. The Weather Research and Forecast Model: Software Architecture and Performance. Proceedings of the 11th ECMWF Workshop on the Use of High Performance Computing in Meteorology. October 25-29, 2005, Reading UK. Ed. George Mozdzynski. (http://wrf-model.org/wrfadmin/docs/ecmwf_2004.pdf).

Park, S., J.B. Klemp, and J. Kim, 2019: Hybrid Mass Coordinate in WRF-ARW and Its Impact on Upper-Level Turbulence Forecasting. Mon. Wea. Rev., 147, 971–985, https://doi.org/10.1175/MWR-D-18-0334.1.

Ramboll. 2013. METSTAT Meteorological Model Statistical Evaluation Package. Ramboll, Novato, California. December 9. (http://www.camx.com/download/support-software.aspx).

Ramboll. 2020a. Revised Final Report: 2028 Future Year Oil and Gas Emission Inventory for the WESTAR-WRAP States – Scenario #1: Continuation of Historical Trends. Ramboll US Corporation, Novato, California. March. (www.wrapair2.org/pdf/WRAP_OGWG_2028_OTB_RevFinalReport_05March2020.pdf).

Ramboll. 2020b. User's Guide Comprehensive Air-quality Model with extensions Version 7.0. Ramboll, Novato, California. May. (http://www.camx.com/files/camxusersguide_v7-00.pdf).

Ramboll. 2021. User's Guide Comprehensive Air-quality Model with extensions Version 7.1. Ramboll, Novato, California. May. (http://www.camx.com/files/camxusersguide_v7-10.pdf).

Ramboll and WESTAR. 2020a. New Mexico Ozone Attainment Initiative Photochemical Modeling Study – Draft Modeling Protocol. Ramboll US Corporation, Novato, CA. Western States Air Resources Council, Santa Fe, NM. May. (https://www.wrapair2.org/pdf/NM_OAI_Modeling_Protocol_v5.pdf).

Ramboll and WESTAR. 2020b. New Mexico Ozone Attainment Initiative Photochemical Modeling Study – Draft Work Plan. Ramboll US Corporation, Novato, CA. Western States Air Resources Council, Santa Fe, NM. May. (https://www.wrapair2.org/pdf/NM_OAI_Work_Plan_v2.pdf).

Ramboll and WESTAR. 2020c. New Mexico Ozone Attainment Initiative Photochemical Modeling Study – 2014 Modeling Platform Development and Model Evaluation. Ramboll US Corporation, Novato, CA. Western States Air Resources Council, Santa Fe, NM. September. (https://www.wrapair2.org/pdf/NM_OAI_2014_BaseCase_MPE_v3.pdf).

Ramboll and WESTAR. 2021. New Mexico Ozone Attainment Initiative Photochemical Modeling Study – Revised 2014v2 Base Case and Model Performance Evaluation. Ramboll US Consulting, Inc., Novato, CA. Western States Air Resources Council, Santa Fe, NM. February. (https://www.wrapair2.org/NMOAI.aspx).

Simon, H., K. Baker and S. Phillips. 2012. Compilations and Interpretation of Photochemical Model Performance Statistics Published between 2006 and 2012. *Atmos. Env.* 61 (2012) 124-139. December. (http://www.sciencedirect.com/science/article/pii/S135223101200684X).

Skamarock, W. C. 2004. Evaluating Mesoscale NWP Models Using Kinetic Energy Spectra. *Mon. Wea. Rev.*, Volume 132, pp. 3019-3032. December. (http://www.mmm.ucar.edu/individual/skamarock/spectra_mwr_2004.pdf) .

Skamarock, W. C., J. B. Klemp, J. Dudhia, D. O. Gill, D. M. Barker, W. Wang and J. G. Powers. 2005. A Description of the Advanced Research WRF Version 2. National Center for Atmospheric Research (NCAR), Boulder, CO. June. (http://www.mmm.ucar.edu/wrf/users/docs/arw_v2.pdf)

Skamarock, W. C., J. B. Klemp, J. Dudhia, D. O. Gill, D. M. Barker, M. G. Duda, X-Y. Huang, W. Wang and J. G. Powers. 2008. A Description of the Advanced Research WRF Version 3. National Center for Atmospheric Research (NCAR), Boulder, CO. June. (https://opensky.ucar.edu/islandora/object/technotes%3A500/datastream/PDF/view)

Skamarock, W. C., J. B. Klemp, J. Dudhia, D. O. Gill, Z. Liu, J. Berner, W. Wang, J. G. Powers, M. G. Duda, D. M. Barker and X-Y. Huang. 2019. A Description of the Advanced Research WRF Model Version 4 (No. NCAR/TN-556+STR). doi:10.5065/1dfh-6p97 (https://opensky.ucar.edu/islandora/object/technotes%3A576/datastream/PDF/download/citation.pdf)

Skamarock, W. C. 2006. Positive-Definite and Monotonic Limiters for Unrestricted-Time-Step Transport Schemes. *Mon. Wea. Rev.*, Volume 134, pp. 2241-2242. June. (http://www.mmm.ucar.edu/individual/skamarock/advect3d_mwr.pdf).

Stoeckenius, T.E., C.A. Emery, T.P. Shah, J.R. Johnson, L.K. Parker, A.K. Pollack. 2009. Air Quality Modeling Study for the Four Corners Region; Prepared by ENVIRON International Corporation, Novato, CA. Prepared for the New Mexico Environment Department, Air Quality Bureau, Santa Fe, NM.

UNC. 2008. Atmospheric Model Evaluation Tool (AMET) User's Guide. Institute for the Environment, University of North Carolina at Chapel Hill. May 30.

(https://www.cmascenter.org/amet/documentation/1.1/AMET_Users_Guide_V1.1.pdf).

UNC. 2018. SMOKE v4.6 User's Manuel. University of North Carolina at Chapel Hill, Institute for the Environment. Chapel Hill, North Carolina. September 24. (https://www.cmascenter.org/smoke/documentation/4.6/manual_smokev46.pdf).

Wesely, M.L. 1989. Parameterization of Surface Resistances to Gaseous Dry Deposition in Regional-Scale Numerical Models. *Atmos. Environ.*, 23, 1293-1304.

Wiedinmyer, C., T. Sakulyanontvittaya and A. Guenther. 2007. MEGAN FORTRAN code V2.04 User Guide. NCAR, Boulder, CO. October 29. (http://acd.ucar.edu/~guenther/MEGAN/MEGANguideFORTRAN204.pdf).

Yarwood, G., J. Jung, G. Z. Whitten, G. Heo, J. Mellberg and M. Estes. 2010. Updates to the Carbon Bond Mechanism for Version 6 (CB6). 2010 CMAS Conference, Chapel Hill, NC. October. (http://www.cmascenter.org/conference/2010/abstracts/emery_updates_carbon_2010.pdf)

Zhang, L., S. Gong, J. Padro, L. Barrie. 2001. A size-segregated particle dry deposition scheme for an atmospheric aerosol module. *Atmos. Environ.*, **35**, 549-560.

Zhang, L., J. R. Brook, and R. Vet. 2003. A revised parameterization for gaseous dry deposition in air-quality models. *Atmos. Chem. Phys*., **3**, 2067–2082.